Regulation of BAP1 tumor suppressor complex by post-translational modifications

par

Nazar Mashtalir

Centre for Research HMR - Hôpital Maisonneuve - Rosemont

Medicine

Thèse présentée à la Faculté de médecine

en vue de l'obtention du grade de PhD

en Sciences Biomedicales

April 25, 2014

Université de Montréal
Faculté des études supérieures et postdoctorales

Cette thèse intitulée:

Regulation of BAP1 tumor suppressor complex by post-translational modifications

Présentée par:
Nazar Mashtalir

a été évaluée par un jury composé des personnes suivantes :

Alain Verreault, président-rapporteur
El Bachir Affar, directeur de recherche
Sylvie Mader, membre du jury
Brian Raught, examinateur externe
Puttaswamy Manjunath, représentant du doyen de la FES

Résumé

Le régulateur transcriptionnel BAP1 est une déubiquitinase nucléaire (DUB) dont le substrat est l'histone H2A modifiée par monoubiquitination au niveau des residus lysines 118 et 119 (K118/K119). Depuis les dernières années, BAP1 emerge comme un gene suppresseur de tumeur majeur. En effet, BAP1 est inactivé dans un plethore de maladies humaines héréditaires et sporadiques. Cependant, malgré l'accumulation significative des connaissances concernant l'occurrence, la pénétrance et l'impact des défauts de BAP1 sur le développement de cancers, ses mécanismes d'action et de régulation restent très peu compris. Cette étude est dédiée à la caractérisation moléculaire et fonctionnelle du complexe multi-protéique de BAP1 et se présente parmi les premiers travaux décrivant sa régulation par des modifications post-traductionnelles.

D'abord, nous avons défini la composition du corps du complexe BAP1 ainsi que ses principaux partenaires d'interaction. Ensuite, nous nous sommes spécifiquement intéressés a investiguer d'avantage deux principaux aspects de la régulation de BAP1. Nous avons d'abord décrit l'inter-régulation entre deux composantes majeures du complexe BAP1, soit HCF-1 et OGT. D'une manière très intéressante, nous avons trouvé que le cofacteur HCF-1 est un important régulateur des niveaux protéiques d'OGT. En retour, OGT est requise pour la maturation protéolytique de HCF-1 en promouvant sa protéolyse par O-GlcNAcylation, un processus de régulation très important pour le bon fonctionnement de HCF-1. D'autre part, nous avons découvert un mécanisme unique de régulation de BAP1 médiée par l'ubiquitine ligase atypique UBE2O. en effet, UBE2O se caractérise par le fait qu'il s'agit aussi bien d'une ubiquitine conjuratrice et d'une ubiquitine ligase. UBE2O, multi-monoubiquitine BAP1 au niveau de son domaine NLS et promeut son exclusion du noyau, le séquestrant ainsi dans le cytoplasme. De façon importante, nos travaux ont permis de mettre de l'emphase sur le rôle de l'activité auto-catalytique de chacune de ces enzymes, soit l'activité d'auto-déubiquitination de BAP1 qui est requise pour la maintenance de sa localisation nucléaire ainsi que l'activité d'auto-ubiquitination d'UBE2O impliquée dans son transport nucléo-cytoplasmique. De manière

significative, nous avons trouvé que des défauts au niveau de l'auto-déubiquitination de BAP1 due à des mutations associées à certains cancers indiquent l'importance d'une propre regulation de cette déubiquitinase pour les processus associés à la suppression de tumeurs.

Mots clés: Chromatine, marque épigénctique, OGT, HCF-1, BAP1, UBE2O, O-GlcNAcylation, régulation protéolytique, ubiquitination, déubiquitinase, ubiquitine ligase atypique, activité auto-catalytique, cancer

Abstract

BAP1 is a nuclear deubiquitinating enzyme (DUB) that acts as a transcription regulator and a DUB of nucleosomal histone H2AK119. In the recent years, it has become clear that BAP1 is a major tumor suppressor, inactivated in a plethora of hereditary and sporadic human malignancies. Although, we now accumulated a significant body of knowledge in respect to the occurrence, penetrance and impact of BAP1 disruption in cancer, its mechanism of action and regulation remained poorly defined. This work is dedicated to the biochemical and functional characterization of the BAP1 multiprotein complex and presents one of the first cases regarding its regulation by post-translational modifications.

First, we defined the initial composition of the BAP1 complex and its main interacting components. Second, we specifically focused on two aspects of BAP1 regulation. We described the cross regulation between the two major components of the complex namely HCF-1 and OGT. We found that HCF-1 is important for the maintenance of the cellular levels of OGT. OGT, in turn, is required for the proper maturation of HCF-1 by promoting O-GlcNAcylation-mediated limited proteolysis of its precursor. Third, we discovered an intricate regulatory mechanism of BAP1 mediated by the atypical ubiquitin ligase UBE2O. UBE2O multi-monoubiquitinates BAP1 on its NLS and promotes its exclusion from the nucleus. Importantly, our work emphasises the role of the autocatalytic activity of both enzymes namely the auto-deubiquitination activity of BAP1, required for the maintenance of nuclear BAP1 and the auto-ubiquitination of UBE2O implicated in its nucleocytoplasmic transport. Significantly, we found that auto-deubiquitination of BAP1 is disrupted by cancer-associated mutations, indicating the involvement of this process in tumor suppression.

Keywords: Chromatin, epigenetic mark, OGT, HCF-1, BAP1, UBE2O, O-GlcNAcylation, proteolytic processing, ubiquitination, deubiquitinase, atypical ubiquitin ligase, autocatalytic activity, cancer

Table of Contents

List of Figures

Dedication:

- Vjacheslav Mykolajovych Korobov PhD, D.Sc (1940-2003) my first supervisor and mentor, great biochemist, wonderful and fair person, whose guidance and spirit helped me to develop my scientific critique and judgment.
- My parents Olga Valentinivna Maksymenko and Bogdan Bogdanovich Mashtalir for raising me, giving me an opportunity and support to pursue a career in the life sciences.
- My grandmother Nelia Nikolaevna Sapozhnikova (1932-1996) for giving me her love and care. A gift on my 12th birthday, her personal medical microscope, inspired my interest to study life on its basic level.

Acknowledgements:

- My mentor and supervisor El Bachir Affar PhD, for teaching me about top quality science, guidance, motivation and support during my PhD studies.
- Elliot Drobetsky PhD, for his cheerful suggestion, and discussions over the years at HMR.
- My friends and colleagues in the lab Helen Yu, Ian Hamond-Martel, Salima Daou, Jessica Gagnon, Nicholas Iannantuono, Helen Pak, Nadine Sen, Haithem Barbour, Diana Adjaoud, Haider H. Dar for helping me in the lab. My old friends and colleagues Serhiy Havrylov PhD, Yurij Rzhepetsky PhD and Tomasz Szostek.
- All authors and co-authors of manuscripts and articles
- Doctoral thesis committee members
- My wife Anastasiya Mashtalir for support during my studies.

Introduction

Chromatin structure and transcription regulation

One of the pillars of life is the ability to acquire information from external stimuli and, depending on its nature, build the proper response to sustain homeostasis (Koshland, 2002). This intrinsic "rationalism" of every living organism is dictated by its genetic information which can be differentially expressed depending on the stimuli or the type of cell that receives it. One of the first examples of regulated gene expression was elucidated through the work done by François Jacob and Jacques Monod (Jacob and Monod, 1961) who used the *E. coli* lactose operon (lac) as a model of a mechanism of gene repression in response to the availability of a preferable energy source. Although the lac operon represents one of the simplest modes of gene expression regulation, the same underlying principle is found within most prokaryotic and eukaryotic genetic regulatory circuits (Lelli et al., 2012).

According to the classical view of gene expression regulation, DNA is considered as a linear genetic element free of obstacles and higher order structures. Genes are thus being differentially transcribed as a function of the RNA polymerase and transcription factors recruitment to promoters. This view persisted for decades in the field of molecular genetics and helped to establish numerous principles of gene expression regulation at the level of transcription factor recruitment, binding and transcription initiation (Lelli et al., 2012). On the other hand, this model did not take into account the numerous biophysical and biochemical constraints that influence gene expression *in vivo* especially in eukaryotic organisms.

Although the circular genetic material (nucleoid) of prokaryotic cell is almost devoid of intergenic elements and introns and is openly located in the cytoplasm, recent studies were able to map regions within the nucleoid with different densities, nuclease

sensitivity and transcriptional activity, suggesting that its expression is regulated by higher order chromatin structures (Dillon and Dorman, 2010; Postow et al., 2004). In contrast to prokaryotes, eukaryotes acquired vast amounts of noncoding/structural/regulatory DNA that comprise up to 98% of all the genetic material (Lelli et al., 2012). This dramatic increase of genome size and constitution required the concurrent establishment of elaborate mechanisms that coordinate its compaction and packaging within the confined space of the nucleus (Kornberg, 1974).

In 1881, the German biologist Walther Flemming coined the term chromatin. Flemming made an observation that the nuclear material of the cell was specifically stained by the basophilic aniline dyes (such as haematoxylin) (Flemming 1882). In years that followed, several discoveries pushed the boundaries of chromatin research: the discovery of histones (Zacharias, 1894), nuclein and "transforming principle" (Avery et al., 1944; Griffith, 1928), followed by the discovery of the structure of DNA (Watson and Crick, 1953). All these, and many more findings, advanced our understanding of the mechanisms of life including chromatin biology and epigenetics (Olins and Olins, 2003).

Chromatin, at its most simplest level, is the stoichiometric deoxyribonucleoprotein complex that contains the DNA molecule wrapped around the histone protein core and is termed the nucleosome (Khorasanizadeh, 2004; Kornberg, 1974; Luger et al., 1997; Olins and Olins, 1974; Senior et al., 1975).

The first electron micrographs of chromatin at its most basic level were acquired by Oudet et al. in 1975 and resembled beads on a string later renamed the 10 nm fiber (Oudet et al., 1975). At that time, it was already known that eukaryotic DNA formed a tight complex with a defined number of histone proteins. The early images of chromatin shed light on how DNA might be compacted inside an interphase nucleus. The early studies on chromatin structure defined that the histones and DNA form repetitive structures of DNA and nucleosome cores, namely the 10 nm fiber. This structure can be further compacted into an even higher order chromatin structures named the 30 nm fibers (Dorigo et al., 2004; Kruithof et al., 2009; Luger et al., 2012; Schalch et al., 2005). Zigzag and solenoid models are the two main models explaining the higher order chromatin structure, although some

studies question the very existence of such structures *in vivo* (Fussner et al., 2011; Nishino et al., 2012). Interestingly, the debate around the exact organisation of chromatin at its higher levels remains open (Luger et al., 2012; Luger and Hansen, 2005). Nonetheless, the 30 nm fiber can be further compacted to form higher order structures, and the degree of compaction of chromatin at this level is highly dependent on the chromosome region, the cell cycle phase and external stimuli (Koundrioukoff et al., 2004; Luger et al., 2012).

Typical nucleosomes include a core histone octamer composed of four pairs of histones, namely H2A/H2B and H3/H4, which act as a spool for the DNA to wrap around. The DNA is wound into a 1.67 left handed supercoil turn around the histone core and encompasses 147 nucleotide base pairs (Luger et al., 1997). The nucleosomes are linked by short DNA sequences, namely linker DNA, which may also be bound by the histone H1, that promotes further chromatin compaction (Caterino and Hayes, 2011; Kornberg, 1974; Oudet et al., 1975).

Histones are highly conserved among most of eukaryotic species (Pontarotti, 2009). The only phyla of the eukaryotic organism devoid of histones are the Dinoflagellates. This group of small free-living flagellate protists seems to have abandoned the classical chromatin architecture and evolved its own unique mode of chromatin packaging. Dinoflagellates genomes protein to DNA ratio is very low (around 1:10). Nonetheless, recent studies found that their genome is compacted by basic proteins that have only distant relation to histones and composed by a family of viral DNA binding proteins (Gornik et al., 2012). On the other hand, other sources predict homology with the DNA binding proteins of Bacteria (Wong et al., 2003).

In eukaryotes, the histone molecule is comprised of α-helical histone fold, and the unstructured histone tail (N-terminal for H3/H4 and C-terminal for H2A/H2B). The histone fold is capable of forming tight heterodimers of H2A/H2B and H3/H4, which can further complex to form tetramers and the core histone particle (Luger et al., 1997). Being highly alkaline in its amino acid composition, the histone octamer forms high affinity complex with DNA. On the contrary, the histone tails remain free of interaction and protrude between the DNA supercoils like antennae. These “antennae” act as major determinants of

chromatin function since they may be marked with numerous signaling and epigenetic post-translational modifications (PTMs) so as to regulate gene expression, DNA replication, DNA repair and epigenetic memory (Campos and Reinberg, 2009; Lelli et al., 2012; Ruthenburg et al., 2007; Shilatifard, 2006). The histone tails do not usually directly act as structural nucleosome elements, but rather play the role of chromatin signalling elements. Numerous PTMs were identified in the histone tail regions. These include the classical PTMs such as serine/threonine phosphorylation, lysine acetylation and ubiquitination, lysine/arginine methylation (Chi et al., 2010; Strahl and Allis, 2000), as well as less studied PTMs such as serine/threonine O-GlcNAcylation and lysine crotonylation (Fujiki et al., 2011; Sakabe et al., 2010; Tan et al., 2011).

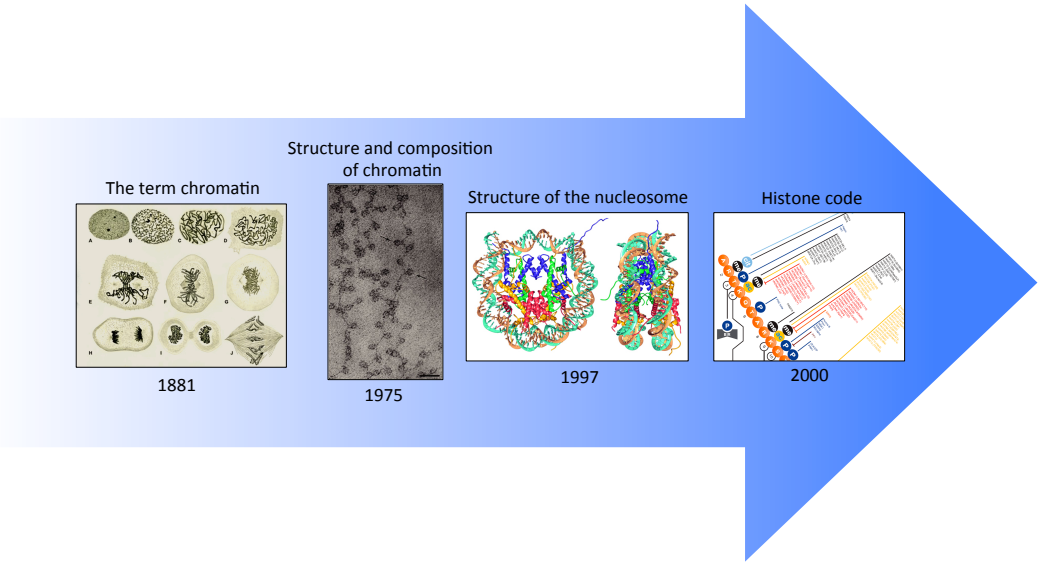

Figure 1 The timeline of chromatin biology. (Flemming, 1882; Luger et al., 1997; Olins and Olins, 2003), Abcam website.

Depending on the region within the genome, chromatin may be highly condensed, such as centromeric or telomeric regions or less condensed such as in active transcription regions. Traditionally, chromatin was thought to exist in two main states: heterochromatin, which is represented by highly compacted nucleosomes and euchromatin, characterised by "loosened" condensation of the nucleosomes (Avramova, 2002; Gaspar-Maia et al., 2011;

Weiler and Wakimoto, 1995). Heterochromatic regions of the nucleus often localize to the nuclear periphery forming the so-called chromocenters/foci. This view of the nuclear architecture persisted for a number of decades and was helpful in understanding how the chromatin architecture would influence gene expression. In recent years, this simplistic view of nuclear organisation dramatically changed, giving rise to a more complex model of chromatin architecture (Oberdoerffer and Sinclair, 2007). The advances in this area of research can be attributed to the development of high fidelity chromatin immunoprecipitation coupled to next generation sequencing analysis ((CHIP-chip/CHIP-seq (Chromatin immunoprecipitation linked to microarray analysis or high throughput sequencing) (Ren et al., 2000; Sealfon and Chu, 2011), chromosome conformation capture (from Chromosome Conformation Capture (3C) to Carbon-Copy Chromosome Conformation Capture (5C) and Genome conformation capture (GCC and Hi-C)(Dekker et al., 2002; Dostie et al., 2006; Lieberman-Aiden et al., 2009; Zhao et al., 2006) along with gene expression profiling ((DNA microarray/seq (RNA expression profiling using microarray analysis or high throughput sequencing)) (Sealfon and Chu, 2011).

Systematic use of these techniques brought about the subdivision of the historical dichotomy between euchromatin/heterochromatin to new and functionally diverse chromatin domains. For example, one study in *Drosophila* cells applied the DamID (DNA adenine methyltransferase identification) and CHIP/seq techniques to study the distribution of 53 well-characterized chromatin regulators so as to create the integral map of their genomic distribution (Filion et al., 2010). This approach is based on the view that a subset of chromatin regulatory elements along with different epigenetic histone marks and DNA modifications can be subdivided into several physically derived chromatin segments. The study divided the chromatin into several distinct but overlapping types. Three types of "repressed" chromatin (schematically indicated as green, blue and black) and two types of "euchromatin" (yellow and red) were distinguished. The green chromatin represents the classical heterochromatin that is marked by its typical epigenetic mark trimethylated H3K9, its reader HP1 and writer the Su(var) 3-9 methyltransferase as well as histone H1. The other repressive type of chromatin schematized as blue most closely resembles the chromatin

established by the polycomb group (PcG) proteins: it recruits the PcG group proteins PCL, PSC, E(z) and is enriched in trimethylated H3K27 histone mark. Most surprisingly, the most abundant type of chromatin that covers roughly half the genome, the black chromatin, is much less diverse in the chromatin bound components, it is devoid of most of the earlier mentioned chromatin elements and consists of large genomic domains of more than 100 kb in length. This type of chromatin recruits the histone H1, lamin (Lam) the regulator of the late polytene chromosomes Suppressor of Underreplication (SUUR) and others and is highly repressive, since the transgenes in this region display low level of expression. The yellow and red euchromatin regions share many similar features and are bound by numerous positive and negative transcriptional regulators as well as the activation transcription marks such as dimethylated H3K4 and trimethylated H3K79. Nonetheless, these two types of euchromatin display different modes of transcription regulation. For example, the yellow chromatin is enriched in trimethylated H3K36 histone mark. The distribution of genes is also different in both types of euchromatin with the red chromatin being enriched in genes important for general cell physiology and involved in DNA repair and nucleic acid metabolism, whereas the yellow chromatin bears more specialized and tissue specific genes involved in signal transduction, extracellular matrix remodelling and transcription factor activity (Filion et al., 2010).

The sequencing of the human genome announced the beginning of a new "post genomic era" in molecular biology (Venter et al., 2001). The result of the human genome project revealed an unexpected outcome: the human genome, expected to be comprised of 50-100 thousand genes contained only ≈ 20 thousand protein coding genes. This number of genes, highly comparable to the mouse genome was only double the number of genes of the *Drosophila melanogaster* and the amebae *Dictyostelium* (12 thousand protein coding genes) (Adams et al., 2000) and half the amount of genes compared to some plants (Goff et al., 2002; Tuskan et al., 2006). This result indicated that the complexity of the human body, its self-awareness, intellect and its ability to construct organized societies are derived from the way genes are regulated, rather than the sheer number. Indeed, the vertebrate genomes encompass tremendous amounts of noncoding/structural DNA along with a whole army of

noncoding RNAs that play an important role in gene expression regulation and in shaping the epigenetic landscape of the cell (Wells, 2011).

The structure of chromatin is subject to an active regulation, this includes the direct chromatin remodeling by the DNA/histone directed ATPases (Ahel et al., 2009; Chan et al., 2005; Chen et al., 2011; Morrison and Shen, 2009; Narlikar et al., 2013; Wu et al., 2007), the chromatin modifying enzymes that target DNA, for example DNA methyltransferases (Goll and Bestor, 2005) and 5-methylcytosine dioxygenases (TET family) (Branco et al., 2012), the histone modifying enzymes such as histone acetyltransferases and deacetylases (Shahbazian and Grunstein, 2007) as well as the histone methyltransferases and demethylases (Klose and Zhang, 2007). Functionally, these proteins may be divided into several groups such as writers, readers and erasers (Patel and Wang, 2013). In order to combine different biochemical properties of these chromatin regulators, these functional groups of proteins often form stable complexes, resulting in the formation of multifunctional epigenetic machineries (Chen et al., 2011; Ho and Crabtree, 2010; Wu et al., 2007; Yokoyama et al., 2004). Several of such protein complexes most relevant to this work are described below in more detail.

Polycomb and Trithorax group protein complexes: regulation of Hox genes and beyond

Hox genes

The coordination of developmental processes in multicellular organisms requires elaborate gene expression regulatory mechanisms. These mechanisms are coordinated by the superfamily of homeotic transcription factors that contain specific DNA binding modules named homeodomains, that bind a specific DNA sequence named the homeobox (Bridges, 1921; McGinnis et al., 1984a; McGinnis et al., 1984b; Scott and Weiner, 1984;

Shah and Sukumar, 2010). Historically, *Hox* genes were regarded as master regulators of morphogenesis and body patterning. The differential expression of *Hox* genes dictates the development of specific body parts (Dolle et al., 1993; Wellik, 2009). This notion arose from the studies in *Drosophila* where *Hox* gene mutants display a specific anterio-posterior homeotic transformation. In this process, the anterior segments of the body acquire the morphology of the more posterior body segments (Bridges, 1921; Lewis, 1978; Scott et al., 1983).

From an evolutionary perspective, the increasing complexity of the animal body plan usually correlates with the increasing number of *Hox* genes, their paralogs and the patterns of their expression (Pearson et al., 2005; Pendleton et al., 1993). For example, one of the simplest body plans in the *Metazoa* is that of the cnidarian *Hydra* has only two Hox genes *Cnox-3* and *Cnox-2* and one ParaHox gene *Cnox-1*. These genes define the anterior part of the body with the tentacles and the mouth opening as well as the posterior part of the body responsible for the binding to the substrate. Further, the expression patterns of *Cnox-3* and *Cnox-2* show that *Cnox-3*, a homologue of the Drosophila *Hox* gene *labial* (*lab*), plays a role in oral anterior patterning. On the contrary, the *Cnox-2*, the homologue of the *Drosophila Deformed* (*Gsx*) that belongs to the ParaHox cluster represses the anterior patterning in the body column (Schummer et al., 1992; Shenk et al., 1993).

The more complex body plan in arthropods such as *Drosophila* is accompanied by the expansion of the *Hox* gene cluster (Carroll, 1995; Pendleton et al., 1993). The *Drosophila* genome encodes eight *Hox* genes divided into two clusters called *Antennopedia* and *Bithorax*. The *Drosophila* developmental model is highly suitable for the study of body patterning since arthropod segmentation is easily detectable throughout their development. The pattern of the *Hox* gene expression correlates with the position of the gene in its corresponding cluster, for example the most anterior segments of the mouth apparatus express the *Antennapedia* member gene *lab* and the most posterior segments of the abdomen express the *Bithorax* family member *Abdominal-B* (*Abd-B*) (Pearson et al., 2005).

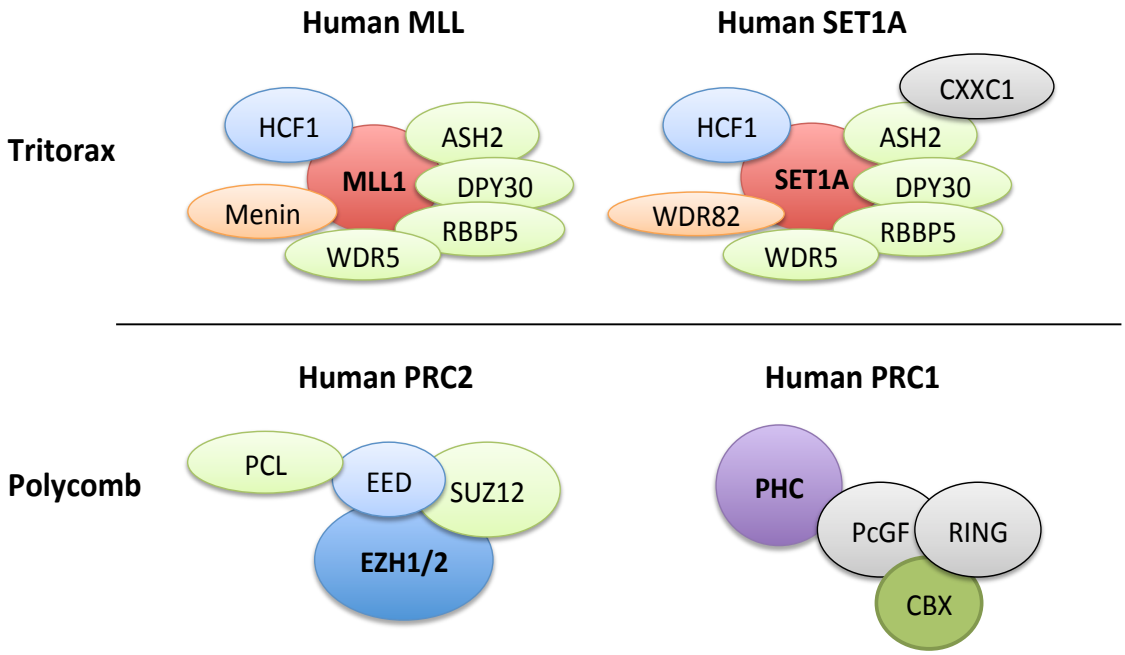

Figure 2. **Structure and composition of the PcG and TrxG protein complexes.** The simplified models of the complexes are shown.

The mammalian genome contains 39 *Hox* genes divided into four clusters (A, B, C and D) (Pendleton et al., 1993). Each cluster contains the *Hox* genes orthologous to the *Drosophila Antennapedia* and *Bithorax* (with some orthologs lost or duplicated depending on the clusters). The considerable increase in the number of the *Hox* genes can be explained by the global duplication of the ancestral chordate genome (Lynch and Wagner, 2009). The complex and often redundant expression pattern of the Hox genes in mammals dictates development of their body plan through complex, and sometimes highly convoluted mechanisms. Pattering of the mammalian body can be visualized by following the *Hox* gene expression along the vertebral column and somites of the mammalian embryo (Cardoso, 1995; Pendleton et al., 1993; Perez-Cabrera et al., 2002).

The polycomb group (PcG) and trithorax group (TrxG) regulatory complexes

Two crucial groups of regulatory genes, the polycomb group (PcG) and the trithorax group (TrxG), dictate the patterns of Hox gene expression and are required for the normal body plan development. The study of these complexes was initiated using genetic experiments in *Drosophila* based on the homeotic transformation phenotypes. The biochemical analysis of the PcG and Trx proteins subsequently revealed that they often constitute large multisubunit chromatin modifying complexes responsible for gene repression and activation respectively (Cao et al., 2002; Kuzmichev et al., 2002; Levine et al., 2002; Wang et al., 2004).

The TrxG proteins come together to form complexes containing the SET (Su(var)3-9, Enhancer-of-zeste and Trithorax) domain containing methyltransferase responsible for histone H3K4 methylation, the epigenetic mark usually associated with transcriptionally active regions in all eukaryotes (Bernstein et al., 2002; Ng et al., 2003). Set1 was first found as a part of the macromolecular complex COMPASS (complex of proteins associated with Set 1) and is the only member of this class of methyltransferases in *Saccharomyces cerevisiae*. COMPASS is responsible for the introduction of all mono-, di-, and trimethylations of H3K4 in yeast (Breen and Harte, 1991; Ingham, 1985; Krogan et al., 2002).

The *Drosophila* genome encodes several SET domain-containing proteins. These include the founding member of the Trithorax (*Trx*) family, Trithorax-related (*Trr*) and *dSet1*. All the members of this methyltransferase family form complexes related to the *Saccharomyces cerevisiae* COMPASS and catalyze the methylation of H3K4 (Eissenberg and Shilatifard, 2010; Hallson et al., 2012; Sedkov et al., 2003).

Trx was first identified as a gene whose mutation leads to “posterior to anterior” transformation phenotype. In contrast, mutations in PcG genes lead to the inverse phenotype (Breen and Harte, 1991). Notably the activation and repressive role of *Trx* and

PcG genes respectively were studied in genetic complementation studies and showed that the *PcG* homeotic transformation phenotypes can be suppressed by the mutations in *Trx* (Shilatifard, 2008).

Mammalian COMPASS-related proteins are represented by at least seven different complexes namely the SETD1A, SETD1B, MLL1 (Mixed lineage leukemia, also known as MLL), MLL2, MLL3, MLL4 and MLL5. SETD1A and SETD1B are the orthologs of the Drosophila *dSet*, the MLL1 and MLL2 related to the *Drosophila Trx*; MLL3 to MLL5 are orthologs of the *Trr* (Hallson et al., 2012; Mohan et al., 2010; Schuettengruber et al., 2007; Sedkov et al., 2003). The members of the COMPASS-like complexes in mammalian cells are responsible for the establishment of the active chromatin state and the removal of the repressive epigenetic marks, for example by the H3K27 demethylase UTX (Lee et al., 2007).

Overview of the PcG complexes

Biochemically, the PcG proteins form two major complexes, PRC1 and PRC2 (Cao et al., 2002; Schuettengruber et al., 2007; Wang et al., 2004). The subsequent studies of PcG proteins resulted in discovery of multiple variants and subdivisions of PRC1 and PRC2 complexes. This is most evident in respect to the mammalian orthologs of the *Drosophila* PRC1 complex, which are often represented by multiple subunit isoforms. The combination of different PcG subunits along with facultative components may results in the formation of tens if not hundreds of complex combinations. In addition to classical PRC1 and PRC2 PcG complexes, several other complexes can be defined such as the Pho repressive complex (Pho-RC) (Klymenko et al., 2006), *Drosophila* Ring-associated factors (dRAF) (Lagarou et al., 2008), and the recently discovered Pc-repressive deubiquitinase complex (PR-DUB), also known as BAP1 complex in mammals (Abdel-Wahab and Dey, 2013; Carbone et al., 2013; Dey et al., 2012; Scheuermann et al., 2010; Yu et al., 2010).

Polycomb repressive complex 2 (PRC2)

The main catalytic product of the PRC2 complex is the repressive di- and trimethylated H3K27 epigenetic mark that is catalyzed by the SET domain containing histone methyltransferase *Enhancer-of-zeste (E (z))* (the EZH1 and EZH2 in mammals). The other components of the complex are represented by the *Suppressor Of Zeste 12* (SUZ12), the *Polycomb like (PCL)* (PLC1, 2 and 3 in mammals), *Extra sex combs (ESC)* (mammalian EED) and the chromatin remodeling factor *Nurf 55* (RbAp46/48 in mammals) (Margueron and Reinberg, 2011). The mammalian complexes also contain the Jumonji- and AT-rich interaction domain (ARID)-domain-containing protein JARID2 that encodes for catalytic inactive methyltransferase, necessary for the proper recruitment of PRC2 to chromatin (Landeira et al., 2010; Pasini et al., 2010). The PRC2 complexes may also interact with a plethora of other transcriptional regulators such as chromatin remodelers, erasers of epigenetic marks (such as the HDACs and KDMs)(Shen et al., 2009; Tong et al., 2012) and most notably the numerous members of the non-coding RNAs (ncRNAs), to facilitate PRC2 recruitment and transcriptional repression (Gupta et al., 2010; Kaneko et al., 2010; Rinn et al., 2007).

The methyltransferase subunits of the PRC2 complex EZH1 and 2, despite being highly similar in their amino acid sequence, play different roles in the maintenance and establishment of the repressive chromatin state and are differentially expressed depending on the proliferative potential of the cell. EZH1 is expressed in both proliferating and quiescent cells. In contrast, EZH2 expression is only detected in proliferating cells. The two EZH subunits also have different contributions to the global level of H3K27 methylation (Margueron et al., 2008; Shen et al., 2008). The EZH1 knockout cells display little changes in their H3K27 methylation levels, whereas the EZH2 knockout cells cannot maintain their H3K27 methylation. Interestingly, EZH1 seems to act mostly in a catalytic activity independent manner, and is able to promote chromatin condensation whereas the EZH2/PRC2 complexes lack this ability. Therefore, the roles of the EZH1 and EZH2 may differ in respect to regulating H3K27 methylation levels. EZH2 appears to be required for

establishing the global H3K27 methylation levels whereas EZH1 might be required for the replenishment of H3K27 methylation following site-specific demethylation (Margueron et al., 2008).

The role of two PRC2 complexes in mammalian cells was extensively studied in the model of myogenic differentiation. The PRC2 complex is essential for maintaining the repressive state of the muscle specific genes (Stojic et al., 2011).

Indeed, during myogenic differentiation, the decrease of EZH2 expression is concomitant with the decrease of the H3K27 methylation; while the levels of EZH1 increase during this process (Caretti et al., 2004; Juan et al., 2009). Moreover, EZH1 is required for the recruitment of the myogenic transcription factor MyoD and Pol II to the early myogenic differentiation gene MyoG (myogenin). In line with these findings, the knockdown of EZH1 inhibits muscle differentiation (Stojic et al., 2011). These findings suggest that EZH1 might have a role in transcriptional activation. Indeed, the study of the global occupancy of EZH1 showed that it co-localizes with transcriptionally active chromatin: H3K4 trimethylation, Poll II occupancy and mRNA production (Mousavi et al., 2012). Of note, the catalytic activity of the EZH1 was shown to be required for normal myogenesis. These findings suggest that EZH1 and EZH2 may play distinct but overlapping roles in transcriptional regulation and maintenance of gene repression (Margueron et al., 2008).

The EED subunit of the PRC2 complex plays a role in the integration of the components of the complex and is required for the recruitment of PRC2 to chromatin. It also seems to play a role in the allosteric activation of the histone methyltransferase activity of EZH2 and the H3K27 methylation mark propagation (Margueron et al., 2009). The knockout of EED leads to the destabilisation of the other components of the complex (Chamberlain et al., 2008). EED also plays a role in the trans-generational propagation of the H3K27 di- and trimethylation marks during the S phase of the cell cycle. The EED recruits the PRC2 complex to the replication fork and promote DNA synthesis-assisted methylation of the newly-incorporated nucleosomes. This is achieved by the PRC2 subunits EZH2 and EED's ability to recognise its own H3K27 methylation epigenetic mark. In

respect to EED, it was shown that the WD40 repeats of the EED form an aromatic cage around the H3K27 methylated mark and is required for the propagation of the repressive chromatin state (Hansen et al., 2008; Margueron et al., 2009). A recent study has shown an intriguing role for EED as an integral subunit of both the PRC2 and the PRC1 complexes. EED was shown to be required for the H3K27 trimethylation as well as for the ubiquitin ligase activity of the PRC1 (Cao et al., 2014).

Although the histone H3K27 trimethylation is considered the main product of PRC2, some non-histone substrates where also described. For example, EZH2 was shown to methylate the cardiac specific transcription factor GATA4 on lysine 299 and attenuate its transcriptional activity by reducing its ability to recruit the p300 acetyltransferase (He et al., 2012). Although in this case, EZH2 activity also promoted gene repression independent of its H3K27 methyltransferase activity. Another study suggests that EZH2 function, at least following its deregulation in disease, may not always be connected with the PRC2 complex (Xu et al., 2012). Moreover, the PRC2 and H3K27 trimethylation-independent function of EZH2 correlates with gene activation. EZH2 interacts with the androgen receptor (AR) and promotes its agonist-independent transcriptional activity in castration-resistant prostate cancer (CRPC) (Xu et al., 2012). Notably the AR/EZH2 interaction is dependent on phosphorylation of EZH2 on Ser 21 by Akt, and links the oncogenic PI3K-Akt signaling pathway to the regulation of gene expression by AR (Xu et al., 2012). These findings suggest that EZH2, in different contexts, may also target substrates other than the H3K27 and be involved in gene activation.

The unconventional role of the PRC2 complex may also include DNA double-strand break (DSB) repair. EZH2 was identified in a screen designed to identify novel DSB response molecules, and is enriched at the sites of IRIF (Ionizing Radiation Induced Foci) along with its catalytic product trimethylated H3K27 (Chou et al., 2010). The exact role of PRC2 in this process is unclear since chromatin at IRIF is considered to be in a more relaxed state as a consequence of DSB repair factors recruitment (Qin and Parthun, 2002; Yu et al., 2005).

Polycomb repressive complex 1 (PRC1)

Drosophila PRC1 complex usually contains the following components in more or less stoichiometric amounts: the founding member of the PcG proteins *Polycomb (Pc), Sex Comb Extra (Sce* or *RING), Posterior Sex Combs (PSC), Polyhomeotic (Ph)* and *Sex Comb on Midleg (Scm)* (Kennison, 1995).

In mammalian species, each of these proteins has multiple homologs. There are three homologs of the *Drosophila Ph* in humans: PH1, PH2, and PH3 and two homologs of *Drosophila Sce*: Ring1B and Ring1A. The six mammalian homologs of *PSC* are termed the PcG RING fingers (PcGFs). These include Bmi-1, the most characterised cofactor, as well as its paralogs MBLR (Mel18 and Bmi1-like RING finger protein), MEL18 and NSPC1 (nervous system Pc1). The *Drosophila Pc* homologs in mammals are represented by the multiple homologs of the Chromobox proteins (Cbx) proteins that usually recognise the PRC2 catalyzed epigenetic mark di- or trimethylated H3K27. *Pc*/Cbx proteins seem to have specific functions such as maintenance of stem cell pluripotency or coordinating lineage commitment (Lanzuolo and Orlando, 2012).

The main catalytic function of the PRC1 complexes is the ubiquitin E3 ligase activity towards the C-terminal histone H2A tail at the position K119 (K118 in *Drosophila*). This activity usually attributed to the core PRC1 subunits Ring1B and Bmi-1 or its paralogs. The crucial N-terminal RING domain engages the ubiquitin charged E2 conjugating enzyme UbcH5c and promotes H2A ubiquitination (Bentley et al., 2011). Ring1B is able to directly ubiquitinate H2A *in vitro*, although its activity is dramatically enhanced by Bmi-1, which is also required for optimal Ring1B activity *in vivo*. The Bmi-1 subunit of the PRC1 also contains a RING domain but is devoid of catalytic activity. Similarly to other double RING ligase complexes, Bmi-1 and Ring1B form a heterodimer complex through their cognate RING domains. The unique basic patch on the Ring1B/Bmi-1 heterodimer promotes direct recognition of the nucleosomal DNA (Bentley et al., 2011). Moreover, a single basic residue (K93) in the RING finger of Ring1B is also required for DNA recognition and ligase activity of the Ring1B/Bmi-1 complex (Mattiroli et al., 2012).

The ubiquitin ligase activity of the PRC1 complex is crucial for the execution of its repressive function and mutation of the RING domain of the Ring1B results in gene derepression despite persistent promoter H3K27 trimethylation (Endoh et al., 2012; Scheuermann et al., 2010; Trojer et al., 2011). The exact mechanism of ubiquitin H2A-mediated repression is unclear, as direct physical changes in the chromatin structure were also observed in PRC1 E3 activity-independent manner (Eskeland et al., 2010; Grau et al., 2011). Nonetheless, the ubiquitinated H2A mark acts as inhibitory signal towards Pol II-mediated transcription initiation by competing with MLL complex mediated di- and tri-methylation of H3 K4 (Nakagawa et al., 2008).

The ubiquitinated H2A appears to be also required for the maintenance of the bivalent chromatin domains (containing the repressive and activation histone marks) in embryonic stem cell. This mechanism appears to stabilize the poised state of the initiated (Ser5 phosphorylated) Pol II. Indeed, Ring1B knockout ES cells display a significant loss of the H2A ubiquitination on such loci, along with the Pol II release and elongation, which result in derepression of the bivalent genes (Stock et al., 2007). The PRC1 complex also participates in the maintenance of the inactivated X chromosome (Xi) (Fang et al., 2004). A high signal of H2A ubiquitination is detectible on the Barr body, and moreover the double Ring1B/Ring1A knockout cells display a loss of H2A ubiquitination on the Xi. Of note, both the PRC1 and PRC2 stably associate with Xi in Xist (X chromosome specific ncRNA)-dependent manner. Nonetheless, the Xi initiation does not seem to require any PcGs (de Napoles et al., 2004; Mak et al., 2002; Silva et al., 2003). Thus, the question about the function of PcGs at the Xi requires further investigations.

The role of H2A ubiquitination as a true epigenetic mark remains unclear. Although being very abundant (5-15% of total H2A), it seems to be erased with each cell division. Indeed the cells that enter the early stages of mitosis almost completely lose chromosomal H2A ubiquitination. This process seems to be inversely correlated with H3S10 phosphorylation, the well-known mitotic histone mark (Bradbury, 1992; Joo et al., 2007; Mueller et al., 1985). The H2A ubiquitination levels are restored immediately after nuclear envelop reestablishment. In *Drosophila* cells, the PSC (PcGFs in human) subunit of the

PRC1 complex remains chromatin-bound throughout DNA replication *in vitro*, indicating that it may be involved in the restoration of the ubiquitin H2A at their proper genomic loci (Francis et al., 2009).

The removal of ubiquitin from H2A also requires a specific and well-controlled deubiquitination reaction. The ever-growing army of DUBs for H2A suggests that this process may be ensured by several enzymes depending on the physiological context, although some overlapping roles might exist (Hammond-Martel et al., 2012).

The primary signals for PRC1 recruitment and H2A ubiquitination remain to be fully defined, and may be ensured by multiple non-overlapping factors. For instance, a role in PRC1 recruitment was attributed to the product of the catalytic activity of the PRC2 complex: the repressive epigenetic mark trimethylated H3K27. Indeed the CBX (*Pc*) PRC1 subunits display the ability to bind trimethyl-H3K27. It was suggested that the PRC1 recruitment and activity is guided and dependent on the PRC2 H3K27 trimethylation as a priming epigenetic mark (Boyer et al., 2006; Cao et al., 2002; Wang et al., 2004). However, this role of the PRC2 in respect to the PRC1 was put to question by several recent studies. Indeed, the EED (the nonanalytic subunit of the PRC2) knockout cells still maintain a significant level of H2A ubiquitination despite the complete loss of trimethylated H3K27. The recruitment of the PRC1 as well as H2A ubiquitination levels at the Xi was independent of the PRC2 (Schoeftner et al., 2006). PRC2-independent H2A ubiquitination was also attributed to the RYBP and YAF2 subtype of the PRC1 complexes. These PRC1 complexes are devoid of the CBX subunit and promote the RYBP/YAF2-dependent, but the trimethyl-H3K27-independent, recruitment of the Ring1B to chromatin and subsequent H2A ubiquitination (Tavares et al., 2012; Wilkinson et al., 2010). Another study describes the atypical PRC1 complex (dRAF in Drosophila also part of the BCOR complex) containing the H3K36me2 demethylase Fbxl10/Kdm2b that appears to be also required for the maintenance of global H2A ubiquitination. The Fbxl10/Kdm2b recruits the Ring1B/NSPC1 ligase complex to CpG islands containing promoters with subsequent H2A ubiquitination (Wu et al., 2013). These results indicate that the non-constitutive components of the complex may contribute significantly to PRC1-mediated repression.

It is noteworthy to point that PRC1 also displays H2A ubiquitination-independent effect on chromatin. *In vitro,* the purified PRC1 complexes promote condensation of the nucleosomal arrays independently of their histone tails and ubiquitination. Furthermore, a study using Ring1B knockout fibroblasts showed that the Ring1B RING domain mutant, unable to interact with E2-conjugating enzyme, was able to restore chromatin condensation and *Hox* gene repression without an increase in H2A ubiquitination (Eskeland et al., 2010; Grau et al., 2011). These results indicate that PRC1 may execute its function through multiple mechanisms that also include a direct effect on chromatin structure. It would be interesting to define the exact mechanism underlying such H2A ubiquitination-independent effect of PRC1.

The catalytic core of the PRC1 can be found in other repressive complexes such as PRC1L4, dRAF, BCOR and E2F6 com. (Gearhart et al., 2006; Lagarou et al., 2008; Ogawa et al., 2002; Trojer et al., 2011). The selective assembly of the different sub-complexes around the Ring1B/PcGF core result in distinct and overlapping roles in gene repression. The dRAF and BCOR seem to share common subunits including the H3K36me2 demethylase Fbxl10/KDM2B and Ring1B/NSPC1 and establish the crosstalk between the H3K36me2 demethylation and histone ubiquitination. The BCOR complex was also shown to be important for BCL6-mediated gene repression (Gearhart et al., 2006; Lagarou et al., 2008).

The complex formed by the cell cycle regulator and transcription factor E2F6, in addition to the core Ring1B/PcGF contains the Myc oncogene regulatory factors such as Max and MGA as well as heterochromatin factors including HP1ϒ and the methyltransferases G9a and GLP. The methyltransferase activity of the G9a/GLP targets H3K9 for di-methylation and promotes the repression of the Myc-responsive genes in G0 cells (Ogawa et al., 2002).

While being a major transcription regulation complex, the PRC1 also appears to function in other chromatin-associated processes, and was suggested to be important for DNA double strand break repair (DSB). Indeed, the components of the PRC1 complex can be recruited to the sites of the DSB and promote the ubiquitination of the histones H2A and

its variant H2AX. This activity of PRC1 is also required for efficient DSB repair and cell survival following genotoxic stress (Gieni et al., 2011; Ismail et al., 2010). The exact function of the H2A/H2AX ubiquitination in DSB repair remains unclear, especially with respect to the ubiquitin ligase activity of the major DSB response E3 ligases RNF8 and RNF168, which catalyze the ubiquitination of H2A on K13/K15 sites (Mattiroli et al., 2012). It would be interesting to define the role and the crosstalk between the two modifications in DSB signaling and repair.

Chromatin recruitment of PcGs

The PRC1 and PRC2 are usually considered not to possess sequence-specific DNA binding activities. This raises the question of how these complexes being targeted to genomic loci to execute their gene repressive roles? Previous studies in *Drosophila* revealed a subset of specific DNA elements called the PcG responsive elements (PRE) (Lanzuolo and Orlando, 2012). The deletion of the PRE elements from the *Hox* locus causes homeotic transformation. Moreover, the insertion of these elements in other unrelated genomic regions promotes PcG recruitment and gene repression. The non-catalytic components of the PcG complexes were also suggested to play a role in their recruitment to chromatin. For example, the ESC-Nurf55 module of the PRC2 complex is the minimal histone-binding element required for histone binding and the HMT activity of the PRC2 (Nekrasov et al., 2007; Yao et al., 2008).

Nonetheless, other studies have shown that the PRE itself is nucleosome-depleted and that the nucleosomes are dynamically evicted and replaced from these regions suggesting that the nucleosomal context is not sufficient/required for the recruitment of PcG complexes (Muller and Kassis, 2006). The Pho protein (Yin Yang1 (YY1) in mammals) is the only PcG member with distinct DNA sequence specificity towards the PRE (Lanzuolo and Orlando, 2012; Shi et al., 1997). Indeed, Pho was found to co-occupy most of the PRE regions with the PRC1 and PRC2 complexes and was shown to interact

with these elements *in vitro* (Xi et al., 2007). On the other hand, other studies suggested that Pho and PhoRC (Pho repressive complex) were not sufficient to promote the recruitment of PcG and were often recruited to chromatin sites that were distinct from those occupied by PRC1 and PRC2 (Dejardin et al., 2005).

The PRE elements in mammals are even less studied. The few elements identified so far are represented by the PRE-kr sequence that can repress the *MafB-Kreisler* locus by recruiting the PRC1 and PRC2 complexes (Sing et al., 2009). The other PRE-like sequence was identified in the HOXD cluster between the HOXD11 and the HOXD12 named the D11.12. It represents a 1.8 kb GC rich DNA sequence capable of inducing the heritable gene repression of the reporter gene. Notably, the D11.12 element incorporates the YY1 binding sequences that were required for repression, indicating the importance of this transcription factor binding for the recruitment of PcG complexes (Woo et al., 2010). Although, the exact mechanisms of PcG recruitment in mammalian cells remain to be defined, the higher order chromatin structure also seems to play an important role. The PcG repressive chromatin is often organised in so-called polycomb bodies and represents a condensed areas of chromatin containing the repressive chromatin marks. Notably, the *Hox* gene cluster can be dynamically associated and displaced from such regions. Indeed, during murine embryogenesis, cells with the repressed *Ho*x cluster are incorporated within the transcriptionally inactive PcG bodies. On the contrary, the activated *Hox* clusters leave the PcG bodies and acquire active chromatin marks (Noordermeer et al., 2011).

The recent discovery of the new PRC complex termed the PR-DUB (BAP1 complex in mammals) raises more questions and possibilities for the mechanism of PcG repression. The PR-DUB in *Drosophila* consists of the deubiquitinating enzyme *Calypso* (BAP1 in mammals) and the polycomb group protein *ASX* (ASXL1, ASXL2, ASXL3 in mammals) (Scheuermann et al., 2010). On the other hand, the mammalian BAP1 complex seems to incorporate additional components such as HCF-1 and OGT and a subset of transcription factors (described below) (Carbone et al., 2013; Sowa et al., 2009; Yu et al., 2010). The deubiquitinase ability of the PR-DUB complex towards ubiquitinated H2A K118 (K119 in mammals) indicates its opposing role towards PRC1 and is thus expected to act as a

transcriptional activator. Nonetheless, the PR-DUB is required for proper *Hox* repression and morphogenesis (Scheuermann et al., 2010). This notion indicates that the dynamic ubiquitination/deubiquitination is required for the PcG induced gene repression, and that the repressed chromatin may be more dynamic than currently appreciated.

Ubiquitin proteasome system

Before the discovery of the ubiquitin-proteasome system (UPS), the only known energy-dependent intracellular protein degradation system was the lysosome. It encompasses a membrane containing hydrolytic enzymes for digestion of the content of phagocytic and pinocytic vesicles for the purpose of generating metabolites and ensuring immune protection (Varshavsky, 2006; Wilkinson, 2005). Although extremely important, this system is highly unspecific and degrades most biopolymers that are trapped within the endocytic vesicles. The notion of both energy dependent and specific protein targeting machinery was elusive until the second half of the 20th century. It was also counterintuitive at that time, that the cell would spend its energy on the destruction of its own proteins. The process of degradation was widely accepted to be passive and moreover, most intracellular proteins were considered to be long-lived (Varshavsky, 2006). It wasn't until the late 1970s that the work by Aaron Ciechanover, Irwin Rose, Avram Hershko and others first described the ATP dependent and ubiquitous pathway of protein degradation by the UPS (Wilkinson, 2005).

Ubiquitination represents the attachment of a 76 AA protein modifier named ubiquitin to the target proteins, which results in their degradation by the cellular protein recycling factory: the proteasome. This classical function of ubiquitination is one of the best studied. Nonetheless, numerous and highly diverse functions of ubiquitination including non-degradative signaling events that can regulate a plethora of cellular functions

were uncovered during the last decade (Geng et al., 2012; Hammond-Martel et al., 2012; Nakayama and Nakayama, 2006; Pickart, 2004).

Protein conjugation, by small protein modifiers, is usual characteristic of eukaryotic cells and is achieved by highly hierarchical and complex biochemical cascades that result in protein post-translational modification. These small protein modifiers include the small ubiquitin like modifier (SUMO), neural precursor cell expressed, developmentally down-regulated 8 (NEDD8), interferon-induced 15 kDa protein (ISG15), autophagy-related protein 8 (ATG8) and ubiquitin-related modifier 1 (URM1) (Kerscher et al., 2006; van der Veen and Ploegh, 2012). These protein conjugation systems regulate diverse and sometimes highly specialized cellular functions. For instance, ATG8 regulates the autophagy pathway (Boya et al., 2013) and the ISG15 regulates the antiviral immune response (Zhao et al., 2013). Here I will focus on protein ubiquitination, as it is most relevant to my work.

Conjugation of ubiquitin to their corresponding substrates is a multistep process that usually requires at least three types of enzymes. The cascade begins when the ubiquitin activating enzyme (E1 also known as UBA1). The E1 is responsible for the first two steps of the process. The E1 catalyzes the activation of ubiquitin by the ATP hydrolysis-dependent adenylation of the ubiquitin C-terminal glycine 76 (G76). The intermediate ubiquitin-adenylate is quickly hydrolysed with the release of free ADP and the formation of ubiquitin-E1 thioester (or charged E1) on the conserved cysteine (C632) of the E1. The next step of the reaction requires the ubiquitin-conjugating enzyme (ubiquitin carrier) (E2). The charged E1 interacts with the E2 and transfers the ubiquitin moiety to the catalytic cysteine on the E2 molecule and this results in the formation of the E2-ubiquitin thioester (or charged E2) (Lee and Schindelin, 2008). The charged E2 is than recruited to the substrate protein with the assistance of the ubiquitin ligase (E3). Depending on the E3 type it may directly participate in the reaction and form an intermediate ubiquitin-E3 thioester (in case of HECT domain E3s) that subsequently discharges the ubiquitin to the ε-amino group of lysine residue of the target protein (Rotin and Kumar, 2009). Otherwise the E3 may act as an adapter between the substrate and the charged E2 (RING and U-box domain

E3s) to promote the transfer of the ubiquitin to the lysine residue of the substrate (Deshaies and Joazeiro, 2009).

Since ubiquitin contains seven lysine residues, it may also be targeted by ubiquitination, resulting in the formation of ubiquitin polymers and thus in substrate polyubiquitination. Depending on the type of chain, polyubiquitination might have different outcomes for the protein substrate. For example lysine 48 (K48)-linked chain attachment will typically result in proteasomal degradation of the target protein (Finley, 2009).

Proteasome is highly conserved multisubunit and ATP-dependent protease complex that specifically targets the proteins marked for degradation. Proteasome is a 2.5 MDa complex that can be functionally and structurally divided into several sub-complexes. The catalytic core particle (CP or 20S subunit) is cylindrical structure that consists of four seven-subunit rings, with two in the middle encompassing three different proteases. The proteases of the CP belong to unique N-terminal nucleophile type of hydrolases and contain one amino-terminal threonine as a single catalytic site. Each protease catalyzes different types of proteolytic reactions with trypsin-like (β2), caspase-like (β1) and hydrophobic residue-targeting (β5) activities. The catalytic centers of the CP subunits face the internal space of the catalytic chamber ensuring the specificity of the reaction toward proteins that were actively brought into the proteasome. The CP proteases with various substrate preferences ensure that proteins reaching the catalytic chamber are efficiently cleaved into small peptides of 6-10 amino acid residues (Finley, 2009; Tomko and Hochstrasser, 2013).

The regulatory particle (RP or 19S subunit) consists of 19 different protein subunits with multiple functions including the six subunits of the AAA type ATPases. One of the main functions of the RP is the ATP-dependent unfolding and translocation of the ubiquitinated protein into the CP. The other important role of the RP include the recognition and recruitment of polyubiquitinated substrates through the ubiquitin receptors and the regulation of the opening of the CP substrate channel, which can be opened only upon the recruitment of the RP complex. The RP also ensures ubiquitin recycling prior to substrate degradation (Finley, 2009).

The protein degradation function of the ubiquitination is essential, indeed the K48 residue of ubiquitin is the only lysine absolutely essential for viability in yeast. Other lysine residues of ubiquitin do not seem to affect viability although the K63 residue is required for the proper response to genotoxic stress (Kolas et al., 2007; Mailand et al., 2007; Stewart et al., 2009; Zhao et al., 2007).

K63-linked chains do not usually promote protein degradation by the proteasome, but are rather involved in signaling processes such as promoting protein translocation or complex assembly. The role and the mechanism of formation of other ubiquitin chains (i.e. K6, K11, K27, K33) or the mixed type and branched chains are much less studied although some regulatory roles for these chains in protein degradation and signaling have been proposed (Kulathu and Komander, 2012).

Ubiquitination is one of the most complex post-translational protein modifications in the cell. The ubiquitination cascade is highly hierarchical, with each step of the process contributing to the specificity and diversity of the outcome signal. The relatively general activating step by E1 supplies the flow of the ubiquitin into the cascade and is represented by only two known enzymes UBA1 and UBA6 (Jin et al., 2007). The E2 enzymes represented by 39 known genes in the human genome play the role of the chain architects and are responsible for the processivity of the reaction and type of chain being build (van Wijk and Timmers, 2010). The E2s also differ in their ability to form chains, with one type acting as priming enzymes, e.g. UBCH5 (Wu et al., 2010) to promote monoubiquitination (adding the first ubiquitin on the substrate) and other type being responsible for chain extension via specific linkages e.g. Cdc34, UBC13/MMS2 (Parker and Ulrich, 2009; Wu et al., 2010). The E3 enzymes, which comprise 600-1000 genes in the human genome represent the vast majority of the components of the ubiquitin system (Deshaies and Joazeiro, 2009; Rotin and Kumar, 2009). The reason for such diversity of the E3s might be explained by their function in substrate recognition. The E3s are responsible for the specificity in the ubiquitination process and often act as intermediate elements between the ubiquitin signaling and other regulatory modifications such as phosphorylation (Ravid and Hochstrasser, 2008). The E3 family is a highly diverse group of enzymes, which differ in

their complexity and domain composition and range from the relatively simple monomeric RING domain ligases to multicomponent ubiquitin ligase machineries such as SCF and APC/C complexes.

Deubiquitinating enzymes (DUBs)

Ubiquitination is a reversible process and a group of specialized proteases namely deubiquitinases (DUBs), are responsible for the removal of the ubiquitin from target proteins. The human genome encodes for at least 100 DUBs. During the recent years, numerous regulatory roles have been defined for the DUBs in counteracting E3 ligases, ubiquitin chain editing, ubiquitin maturation and recycling (Komander et al., 2009). Notably deregulation of numerous DUBs might be involved in several human illnesses such as neurodegeneration diseases, inflammation and malignant neoplasias (Carbone et al., 2013; Leonard et al., 2001; Tsou et al., 2013; Williams et al., 2011).

The DUBs superfamily of enzymes can be subdivided into several classes depending on the type of their catalytic domain. The DUBs that contain a cysteine in their catalytic domain can be classified as ubiquitin C-terminal hydrolases (UCH), ubiquitin specific proteases (USP), ovarian tumour proteases (OTU) and Machado-Josephin domain (MJD)-containing families. Only one class of enzymes of MNP+/JAMM family represents the metalloprotease DUBs that contain Zn^{2+} in their catalytic site.

The DUB superfamily of enzymes evolved multiple mechanisms to promote their specificity towards the isopeptide bond between the GG tail of the ubiquitin and the lysine of the target molecule. The specificity of the DUBs towards ubiquitin versus the UBLs can be explained by the nature of its C-terminal GG region and its neighbouring amino acid residues. Indeed, the unique sequence of LRLRGG in the ubiquitin is crucial for the DUB ability to hydrolyse the ubiquitin isopeptide bond (James et al., 2011). A recent study discovered that the single substitution of the leucine 73 to proline (UbL73P) generates

conjugation proficient ubiquitin resistant to hydrolysis by most DUBs (Bekes et al., 2013).

The relatively rigid structure of the ubiquitin fold makes it an ideal target for protein/protein interactions. For example, the hydrophobic patch around isoleucine 44 (I44) is crucial for the recognition by most DUBs and ubiquitin binding domains (UBDs) (Dikic et al., 2009; Komander et al., 2009). Nonetheless, some DUBs may display a dual specificity toward more than one UBL. For example, USP21 can cleave NEDD8 as well as the ubiquitin (Ye et al., 2011). Most of the DUBs are specific toward the isopeptide bond, but in some unique cases the DUB may possess the peptidase activity as well. USP1 was shown to promote its own autocatalytic cleavage. The USP1 is able to bind and promote the removal of the N-terminal UBL domain. In this case the USP catalytic domain of the DUB recognises the LLGG motif within the protein that mimics the C-terminus of the ubiquitin (Huang et al., 2006).

DUBs display different degrees of specificity toward ubiquitin chains as linkage specific DUBs recognise particular polyubiquitin chain. For example, the JAMM/MNP+ family DUBs display high degree of specificity towards the K63 linked chains and most members of this family where shown to target this type of polyubiquitin. This includes the proteasome-associated DUB POH1, the DSB repair-associated DUB, BRCC36 and the endocytosis regulators, AMSH and AMSH-LP (Cooper et al., 2009; Sato et al., 2008). The crystal structure of AMSH-LP shed light on the mechanism of recognition and proteolysis of K63 chains by this DUB. The JAMM/MNP+ domain engages in interactions with the proximal and the distal ubiquitin molecules. Notably, the interaction also involves the recognition of the K63 isopeptide bond itself (Cooper et al., 2009; Sato et al., 2008). The K48 specific DUBs are represented by the proteasome-associated USP14 and the OTU family DUBs such as OTUB1 (Hu et al., 2005; Mevissen et al., 2013). Of note, there are several modes of recognition of the ubiquitin chains by DUBs that result in an exo- (the proximal or the distal ubiquitin moieties are recognised) or endo-catalytic (the enzyme recognises internal ubiquitin moieties) activities (Komander et al., 2009). For example, USP14 is considered a typical exo-catalytic DUB and can generate free ubiquitin by binding and deubiquitinating specifically the distal ubiquitin moiety (Hu et al., 2005). A

unique mode of polyubiquitin chain recognition is displayed by USP5 (IsoT) whereby the UBP-ZnF domain of this DUB engages in the interaction with ubiquitin in its C-terminal region. Thus, only unanchored ubiquitin chains can be recognised and cleaved allowing the cleavage of both the K48 and K63 chains (Reyes-Turcu et al., 2006). This function of USP5 allows the recycling of free ubiquitin, as mutations in the yeast ortholog of USP5, Ubp6, induce proteasomal protein degradation defects due to the depletion of the free ubiquitin pool (Amerik et al., 1997; Hanna et al., 2007). The endo- type catalytic activity is displayed by numerous DUBs (e.g., AMSH-LP, CYLD, USP8 and USP9X). The endo- and exo- activity modes of specific DUBs might result in the generation of monoubiquitinated substrates. Although much less is known about the removal of the last monoubiquitin moiety from substrates, it is possible that it can be further processed by additional DUBs. For example the UCH family DUBs (BAP1 and UCH37) are suggested to remove the proximal ubiquitin in monoubiquitinated substrates (Johnston et al., 1999). On the other hand monoubiquitinated substrates can be subjected to ubiquitin chain extension by ubiquitin E3 (or E4) ligases (Liu et al., 2010). The coordinated action of the DUB and the E3 in this process may result in ubiquitin chain type switching. For instance, a switch from non-degradative K63 chains to degradative K48 signal is exemplified by the action of the E3/DUB hybrid A20 (Wertz et al., 2004).

In addition to deubiquitinating specific substrates, several other general functions of the DUBs were described. These include the maturation of the ubiquitin precursor to yield the functional ubiquitin, recycling of the ubiquitin upon protein degradation, counteracting and regulating the E2 and E3 enzyme activities as well as ubiquitin chain editing/trimming.

The ubiquitin is translated as precursor from several genes. These include the UBC, UBB, UBA52 and UBA80 that are fused as a linear ubiquitin chain or to the ribosomal proteins (L40 and S27a). It remains to be defined which DUBs are responsible for the maturation of ubiquitin (Kimura and Tanaka, 2010).

The deubiquitinating enzyme BAP1 as a core subunit of a multiprotein chromatin-modifying complex

BAP1 (BRCA1 associated protein 1) belongs to the superfamily of the deubiquitinating enzymes (DUBs) and more specifically to the ubiquitin C-terminal hydrolase (UCH) family of cysteine proteases. It was first identified as an interacting partner of BRCA1 (Breast cancer-associated 1). This pioneering study showed that it interacts with the RING domain of BRCA1 by the means of its C- terminal region. (Jensen et al., 1998). This study also showed that BAP1 was mutated in several cases of lung cancer and was able to enhance the tumor suppression activity of BRCA1 in the breast cancer cell line MCF7. Interestingly the L691P mutation introduced at the C-terminus of BAP1 disrupted its interaction with BRCA1. Notably, BAP1 also interacts with BARD1, a major partner of BRCA1 partner. Interestingly, the interaction region in BAP1 is located on the opposite side of the protein closer to the UCH domain (AA 182-365) (Nishikawa et al., 2009). To date the significance of BAP1 interaction with BRCA1/BARD1 remains unclear, although one study indicated that BAP1 interfere with BRCA1/BARD1 ubiquitin ligase activity *in vitro* by disrupting the proper heterodimer formation (Nishikawa et al., 2009). This effect of BAP1 was independent of its catalytic activity. Of note, this study remains controversial since it predicts a negative role of BAP1 in the regulation of DNA double strand break (DSB) repair by homologous recombination, which appears to requires BRCA1/BARD1 activity (Ohta et al., 2011). Studies by our group indicate the opposite; the inhibition of BAP1 impaired proper HR and interfered with RAD51 and BRCA1 recruitment to DSB sites (Yu et al., 2014).

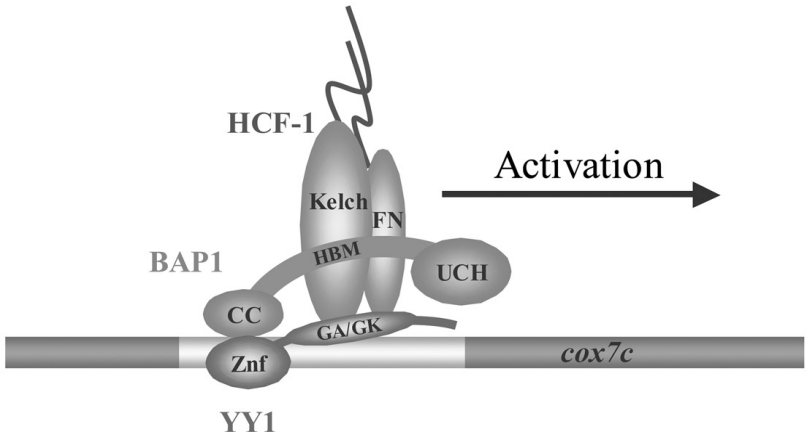

Figure 3. Model representing the recruitment of BAP1 and HCF-1 to the *cox7c* promoter by the transcription factor YY1(Yu et al., 2010).

Recent studies showed that BAP1 is involved in transcription regulation, tumor suppression and development (Abdel-Wahab and Dey, 2013; Dey et al., 2012; Harbour et al., 2010; Je et al., 2012; Machida et al., 2009; Misaghi et al., 2009; Scheuermann et al., 2010; Testa et al., 2011; Ventii et al., 2008; Yu et al., 2010). The first studies by our group and others (Machida et al., 2009; Misaghi et al., 2009; Sowa et al., 2009; Yu et al., 2010) showed that BAP1 nucleates multiprotein complexes with average molecular weight around 1.6 MDa, that composed of numerous transcription and chromatin regulators (Yu et al., 2010). Tandem affinity purification (TAP)/Mas spectrometry (MS) analysis revealed stoichiometric (according to gel staining and semiquantitative analysis of MS peptides) interaction partners of BAP1 along with substoichiometric components. Highly abundant components of the complex are represented by the chromatin-associated protein Host Cell Factor-1 (HCF-1), polycomb group proteins additional sex combs like 1 and 2 (ASXL1/2), histone demethylase KDM1B (LSD2), O-linked N-acetylglucosamine transferase (OGT), forkhead transcription factors FOXK1/FOXK2 and histone acetyl transferase 1 (HAT1) (Machida et al., 2009; Misaghi et al., 2009; Sowa et al., 2009; Yu et al., 2010). Less abundant but consistently recovered components were identified as polycomb group protein

and the zinc finger transcription factor Yin Yang1 (YY1), and the atypical ubiquitin carrier UBE2O (Sowa et al., 2009; Yu et al., 2010).

The overall composition of the BAP1 complex suggests its major involvement in the regulation of the chromatin landscape by multiple mechanisms. These include a potential role of the BAP1 complex as a writer of chromatin modifications by OGT and HAT1 (O-GlcNAcylation and acetylation of histones, respectively), a chromatin mark reader by ASXL1/2 (presence of PHD motifs that bind methylated lysine residues) and a chromatin modification eraser by BAP1 and LSD2 (deubiquitination and demethylation of histones) (Sowa et al., 2009; Yu et al., 2010).

Our group showed that BAP1 is implicated in transcriptional regulation and forms a ternary complex with the transcription cofactor HCF-1 and the transcription factor YY1. BAP1 forms a tight complex with HCF-1 through its HCF-1 binding motif (HBM motif, see also below). Indeed, immunodepletion studies showed that all the cellular pool of BAP1 is associated with HCF-1, although only a fraction of total HCF-1 was complexed with BAP1, which is not surprising taking into account that HCF-1 is a highly abundant chromatin-associated protein. The interaction of BAP1 with YY1 is transient, but this transcription factor was recoverable in the co-IP experiments. In addition, we showed that YY1 and HCF-1 directly interact with BAP1 through non-overlapping protein regions. Interestingly the loss of the HCF-1 interaction with BAP1 by the deletion of the HBM motif resulted in a decreased abundance of the YY1 in the complex. This result indicates that, although a direct interaction occurs between BAP1 and YY1, high affinity HCF-1 binding is required to stabilize the ternary complex. Importantly, we showed that BAP1 was able to promote transcription activation through its DUB activity, since the catalytic dead C91S mutant failed to do so (Yu et al., 2010).

To define the BAP1-dependent transcriptome, we performed mRNA expression microarray analysis in the condition of BAP1 depletion by RNAi. Numerous genes were deregulated following the loss of BAP1, including genes involved in cell cycle regulation, DNA damage response, cell survival and apoptosis as well as cell metabolism (Yu et al., 2010). This result suggests that the BAP1 complex is involved in the transcription

regulation of numerous aspects of cell physiology. To further characterize the role of BAP1 in transcription, we used one of the genes strongly down regulated following BAP1 depletion. The *Cox7c* encodes for one subunit of the holoenzyme that mediates the terminal step of the mitochondrial electron transport chain. Since it was known that YY1 is involved in the regulation of multiple aspects of the cell metabolism (Blattler et al., 2012) including the expression of *Cox7c*, we analyzed the role of the BAP1 complex in the regulation of this gene. The RNAi mediated depletion of BAP1 or HCF-1 resulted in the down regulation of *Cox7c* protein level. On the other hand, the knockdown of YY1 resulted in the activation of *Cox7c* expression (Figure 3). The RNAi-mediated down regulation of YY1 also reduced the abundance of the BAP1 and HCF-1 on the *Cox7c* promoter region, indicating that YY1 plays the role of the recruiting factor for the BAP1/HCF-1 complex to regulate transcription (Yu et al., 2010).

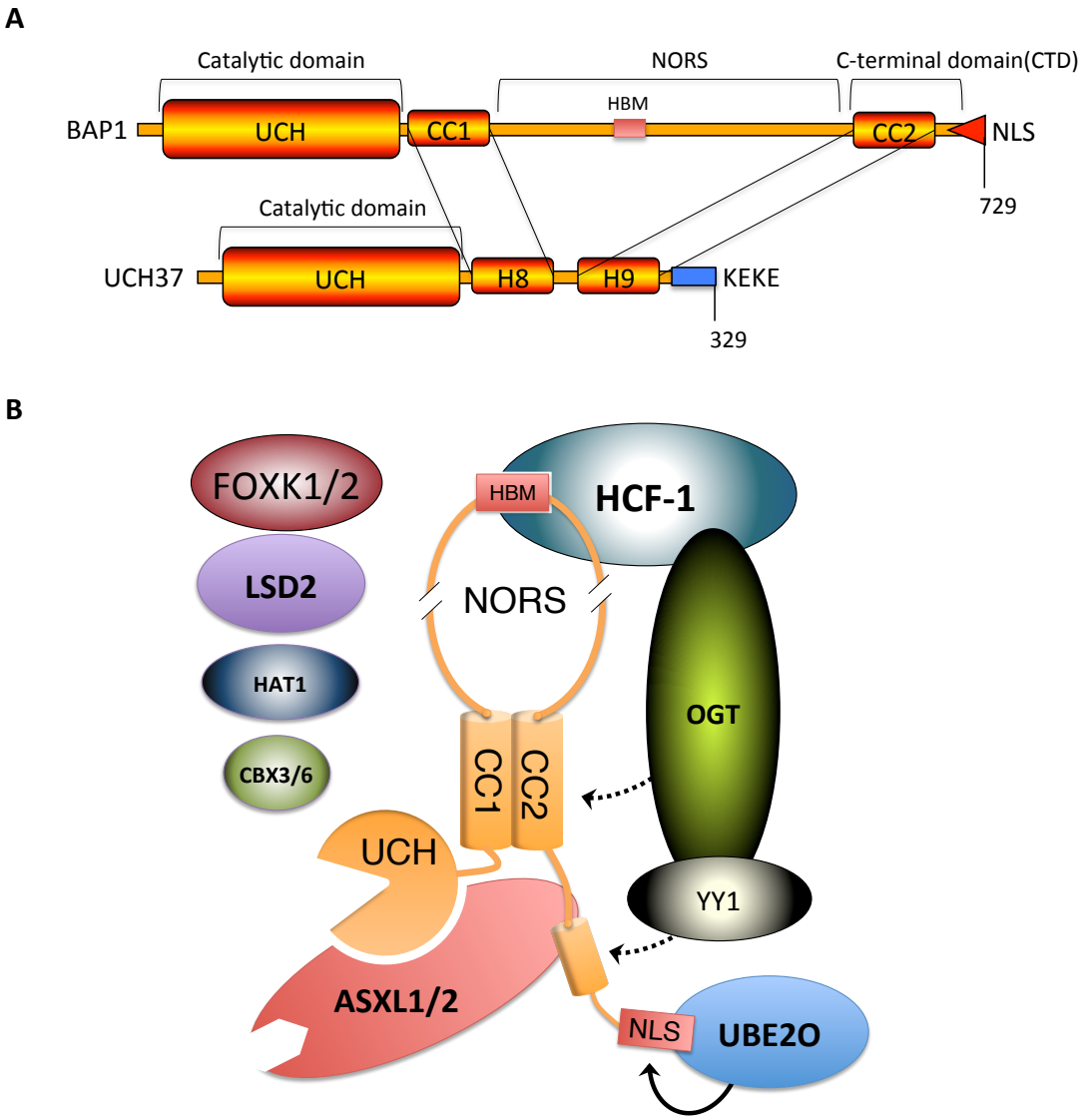

Figure 4. **Schematic representation of BAP1 and its multiprotein complex. A)** Comparison of human BAP1 and UCH37. **B)** Inventory of the components of the BAP1 complex. Dashed arrows indicate low affinity interactions. The binding regions of FOXK1/2, LSD2, HAT1 and CBX factors are unknown.

Of note, the BAP1 complex analysis recovered several other transcription factors such as FOXK1/2, NRF-1, the ETS family transcription factors Elf-1, Elf-2 and Elf-3 (Yu et al., 2010) (and unpublished data from our laboratory). These sequence specific DNA binding transcription factors may play major roles in coordinating the recruitment of the BAP1 complex to gene promoter regions as we described for YY1.

BAP1 as a tumor suppressor in multiple hereditary and sporadic cancers

The work during the recent years has defined BAP1 as a major tumour suppressor mutated and inactivated in numerous sporadic and hereditary cancers (Carbone et al., 2013).

The first studies on BAP1 showed that it is mutated in lung cancer (Jensen et al., 1998). The subsequent study showed a prevalence of BAP1 homozygous mutations and loss (84%) in the rare melanoma of the eye (involving iris, ciliary body, or choroid or collectively uvea). In the same study, the authors showed that siRNA-mediated knockdown of BAP1 in melanoma cell lines promoted morphological changes similar to metastatic melanomas. Notably, the mRNA expression profiling of the BAP1-depleted cells revealed the upregulation of genes implicated in cell invasion such as CDH1 and the proto-oncogene KIT, which are often associated with aggressive invasive melanomas. On the other hand, the genes involved in the normal melanocyte differentiation such as neural crest migration gene ROBO1, and melanocyte differentiation genes CTNNB1, EDNRB and SOX10 were down-regulated. Therefore the loss of BAP1 may promote the acquisition of the characteristics of invasiveness associated with metastatic uveal melanoma (Harbour et al., 2010).

In a study aimed at identifying the genes that increase the risk of asbestos/erionite-induced mesotheliomas, BAP1 was found to be mutated in this cancer (Testa et al., 2011). The two families described in this study were characterized by germline heterozygous

mutations in the BAP1 gene, which results in the production of a truncated non-functional protein. Notably, the individuals from both families had high incidence of mesotheliomas, as well as other tumours such as uveal melanomas. Importantly, the tumour samples also showed the loss of the second allele of BAP1 (Testa et al., 2011). Interestingly, a high incidence of BAP1 mutations was also observed in sporadic cases of malignant pleural mesotheliomas (MPM) (Bott et al., 2011). The authors performed a copy number variation study in a subset of 53 cases of MPM using Comparative Genomic Hybridization array (CGH array). The data indicated that BAP1 was inactivated in 23% of tumor samples analyzed. Analysis of BAP1 gene in 25 MPM cell lines also revealed that 6 of them had BAP1 loss or mutations. The fact that a significant proportion of BAP1 mutations/deletions were heterozygous indicates that BAP1 may be a haploinsufficient tumor suppressor (Bott et al., 2011). BAP1 germline mutations were also found in familial cases of the atypical melanocytic tumor syndrome (Wiesner et al., 2011). The affected individuals developed multiple skin neoplasms that were highly heterogeneous in morphology and histopathology ranging from the epithelioid nevi to atypical melanocytic proliferation that showed overlapping features with melanoma. Some individuals also developed uveal and cutaneous melanomas. As in the case of MPM, the melanoma tumours showed the loss of the second BAP1 allele (Carbone et al., 2012; Wiesner et al., 2011).

BAP1 is also mutated in a subset of renal cell carcinoma (Pena-Llopis et al., 2012). In this study, BAP1 was also found to be a two hit tumour suppressor. The prevalence of BAP1 loss was 14% (24/176) (Pena-Llopis et al., 2012).

The role of BAP1 as a tumor suppressor in myeloid malignancies was recently suggested by the work using the BAP1 knockout mouse. Although the BAP1 constitutive knockout is early embryonic lethal, the creERT2 tamoxifen conditional knockout mice at adult age can be generated. The animals with BAP1 deletion developed severe anemia accompanied by myeloproliferative/myelodysplastic syndrome within 4 weeks after tamoxifen injections with features close to human myelodysplastic syndrome /chronic myelomonocytic leukemia (MDS/CMML), which was accompanied by ineffective

erythropoiesis and thrombopoiesis. The authors also found that BAP1 expression is significantly decreased in MDS patients compared to healthy controls (Dey et al., 2012).

The tumour-associated rearrangements in BAP1 locus range from the whole region deletion to point mutations. Indeed, the 3p21.1 chromosome cluster containing several genes is a known cancer hot spot (Ji et al., 2005). BAP1 is also subjected to mutations that induce frame shifts or in frame insertion/deletions and changes in splicing site. Point mutations result in amino acid substitutions or acquisition of stop codons (Abdel-Rahman et al., 2011; Carbone et al., 2013; Harbour et al., 2010; Pena-Llopis et al., 2012; Wadt et al., 2012; Wiesner et al., 2012; Wiesner et al., 2011; Yoshikawa et al., 2012). Point mutations are of particular interest for the determination of BAP1 mechanism of action and regulation, since they do not usually result in a drastic dysfunction of the protein, but rather reveal specific protein regions critical for its function. The amino acid substitutions and small in-frame deletions are thus of particular interest.

The most often and well characterized point mutations occur within the catalytic UCH domain of BAP1. They either affect the catalytic triad itself (C91, H169 and D184) or amino acids within its close vicinity (i.e. F81, A95, S172), thus resulting in the disruption or decrease of the BAP1 catalytic activity (Abdel-Rahman et al., 2011; Carbone et al., 2012; Carbone et al., 2013; Harbour et al., 2010; Pena-Llopis et al., 2012; Wadt et al., 2012; Wiesner et al., 2012; Wiesner et al., 2011; Yoshikawa et al., 2012). The second most mutated region is the C- terminus of BAP1 (C-terminal domain (CTD) and the Nuclear localization signal (NLS)). This region is highly conserved and point mutations here may affect the ability of BAP1 to form the multiprotein complex or its subcellular localization. For example the small in frame deletion of the 666-669 region (Harbour et al., 2010) completely abrogates BAP1 catalytic activity towards the ubiquitinated histone H2A by disrupting the interaction with ASXL1 and ASXL2 (Salima Daou et al., submitted). Another interesting subset of mutations occurred in the N-terminal part of the CTD (Figure 4) (Harbour et al., 2010). The nuclear localization was also shown to be crucial for BAP1 tumor suppression function (Ventii et al., 2008). Indeed, cancer-associated mutations often result in deletions of the NLS region of BAP1, inducing its cytoplasmic localization. In this

regard another subset of mutations, represented by small in frame deletions/insertions (Δ631-634 and Δ637-638InsN) induce BAP1 cytoplasmic sequestration. We found that this effect occurs through disrupted auto-deubiquitination activity of BAP1 towards its NLS region. Notably these mutations did not affect the BAP1 DUB activity towards its substrate, the ubiquitinated H2A. These results indicate that the loss of BAP1 tumour suppression function also occurs as a result of its aberrant subcellular localization (Mashtalir et al., 2014).

The effect of numerous mutations in BAP1 still remains to be determined, including multiple point mutations found in the middle (NORS) region of BAP1 (Figure 4). This region contains the HBM, which is important for the HCF-1 interaction with BAP1 (Machida et al., 2009; Yu et al., 2010). Interestingly, mutations of HBM were identified in renal carcinoma, resulting in loss of the BAP1/HCF-1 interaction and as a result loss of its antiproliferative activity (Pena-Llopis et al., 2012).

HCF-1 as an integrative platform for regulation of the chromatin landscape

Initial research on BAP1 function and mechanism of action focused on its interaction with the most abundant component of the complex: HCF-1. HCF-1 was first identified as a transcriptional cofactor of the herpes simplex virus-1 (HSV-1) transactivation factors VP16 and the cellular factor POU2F1, important for viral immediate early (IE) gene expression (Herr, 1998; Mahajan and Wilson, 2000; Wilson et al., 1993; Wysocka and Herr, 2003). Since then, HCF-1 was implicated in multiple cellular functions i.e. cell cycle progression, RNA splicing metabolism and circadian rhythm regulation (Ajuh et al., 2002; Ruan et al., 2012; Zhang et al., 2009).

Several functionally and structurally distinct regions can be defined in the HCF-1 protein sequence (See the results section). The N-terminal region of HCF-1 contains five repeats of β-propeller-like Kelch domain. This structure is crucial for the recruitment of

HCF-1 to specific transcription regulators that participate in protein/protein interactions with HCF-1 via the so-called HCF-1 binding motif (HBM). This short amino acid stretch represented by [E/D]-H-X-Y consensus comprised within numerous transcription factors and epigenetic regulators including HSV coactivator VP16, the transcription factors PGC-1, LZIP, E2F1/3/4, THAP1-4 and the deubiquitinase BAP1 (Freiman and Herr, 1997; Tyagi et al., 2007; Vercauteren et al., 2008; Wilson et al., 1993; Wilson et al., 1995; Yokoyama et al., 2004; Yu et al., 2010). Adjacent to the Kelch domain, HCF-1 contains a large basic domain implicated in protein/protein and intramolecular interactions and required for interactions with paired amphipathic helix protein SIN3A, the O-linked N-acetylglucosamine transferase OGT (Daou et al., 2011) and the transcription factors GABP2 (Vogel and Kristie, 2000b) and ZBTB17 (Piluso et al., 2002).Schema

The middle region of HCF-1 contains a unique proteolytic processing domain (PPD) involved in protein maturation and protein/protein interactions with transcription co-activator/co-repressor protein four-and-a-half LIM domain-2 (FHL2) and OGT (Daou et al., 2011; Vogel and Kristie, 2006). The C-terminal region of HCF-1 is comprised of the acidic region and a tandem of fibronectin type 3 domain: FN3-1 and FN3-2. The C-terminus of HCF-1 has been implicated in the interaction with protein phosphatase 1 (PP1) (Ajuh et al., 2000) and PDCD2, which acts as HCF-1 negative regulator and supresses its ability to promote cell proliferation (Scarr and Sharp, 2002).

HCF-1 is synthesized as a large (300kDa) precursor that is being quickly processed by limited proteolysis in its central PPD region (Vogel and Kristie, 2000a, 2006; Wilson et al., 1993; Wilson et al., 1995). The domain is composed of 8 reiterations of 20 amino acid residues, six of which (PPD1, 2,3, 5, 6, 8) can be proteolytically processed, yielding the N- and C- terminal fragments of different molecular weights (Vogel and Kristie, 2000a, 2006; Wilson et al., 1993; Wilson et al., 1995).

Following processing, the N- and C- terminal polypeptides of HCF-1 remain tightly associated. This interaction is attributed to the so-called self-association sequences (SAS) of HCF-1. The N- terminal SAS-N is adjacent to the Kelch domain and the SAS-C is located at the FN3-1 domain within the C-terminus of the protein. The recent crystal

structure of the SAS domain of HCF-1 revealed the mechanism of its self-association. The SAS-N sequence of the protein complements the missing beta strand structures of the incomplete C-terminal FN3-1 domain. This interaction is also important for proper Oct-1/VP16/HCF-1 complex formation and transactivation (Park et al., 2012).

HCF-1 orthologs can be found in all metazoan species. The N-and C-termini, Kelch domain, SAS motif and FN3 domains of HCF-1 are highly conserved. The middle region of the protein differs among the HCF-1 orthologs. Notably, the posttranslational proteolytic processing is characteristic of most HCF-1 orthologs excluding *Caenorhabditis elegans* HCF (CeHCF) (Liu et al., 1999). Intriguingly, the mechanism of the invertebrate HCF-1 proteolysis is different from the vertebrate species. For example the *Drosophila* dHCF is missing the PPD domain, but contains the characteristic taspase-1 cleavage site required for its processing by this protease (Capotosti et al., 2007). This observation indicates that, although the mechanisms of proteolytic processing are different for invertebrates and vertebrates, the cleavage itself is crucial for normal HCF-1 function. Indeed, the proteolytic processing of the human HCF-1 was shown to be required for normal progression through mitosis (Julien and Herr, 2003, 2004).

HCF-1 is a highly abundant nuclear factor found in numerous transcription regulatory complexes. Interestingly HCF-1 participates in both repressive as well as activation transcriptional regulatory complexes. For example HCF-1 can be found in MLL1, MLL5, SETD1A trithorax like, MOF-NSL acetyltransferase and TET 2/3 5-metylcytosine hydroxylase transcription activation complexes as well as the repressive SIN3A/HDAC1/2 and THAP1/3 histone deacetylase complexes (Cai et al., 2010; Deplus et al., 2013; Fujiki et al., 2009; Mazars et al., 2010; Tyagi et al., 2007; Wysocka et al., 2003; Yokoyama et al., 2004).

The role of the HCF-1 as an important factor for gene activation was first studied in the context of the HSV genome expression during the virus lytic cycle. It was suggested that HCF-1 promotes viral IE gene expression by recruiting chromatin modifying and remodeling factors to promote the active chromatin state. This includes the recruitment of the SETD1/MLL family methyltransferases to introduce the activating H3K4 methylation

marks as well as the LSD1 and JMJD2 histone lysine demethylases to remove the repressive histone methylation. Notably, the inhibition of LSD1 by RNAi or by a pharmacological inhibitor severely affected the ability of the HSV to promote its lytic cycle. The authors suggested that upon viral infection the intrinsic cellular response mechanisms promote the heterochromatinization of the integrated viral genome by the H3K9 methyltransferases. In order to achieve an efficient lytic cycle, this process has to be counteracted by the HCF-1/LSD1 and HCF-1/SETD1 in order to revert the HSV genome to a transcriptionally active state (Liang et al., 2009).

HCF-1 also seems to play role in chromatin structure by recruiting the chromatin assembly factors, histone chaperones and the chromatin remodeling ATPases. This includes the recruitment of the H3/H4 histone chaperones Asf1a and Asf1b. HCF-1 interacts with Asf1b through it C-terminal FN3 domains and was shown to be important for the replication of viral DNA by tethering the chromatin assembly components to the viral replication machinery (Peng et al., 2010).

HCF-1 resides in a complex with the chromatin-remodeling enzyme of the SWI/SNF family CHD8 (Cai et al., 2010; Smith et al., 2005). Although CHD8 is implicated in gene repression, it might have a potential opposite role in the transcription activation complexes with the HCF-1/MLL methyltransferase and the HCF-1/MOF-NSL acetyltransferase (Cai et al., 2010). The HCF-1/SETD1 complex was also shown to be engaged in the NURF chromatin-remodeling complex, suggesting its potential role in the establishment of heterochromatin boundaries (Li et al., 2011).

The role of HCF-1 in gene expression activation can be exemplified by its interaction with acetyltransferase complexes such as the MOF-NSL and the ATAC (ADA2-containing). HCF-1/MOF-NSL complex promotes acetylation of the histone H4K5-8-16 and the HCF-1/ATAC or HCF-1/SAGA complexes promote acetylation of both H3 and H4 (Cai et al., 2010; Krebs et al., 2011; Smith et al., 2005; Spedale et al., 2012).

At the functional level, HCF-1 was identified as one of the major players in the control of the cell cycle. HCF-1 cooperates with E2F transcription factors, which are required for G1/S transition. Members of the E2F family play crucial role in the

transcriptional control of their target genes required for S phase initiation and progression (Tyagi et al., 2007; Wysocka et al., 2003). This group of transcriptional regulators include activating members such as E2F1 and E2F3 as well as repressive factors, e.g., E2F4. During the initiation of S phase, HCF-1 appears to recruit the MLL/SETD1 complexes to the E2F1/3 target genes and promotes the trimethylation of histone H3K4 to activate the transcription of target genes. On the other hand, HCF-1 seems to be also required for the recruitment of repressive HDAC/SIN3A complexes by E2F4 transcription factor (Tyagi et al., 2007; Wysocka et al., 2003).

Nonetheless, HCF-1 seems to function at least in part as an integral protein interaction platform that can involve multivalent protein/protein interactions to recruit the necessary regulatory components to the transcription start sequence (Dejosez et al., 2010).

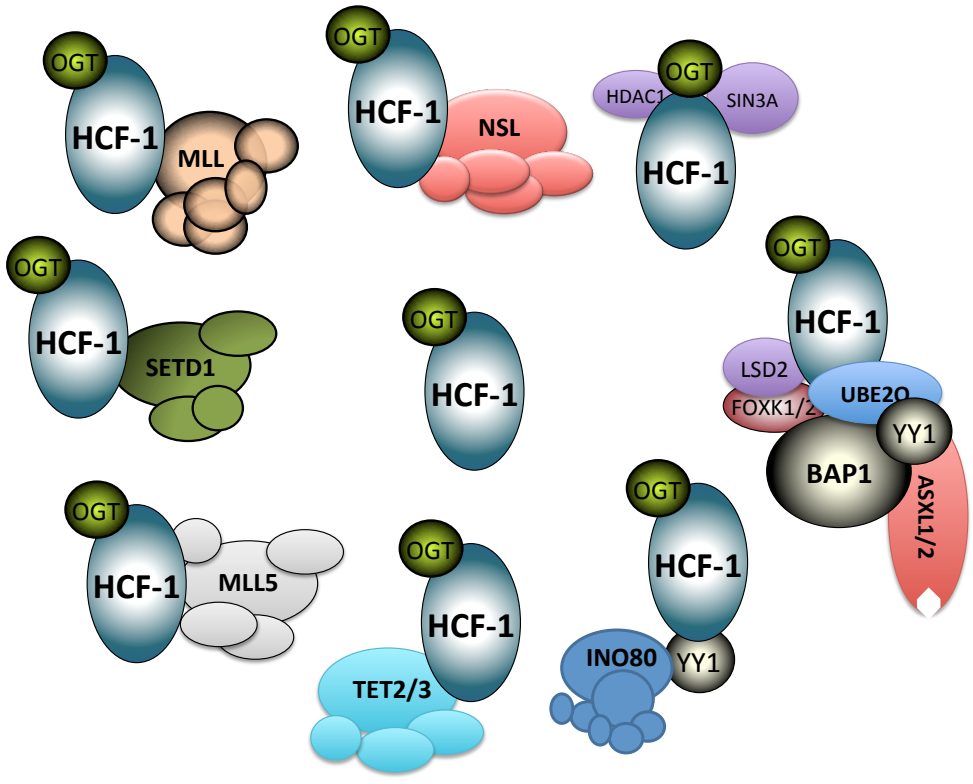

Figure 5. HCF-1/OGT protein complex as a structural and functional component in a subset of chromatin modifying machineries.

Analysis of transcription regulatory complexes that contain HCF-1 using tandem affinity purification (TAP), also usually recovers significant amounts of OGT (Wysocka et al., 2003). This is also true for TAP purifications of OGT itself (Deplus et al., 2013) (Salima Daou, Nazar Mashtalir and El Bachir Affar unpublished data). In fact TAP purifications from multiple sources indicate that HCF-1/OGT forms a stable complex that can act as an integral regulatory unit of multiple if not all the HCF-1 containing chromatin regulatory machineries (Figure 7)(Cai et al., 2010; Dejosez et al., 2010; Fujiki et al., 2009; Wysocka et al., 2003; Yao et al., 2008; Yu et al., 2010). Indeed, we found a tight co-regulation between HCF-1 and OGT. HCF-1 is required to stabilize the nuclear pool of OGT; and OGT is in turn required for HCF-1 proteolytic maturation (see also results and discussion sections)(Daou et al., 2011).

OGT: one response to multiple questions

The O-linked N-acetylglucosamine transferase (OGT) is an essential and ubiquitous eukaryotic enzyme that catalyzes the transfer of N-acetyl glucosamine sugar moiety to hydroxyl groups of serine and threonine amino acid residues of proteins. Until recently OGT was known to be the only enzyme capable of catalyzing sugar/protein O-GlcNAcylation. It was also discovered that a secreted form termed eOGT could catalyze the O-GlcNAcylation of extracellular matrix proteins (Sakaidani et al., 2011). Nonetheless, OGT remains the sole enzyme responsible for O-GlcNAcylation of intracellular protein targets. Despite the fact that thousands of proteins were reported to be O-GlcNAcylated, the exact functions of this posttranslational modifications remain unclear (Wang et al., 2012; Wang et al., 2010). The widespread abundance of O-GlcNAcylation and the occurrence of only one enzyme responsible for this modification suggest a highly pleiotropic nature of OGT. Protein modification by O-GlcNAcylation was shown to have multiple outcomes on target proteins including changes in stability, localization, folding and activity (Hart et al.,

2011). The dynamic changes of protein O-GlcNAcylation as a function of cell cycle phases, differentiation, and stress were also reported (Hart et al., 2007; Wells et al., 2001). O-GlcNAcylation was implicated in a wide variety of cellular processes ranging from nutrient sensing, protein degradation, innate immune response and PI3-kinase signaling to regulation of gene expression, epigenetic memory and circadian rhythm modulation. Aberrant O-GlcNAcylation has been reported in several human conditions such as neurodegenerative disease, diabetes and cancer (Akimoto et al., 2000; Caldwell et al., 2010; Dias and Hart, 2007; Ma and Vosseller, 2013; Yang et al., 2008).

O-GlcNAcylation is a reversible process and the hydrolysis of this modification is catalyzed by the sole enzyme O-linked N-acetylglucosamine hydrolase (OGA). OGA appears to have a dual activity, which in addition to its O-GlcNAcylhydrolase activity can promote protein acetylation (Comtesse et al., 2001). The apparent simplicity in the component composition of the O-GlcNAcylation/hydrolysis pathway and thousands of regulated substrates raise the questions about the specificity of O-GlcNAcylation. These questions can be partly addressed by the fact that OGT is a highly abundant component integrated within a large number of protein complexes (Cai et al., 2010; Dejosez et al., 2010; Fujiki et al., 2009; Wysocka et al., 2003; Yao et al., 2008; Yu et al., 2010). This is exemplified by a subset of transcription/epigenetic regulatory complexes in which OGT is often found with its partner HCF-1 activating or repressing transcription. Therefore, the OGT interaction partners recruit it to different substrates, thus ensuring the specificity of GlcNAcylation.

OGT is a highly conserved enzyme found in all metazoan organisms, although some similar enzymes with unknown function have been recently found in Bacteria (Martinez-Fleites et al., 2008). The human OGT is translated as a 1028 amino acid polypeptide that contains 11.5 tetratricopeptide repeats (TPR) sequences at its N-terminus and a three lobed catalytic domain at its C-terminus. As in many other proteins, the TPR motifs of the enzyme participate in protein/protein interactions and substrate recognition (Clarke et al., 2008; Iyer and Hart, 2003). The catalytic domain of OGT is closely related to the GT-B superfamily of glycosyltransferases but unlike most members of this group of enzymes, it

contains a relatively large internal domain of 120 AA between N- and C- lobes of the enzyme. OGT is also unique because it is the only enzyme of the GT-B superfamily capable of catalyzing GlcNAcylation of peptide substrates (Lairson et al., 2008). The other unique feature the OGT catalytic domain is its ability to act as a phosphatidylinositol (3,4,5)-trisphosphate (PIP3) binding domain that is responsible for the insulin-induced translocation of the enzyme to the plasma membrane (Yang et al., 2008). The catalytic reaction involving OGT requires UDP-GlcNAc as the GlcNAc donor and the reaction energy is acquired from the pyrophosphate bond (Lairson et al., 2008).

The requirement of UDP-GlcNAc for the O-GlcNAcylation reaction raised the interesting possibility that OGT might be a nutrient sensor. UDP-GlcNAc is a major product of the hexosamine biosynthetic pathway (HBP) witch is recognised as a sensor of nutrients in the cells (Marshall et al., 1991). Indeed, the production of UDP-GlcNAc is highly sensitive to nutrient availability and constitutes a limiting factor for O-GlcNAcylation reactions. This highly sensitive interplay between UDP-GlcNAc concentration and target protein O-GlcNAcylation might have profound effects on the cellular response to nutrient availability at multiple levels ranging from modulation of plasma membrane-mediated signaling to regulation of gene expression (Hart et al., 2011).

Another fascinating regulatory effect of protein O-GlcNAcylation is that it targets the S/T residues of proteins, which are also targeted by most protein kinases in the cell. In this respect, O-GlcNAcylation could directly compete with protein phosphorylation, and vice versa. Indeed, multiple proteomic studies found an inverse correlation between the two modifications (Hart et al., 2007; Hart et al., 2011; Wang et al., 2010).

OGT is a nucleo/cytoplasmic protein, approximately equal levels of the enzyme being present in both compartments (Daou et al., 2011). The nuclear function of OGT is described in multiple studies showing its involvement in numerous repressive and activating protein complexes. This includes the already described HCF-1 containing complexes such as the H3K4 methyltransferases MLL1, MLL5, SETD1, the DNA 5-methylcytosine hydroxylases TET1/2/3, the histone acetyltransferase MOF-NSL as well as

the repressive histone deacetylase complex SIN3A (Cai et al., 2010; Chen et al., 2013; Deplus et al., 2013; Fujiki et al., 2009; Ito et al., 2014; Yang et al., 2002).

Recently the *Drosophila* polycomb group protein Super sex combs (*Sxc*) have been shown to be an ortholog of the human OGT. *Sxc* is recruited to the *Hox* gene cluster and promotes its transcriptional repression. Homozygous mutants of *Sxc* are usually early embryonic lethal. Moreover, some *Sxc* heterozygous mutants display severe homeotic transformation phenotype and late pupal lethality. It is currently unknown whether this effect will be recapitulated in mammals (Gambetta et al., 2009; Sinclair et al., 2009).

Recent studies have also shown that OGT may directly target nucleosomal histones and establish O-GlcNAcylation as a novel epigenetic mark (Chen et al., 2013; Fujiki et al., 2011; Sakabe et al., 2010). For example the study by Hart's group found O-GlcNAcylation sites on Histone H2A (T101), H2B (S36) and H4 (S47). Most histone modifications were found in the nucleosome histone folds, but not in histone tails where most of the epigenetic modifications occur (Sakabe et al., 2010). Another study showed that histone H2B is predominantly O-GlcNAcylated at S112. The authors generated a modification-specific antibody and intriguingly found that S112 O-GlcNAcylation is required for histone H2B monoubiquitination at position K120, a histone mark important for positive regulation of mRNA elongation by Pol II (Fujiki et al., 2011).

Most recently, several studies revealed new roles of OGT in transcription regulation. It was shown that OGT interacts with the TET1/2/3 5-methylcytosine hydroxylases, enzymes responsible for the oxidation of methylated DNA and represent the most promising candidates for active DNA demethylation (Kohli and Zhang, 2013). Interestingly, several groups found that the TET family members where required for proper recruitment of OGT to chromatin (Chen et al., 2013; Deplus et al., 2013; Ito et al., 2014). One study showed that the interaction between TET2 and OGT was required for the proper histone H2B ubiquitination at position K120 (Chen et al., 2013). On the other hand, another study showed the importance of the TET2/OGT/HCF-1 interaction for proper recruitment of the SETD1 complex to chromatin for H3K4 trimethylation and gene activation (Deplus et al., 2013).

With respect to the BAP1 complex, the exact role of OGT and the functional link with deubiquitination remains to be defined. Nonetheless, one study revealed that the HCF-1/OGT/BAP1 complex is an important regulator of gluconeogenesis. This complex appears to directly bind the energy balance regulatory transcription factor PGC1α and promotes its O-GlcNAcylation. Subsequently this modification promotes the stabilization of hepatic PGC1 α levels by its direct deubiquitination by BAP1 (Ruan et al., 2012).

UBE2O: breaking the rules of the classical ubiquitin cascade

One of the most unusual components of the BAP1 complex is UBE2O/E2-230k. UBE2O belongs to the E2 ubiquitin carrier class of enzymes, and contains the UBC domain proficient in the transfer of ubiquitin (Berleth and Pickart, 1996; Haldeman et al., 1995; Klemperer et al., 1989). UBE2O displayed many unusual biochemical features. Unlike most of the classical E2s, UBE2O was found to be relatively less sensitive to iodoacetamide, a cysteine-alkylating agent, indicating the possibility of conformational changes in the enzyme or the possible involvement of multiple redundant cysteines. In contrast, UBE2O was shown to be highly sensitive to inorganic arsenate, the alkylating agent that predominantly targets cysteines in close proximity and promotes their crosslinking. This finding prompted the authors to hypothesize that a unique mechanism of cysteine relay might be involved in the ubiquitin conjugation process engaging at least two steps of intramolecular ubiquitin transfer (Berleth and Pickart, 1996; Haldeman et al., 1995; Klemperer et al., 1989). The large size of UBE2O (140 kDa) was also unusual, since most of the E2s are small (15-25kDa) single domain enzymes (van Wijk and Timmers, 2010). UBE2O was also able to target artificial substrates in vitro (i.e. histone H2B) and this reaction did not seem to require additional E3s. These initial studies indicated that UBE2O might function as an atypical ubiquitin E2/E3 hybrid (Berleth and Pickart, 1996).

UBE2O belongs to the class IV of ubiquitin conjugating enzymes (van Wijk and Timmers, 2010; Yokota et al., 2001). This classification of E2s is based on the characteristics of the N- and C-terminal extensions relative to their "central" UBC domain. Class I is represented by the enzymes with no extensions and containing essentially the catalytic core (i.e. UbcH5c, Ubc7 and Ubc13). Class II enzymes have N-terminal extensions (i.e. UbcH6 and UbcH10) and class III members possess C- terminal extensions (i.e. CDC34). In contrast, class IV family of E2s contain both N and C- terminal extensions flanking their UBC domains. The extensions to the UBC domain are known to regulate multiple features of the E2s including their localization, E3 binding specificity and activity (van Wijk and Timmers, 2010).

Only three members of the class IV enzymes represent this small and poorly characterized family of ubiquitin carriers. This family includes the anti-apoptotic protein BIRC6/Apollon/BRUCE, UBE2O and Ube2Z. The latter was shown to be specifically charged by UBA6 (Jin et al., 2007). Notably, BRUCE was also shown to act as an E3-independent ubiquitin conjugating enzyme. It was shown that BRUCE uses its N-terminal BIR (baculoviral IAP inhibitor of apoptosis repeats) and C-terminal UBC domain to bind and promote ubiquitination and degradation of pro-apoptotic proteins such as SMAC and Caspase-9 (Bartke et al., 2004; Hao et al., 2004; Morizane et al., 2005). Recently BRUCE was also shown to promote the ubiquitination-dependent removal of the mid-body ring during the late stages of the cytokinesis (Pohl and Jentsch, 2008). Interestingly, BRUCE is the closest homolog of UBE2O in humans, although this homology can be found only within its UBC domain.

The function and the physiological role of UBE2O remained largely unknown. It was shown that UBE2O is differentially expressed in multiple tissues (Nagase et al., 2000; Yokota et al., 2001). The expression of UBE2O was also shown to be dramatically increased during erythroid differentiation (Wefes et al., 1995). In addition, UBE2O appears to be highly expressed in striated and heart muscle tissues as well as the brain (Nagase et al., 2000; Wefes et al., 1995; Yokota et al., 2001; Zhang et al., 2013a). These results indicate that although UBE2O seems to be a ubiquitous enzyme, its expression might also

be induced in response to specific stimuli (i.e. adipose, muscle and erythroid differentiation).

Recent studies started to reveal some physiological roles of UBE2O. This enzyme seems to be involved in the regulation of TNF receptor-associated factor 6 (TRAF6)-mediated nuclear factor NF-kappa-B (NF-κB) activation. UBE2O interacts with TRAF6 and inhibits its ubiquitination by K63-linked polyubiquitin chains and subsequently promotes persistent signal transduction (Zhang et al., 2013b). This inhibition occurred independently of UBE2O catalytic activity and the UBC domain in general. The UBE2O binding to TRAF6 was shown to compete with myeloid differentiation primary response protein MyD88 adapter binding and inhibit its IL-1β-induced activation (Zhang et al., 2013b). The same group also studied the role of UBE2O in the regulation of bone morphogenic protein (BMP)/ Mothers against decapentaplegic homolog 6 (SMAD6) signaling. UBE2O was found to mono-ubiquitinate SMAD6 and potentiate its activating role towards BMP7-induced SMAD1 phosphorylation and transcriptional responses (Zhang et al., 2013a). UBE2O appears to play a major role as a positive regulator of BMP signaling through mono-ubiquitination of SMAD6 during adipocyte differentiation. The main caveat of these two studies is that they used a truncated form of UBE2O (Zhang et al., 2013a).

A crucial role of UBE2O in the regulation of retrograde vesicle trafficking and actin nucleation was recently discovered as a result of an E2 enzymes targeting screen (Hao et al., 2013). The authors studied the role of the ubiquitin ligase TRIM27 in the ubiquitination of the actin nucleation factor WASH. TRIM27 is responsible for the K63 ubiquitin chain formation on the conserved hydrophobic region of WASH and is required for actin nucleation and retrograde transport. In this work, UBE2O is regarded as a simple ubiquitin carrier that works with TRIM27, although according to our predictions of UBE2O targeting sequence, it is possible that UBE2O directly ubiquitinates WASH (Hao et al., 2013).

We found that UBE2O directly interact with and ubiquitinates BAP1 nuclear localization signal (NLS), regulating the subcellular localization of this DUB. This ubiquitination can be actively counteracted by the BAP1 auto-deubiquitination (auto-DUB) activity, a mechanism disrupted in cancer. Moreover we identified a consensus sequence

for UBE2O targeting and revealed a subset of proteins with such a sequence and validated several of them as UBE2O substrates (Mashtalir et al., 2014) (see also the result section).

Articles

Crosstalk Between O-GlcNAcylation And Proteolytic Cleavage Regulates The Host Cell Factor-1 Maturation Pathway Ψ

Salima Daou[1*], Nazar Mashtalir[1*], Ian Hammond-Martel[1], Helen Pak[1], Helen Yu[1], Guangchao Sui[2], Jodi L. Vogel[3], Thomas M. Kristie[3] and El Bachir Affar[1,4]

[1]Maisonneuve-Rosemont Hospital Research Center, Department of Medicine, University of Montréal, Montréal, Canada
[2]Wake Forest University School of Medicine, Winston-Salem, NC, USA.
[3]Laboratory of Viral Diseases, National Institute of Allergy and Infectious Diseases, National Institutes of Health, Bethesda, MD, USA.

Running title: O-GlcNAcylation regulates HCF-1 proteolysis

[*]Equal contribution to this work

[4]Correspondence

I contributed to this study as a co-first author. I made the first observation of OGT dependent HCF-1 processing. I performed the experiments regarding the OGT stability, subcellular localization and ubiquitination, PPD processing in vivo and HCF-1 chromatin association (overall 50% of experiments). I wrote parts of the article, prepared the manuscript for submission and performed the experiments requested by the reviewers during the revision.

Ψ-This paper was published in Proceedings of the National Academy of Sciences in February 2011.

ABSTRACT

Host Cell Factor 1 (HCF-1) plays critical roles in regulating gene expression in a plethora of physiological processes. HCF-1 is first synthesized as a precursor, and subsequently specifically proteolytically cleaved within a large middle region termed the proteolytic processing domain (PPD). Although the underlying mechanism remains enigmatic, proteolysis of HCF-1 regulates its transcriptional activity and is important for cell cycle progression. Here we report that HCF-1 proteolysis is a regulated process. We demonstrate that a large proportion of the signaling enzyme O-linked-N-acetylglucosaminyl transferase (OGT) is complexed with HCF-1 and this interaction is essential for HCF-1 cleavage. Moreover, HCF-1 is, in turn, required for stabilizing OGT in the nucleus. We provide evidence indicating that OGT regulates HCF-1 cleavage via interaction with and O-GlcNAcylation of the HCF-1 PPD. In contrast, although OGT also interacts with the basic domain in the HCF-1 amino-terminal subunit, neither the interaction nor the O-GlcNAcylation of this region are required for proteolysis. Moreover, we show that OGT-mediated modulation of HCF-1 impacts the expression of the herpes simplex virus immediate early genes, targets of HCF-1 during the initiation of viral infection. Together the data indicate that O-GlcNAcylation of HCF-1 is a signal for its proteolytic processing and reveal a novel crosstalk between these post-translational modifications. Additionally, interactions of OGT with multiple HCF-1 domains may indicate that OGT has several functions in association with HCF-1.

INTRODUCTION

HCF-1 is a ubiquitously expressed chromatin-associated protein and a major transcriptional regulator controlling numerous cellular processes including cell cycle progression (reviewed in (Kristie et al. 2009)).

HCF-1 undergoes a unique mode of limited proteolysis involving a series of 20 aa reiterations within the central proteolytic processing domain (PPD) (Kristie and Sharp 1993; Wilson et al. 1995). Although the mechanism of cleavage remains to be fully defined, previous studies suggested that HCF-1 might possess an autoproteolytic activity (Vogel and Kristie 2000). HCF-1 cleavage occurs at one or more reiterated sites at the PPD, generating several N-terminal and C-terminal subunits that form stable heterodimers via two corresponding pairs of motifs, termed self association sequences (SAS) (Wilson et al. 2000).

Earlier studies indicated that proteolytic processing of HCF-1 is required to coordinate two major functions of HCF-1 in cell cycle progression (Julien and Herr 2003). The HCF-1 N subunit is necessary and sufficient to promote the G1 to S transition, while the C subunit is required for progression through mitosis (Julien and Herr 2003). However, the molecular properties that characterize the functions of the precursor versus the mature forms of HCF-1 remain unclear. It is likely that the gain or loss of specific protein interactions is one major consequence of HCF-1 processing. For instance, the coactivator/corepressor FHL2 interacts with the HCF-1 precursor via a motif located in the central region of the PPD. HCF-1 processing removes this motif, thus decreasing the activation of an HCF-1-dependent target gene (Vogel and Kristie 2006).

OGT is a highly conserved enzyme that participates in critical nuclear and cytoplasmic signalling events (Butkinaree et al. 2010; Slawson et al. 2010). Similar to phosphorylation, OGT modifies S/T residues of target proteins with a single N-acetylglucosamine (O-GlcNAc); regulating protein function by influencing protein interactions, enzymatic activity, and subcellular localization. Furthermore, O-GlcNAc modification is highly dynamic and ample evidence indicates the existence of extensive

crosstalk between O-GlcNAcylation and phosphorylation in controlling biological processes (Butkinaree et al. 2010; Slawson et al. 2010). The reversibility of O-GlcNAcylation is ensured by a unique beta-N-acetylglucosaminidase (OGA) which is also highly conserved (Hu et al. 2010). OGT interacts with numerous cellular proteins, most notably transcription factors and regulators. Significantly OGT was previously shown to interact with and glycosylate the HCF-1 N subunit (Wang et al. 2010; Wysocka et al. 2003). However, the biological significance and mechanism of this O-GlcNAcylation remain unknown. Here, we reveal a novel physical and functional link between O-GlcNAcylation and limited proteolysis.

RESULTS

HCF-1 regulates the stability of nuclear OGT.

HCF-1 possesses a unique modular structure consisting of an amino-terminal Kelch domain followed by: (i) a region rich in basic residues; (ii) the PPD containing the 20 aa reiterations that are the sites of specific proteolysis; (iii) an acidic activation domain; (iv) and a set of fibronectin repeats (Fig.1A). HCF-1 was previously shown to interact with OGT (Wysocka et al. 2003). However the abundance of nuclear OGT stably associated with HCF-1 relative to the entire nuclear pool was not known. To address this, we immunodepleted HCF-1 from HeLa nuclear extracts (Fig.1B). Quantification of OGT levels in the HCF-1 complexes fraction (IP) and the flow through (FT) revealed that nearly 50% of the total nuclear OGT is stably associated with HCF-1. The association of a large proportion of OGT with HCF-1 suggests important roles of this complex. Strikingly, depletion of HCF-1 in HeLa cells by shRNA induced a corresponding dose-dependent decrease of OGT (Fig.1C). This result was confirmed by a pool of 4 siRNA oligonucleotides targeting HCF-1 (Fig.1C). Conversely, overexpression of HCF-1 induced an increase in OGT protein levels (Fig.1D). The reduction in OGT levels in the absence of HCF-1 were not due to a reduction in *OGT* mRNA levels (Fig.1E). Moreover, no detectable HCF-1 was found to be associated with the *OGT* promoter (Fig.1F). In contrast, HCF-1 was

readily detected on the promoter of *p107* RB family member (Fig.1F), a known HCF-1 target gene (Tyagi et al. 2007).

The above results suggested that HCF-1 regulates OGT stability via a post-transcriptional mechanism. Since OGT is distributed in both the cytoplasm and the nucleus while HCF-1 is primarily localized in the nucleus, we determined whether the nuclear pool of OGT was preferentially stabilized by HCF-1. Subcellular fractionation showed that the nuclear pool of OGT is significantly reduced relative to the corresponding cytoplasmic pool following depletion of HCF-1 (Fig.2A). These results were confirmed by immunostaining following knockdown of HCF-1 where a significant reduction of nuclear OGT could be observed in the HCF-1 depleted cells (Fig.2B). To determine whether OGT is regulated by proteasomal degradation, we transfected expression plasmids for OGT and ubiquitin, followed by treatment with the proteasome inhibitor MG132. After OGT immunoprecipitation, we observed a typical ubiquitination smear, which was increased by MG132 treatment (Fig.2C). We note that MG132 has a minor effect on OGT protein levels. This is due to the relatively long half-life of OGT (~ 12 hours) (Marshall et al. 2005). We also observed an increase in the ubiquitination of endogenous OGT following extended treatment with MG132 (Fig.S1). Next, we conducted a cycloheximide chase upon HCF-1 knockdown and found that OGT was slightly reduced overtime while no change or even a small increase was observed for the shControl transfected cells (Fig.2D).

OGT is required for HCF-1 proteolytic processing.

It was previously reported that OGT interacts with and glycosylates HCF-1 (Wysocka et al. 2003), suggesting an important reciprocal regulation. Strikingly, depletion of OGT induced an accumulation of the HCF-1 precursor with a corresponding decrease in the HCF-1 cleavage products (Fig.3A). Quantification indicated that shRNA constructs, which depleted OGT to different extents, correlated in an inverse manner with the ratio of HCF-1 cleavage products (HCF-1 FL/HCF-1 cleaved forms). As expected, the extent of OGT knockdown also correlated with a proportional decrease of global O-GlcNAc modification. Transfection of siRNA oligonucleotide pools, which induced a substantial

knockdown of OGT, also resulted in a significant accumulation of HCF-1 FL (Fig.3A). OGT knockdown also inhibited HCF-1 cleavage in other cell types indicating that this inhibition is not cell-type specific (Fig.3A). Conversely overexpression of OGT along with HCF-1 FL resulted in: (i) an increase in global protein O-GlcNAcylation levels; (ii) a decrease in HCF-1 FL levels; and (iii) an increase in the levels of HCF-1 N and C polypeptides (Fig.3B). The effect on HCF-1 cleavage was dependent on OGT catalytic activity (Fig.S2).

O-GlcNAc modification is dynamic and cycling is ensured by the concerted action of OGT and OGA (Hurtado-Guerrero et al. 2008; Love et al. 2010). We reasoned that overexpressed OGA would shift the equilibrium toward O-GlcNAc removal with a concomitant effect on HCF-1 cleavage. Although no significant changes were seen on the cleaved forms of HCF-1 following overexpression of OGA, a noticeable increase in the level of HCF-1 precursor was observed (Fig.3C). The decrease of global O-GlcNAc with overexpressed OGA was considerably less significant than with OGT RNAi (Fig.3C).

Components of the nuclear pore complex are known to be heavily glycosylated by OGT suggesting that O-GlcNAc modification might be required for the nuclear import of proteins (Davis and Blobel 1987; Hanover et al. 1987; Jinek et al. 2004). Although not firmly established, HCF-1 appears to be cleaved in the nucleus (Wilson et al. 1995). We reasoned that depletion of OGT might induce cytoplasmic sequestration of HCF-1 FL from accessing factors required for its cleavage in the nucleus. However, in the absence of OGT, most of the HCF-1 FL is in the nucleus, indicating that the lack of HCF-1 cleavage was not due to a defect in nuclear import (Fig.3D). To further confirm these results, cells were stained for HCF-1 following shRNA knockdown of OGT. While substantial depletion of OGT was achieved, no noticeable cytoplasmic accumulation of HCF-1 was observed (Fig.S3). Interestingly, in contrast to HCF-1 cleavage, no effect of OGT knockdown was observed on the histone methyltransferase and transcription regulator MLL1, which is also subjected to specific proteolytic cleavage (Hsieh et al. 2003) (Fig.S4). We concluded therefore that OGT is required for HCF-1 cleavage.

OGT interacts with and glycosylates full length HCF-1.

To investigate the mechanism of HCF-1 maturation, we sought to characterize the OGT interaction with HCF-1. First, we cotransfected HA-HCF-1 FL or HA-HCF-1 N (1-1010aa) with Myc-OGT, and found that significantly more OGT is immunoprecipitated with HA-HCF-1 FL than HA-HCF-1 N (Fig.S5A), suggesting that the major determinants of OGT/HCF-1 interaction are contained within HCF-1 sequences that are not present in the HCF-1 N protein.

Next we used the WT or an uncleavable form of HCF-1 mutant (NC) in which the critical glutamic acid of each repeat had been mutated to alanine (Vogel and Kristie 2006). Immunoprecipitation assays revealed that the uncleavable HCF-1 mutant was even more efficient in co-immunoprecipitation of OGT than the WT HCF-1 (Fig. S5B). These effects were also observed following co-expression of HCF-1 WT or the uncleavable mutant with OGT. In this case, OGT expression induced processing of the HCF-1 WT but not the HCF-1 NC mutant (Fig.S5C). Of note, Myc-OGT was substantially stabilized in cells co-transfected with HCF-1 NC accounting partly for the more efficient co-immunoprecipitation. However, the ratio of the IP/Input supported the conclusion that OGT interacts more efficiently with the uncleaved HCF-1 than the HCF-1 WT (Fig.S5C). Next, *in vitro* GST-pull down assays using recombinant GST-OGT and various *in vitro* translated forms of HCF-1 (FL, N and C subunits) indicated that the GST-OGT interacts more efficiently (~10 fold) with the HCF-1 precursor than the HCF-1 N subunit (Fig.S6). No interaction was observed with the HCF-1 C (Fig.S6). To determine whether HCF-1 FL is O-glycosylated, we immunoprecipitated HCF-1 and found that the precursor reacts with the anti-O-GlcNAc antibody, suggesting that O-GlcNAcylation of HCF-1 precedes its processing (Fig.S7). We also note that large C-terminal fragments corresponding most likely to processing intermediates are O-glycosylated, however the most processed forms of HCF-1 C-terminal subunits appear to be very poorly O-glycosylated.

OGT interaction with and O-GlcNAcylation of the HCF-1 N-terminal subunit are not required for HCF-1 proteolytic cleavage.

To determine the role of O-GlcNAc in the proteolytic processing of HCF-1, we utilized two approaches. We first conducted GST-pulldown assays with subdomains of the HCF-1 N subunit and observed that the HCF-1 basic region interacts with OGT (Fig.S8A). We further determined that a region between 500 and 550 aa of HCF-1 is sufficient for this interaction (Fig.S8A). Therefore, we generated a mutant of HCF-1 lacking this domain (Δ500-650 aa) (HA-HCF-1 ΔOBM) (Fig.S8B). Interestingly, this mutant was cleaved as efficiently as the WT HCF-1 (Fig.S8C, left panel). Moreover, the interaction of this HCF-1 mutant with OGT was almost unchanged in comparison to the WT HCF-1 (Fig.S8C, left panel). Next, we analysed the O-GlcNAcylation levels of this HCF-1 mutant and observed that while a significant decrease in the O-GlcNAcylation of the cleaved forms of HCF-1 was evident, there was no substantial change in the overall O-GlcNAcylation of the uncleaved FL HCF-1 (Fig.S8C, right panel). The data indicate that neither the interaction of OGT with the N subunit nor its O-GlcNAcylation is responsible for the OGT mediated proteolysis of HCF-1. To confirm these results, we mutated all of the known O-GlcNAcylation sites located in the HCF-1 N subunit (Wang et al. 2010) (HA-HCF-1 ΔO-Glc) (Fig.S8B). Similar to the HCF-1 DOBM mutant, a substantial decrease in HCF-1 O-GlcNAcylation was observed for the cleaved forms while no major changes in the O-GlcNAcylation levels of the uncleaved HCF-1 were seen (Fig.S8C, right panel). Importantly the extent of HCF-1 cleavage remained essentially similar to the WT form suggesting that O-GlcNAc modification of the basic region within the HCF-1 N is not required for processing (Fig.S8C, left panel).

OGT interacts with, O-glycosylates, and promotes the cleavage of the PPD.

To provide further mechanistic insights into the role of OGT in HCF-1 processing, we investigated the role of the PPD in promoting the OGT/HCF-1 interaction. First we transfected cells with the uncleavable HCF-1 FL (HCF-1 NC) or HCF-1 lacking the PPD

(HCF-1 Δ PPD) and compared the interaction with OGT. As shown in Fig.4A, the HCF-1 lacking the PPD interacted less efficiently (~ 20-fold less) with OGT than the uncleavable form suggesting that the PPD is the major OGT-interacting domain. Previously it was demonstrated that the PPD was sufficient for cleavage in cells, although it is very poorly processed (Wilson et al. 1995). Therefore, we generated PPD expression constructs with and without a Nuclear Localization Signal (NLS) (Fig.S9A). In contrast to the PPD without the NLS (Myc-PPD), which was moderately cleaved, the PPD with the NLS (Myc-NLS-PPD) was dramatically cleaved and only a faint band of residual uncleaved PPD could be detected (Fig.S9B). Of note, the Myc-NLS sequences (~3 kDa) enabled us to detect the smallest cleaved form of the Myc-NLS-PPD (PPD repeat 1-2).

As detected by immunofluorescence, the Myc-PPD was distributed in the cytoplasm and nucleus (Fig.4B). In contrast, the Myc-NLS-PPD accumulated in the nucleus (Fig.4B). Interestingly, cells expressing Myc-NLS-PPD exhibited a typical pronounced nuclear OGT staining (Fig.4B), similar to mock transfected cells (Fig.2B). However, in cells expressing Myc-PPD, OGT was distributed evenly between cytoplasm and nucleus (Fig.4B), suggesting that this form of the PPD directly interacts with OGT and interferes with its nuclear localization. This result was confirmed by subcellular fractionation, i.e., cells expressing Myc-PPD exhibit significantly higher OGT levels in the cytoplasm (Fig. S10). Next, we found that the HCF-1 PPD (Myc-PPD) was sufficient to co-IP OGT (Fig.4C). In contrast, the smallest cleaved form of PPD does not interact with OGT indicating that this set of reiterations (R1-2) is not sufficient to mediate the association with OGT. Since the Myc-NLS-PPD appears to be dramatically cleaved, we reasoned that this domain might interact with OGT and be a target of OGT mediated O-GlcNAcylation prior to its cleavage. In support of this, the Myc-PPD was modified by O-GlcNAc in an OGT-dependent manner (Fig.4D and Fig. S11). To further characterize the role of OGT in promoting HCF-1 cleavage, we took advantage of the PPD without the NLS, which localizes in both cytoplasm and nucleus (Fig.4B), interacts with OGT, and is moderately cleaved (Fig.4C). Following over-expression of OGT, we observed a decrease in the levels of both the FL Myc-PPD and the cleavage products (Fig.4E). Conversely, knockdown of OGT induced an

accumulation of FL Myc-PPD (Fig S12). These results indicate that OGT directly promotes the cleavage of the HCF-1 PPD and intermediate processing forms.

Depletion of OGT enhances HCF-1 target gene expression.

Since we observed a significant accumulation of HCF-1 FL in the nucleus following depletion of OGT, we first determined whether it associates with chromatin. The chromatin/nuclear matrix fraction of HeLa cells was prepared from control and OGT-depleted cells and treated with MNase (Sanders 1978). As shown in Fig.5A, HCF-1 was released into the soluble fraction following MNase treatment, indicating its association with chromatin.

Finally, to determine the biological consequences of OGT mediated regulation of HCF-1 cleavage, we assessed the impact of OGT depletion on HCF-1 mediated gene expression using the well characterized model of HCF-1-dependent activation of the herpes simplex virus (HSV) IE genes (Kristie et al. 2009). HFF cells transfected with control or OGT siRNAs were infected with HSV and the levels of viral and control cellular mRNAs were determined by qRT-PCR. As shown in Fig.5B, depletion OGT (~80%) resulted in a substantial increase in the ratio of HCF-1 precursor to the HCF-1 cleavage products as compared to cells transfected with control siRNAs. Importantly, depletion of OGT also resulted in a consistent increase (~1.5 to 2.5-fold) in viral IE gene expression (Fig.5B). In contrast, no impact was seen on expression of the control *GAPDH* or *TBP* mRNA levels. As factors such as the Sp1 transcription factor, a known component of the viral HSV IE gene expression regulatory circuit, as well as RNA polymerase II can be regulated by O-GlcNAcylation (Kelly et al. 1993; Yang et al. 2001), we also analyzed the expression of a set of Sp1 target genes in cells depleted of OGT. In contrast to the impact on HSV IE gene expression, we did not detect any significant changes in the expression of these Sp1 target genes (Fig. S13). Thus, although we can not exclude possible effects resulting from O-GlcNAcylation of other cellular factors, the loss of Sp1 or RNA polymerase II O-GlcNAcylation does not likely account for the observed increase in HSV immediate-early gene expression. The results are consistent with previous data indicating that the full-

length, non-processed form of HCF-1 was more efficient in induction of viral IE reporter genes (Vogel and Kristie 2006).

DISCUSSION

Site-specific limited proteolytic cleavage is exploited as a signaling mechanism in nearly all living organisms. Moreover, the importance of this post-translational modification is emphasized by the fact that, in mammals, numerous physiopathological processes have evolved elaborate protein cleavage machineries.

Mammalian HCF-1 is subjected to proteolytic cleavage via limited site-specific proteolysis within unique reiterations of the PPD. Interestingly, *C elegans* HCF does not have a domain homologous to PPD and is not cleaved (Liu et al. 1999). The *Drosophila* HCF, although also cleaved, does not contain cleavage sites homologous to the mammalian HCF-1 PPD (Mahajan et al. 2003). This suggests that a need developed for HCF-1 proteolytic processing, although distinct mechanisms of cleavage have apparently evolved. Indeed, it has been shown that the *Drosophila* HCF is cleaved by the protease taspase 1, while human and mouse HCF-1 are cleaved in a taspase 1-independent manner (Capotosti et al. 2007).

Here, we demonstrate that OGT is required for HCF-1 cleavage. Interestingly O-GlcNAcylation is shown here to promote proteolytic cleavage, protein phosphorylation also impacts proteolytic cleavage by either stimulation or inhibition (Kurokawa and Kornbluth 2009), thus highlighting the importance of post-translational modifications in tightly regulating limited proteolysis. In addition to the previously established role of OGT in inhibiting proteasomal degradation via O-GlcNAcylation of the proteasome or its substrates (Cheng and Hart 2001; Han and Kudlow 1997; Zhang et al. 2003), we have here uncovered an additional role for this enzyme in signalling limited proteolysis. Since both proteolytic cleavage and O-GlcNAcylation modulate the function of several transcription regulators, it would be interesting to determine whether this crosstalk represents a more global signaling event.

The role of OGT in association with HCF-1 is likely to have several functions. With respect to the regulation of HCF-1 cleavage, it is possible that the PPD encodes a dormant protease that is stimulated by O-GlcNAcylation, following a significant conformational change. This model would provide a level of control that prevents promiscuous and

untimely autocleavage of HCF-1. Alternatively, O-GlcNAcylation of the PPD may provide a signal for recruitment of an, as yet unidentified, protease. Importantly, the PPD is not simply a domain containing proteolytic cleavage sites but is also a domain that interacts with HCF-1 binding partners. OGT mediated O-GlcNAcylation of the PPD or PPD interacting partners could result in an enhancement of cleavage via disruption of protective interactions. Thus, OGT-mediated cleavage of HCF-1 can provide a mechanism for controlling the dosage and functional competency of HCF-1 and its processed subunits. In support of this, depletion of OGT results in accumulation of the full-length HCF-1 and a stimulation of HCF-1 dependent transcriptional activation of the HSV IE genes. Finally, an additional implication of the interaction of OGT with HCF-1 is the reciprocal impact of HCF-1 on OGT stability. Thus, as OGT interacts more efficiently with the HCF-1 precursor, it may therefore modulate its own stability.

In addition to modulating HCF-1 cleavage, OGT is also likely to have additional functional roles in association with HCF-1. In addition to its interaction with the HCF-1 PPD, OGT also interacts with the basic domain of HCF-1 and remains associated with the cleaved HCF-1 subunits. Thus, OGT might modulate HCF-1 interactions with chromatin-associated regulators. Notably, OGT is a metabolic sensing enzyme. It would be of continued interest to investigate whether changes in metabolic conditions impact HCF-1 processing and/or function, which in turn would affect cell growth and cell cycle progression. Thus, as HCF-1 is a major regulator of cellular metabolism (Dejosez et al. 2008; Vercauteren et al. 2008), O-GlcNAcylation of HCF-1 might provide a link between cellular metabolism and cell proliferation**.**

MATERIALS AND METHODS

Plasmids and Antibodies

shRNA constructs, expression plasmids, and antibodies used in this study are described in supplemental information.

Cells and virus

HeLa, U2OS, HFF (human foreskin fibroblast), and 293T cells were maintained according to standard protocols. Infections of HFF cells with HSV-1, cell transfections, and western blotting were done as described in supplemental information.

Immunodepletion and Immunoprecipitation

Immunodepletion of HeLa nuclear extracts with anti-HCF-1 or control IgG were done as described in supplemental information.

Biochemical fractionation of subcellular compartments

Nuclear and cytoplasmic fractions were obtained using a hypotonic lysis buffer as described (Nakatani and Ogryzko 2003). Chromatin fractions and digestion with MNase were conducted as described (Groisman et al. 2003).

In vitro GST-pulldown assays

Recombinant GST-OGT fusion protein was purified using glutathione agarose beads and used for pull down assays as described in the text and supplemental information.

Immunofluorescence

Cells were fixed with paraformaldehyde and stained with the appropriate antibodies as detailed in the supplemental information.

mRNA expression analysis and chromatin immunoprecipitations

mRNA was prepared according to standard procedures and cDNAs were used for real time qRT-PCR analysis of cellular and viral mRNA levels. Chromatin immunoprecipitation (ChIP) was done essentially as previously described (Bottardi et al. 2009) with minor modifications as described in supplemental information .

Acknowledgments

This work was supported by grants to E.B.A. from the Terry Fox Foundation (grant#018144). Work in T.K's laboratory was supported by the Laboratory of Viral Diseases, Division of Intramural Research, National Institute of Allergy and Infectious Diseases, NIH. E.B.A. is a scholar of Le Fonds de la Recherche en Santé du Québec. S.D. is a PhD Scholar of the Islamic Bank for Development. N.M. is a PhD Scholar of Le Fonds Québécois de la Recherche sur la Nature et les Technologies. H. Y. is a PhD Scholar of the Canadian Institutes for Health Research. We are grateful to Winship Herr for his generous gift of HCF-1 constructs and antibodies and to James J.D. Hsieh for his kind gift of MLL1 construct. We thank Elliot Drobetsky for the critical reading of the manuscript.

The authors declare no conflict of interest.

REFERENCES

Bottardi, S., et al. (2009), 'Ikaros and GATA-1 combinatorial effect is required for silencing of human gamma-globin genes', *Mol Cell Biol,* 29 (6), 1526-37.

Butkinaree, C., Park, K., and Hart, G. W. (2010), 'O-linked beta-N-acetylglucosamine (O-GlcNAc): Extensive crosstalk with phosphorylation to regulate signaling and transcription in response to nutrients and stress', *Biochim Biophys Acta,* 1800 (2), 96-106.

Capotosti, F., Hsieh, J. J., and Herr, W. (2007), 'Species selectivity of mixed-lineage leukemia/trithorax and HCF proteolytic maturation pathways', *Mol Cell Biol,* 27 (20), 7063-72.

Cheng, X. and Hart, G. W. (2001), 'Alternative O-glycosylation/O-phosphorylation of serine-16 in murine estrogen receptor beta: post-translational regulation of turnover and transactivation activity', *J Biol Chem,* 276 (13), 10570-5.

Davis, L. I. and Blobel, G. (1987), 'Nuclear pore complex contains a family of glycoproteins that includes p62: glycosylation through a previously unidentified cellular pathway', *Proc Natl Acad Sci U S A,* 84 (21), 7552-6.

Dejosez, M., et al. (2008), 'Ronin is essential for embryogenesis and the pluripotency of mouse embryonic stem cells', *Cell,* 133 (7), 1162-74.

Groisman, R., et al. (2003), 'The ubiquitin ligase activity in the DDB2 and CSA complexes is differentially regulated by the COP9 signalosome in response to DNA damage', *Cell,* 113 (3), 357-67.

Han, I. and Kudlow, J. E. (1997), 'Reduced O glycosylation of Sp1 is associated with increased proteasome susceptibility', *Mol Cell Biol,* 17 (5), 2550-8.

Hanover, J. A., et al. (1987), 'O-linked N-acetylglucosamine is attached to proteins of the nuclear pore. Evidence for cytoplasmic and nucleoplasmic glycoproteins', *J Biol Chem,* 262 (20), 9887-94.

Hsieh, J. J., et al. (2003), 'Proteolytic cleavage of MLL generates a complex of N- and C-terminal fragments that confers protein stability and subnuclear localization', *Mol Cell Biol,* 23 (1), 186-94.

Hu, P., Shimoji, S., and Hart, G. W. (2010), 'Site-specific interplay between O-GlcNAcylation and phosphorylation in cellular regulation', *FEBS Lett,* 584 (12), 2526-38.

Hurtado-Guerrero, R., Dorfmueller, H. C., and van Aalten, D. M. (2008), 'Molecular mechanisms of O-GlcNAcylation', *Curr Opin Struct Biol,* 18 (5), 551-7.

Jinek, M., et al. (2004), 'The superhelical TPR-repeat domain of O-linked GlcNAc transferase exhibits structural similarities to importin alpha', *Nat Struct Mol Biol,* 11 (10), 1001-7.

Julien, E. and Herr, W. (2003), 'Proteolytic processing is necessary to separate and ensure proper cell growth and cytokinesis functions of HCF-1', *EMBO J,* 22 (10), 2360-9.

Kelly, W. G., Dahmus, M. E., and Hart, G. W. (1993), 'RNA polymerase II is a glycoprotein. Modification of the COOH-terminal domain by O-GlcNAc', *J Biol Chem,* 268 (14), 10416-24.

Kristie, T. M. and Sharp, P. A. (1993), 'Purification of the cellular C1 factor required for the stable recognition of the Oct-1 homeodomain by the herpes simplex virus alpha-trans-induction factor (VP16)', *J Biol Chem,* 268 (9), 6525-34.

Kristie, T. M., Liang, Y., and Vogel, J. L. (2009), 'Control of alpha-herpesvirus IE gene expression by HCF-1 coupled chromatin modification activities', *Biochim Biophys Acta,* 1799 (3-4), 257-65.

Kurokawa, M. and Kornbluth, S. (2009), 'Caspases and kinases in a death grip', *Cell,* 138 (5), 838-54.

Liu, Y., Hengartner, M. O., and Herr, W. (1999), 'Selected elements of herpes simplex virus accessory factor HCF are highly conserved in Caenorhabditis elegans', *Mol Cell Biol,* 19 (1), 909-15.

Love, D. C., Krause, M. W., and Hanover, J. A. (2010), 'O-GlcNAc cycling: emerging roles in development and epigenetics', *Semin Cell Dev Biol,* 21 (6), 646-54.

Mahajan, S. S., Johnson, K. M., and Wilson, A. C. (2003), 'Molecular cloning of Drosophila HCF reveals proteolytic processing and self-association of the encoded protein', *J Cell Physiol,* 194 (2), 117-26.

Marshall, S., Okuyama, R., and Rumberger, J. M. (2005), 'Turnover and characterization of UDP-N-acetylglucosaminyl transferase in a stably transfected HeLa cell line', *Biochem Biophys Res Commun,* 332 (1), 263-70.

Nakatani, Y. and Ogryzko, V. (2003), 'Immunoaffinity purification of mammalian protein complexes', *Methods Enzymol,* 370, 430-44.

Sanders, M. M. (1978), 'Fractionation of nucleosomes by salt elution from micrococcal nuclease-digested nuclei', *J Cell Biol,* 79 (1), 97-109.

Slawson, C., Copeland, R. J., and Hart, G. W. (2010), 'O-GlcNAc signaling: a metabolic link between diabetes and cancer?', *Trends Biochem Sci,* 35 (10), 547-55.

Tyagi, S., et al. (2007), 'E2F activation of S phase promoters via association with HCF-1 and the MLL family of histone H3K4 methyltransferases', *Mol Cell,* 27 (1), 107-19.

Vercauteren, K., Gleyzer, N., and Scarpulla, R. C. (2008), 'PGC-1-related coactivator complexes with HCF-1 and NRF-2beta in mediating NRF-2(GABP)-dependent respiratory gene expression', *J Biol Chem,* 283 (18), 12102-11.

Vogel, J. L. and Kristie, T. M. (2000), 'Autocatalytic proteolysis of the transcription factor-coactivator C1 (HCF): a potential role for proteolytic regulation of coactivator function', *Proc Natl Acad Sci U S A,* 97 (17), 9425-30.

--- (2006), 'Site-specific proteolysis of the transcriptional coactivator HCF-1 can regulate its interaction with protein cofactors', *Proc Natl Acad Sci U S A,* 103 (18), 6817-22.

Wang, Z., et al. (2010), 'Extensive crosstalk between O-GlcNAcylation and phosphorylation regulates cytokinesis', *Sci Signal,* 3 (104 ra2), 1-22.

Wilson, A. C., Peterson, M. G., and Herr, W. (1995), 'The HCF repeat is an unusual proteolytic cleavage signal', *Genes Dev,* 9 (20), 2445-58.

Wilson, A. C., et al. (2000), 'HCF-1 amino- and carboxy-terminal subunit association through two separate sets of interaction modules: involvement of fibronectin type 3 repeats', *Mol Cell Biol,* 20 (18), 6721-30.

Wysocka, J., et al. (2003), 'Human Sin3 deacetylase and trithorax-related Set1/Ash2 histone H3-K4 methyltransferase are tethered together selectively by the cell-proliferation factor HCF-1', *Genes Dev,* 17 (7), 896-911.

Yang, X., et al. (2001), 'O-linkage of N-acetylglucosamine to Sp1 activation domain inhibits its transcriptional capability', *Proc Natl Acad Sci U S A,* 98 (12), 6611-6.

Zhang, F., et al. (2003), 'O-GlcNAc modification is an endogenous inhibitor of the proteasome', *Cell,* 115 (6), 715-25.

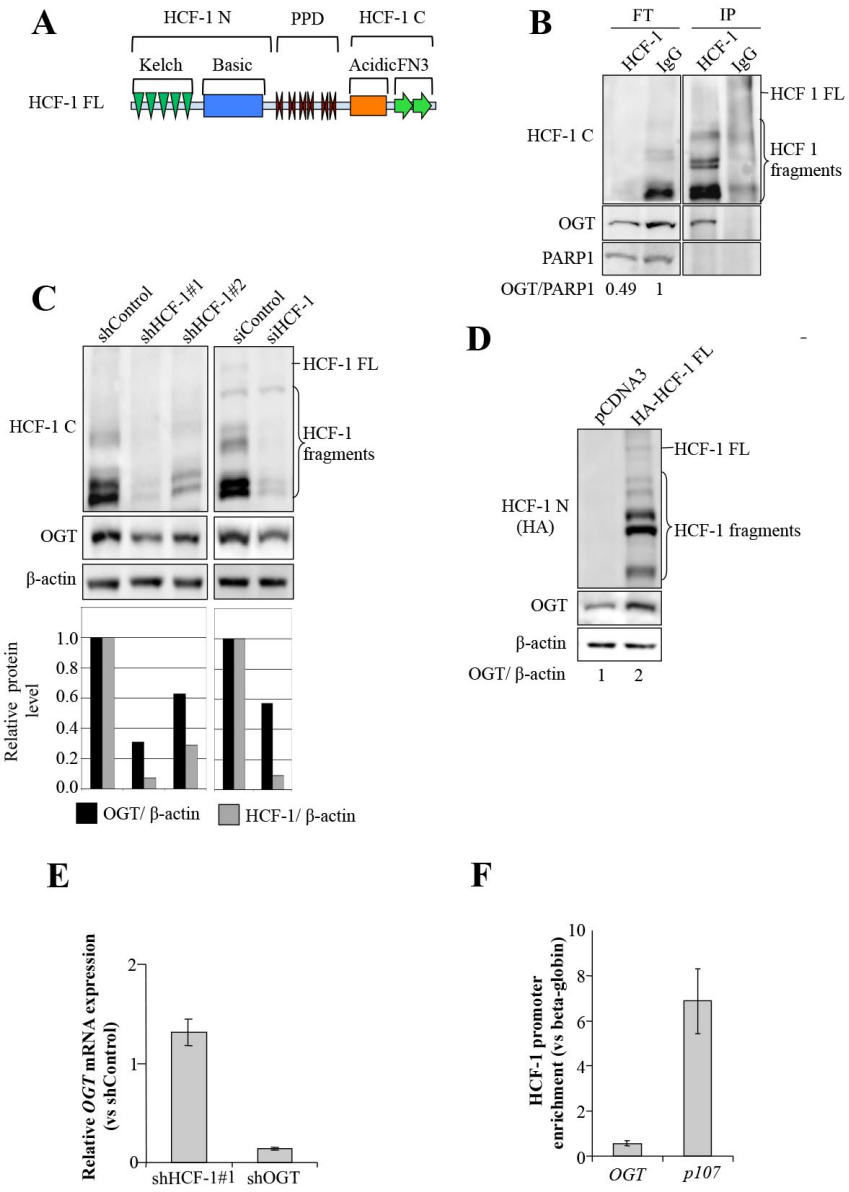

Figure 1

HCF-1 is required for the maintenance of proper OGT levels.

(**A**) Schematic representation of the domains of the human HCF-1. (**B**) Immunodepletion of HeLa nuclear extracts using anti-HCF-1. OGT and HCF-1 were detected in the HCF-1 immunoprecipitate (IP) and flow through (FT) by western blot. The nuclear protein PARP1 was used as a negative control. Quantification of OGT was done relative to PARP1. (**C**)

Depletion of HCF-1 using shRNA plasmids or siRNA oligonucleotide pools induces OGT downregulation. Quantification of OGT or HCF-1 was done relative to β-actin. (**D**) Overexpression of HCF-1 increases OGT protein levels. HeLa cells were transfected with HCF-1 FL and 2 days post-transfection, cells were harvested for immunoblotting. (**E**) *OGT* mRNA is not affected by HCF-1 depletion. U2OS cells mRNAs were isolated and cDNAs were quantitated by qRT-PCR relative to *GAPDH*. shRNA for OGT was included as an internal control. All experiments were repeated at least 3 times and the data are presented as mean ± SD. (**F**) Promoter occupancy by HCF-1. ChIP assays were done using U2OS cell chromatin and anti-HCF-1 or IgG control. The enrichment of factors was calculated relative to the occupancy of the *β-globin* promoter. All experiments were repeated at least 3 times and data are presented as mean ± SD.

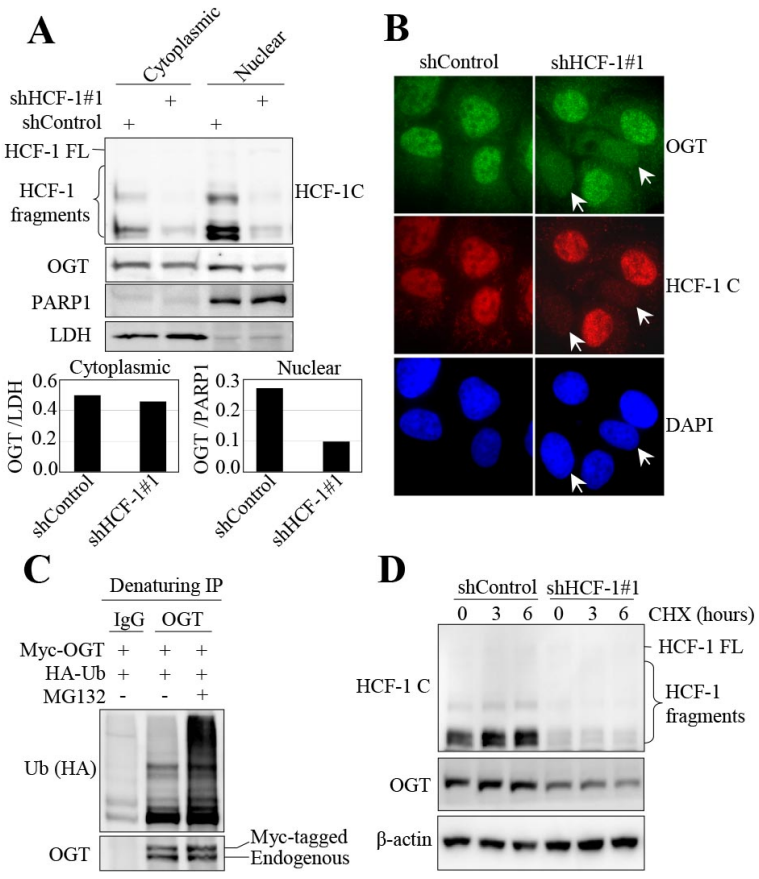

Figure 2

HCF-1 regulates the stability of OGT.

Nuclear OGT is preferentially downregulated following HCF-1 depletion (A-B). (**A**) Biochemical fractionation of nuclear and cytoplasmic compartments following HCF-1 knockdown in U2OS. PARP1 and LDH, which are localized in the nucleus and cytoplasm, respectively, were used as controls for fractionation. Quantification of cytoplasmic versus nuclear OGT was done relative to LDH or PARP1, respectively. (**B**) Immunofluorescence

detection of OGT in U2OS cells following HCF-1 knockdown. (**C**) OGT is ubiquitinated and regulated by proteasomal degradation. 293T cells were transfected with Myc-OGT and HA-ubiquitin (HA-Ub). Two days post-transfection, cells were treated with 20 μM MG132 for 4 hours prior to harvesting for immunoprecipitation and western blotting. (**D**) OGT protein stability is decreased following HCF-1 depletion. U2OS cells were transfected with HCF-1 shRNA plasmids. Three days later, cells were treated with CHX (100 μg/ml) and harvested for western blotting.

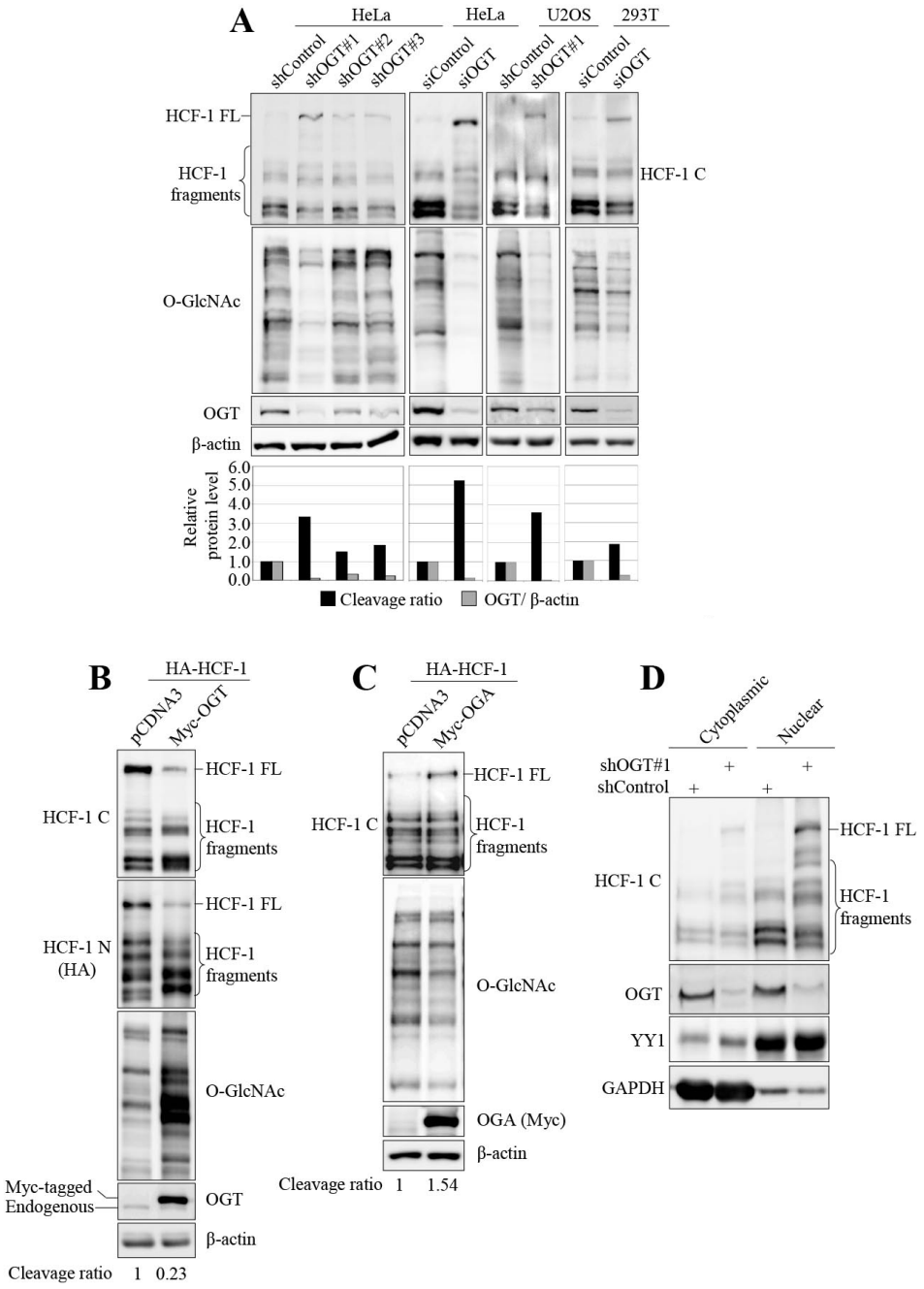

Figure 3

OGT is required for HCF-1 proteolytic cleavage.

(**A**) OGT depletion induces accumulation of the HCF-1 precursor with a decrease in the levels of the cleaved forms. Cells were transfected with either OGT shRNA or OGT siRNA oligonucleotide pools and harvested for western blotting. Quantification of OGT is relative to β-actin. The HCF-1 cleavage ratio was estimated by dividing the signal value of the precursor by the sum of the signal values of the cleaved forms. (**B**) Overexpression of OGT promotes HCF-1 cleavage. 293T cells were transfected with either pcDNA3 control or Myc-OGT along with HA-HCF-1 FL. Two days post-transfection, cells were harvested for western blotting. (**C**) Overexpression of OGA inhibits HCF-1 cleavage. 293T cells were transfected with either pcDNA3 control or Myc-OGA along with HA-HCF-1 FL. Two days post-transfection, cells were harvested for western blotting. (**D**) Subcellular fractionation following knockdown of OGT. HeLa cells were transfected with OGT shRNA plasmids and harvested for fractionation and western blotting. YY1 and GAPDH were used as markers for nucleus and cytoplasm, respectively.

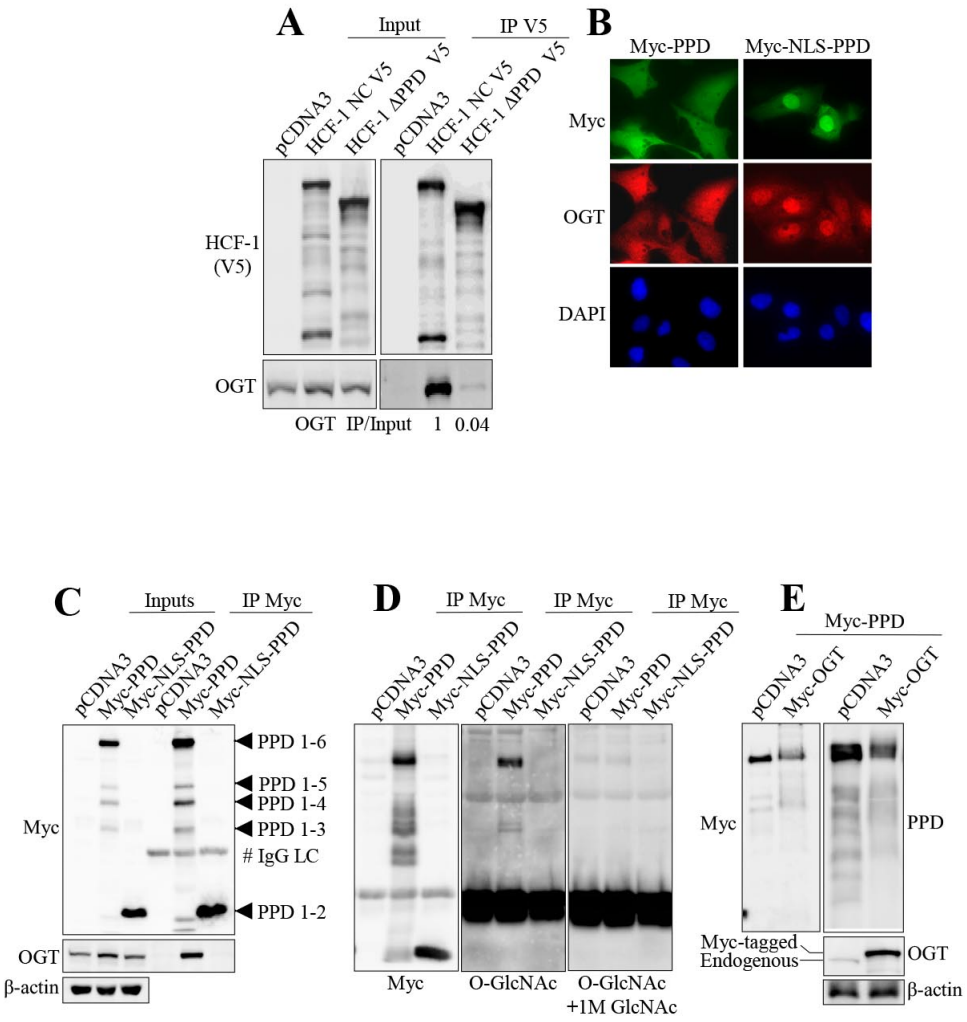

Figure 4

OGT interacts with HCF-1 PPD and mediates its cleavage.

(**A**) Interaction of OGT with HCF-1 lacking PPD or HCF-1 FL. 293T cells were transfected with either HCF-1 NC V5 or HCF-1 ΔPPD V5. Two days post-transfection, total cell

extracts were used for immunoprecipitation using an anti-V5. (**B**) Immunofluorescence localization of PPD with or without a nuclear localization signal. U2OS cells were transfected with either Myc-PPD or Myc-NLS-PPD. Two days post-transfection, cells were used for immunostaining using an anti-Myc. (**C**) Interaction of PPD with OGT. 293T cells were transfected with either Myc-PPD or Myc-NLS-PPD. Two days post-transfection, total cell extracts were used for immunoprecipitation using an anti-Myc. (**D**) O-GlcNAcylation of PPD with OGT. 293T cells were transfected with either Myc-PPD or Myc-NLS-PPD and Myc-OGT. Two days post-transfection, total cell extracts were used for immunoprecipitation under denaturing conditions using an anti-Myc. To ensure the specificity of signal, the O-GlcNAc antibody was pre-incubated for 1 H with 1 M of N-acetylglucosamine before being applied to the membrane. (**E**) Overexpression of OGT promotes PPD proteolytic cleavage. 293T cells were transfected with Myc-PPD along with pCDNA3 or Myc-OGT. Two days post-transfection, total cell extracts were used for immunoblotting.

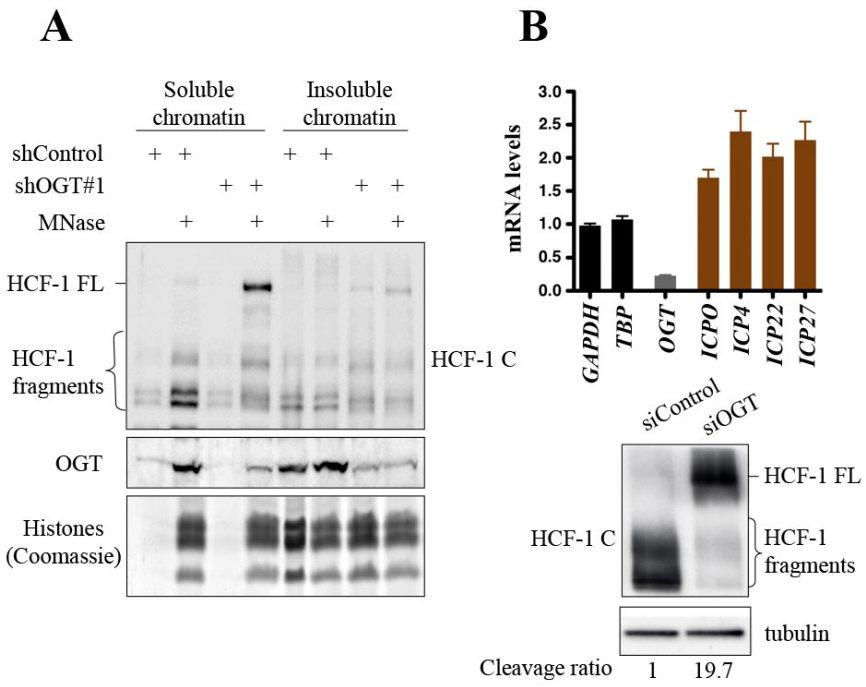

Figure 5

Uncleaved HCF-1 associates with chromatin and enhances HCF-1-mediated viral gene expression.

(**A**) HCF-1 precursor is associated with chromatin. HeLa were transfected with either non-targeting control or OGT shRNA plasmids. Three days post-transfection, cells were harvested for cell fractionation. The chromatin/nuclear matrix fraction was treated with micrococcal nuclease (MNase) to release nucleosomes. Proteins were detected in the soluble and pellet fractions by immunoblotting or coomassie blue staining. (**B**) HFF cells were transfected with control or OGT siRNAs. Three days post transfection, cells were infected with 0.1 PFU HSV-1 and harvested for mRNA analysis (top panel) and immunoblotting (bottom panel). Levels of control cellular (*GAPDH and TBP*), *OGT*, and viral IE mRNAs in OGT depleted cells are shown relative to levels in control siRNA

transfected cells. All experiments were repeated at least 3 times and data are presented as mean ± SD.

SUPPLEMENTAL INFORMATION

Supplemental Information contains additional methods; thirteen figures; the sequences of the OGT and HCF-1 shRNA constructs and additional references.

SUPPLEMENTARY FIGURES

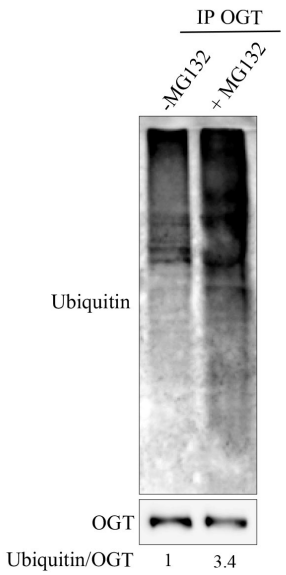

Figure S1.

Endogenous OGT is ubiquitinated and degraded by the proteasome.

293T cells were treated with 20 μM MG132 for 10 hours. Denatured whole cell extracts were used to immunoprecipitate OGT which was subjected to immunoblotting with the indicated antibodies.

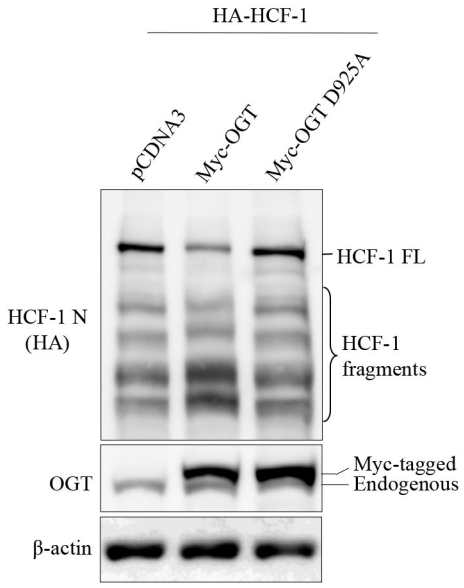

Figure S2.

OGT regulates HCF-1 cleavage in catalytic activity-dependent manner.

293T cells were transfected with HA-HCF-1 FL expression plasmid along with pCDNA3, Myc-OGT or Myc-OGT D925A. Two days post-transfection, total cell extracts were used for immunoblotting with the indicated antibodies.

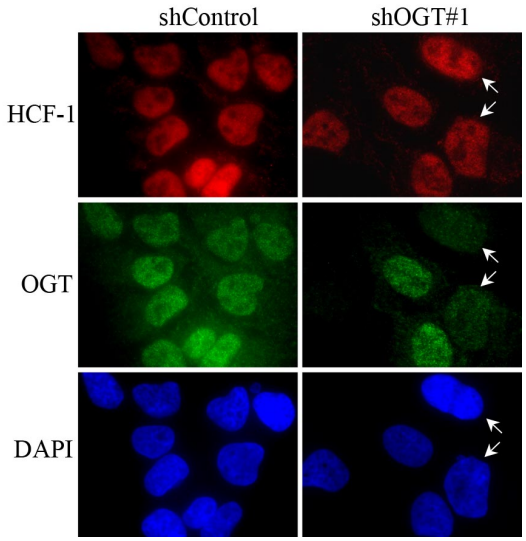

Figure S3.

Depletion of OGT does not interfere with HCF-1 nuclear import.

Immunofluorescence detection of HCF-1 following knockdown of OGT. U2OS cells were transfected with either non-targeting control or OGT shRNA plasmid for 3 days prior to fixation and immunostaining. Arrows indicate cells depleted for OGT.

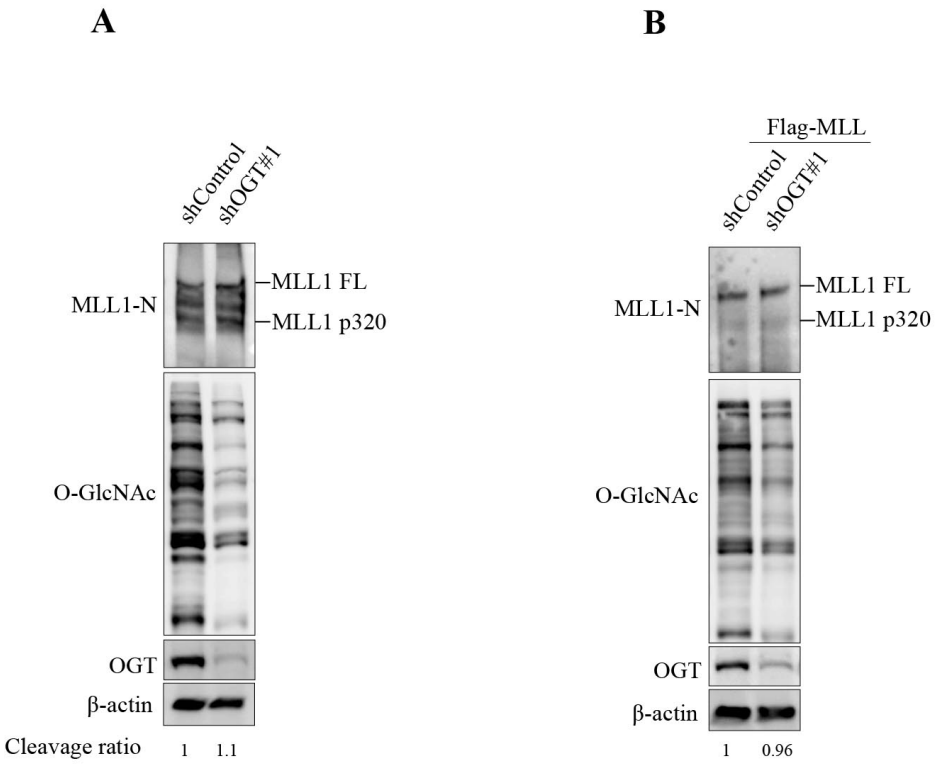

Figure S4.

OGT is not required for proteolytic cleavage of mixed lineage leukaemia MLL1.

(**A**) HeLa cells were transfected with either non-targeting control or OGT shRNA plasmids. Three days post-transfection, cells were harvested for immunoblotting. (**B**) HeLa cells were transfected with either non-targeting control or OGT shRNA plasmids along with Flag-MLL1 expression plasmid. Three days post-transfection, cells were harvested for western blotting.

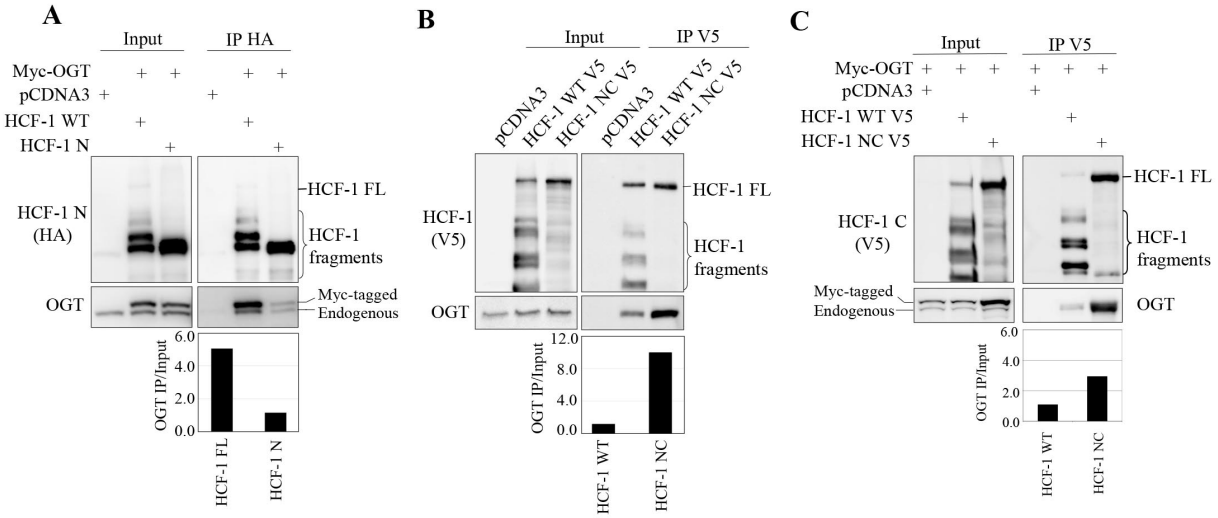

Figure S5.

OGT interacts more efficiently with the HCF-1 precursor.

(**A**) Interaction of OGT with HCF-1 N subunit or HCF-1 FL. HeLa cells were transfected with either HA-HCF-1 FL or HA-HCF-1 N (1-1010 aa) along with Myc-OGT. Two days post-transfection, total cell extracts were used for immunoprecipitation using anti-HA and immunoblotting using the indicated antibodies. The efficiency of interaction was determined by densitometry quantification of OGT in the IP fraction versus OGT in the input cell extract for each condition. Note that transfected cells with both Myc-OGT and HCF-1 show a substantial increase in the levels of transfected OGT. In contrast, the signal of endogenous OGT is not significantly changed between control and HCF-1 conditions as the ratio of non-transfected cells versus transfected cells is high. (**B**) Interaction of OGT with uncleaved HCF-1 or HCF-1 FL. 293T cells were transfected with either HCF-1 FL V5 or HCF-1 NC V5 and used for immunoprecipitation using anti-V5. The efficiency of interaction was determined as in panel A. (**C**) Interaction of overexpressed OGT with uncleaved HCF-1 or HCF-1 FL. 293T cells were transfected with either HCF-1 FL V5 or

HCF-1 NC V5 expression plasmids along with Myc-OGT. Two days post-transfection, total cell extracts were used for immunoprecipitation using an anti-V5. The immunocomplexes were subjected to western blotting. The efficiency of interaction was determined as in panel A. We note that: (i) large HCF-1 fragments containing portions of PPD interact more with OGT than HCF-1 N terminal subunit (ii) the uncleaved full length HCF-1 containing intact PPD interacts more efficiently with OGT than HCF-1 cleaved fragments.

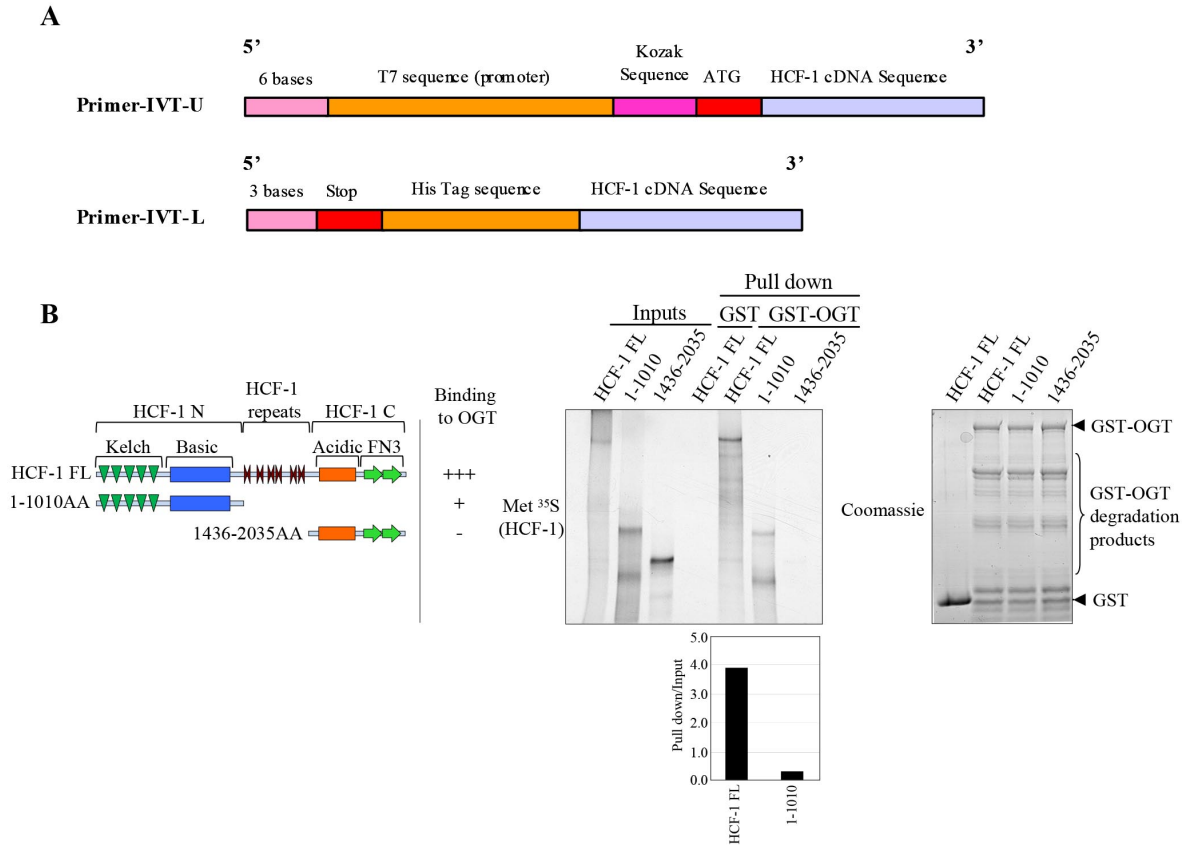

Figure S6.

Interaction *in vitro* between OGT and HCF-1 FL, HCF-1 N or HCF-1 C subunits.

(**A**) Schematic representation of primers design for IVT of HCF-1 fragments. (**B**) HCF-1 full length interacts more efficiently with OGT than HCF-1 cleaved fragments. GST-tagged OGT bound to GSH beads was incubated with various fragments of *in vitro* translated ^{35}S labeled-HCF-1 for 8 hours. Following extensive washes, the bead-associated complexes were analyzed by coomassie blue staining for GST-OGT and autoradiography for HCF-1. The efficiency of interaction was determined by densitometry quantification of OGT in the pull down fraction versus OGT in the input fraction for each interaction. These *in vitro* studies indicate that OGT interacts with the N-terminus subunit of HCF-1. We note that the full-length HCF-1 (with intact PPD) interacts more strongly with OGT comparatively to HCF-1 N subunit.

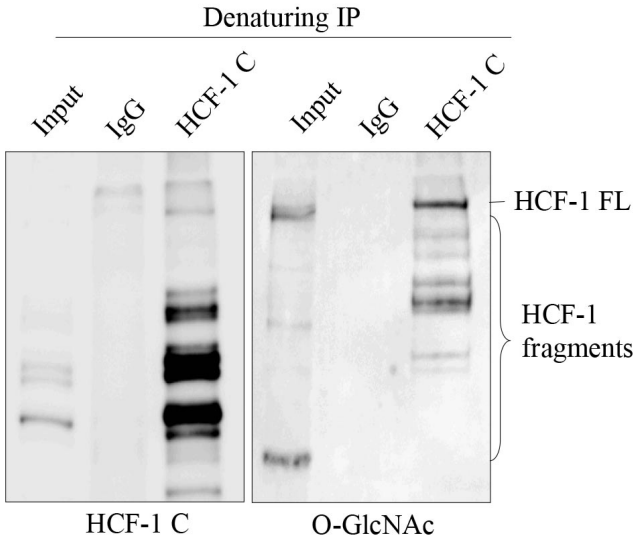

Figure S7.

The HCF-1 precursor is O-glycosylated.

U2OS cell extracts were used for immunoprecipitation under denaturing conditions with an anti-HCF-1 C-terminal antibody. The immunocomplexes were used for western blotting with the indicated antibodies.

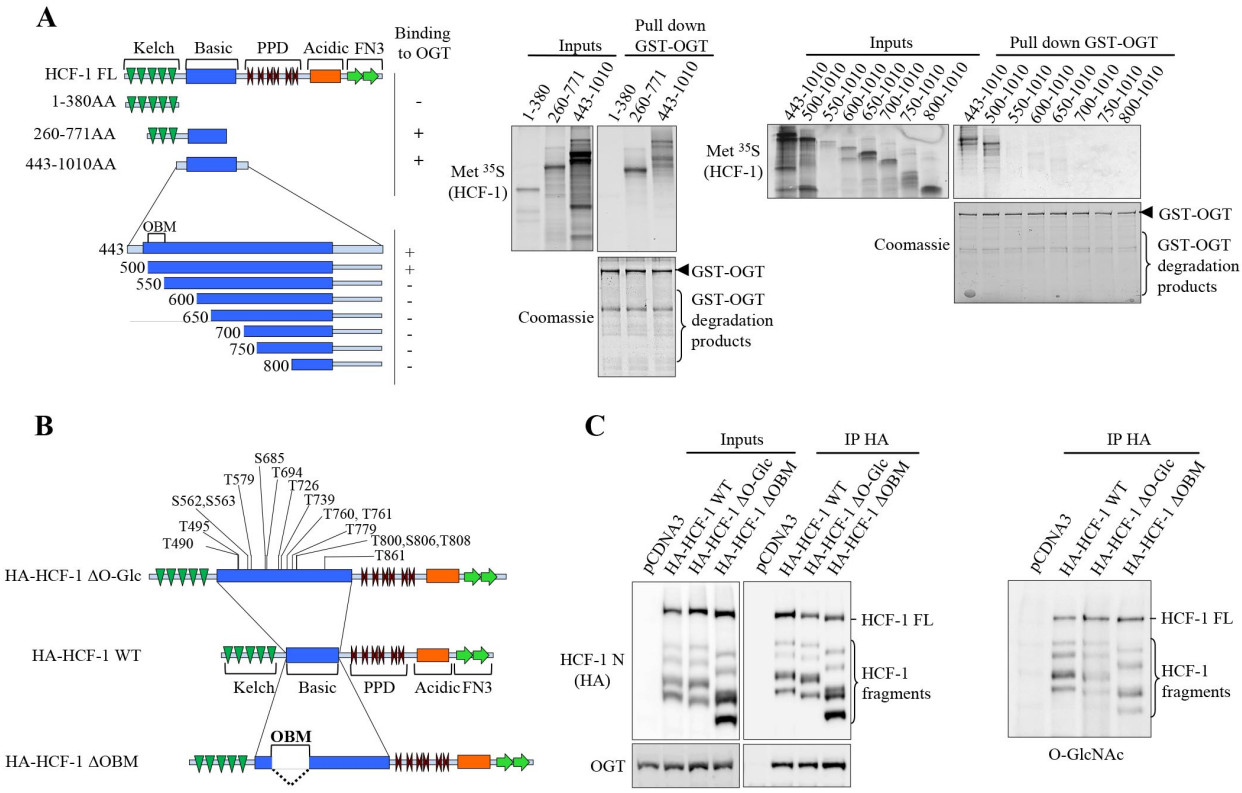

Figure S8.

HCF-1 N-terminal subunit interaction with OGT or its O-GlcNAcylation are not required for HCF-1 proteolytic cleavage.

(**A**) Identification of OGT-binding domain in HCF-1 N. GST-tagged OGT bound to GSH beads was incubated with various fragments of *in vitro* translated ^{35}S labeled-HCF-1. The bead-associated complexes were analyzed by coomassie blue staining for GST-OGT and HCF-1 was analyzed by autoradiography. (**B**) Schematic representation of the S/T O-GlcNAcylation residues mutated in HCF-1 (HA-HCF-1 ΔO-Glc) and the deleted OGT-binding motif OBM in HCF-1 (HA-HCF-1 ΔOBM). (**C**) O-GlcNAcylation status, proteolytic processing and interaction of HCF-1 mutants with OGT. 293T cells were transfected with HA-HCF-1 WT, HA-HCF-1 ΔOBM or HA-HCF-1 ΔO-Glc. Two days post-transfection, cells were harvested for immunoprecipitation using an anti-HA. We note that O-glycosylation of HCF-1 N subunit does not appear to play a role in HCF-1 cleavage

since (i) mutation of multiple glycosylation sites in the N-terminal subunit or (ii) deletion of the OGT-interacting motif in this subunit does not affect HCF-1 maturation. Thus the N-terminal subunit, although it provides a distinct domain of interaction with OGT, is dispensable for HCF-1 cleavage. It remains possible that the interaction of the HCF-1 N-terminal subunit with OGT is important for other HCF-1 functions that are distinct from the role of OGT in HCF-1 proteolytic processing.

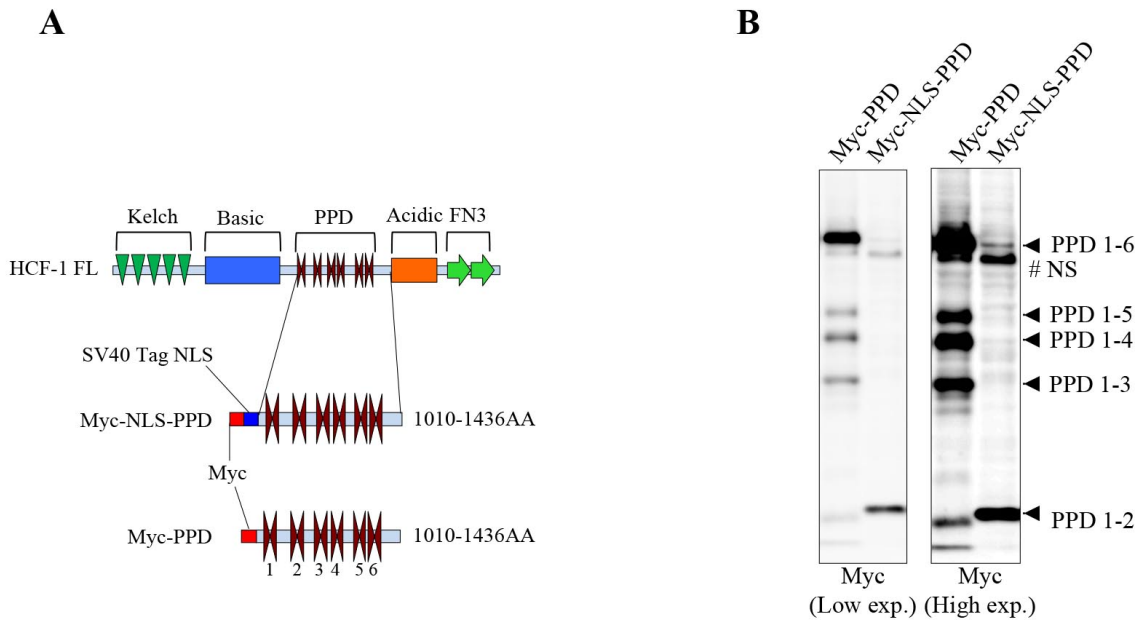

Figure S9.

Expression of HCF-1 PPD with or without a nuclear localization signal.

(**A**) Schematic representation of human HCF-1 showing the PPD with the designed constructs.

(**B**) 293T cells were transfected with either Myc-PPD or Myc-NLS-PPD expression plasmids. Two days post-transfection, total cell extracts were used for immunoblotting with anti-Myc antibody. NS, non specific band.

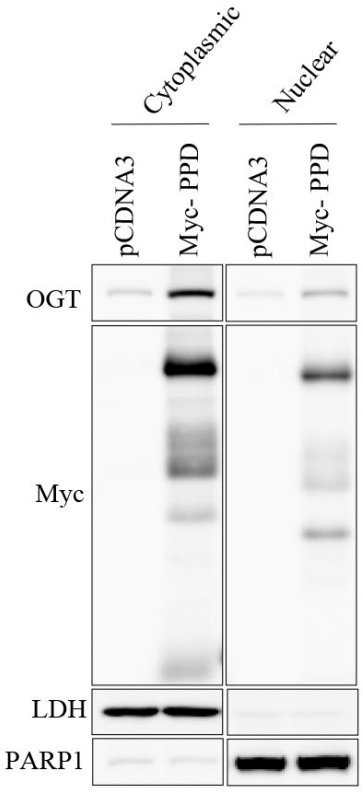

Figure S10.

HCF-1 PPD stabilizes OGT in the cytoplasm.

293T cells were transfected with Myc-PPD or Myc-NLS-PPD expression plasmids along with Myc-OGT expression plasmid. Forty-eight hours later, cells were homogenized using a dounce homogenizer to separate cytoplasm and nuclei. Homogenates was centrifuged at 3500 g for 15 min, and the cytoplasmic fraction (supernatant) and nuclear fraction (pellet) were collected. Fractions were subjected to immunoblotting with the indicated antibodies. PARP1 and LDH, which are localized in the nucleus and cytoplasm, respectively, were used as controls for fractionation.

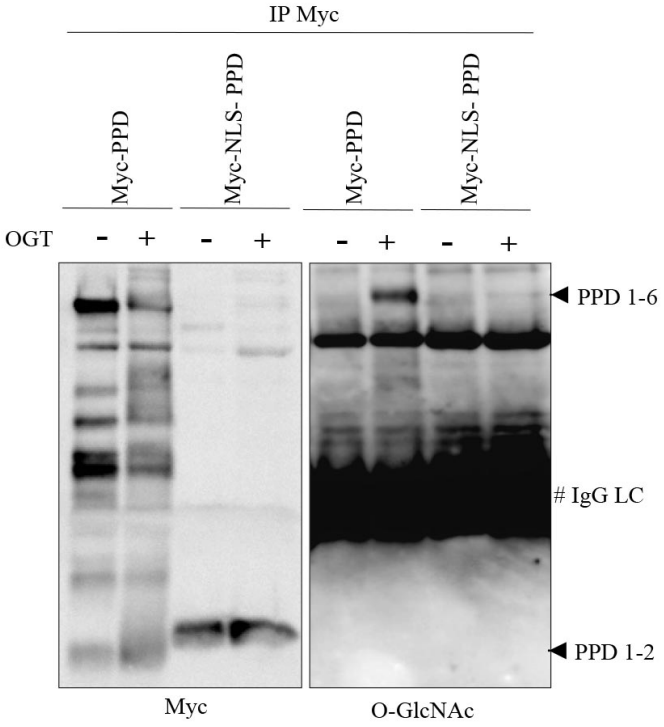

Figure S11.

O-GlcNAcylation of HCF-1 PPD is dependent on OGT.

293T cells were transfected with Myc-PPD or Myc-NLS-PPD expression plasmids along with OGT expression plasmid or pCDNA3. Forty-eight hours later, extracts of the cells were subjected to IP in denaturing conditions with anti-Myc antibody. Samples were analyzed by immunoblotting with the indicated antibodies.

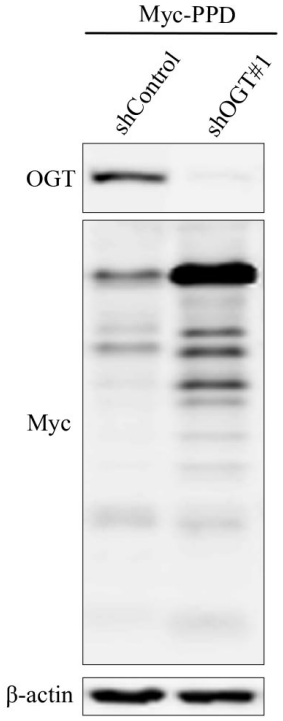

Figure S12.

RNAi of OGT inhibits cleavage of HCF-1 PPD.

HeLa cells were transfected with the indicated shRNA constructs along with Myc-PPD plasmid and pBABE-puro. The next day, the cells were selected with 2 μg/ml of puromycin for 48 hours. Following selection, the cells were harvested and subjected to immunoblotting with the indicated antibodies.

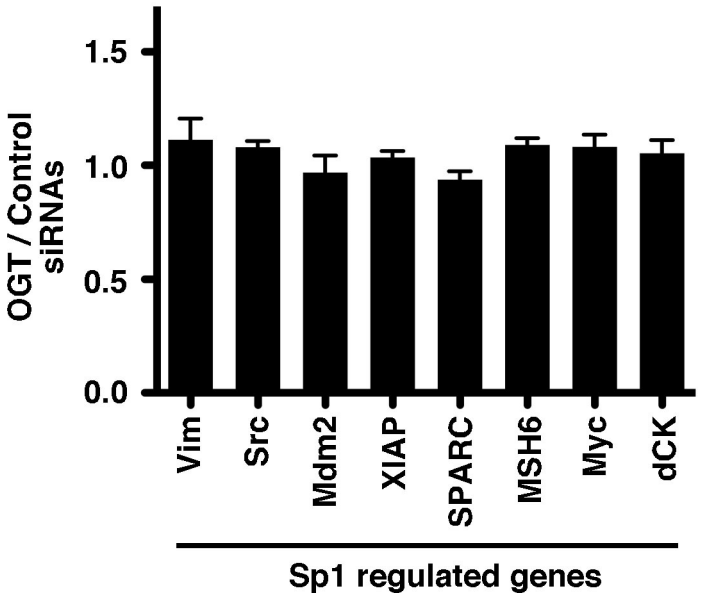

Figure S13.

Depletion of OGT does not affect Sp1 target gene expression.

HFF cells were transfected with control or OGT siRNAs. Three days post transfection, cells were infected with 0.1 PFU HSV-1 and harvested for mRNA analysis. Levels of Sp1 target gene mRNAs in OGT-depleted cells are shown relative to levels in control siRNA transfected cells. All experiments were repeated at least 3 times and data are presented as mean ± SD.

MATERIALS AND METHODS

Plasmids and Antibodies

shRNA constructs for human *OGT* or *HCF-1* were generated as described previously (Sui et al. 2002). The cDNAs of human *OGT* and *OGA* were cloned from HeLa cell RNA by RT-PCR. GST-OGT was generated by subcloning the *OGT* cDNA into pGEX-4T1 vector. Mammalian constructs to express N-terminal Myc-tagged OGT or OGA were generated by subcloning into the pDEST-N-Myc Gateway® plasmid (Invitrogen). The Myc-OGT D925A catalytic inactive mutant (Clarke et al. 2008) was generated by site-directed mutagenesis. The HCF-1 N (1-1010 aa) containing mutations in the O-glycosylation sites (S/T to A) was generated by direct gene synthesis (Biobasic Inc), and introduced into pCDNA3 (HA-HCF-1 FL ΔO-Glc). The HCF-1 lacking the OGT-binding motif (HA-HCF-1 ΔOBM) was generated by PCR-based subcloning into pCDNA3. The plasmids pCGN-HCF-1 FL and pCGN-HCF-1 N1011 were generously provided by Dr. Herr (Wilson et al. 1993; Wilson et al. 2000). The Myc-PPD and Myc-NLS-PPD expression constructs were generated by PCR-based subcloning of HCF-1 sequence (3028-4305 bp) into pDEST-N-Myc. The expression vectors V5-tagged wildype HCF-1 and the uncleavable HCF-1 have been described (Vogel and Kristie 2006). The HCF-1 D PPD V5 containing a deletion of the PPD (998-1456 aa) was derived from the WT HCF-1 (23). A plasmid containing the full length MLL1 was kindly provided by Dr. Hsieh (Hsieh et al. 2003). The anti-HCF-1 PPD antibody has been described (Kristie et al. 1995; Kristie 1997). Additional antibodies were as follows: anti-HCF-1 (A301-400A) and anti-MLL1-N300 (A300-086A), Bethyl Laboratories; anti-βactin (MAB1501) and GAPDH (MAB374), Millipore; anti-OGT (H300, sc-32921)**,** anti-OGT (A6, sc-74547), anti-ubiquitin (P4D1, sc-8017), anti-PARP-1 (F2, sc-8007), anti-YY1 (H10, sc-7341) and rabbit IgG (sc-2027), Santa Cruz Biotechnology; anti-O-Linked N-Acetylglucosamine (RL2, GTX22739), GeneTex; anti-HA (16B12, MMS-101P), anti-c-Myc (MMS-150P), Covance; anti-V5 (SV5, ab27671), Abcam.

Cell culture, RNAi and immunoblotting

HeLa, U2OS and HEK293T (293T) cells were maintained according to standard culture protocols. Cells were transfected with either 5 μg of non-targeting control or RNA interference plasmids (shRNA) along with 0.2 μg pBABE puromycin resistance-encoding vector using Lipofectamine 2000 (Invitrogen). The transfected cells were selected after 1 day by adding 2 μg/ml of puromycin for HeLa and 3 μg/ml for U2OS and 293T, for 2 additional days as described (Affar et al. 2006). For siRNA, cells were transfected with either 200 pmol of non-targeting control, *hOGT* (L-019111-00) or *hHCF-1* (L-019953-00) siRNAs ON-TARGETplus SMARTpool (Dharmacon). Three days post-transfection, cells were harvested for western blotting. HFF cells were transfected with control or OGT siRNAs. Three days post-transfection, cells were infected with 0.1 PFU HSV-1 and harvested for mRNA analysis and western blotting. Total cell extracts were prepared in lysis buffer (50 mM Tris-HCl, pH 7.3; 5 mM EDTA; 50 mM KCl; 0.1% NP-40; 1 mM phenylmethylsulfonyl fluoride (PMSF); 1 mM dithiothreitol and protease inhibitors cocktail (Sigma), and protein concentration was determined by Bradford assay. SDS-PAGE and Western blotting were done according to standard procedures. The band signals were acquired with a LAS-3000 LCD camera coupled to MultiGauge software (Fuji, Stamford, CT, USA). Densitometric analysis of protein bands and radioautographs were done using Gel-Pro Analyzer 3.1 (Media Cybernetics Inc).

Immunodepletion and Immunoprecipitation

Immunodepletion of nuclear extracts was conducted using HeLa nuclear extracts (~100 μg of proteins) incubated overnight at 4 ºC with 2 μg of anti-HCF-1 (A301-400A) or control IgG in IP buffer (50 mM Tris, pH 7.3; 150 mM NaCl; 5 mM EDTA; 10 mM NaF; 1% Triton X-100; 1 mM PMSF and protease inhibitors cocktail (Sigma)). The immuno-complexes were collected on protein A agarose beads which were saturated with 1% BSA in IP buffer. Immuno-complexes were washed twice with the IP buffer supplemented with 1% BSA. Bound proteins were eluted and subjected, along with the flow through fractions,

to western blotting. Co-immunoprecipitations to determine proteins interactions and O-GlcNAc protein modification levels were conducted essentially as described above using 2 mg of total cell lysates prepared in lysis buffer (50 mM Tris, pH 7.3; 150 mM NaCl; 5 mM EDTA; 10 mM NaF; 1% Triton X-100; 1 mM PMSF, protease inhibitors cocktail (Sigma) and 10 μM *PUGNAc* (*Toronto* Research Chemicals). Denaturing immunoprecipitations were done using the same lysis buffer containing 300 mM NaCl and 1% SDS. After boiling for 3 mins, the samples were diluted 10 fold with the same buffer used above without SDS prior to immunoprecipitation.

***In vitro* interaction assays**

Recombinant GST-OGT fusion protein was purified using glutathione agarose beads (Sigma) and 2 to 3 μg of beads containing bound proteins were incubated with 10 μl of *in vitro* translated *methionine-*^{35}S labelled HCF-1 (*TNT*® T7 Quick Coupled Transcription/Translation System, Promega) for 6 to 8 hours at 4 ºC in 50 mM Tris, pH 7.5; 50 mM NaCl; 0.02% Tween 20; 1 mM PMSF and 500 μM dithiothreitol). The beads were extensively washed with the same buffer, and bound proteins eluted in Laemmli buffer and subjected to autoradiography or western blotting. The primers used for the amplification of **HCF-1 fragments used IVT assays are provided below.**

Immunofluorescence

Cells were fixed for 20 min using 3 % paraformaldehyde in phosphate-buffered saline (PBS), permeabilized in PBS containing 0.5 % NP-40 for 20 min. Following incubation in blocking solution (PBS containing 0.1% NP-40 and 10% FBS), cells were stained with the polyclonal anti-HCF-1 **(A301-400A)**, **the monoclonal anti-OGT** (A6) or the monoclonal anti-c-Myc (MMS-150P). Anti-mouse Alexa Fluor® 594 or Alexa Fluor® 488, and Anti-rabbit Alexa Fluor® 488 or Alexa Fluor® 594 (Invitrogen) were used as secondary antibodies. Nuclei were stained with 4', 6-diamidino-2-phenylindole (DAPI). Images were acquired using Leica DMRE microscope, HCX PL APO 63X/ 1.32-0.6 OIL CS objective and Retiga Ex (Qimaging) camera.

mRNA expression analysis

RNA was prepared using Trizol reagent (Invitrogen) and the RNeasy kit (QIAGEN). Total mRNA was used for reverse transcription using the Superscript III reverse transcriptase and oligo$(dT)_{12\text{-}18}$ primers (Invitrogen). The obtained cDNAs were subjected to Real time PCR using SYBR Green detection kit (Invitrogen) to determine levels of individual mRNAs. PCR was conducted on an iCycler iQ apparatus (Bio-Rad). The primers used are listed below.

Chromatin immunoprecipitation analysis

Chromatin immunoprecipitation (ChIP) experiments were done essentially as previously described (Bottardi et al. 2009) with the following modifications. U2OS cells (5×10^6) were incubated with EGS (ethylene glycolbis [succnimidyl succinate], Sigma-Aldrich) as described (Nowak et al. 2005; Zeng et al. 2006) and were cross-linked with 1% formaldehyde in PBS for 10 min. Following quenching with glycine, cells were scraped in cold PBS, washed with buffer A (50 mM Tris-HCl, pH 8.0; 0.1% NP40; 2 mM EDTA; 10% glycerol; 1 mM PMSF and protease inhibitors cocktail, Sigma) and then sonicated in Buffer B (50 mM Tris-HCl, pH 8.0; 1% SDS; 10 mM EDTA; 1 mM PMSF and protease inhibitors cocktail). After centrifugation and pre-clearing, the suspension was incubated with anti-HCF-1 (A301-400A) or an IgG control. DNA was purified from immunocomplexes and quantitated by qPCR using the $2^{-\Delta\Delta^{CT}}$ method, where $\Delta\Delta$CT is calculated as follows: (ChIP CT– input CT of the control antibody) – (ChIP CT – input CT of the target antibody). The results are shown as a ratio of target gene promoter to a reference gene promoter. The primers are listed below.

SUPPLEMENTAL REFERENCES

Affar, E. B., et al. (2006), 'Essential dosage-dependent functions of the transcription factor Yin Yang 1 in late embryonic development and cell cycle progression', *Mol. Cell Biol.,* 26 (9), 3565-81.

Bottardi, S., et al. (2009), 'Ikaros and GATA-1 combinatorial effect is required for silencing of human gamma-globin genes', *Mol Cell Biol,* 29 (6), 1526-37.

Clarke, A. J., et al. (2008), 'Structural insights into mechanism and specificity of O-GlcNAc transferase', *EMBO J,* 27 (20), 2780-8.

Hsieh, J. J., Cheng, E. H., and Korsmeyer, S. J. (2003), 'Taspase1: a threonine aspartase required for cleavage of MLL and proper HOX gene expression', *Cell,* 115 (3), 293-303.

Kristie, T. M. (1997), 'The mouse homologue of the human transcription factor C1 (host cell factor). Conservation of forms and function', *J Biol Chem,* 272 (42), 26749-55.

Kristie, T. M., et al. (1995), 'The cellular C1 factor of the herpes simplex virus enhancer complex is a family of polypeptides', *J Biol Chem,* 270 (9), 4387-94.

Nowak, D. E., Tian, B., and Brasier, A. R. (2005), 'Two-step cross-linking method for identification of NF-kappaB gene network by chromatin immunoprecipitation', *Biotechniques,* 39 (5), 715-25.

Sui, G., et al. (2002), 'A DNA vector-based RNAi technology to suppress gene expression in mammalian cells', *Proc. Natl. Acad. Sci. U. S. A.,* 99 (8), 5515-20.

Vogel, J. L. and Kristie, T. M. (2006), 'Site-specific proteolysis of the transcriptional coactivator HCF-1 can regulate its interaction with protein cofactors', *Proc Natl Acad Sci U S A,* 103 (18), 6817-22.

Wilson, A. C., et al. (1993), 'The VP16 accessory protein HCF is a family of polypeptides processed from a large precursor protein', *Cell,* 74 (1), 115-25.

Wilson, A. C., et al. (2000), 'HCF-1 amino- and carboxy-terminal subunit association through two separate sets of interaction modules: involvement of fibronectin type 3 repeats', *Mol Cell Biol,* 20 (18), 6721-30.

Zeng, P. Y., et al. (2006), 'In vivo dual cross-linking for identification of indirect DNA-associated proteins by chromatin immunoprecipitation', *Biotechniques,* 41 (6), 694, 96, 98.

Autodeubiquitination protects the tumor suppressor BAP1 from cytoplasmic sequestration mediated by the atypical ubiquitin ligase UBE2O [Ω]

Nazar Mashtalir[1], Salima Daou[1], Haithem Barbour[1], Nadine N Sen[1], Jessica Gagnon[1], Ian Hammond-Martel[1], Haider H Dar[1], Marc Therrien[2] and El Bachir Affar[1,3]

[1]Maisonneuve-Rosemont Hospital Research Center, Department of Medicine, University of Montréal, QC, Montréal, H1T 2M4, Canada

[2]Institute for Research in Immunology and Cancer, Laboratory of Intracellular Signaling, University of Montréal, Montréal, QC, H3T 1J4, Canada

[3]Correspondence

Running title: UBE2O ligase regulates the tumor suppressor BAP1.

I contributed to this study as first author. Experimentally I contributed to 89% of the figures. I have conceptual contribution to most findings of the study. I wrote the initial manuscript (Result section, figure legends, materials and methods and part of discussion), prepared the manuscript for submission and performed majority of the experiments for article revision.

Ω-This paper was published in Molecular Cell in April 2014.

SUMMARY

The tumor suppressor BAP1 interacts with chromatin-associated proteins and regulates cell proliferation, but its mechanism of action and regulation remain poorly defined. We show that the ubiquitin conjugating enzyme UBE2O multi-mono-ubiquitinates the nuclear localization signal of BAP1, thereby inducing its cytoplasmic sequestration. This activity is counteracted by BAP1 auto-deubiquitination through intramolecular interactions. Significantly, we identified cancer-derived BAP1 mutations that abrogate auto-deubiquitination and promote its cytoplasmic retention, indicating that BAP1 auto-deubiquitination ensures tumor suppression. The antagonistic relationship between UBE2O and BAP1 is also observed during adipogenesis, whereby UBE2O promotes differentiation and cytoplasmic localization of BAP1. Finally, we established a putative targeting consensus sequence of UBE2O and identified numerous chromatin remodeling factors as potential targets, several of which tested positive for UBE2O-mediated ubiquitination. Thus, UBE2O defines an atypical ubiquitin-signaling pathway that coordinates the function of BAP1 and establishes a paradigm for regulation of nuclear trafficking of chromatin-associated proteins.

HIGHLIGHTS

- UBE2O ubiquitinates BAP1 on its NLS, and regulates its subcellular localization
- The mechanism of BAP1 auto-deubiquitination is disrupted in cancer
- UBE2O and BAP1 have antagonistic roles in cell cycle regulation and differentiation
- UBE2O targets itself and a subset of chromatin regulators

INTRODUCTION

The covalent attachment of ubiquitin to target proteins, i.e., ubiquitination, regulates both protein stability and function, and is fundamental to diverse biological processes (Hammond-Martel et al., 2012; Jackson and Durocher, 2013). The deubiquitinase (DUB) BAP1 is a transcriptional regulator required for mammalian development (Dey et al., 2012; Yu et al., 2010). BAP1 is also a tumor suppressor inactivated in various cancers, and reconstitution studies in cancer cells harboring BAP1 mutations indicated that both BAP1 catalytic activity and nuclear localization are required for its growth suppressive properties (Carbone et al., 2013; Ventii et al., 2008). Moreover, RNAi-mediated depletion of BAP1 also induces defects in cell cycle progression indicating that this protein is a key regulator of cell proliferation (Machida et al., 2009). At the molecular level, BAP1 assembles a large multi-protein complex consisting of numerous transcription factors and chromatin-associated proteins including the Host Cell Factor-1 (HCF-1), the Polycomb Group (PcG) proteins Additional Sex Combs Like 1 and 2 (ASXL1/2), the histone demethylase KDM1B, the O-linked N-acetylglucosamine transferase (OGT), the forkhead transcription factors FOXK1/FOXK2, and the zinc finger transcription factor Yin Yang1 (YY1) (Machida et al., 2009; Misaghi et al., 2009; Sowa et al., 2009; Yu et al., 2010).

The *Drosophila* BAP1, Calypso, is a PcG protein that interacts with Additional Sex Combs (ASX), localizes at PcG-target gene regulatory regions, and represses HOX gene expression. Calypso/ASX heterodimer, termed PR-DUB (Polycomb repressive DUB), deubiquitinates histone H2A (Scheuermann et al., 2010), a chromatin modification involved in chromatin remodeling and gene silencing (Lanzuolo and Orlando, 2012).

We and others previously identified the ubiquitin conjugating enzyme UBE2O as a substoichiometric factor that co-purifies with the human BAP1 (Machida et al., 2009; Sowa et al., 2009; Yu et al., 2010), suggesting that it might be involved in the coordination of BAP1 function. UBE2O belongs to the E2 family of ubiquitin-conjugating enzymes, although, unlike most members of this family, it is unusually large (140 kDa) (van Wijk and Timmers, 2010). Pioneering studies from Pickart's group suggested that UBE2O might

function as an E2/E3 hybrid (Berleth and Pickart, 1996; Klemperer et al., 1989). This was essentially based on the observation that UBE2O can ubiquitinate free histones *in vitro*, in the presence of E1 enzyme only. It has been proposed that ubiquitination by UBE2O involves an intramolecular thioester relay mechanism since this enzyme is inhibited by phenylarsine oxide (PAO) which can crosslink adjacent cysteines (Klemperer et al., 1989). Otherwise, the physiological substrates of UBE2O are largely unknown. Nonetheless, it was recently shown that UBE2O regulates TRAF6-dependent NF-κB in a catalytic activity-independent manner (Zhang et al., 2013b), monoubiquitinates SMAD6 during bone morphogenetic protein signaling (Zhang et al., 2013a), and coordinates endosomal protein trafficking (Hao et al., 2013) thus implicating UBE2O in numerous cellular processes. In this study, we uncover a novel ubiquitin-signaling pathway, mediated by UBE2O, that has important implications for chromatin-associated processes.

RESULTS

The ubiquitin conjugating enzyme UBE2O interacts with and ubiquitinates BAP1

We previously described the purification of complexes formed by wild type and catalytic dead BAP1 (C91S) (Yu et al., 2010). The complexes were essentially identical, although when probed with an anti-ubiquitin antibody, the C91S complex exhibited a dramatic increase in signal (Figure 1A). We also routinely observed mono-ubiquitination of BAP1 in transfected cells, independently of its DUB activity (Figure 1A and Figure S1A-E). This suggests that BAP1 might be functionally regulated by distinct ubiquitination events in DUB activity-dependent and -independent manner. To identify E3 ligases responsible for the ubiquitination of BAP1, we initially considered UBE2O which was more abundant in the C91S versus the wild type BAP1 complex (Figure 1A). The UBE2O association with BAP1 was not affected by mutation of the HCF-1 Binding Motif (HBM) which eliminates HCF-1, a major component of the complex (Figure 1A). Glycerol density

gradient fractionation of nuclear extracts indicated that UBE2O co-sediments with the BAP1 complex (Figure 1B). Next, we co-transfected BAP1 or C91S with UBE2O or its catalytic dead mutant C1040S (hereafter UBE2O CD) and ubiquitin into 293T cells. Strikingly, UBE2O ubiquitinates BAP1, and modified forms were more abundant in the C91S mutant (Figure 1C). Incubation of UBE2O-modified BAP1 C91S with an excess of USP2 DUB catalytic domain resulted in its complete deubiquitination further demonstrating ubiquitin conjugation (Figure S1F). Of note, deletion of the UCH catalytic domain results in the abolishment of the constitutive mono-ubiquitination (Figure S1G). On the other hand, a similar UBE2O-dependent ubiquitination pattern could be observed for BAP1 C91S or BAP1 ΔUCH indicating that UBE2O-mediated ubiquitination is distinct from its constitutive mono-ubiquitination.

To control for the specificity of UBE2O-mediated BAP1 ubiquitination, we evaluated other E2s and none was able to ubiquitinate BAP1 (Figure S1H,I). We also tested two known H2A DUBs, i.e., USP16 and MYSM1, as well as the SUMO protease SENP2, and no UBE2O-mediated ubiquitination could be observed (Figure S1J). Using multiple sequence alignment, we identified three main conserved regions in UBE2O namely CR1 (conserved region 1), CR2 (conserved region 2) and UBC (Ubiquitin conjugating) (Figure 1D, Figure S1K). Secondary structure prediction analysis revealed all-β domains within CR1 and CR2 and the typical α/β UBC fold. Deletion of either N- (ΔCR1-CR2) or C-terminal (ΔC) regions of UBE2O completely disrupted BAP1 ubiquitination (Figure 1D, E). Moreover, deletion of only the N-terminal CR1 region (ΔCR1-A) was sufficient to abolish UBE2O catalytic activity. Hence, the integrity of multiple domains of UBE2O is required for ubiquitination of BAP1.

UBE2O catalyzes the multi-mono-ubiquitination of BAP1

To determine the mechanism of UBE2O action on BAP1, we established an *in vitro* assay for BAP1 ubiquitination using wild type and C91S complexes immobilized on the beads (Figure S2A). UBE2O-mediated ubiquitination appears to be highly specific for the C91S mutant as no modified forms were observed for other BAP1 partners (Figure 2A).

Moreover, ubiquitination of the C91S mutant did not disrupt complex integrity, since none of the complex components was released into the soluble fraction in a UBE2O-dependent manner (Figure 2A). Notably, we did not detect ubiquitination of wild type BAP1 as opposed to C91S, and this ubiquitination was completely abolished by the UBE2O inhibitor PAO (Figure 2A, Figure S2B). We note that UBE2O, purified from HeLa cells under high or low salt conditions or from bacteria, ubiquitinates C91S to similar extents (Figure S2C,D). Importantly, although less efficient, ubiquitination was also observed using bacteria-purified BAP1 and UBE2O (Figure S2E). Therefore UBE2O is an atypical E2/E3 enzyme with substrate binding and ubiquitin conjugating functions.

To further confirm that auto-deubiquitination prevents accumulation of ubiquitin on BAP1, the beads-bound wild type complex was pretreated with N-ethylmaleimide (NEM), which resulted in a significant ubiquitination of BAP1 by UBE2O (Figure S2A, Figure 2B). Next, we used methylated ubiquitin, which is unable to form poly-ubiquitin or linear chains in the *in vitro* reaction (Figure 2C). The reaction with methylated ubiquitin was as efficient as with the unmodified ubiquitin and resulted in a similar ubiquitination pattern, indicating that UBE2O multi-mono-ubiquitinates BAP1. The same observation was made *in vivo* when a K0 ubiquitin mutant, incapable of chain formation, was used for co-transfection of 293T cells with the C91S mutant and UBE2O (Figure 2D). Next, 293T cells were co-transfected with wild type BAP1 or C91S mutant and UBE2O, and then treated with the proteasome inhibitor MG132 (Figure 2E). The typical multi-mono-ubiquitination pattern of BAP1 was unchanged after proteasome inhibition, indicating that UBE2O is unable to directly catalyze poly-ubiquitin chain elongation with subsequent degradation of BAP1. Immunodetection of endogenous CDC25A was conducted as a control for proteasome inhibition. Next, we tested several E3s that interact with either UBE2O or BAP1 and no further chain elongation was observed (Figure S2F-I). To further confirm that the stability of BAP1 is not directly regulated by UBE2O, we performed siRNA knockdown of UBE2O in MCF7 cells, which express high protein levels of this enzyme, followed by treatment with cycloheximide (CHX) (Figure 2F). Endogenous BAP1 appears to be highly stable and UBE2O knockdown did not significantly change BAP1 protein levels. We concluded that

UBE2O catalyzes BAP1 multi-mono-ubiquitination without directly promoting its proteasomal degradation under normal growth conditions. Of note, UBE2O depletion also did not affect the constitutive mono-ubiquitination of BAP1 observed in cells transfected with this DUB (Figure S2J).

The NLS of BAP1 is required for UBE2O-mediated ubiquitination

Using a GST pull down assay, we found that the BAP1 C-terminal region (598-729 aa), which includes the C-terminal domain (CTD) and NLS, is necessary and sufficient for UBE2O binding (Figure 3A). Surprisingly, co-expression of UBE2O with CTD-NLS promoted the latter's degradation by the proteasome, since it could be reversed by MG132 (Figure 3B, left panel and Figure S3A, B). Immunoprecipitation of the CTD-NLS revealed an ubiquitination pattern similar to that of the full length BAP1 (4-5 sites of multi-mono-ubiquitination), although some high molecular weight smears were also detected (Figure 3B, right panel). Next, we found that both wild type and K0 ubiquitin mutants promoted UBE2O-mediated multi-mono-ubiquitination and degradation of the CTD-NLS (Figure S3C). Moreover, knockdown of endogenous UBE2O rescued the degradation of CTD-NLS (Figure 3C). These results confirm that the CTD-NLS represents both the interaction and ubiquitination region for UBE2O. The degradation of CTD-NLS can be explained by the small size of this region (only 101aa), in line with a recent discovery by Ciechanover's group indicating that monoubiquitinated substrates of less than 150 aa can be degraded without further ubiquitin chain formation (Shabek et al., 2012). Next, we purified the complex of the BAP1ΔCTD mutant that possesses a large deletion of aa 631-693 leaving only the NLS region intact (aa 699-729) (Figure 3D). The abundance of UBE2O was nearly unchanged between the wild type and the mutant indicating that UBE2O binds the NLS region. BAP1 possesses a complex NLS region (Figure S3D,E). We designed a set of BAP1 NLS mutants in the C91S background to render the ubiquitination analysis more sensitive. We found that both C91SΔ688-716 and C91SΔ711-729 mutants were unable to bind and to be ubiquitinated by UBE2O (Figure 3E). Therefore, the NLS region that includes the RRR (aa 699-701) site, the hydrophobic GVSIGRL patch (aa 703-709) as well

as the basic amino acid stretch RRKRSRPYKAKRQ (aa 717-729) is required for binding and ubiquitination by UBE2O. The region of basic amino acids RRKRSR (aa 717-722) is strictly required for binding and ubiquitination by UBE2O (Figures 3E, Figure S3F-G). Thus, multiple determinants of this composite and highly conserved NLS are required for UBE2O-mediated ubiquitination of BAP1 (Figure S3H).

UBE2O ubiquitinates the NLS of BAP1 and regulates its subcellular localization

To identify the UBE2O ubiquitination sites on BAP1, we performed an anti-Flag affinity purification of C91S co-transfected with ubiquitin and UBE2O (Figure 4A). MS peptide analysis revealed 14 unique ubiquitination sites in BAP1, 9 of which were detected more than once (Figure 4B). Analysis of all ubiquitination events revealed that 50 % are located in the area of NLS, which represents only 4 % of the protein. Next, we introduced a series of lysine to arginine mutations in the CTD-NLS region (12 K/R) or in the NLS alone (5 K/R) of C91S (Figure 4C). Mutation of all lysine sites in the CTD-NLS (12 K/R) strongly reduced C91S ubiquitination; moreover, mutation of lysines in the NLS (5 K/R) region had an identical effect on C91S ubiquitination compared with the 12 K/R mutant. Interestingly, the binding of UBE2O to either mutants of C91S was unchanged indicating that K/R mutations do not significantly affect UBE2O binding affinity. Taken together, these results indicate that UBE2O ubiquitinates primarily the NLS of BAP1.

Ubiquitination was reported to promote nuclear export of proteins (Groulx and Lee, 2002; Li et al., 2003). Therefore, we evaluated whether the ubiquitination of BAP1 affects its subcellular localization. BAP1 is prominently nuclear, but displayed strong cytoplasmic staining when co-expressed with UBE2O. This effect depends on the catalytic activity of UBE2O. Notably, the effect of UBE2O on the C91S mutant was more pronounced with almost all cells showing cytoplasmic or nucleo-cytoplasmic localization (Figure 4D). In addition, the C91S mutant usually displayed a more pronounced cytoplasmic localization compared to the wild type BAP1. Of note, overexpression of UBE2O, but not its catalytic dead form, also promoted cytoplasmic localization of endogenous BAP1 (Figure S4). To probe whether this effect is due to its inability to deubiquitinate its NLS, we compared the

nuclear localization of BAP1 and C91S (5 K/R) mutants (Figure 4E). Remarkably, the K/R mutation rescued the C91S mutant from the cytoplasmic sequestration, thus supporting the notion that NLS auto-deubiquitination is involved in the regulation of BAP1 nuclear import/export.

Intramolecular interaction in BAP1 is required for efficient NLS auto-deubiquitination

UCH37 is highly similar to BAP1 and its crystal structure suggests that an intramolecular interaction occurs between the UCH and the CTD (Figure S5A) (Burgie et al., 2011). Since catalytically dead UCH37 C88A is also strongly ubiquitinated by an unknown E3 ligase (Figure S5B), we reasoned that both BAP1 and UCH37 might use their respective CTD regions for interaction with the UCH domain (Figure S5C). Examination of CTD and UCH flanking sequences of BAP1 revealed putative coiled coil motifs that can engage in intramolecular interactions (Figure S4D). Next, we used the crystal structure of UCH37 to generate a superimposed model of BAP1 (Figure 5A). This model suggests that the CTD region (containing the CC2) forms an interaction interface with the CC1 and the UCH domain. We note that this model cannot predict the structure of the NLS and NORS regions, which are not present in UCH37. To validate our computational prediction, we designed a series of deletion mutants in the N- terminus of BAP1 including the UCH domain alone and a larger fragment that includes CC1 (UCH-CC1) (Figure 5B). Co-IP between the fragments revealed that both UCH and UCH-CC1 interact with CTD-NLS (Figure 5C). To test whether this interaction can promote deubiquitination of CTD-NLS, we took advantage of the earlier observation that CTD-NLS can be degraded as a result of ubiquitination by UBE2O. We designed a complementation/rescue system in which the degradation of CTD-NLS would be counteracted by the N-terminus of BAP1. Indeed, the degradation of CTD-NLS was efficiently rescued only by UCH-CC1 but not by UCH alone, and this was dependent on the catalytic activity of BAP1 (Figure 5D). This suggests that despite direct CC2/UCH interaction, the CC1/CC2 interface plays an important role in NLS deubiquitination. To further test the requirement of the CC1/CC2 in the context of the

full-length protein, CC1 and CTD deletion mutants were used (Figure 5B). Deletion of the CTD (ΔCTD) or CC2 (ΔCC2) almost completely blocked the auto-deubiquitination activity of BAP1 despite the presence of a catalytically proficient UCH domain (Figure 5E). The CC1 deletion mutant had a less pronounced auto-deubiquitination defect consistent with the fact that CC2 interacts with both CC1 and UCH. To test whether the deficiency in the ability of BAP1 to auto-deubiquitinate the NLS affects its localization, cell lines stably expressing the wild type or mutants BAP1 were generated. IF analysis revealed that the wild type BAP1 displayed a typical nuclear localization, whereas the ΔCTD and ΔCC2 mutants had a stronger cytoplasmic localization similar to the C91S mutant (Figure 5J). Notably the ΔHBM mutant displayed normal localization similar to wild type BAP1. Thus BAP1 auto-deubiquitination depends on an intramolecular binding between CC2 and UCH-CC1 and is important to counteract the E3 ligase activity of UBE2O towards the NLS.

BAP1 NLS auto-deubiquitination is disrupted by cancer-associated mutations of CTD

Our results suggest that disruption of auto-deubiquitination leads to improper BAP1 localization. We thus searched for cancer mutations in BAP1 that may target the UCH-CC1 interaction interface with CC2. We first tested G13V and F660A mutations and none had a noticeable effect on BAP1 auto-deubiquitination (Figure S5E,F). Next, we considered two small in frame deletions of CC2 (ΔE631-A634 and ΔK637-C638InsN) (Harbour et al., 2010) (Figure 5B). We conducted complex purification of BAP1, ΔE631-A634 and ΔK637-C638InsN, and strikingly observed in both mutants an intense band around 230 kDa that corresponds to UBE2O (Figure 5F). Other major components of the complex such as OGT and HCF-1 showed no apparent differences (Figure 5F). The CC2 directly interacts with UCH, so mutations in this region may interfere with the catalytic activity of BAP1. To test this, we used an *in vitro* deubiquitination assay using a BAP1 natural substrate, i.e., the nucleosomal histone H2A ubiquitinated at position K119 (Figure S5G, H, I). The activities of both cancer mutants were very similar to BAP1, whereas the control C91S failed to deubiquitinate H2A (Figure 5G). Next, to evaluate whether these cancer mutations affect the auto-deubiquitination activity of BAP1, we exploited the UCH/CTD rescue system and

the ability of UBE2O to promote degradation of the BAP1 CTD-NLS. We cloned the CTD-NLS region of ΔK637-C638InsN mutant, and a mutant with a large internal deletion in CC2 (Δ636-655) as a control (Figure 5B). Remarkably, complementation with UCH-CC1 rescued the wild type CTD-NLS, but not the ΔK637-C638InsN and Δ635-655 (Figure 5H). Next, we sought to investigate these mutations in the context of the full-length protein. The effect of UBE2O on the cancer mutants was almost as dramatic as on the C91S despite their catalytic proficiency (Figure 5I). Finally, ΔE631-A634 and ΔK637-C638InsN mutants displayed increased cytoplasmic localization similar to the C91S mutant (Figure 5J).

UBE2O is regulated by active nucleo-cytoplasmic transport mechanisms and promotes BAP1 cytoplasmic localization during adipocyte differentiation

UBE2O possesses two functional NLS motifs, but the full-length enzyme displayed predominant cytoplasmic localization (Figure S6A-E). Next, purification of UBE2O-associated proteins followed by MS analysis revealed numerous components of the nuclear import/export machinery as well as several kinases that might coordinate its nuclear trafficking (Figure S6F). Taking into account that UBE2O is a heavily phosphorylated enzyme (Figure S6G), we sought to determine the impact of kinase inhibition on UBE2O localization. We treated cells with a panel of kinase inhibitors of various specificities and observed a nuclear translocation of UBE2O with the CDK-inhibitors Purvalanol A and RO-3306 (Figure 6A,B). Interestingly, UBE2O catalytic dead form was strongly retained in the nucleus indicating the importance of catalytic activity in coordinating its nucleo-cytoplasmic transport. Consistent with its potential role in negatively regulating BAP1 function, siRNA-depletion of UBE2O increased cell proliferation whereas siRNA-depletion of BAP1 resulted in decreased cell proliferation (Figure 6C). Of note, no noticeable changes in UBE2O or BAP1 localization were observed in unperturbed cycling cells (Data not shown), suggesting that only very limited pools of UBE2O or BAP1 might be imported or exported respectively. Taking into account that BAP1 tightly coordinate cell proliferation, we reasoned that a substantial change in BAP1 localization might be observed during permanent cell cycle exit. Since UBE2O was implicated in promoting adipocyte

differentiation in the mouse embryo cell line C3H10T1/2, we recapitulated this effect using the 3T3-L1 cellular model of adipocyte differentiation as determined by immunoblotting for aP2 and Perilipin (PLIN) adipogenic markers and Oil Red O staining (Figure 6D,E). Significantly, a fraction of BAP1 become excluded from the nucleus as 3T3-L1 cells differentiate into adipocytes (Figure 6F). In addition, mutation of the UBE2O-ubiquitination sites in BAP1 resulted in a substantial retention of this DUB in the nucleus. Since BAP1 5K/R mutant still interact with UBE2O and is ubiquitinated on other sites, we also replaced the NLS region of BAP1, containing the UBE2O-interacting motif, with T-large antigen NLS which prominently prevented the cytoplasmic localization of this DUB during differentiation.

UBE2O targets a subset of bipartite NLS-containing transcription regulators

UBE2O displays prominent UBC-dependent auto-catalytic activity *in vitro* and *in vivo* (Figure 7A and Figure 1C), which is inhibited by PAO (Figure S2B, Figure 7A). In addition, a nuclear retention of UBE2O, more pronounced for the catalytic dead form was observed following treatment with CDK inhibitors (Figure 6A,B). Thus, we sought to determine if NLS sequences within UBE2O may constitute auto-ubiquitination sites. Strikingly the NLS1/A mutant was completely auto-ubiquitination-deficient similar to UBE2O CD, whereas mutation of NLS2 had no significant effect on UBE2O auto-ubiquitination (Figure S6A, Figure 7B). In addition, the bipartite NLS regions of UBE2O and BAP1 contain a highly conserved patch of aliphatic hydrophobic amino acids (VLI patch) between the minor and major NLS sites (linker region) (Figure 7C). Mutation of the VLI patch disrupted auto-ubiquitination (Figure S7A). Of note, the NLS1 architecture is highly conserved between most UBE2O orthologs (Figure S6E). These results prompted us to search whether this subtype of bipartite NLS may serve as a specific signal for UBE2O recognition and ubiquitination in other proteins. Several candidates were identified, notably chromatin-associated proteins, suggesting that UBE2O might exert extensive control over nuclear signaling pathways (Figure S7F). We selected four proteins, i.e., p400, CDT1, INO80 and CXXC1, predicted as potential UBE2O substrates. INO80 and p400 are

members of SWI/SNF family of chromatin-remodeling ATPases (Jin et al., 2005; Vassilev et al., 1998) containing the predicted NLS sequences (Figure 7C). CXXC1 is the CpG island binding protein and component of the SET1 complex (Lee and Skalnik, 2005) that contains two predicted NLS sequences with NLS2 containing the putative UBE2O binding motif. The DNA replication factor CDT1 also harbors a potential binding and ubiquitination site for UBE2O (Nishitani et al., 2000). INO80, p400 and CDT1 were degraded following co-expression with UBE2O in a catalytic-activity dependent manner, ostensibly as a result of ubiquitin chain extension by unknown E3 ligases (Figure 7D, Figure S7B). CXXC1 showed several slow migrating bands suggesting its ubiquitination without degradation (Figure 7D, right panel). Next, we selected INO80 and CXXC1 as two contrasting examples of UBE2O action for further characterization of their ubiquitination by UBE2O (Figure 7D). When the immunoprecipitated INO80 was loaded in equal amounts, the ubiquitin blot showed a typical polyubiquitin smear in the stacking gel (Figure 7D, left panel). The ubiquitination profile of CXXC1 was similar to that of BAP1 and UBE2O with several distinct multi-mono-ubiquitin bands (Figure 7D, right panel). Ubiquitination of INO80 and CXXC1 by UBE2O had a pronounced effect on their subcellular localization, as both proteins displayed stronger cytoplasmic localization following co-expression of wild type but not UBE2O CD mutant (Figure 7E). We also found a potential UBE2O binding consensus in ALC1, another nuclear SWI/SNF family chromatin-remodeling enzyme (Ahel et al., 2009), but UBE2O had no effect on ALC1 ubiquitination and localization (Figure S7C,D,E). This can be explained by the absence of the major NLS stretch in the vicinity of the consensus and/or the location of the consensus in the masked fold of its Macro domain. Therefore, UBE2O targets a subset of chromatin remodeling and modifying factors containing a bipartite NLS with a specific VLI patch in the linker region with the exception of CDT1, which contains the major NLS stretch upstream of the UBE2O consensus. Thus, substrate ubiquitination by UBE2O can induce cytoplasmic localization, which might be accompanied by further proteasomal degradation as a consequence of ubiquitin chain extension by other E3 ligases.

DISCUSSION

Regulation of BAP1 by UBE2O-mediated ubiquitination

Here, we define a regulatory mechanism involving the E2/E3 hybrid UBE2O which multi-mono-ubiquitinates BAP1 in the NLS region. Under normal growth conditions, BAP1 is predominantly nuclear whereas UBE2O is mainly cytoplasmic suggesting that BAP1 ubiquitination is highly regulated. In particular, this compartmentalization raises the question regarding the cellular compartment where the ubiquitination actually occurs. UBE2O could be imported into the nucleus to ubiquitinate BAP1 and promote its ubiquitin-mediated nuclear export as observed for other proteins (Groulx and Lee, 2002; Li et al., 2003). Since we did not observe a noticeable accumulation of endogenous UBE2O in the nucleus, it is possible that only a small fraction of UBE2O is imported into this compartiment at any given time. Controling UBE2O import itself would provide another level of regulation for the fine-tuning of BAP1 ubiquitination. Indeed, (i) BAP1 and UBE2O exert antagonistic functions during cell proliferation, (ii) CDK inhibitors promoted UBE2O nuclear localization with a stronger effect towards its catalytic dead form, (iii) UBE2O exhibits an auto-ubiquitination activity towards its own NLS, and (iv) two recent studies revealed that the K521 residue (K516 in mouse), part of UBE2O NLS1, is ubiquitinated *in vivo* (Figure S6G)**.** Our data do not exclude the possibility that, under specific conditions, BAP1 might be exported to the cytoplasm prior to its ubiquitination, although we did not identify any export signal in BAP1. Further studies are needed to dissect the possible mechanisms of UBE2O nucleocytoplasmic transport including its regulation.

On the other hand, since ubiquitination of BAP1 is counteracted by auto-deubiquitination, one can predict that a yet to be identified signal is needed to inactivate BAP1 catalytic activity. This initiating event would render this DUB susceptible to ubiquitination by UBE2O. BAP1 could be modified by other post-translational modifications that inhibit its auto-deubiquitination. In fact, several phosphorylation and ubiquitination sites of BAP1 were identified in proteomics studies (Figure S6H), and in this study we identified several ubiquitination sites on UCH, some of which might result from

the action of other E3 ligases. Under normal cell growth conditions, UBE2O-mediated ubiquitination of BAP1 might not necessarily lead to a net accumulation of BAP1 in the cytoplasm, since this could be a protracted process that is concomitant with both *de novo* synthesis of BAP1 and further degradation or re-import of this DUB. We speculate that this could be an editing mechanism that might coordinate the transcriptional competency of BAP1. In contrast, during adipocyte differentiation, we observed a net cytoplasmic redistribution BAP1 that would drastically impact its transcriptional activity. It is also possible that BAP1 might exert cytoplasmic functions in terminally differentiated adipocytes. We note that, since our conclusion is based on ectopically expressed BAP1, further work is needed to establish this regulation for the endogenous enzyme and to provide insights into the possible concerted action of post-translational modifications in regulating the trafficking and function of this DUB.

Auto-deubiquitination of BAP1 and its disruption in cancer

Auto-deubiquitination of DUBs was previously observed for UCH-L1, which was able to counteract its own ubiquitination by an unknown E3 ligase (Meray and Lansbury, 2007). Interestingly, in our study, we noticed a similar mechanism regulating UCH37. We also note that UCH37 and BAP1 share a common ancestry. Although vertebrate BAP1 acquired the long NORS region, which contains the HCF-1 interaction motif, the intramolecular interaction between the amino and carboxy termini seems to be evolutionary conserved. It is possible that DUB auto-deubiquitination might constitute a regulatory mechanism, which is more widely used than currently appreciated.

Cancer-associated mutations in BAP1 disrupt its function by multiple means. Large deletions in the BAP1 gene result in dysfunctional proteins. Point mutations in the UCH domain of BAP1 often target the catalytic site or its immediate environment resulting in disruption of catalytic activity. The cancer-derived mutations of BAP1 in the catalytic site are predicted to impact both auto-deubiquitination as well as DUB activity towards other substrates. Histone H2A is a substrate of BAP1 (Scheuermann et al., 2010; Yu et al., 2014), and other substrates such as HCF-1 and OGT were previously also described (Machida et

al., 2009; Misaghi et al., 2009; Ruan et al., 2012). In this study, we identified two cancer-mutations in the coiled-coil motif of the C-terminal region that remarkably did not compromise BAP1 complex assembly, but instead promoted UBE2O association with this DUB. It would be interesting to further determine whether this is a result of structural changes in BAP1 that facilitate UBE2O binding, or rather is a consequence of increased cytoplasmic sequestration of BAP1. Importantly, the two cancer-derived mutations selectively compromised the auto-deubiquitination activity of BAP1 without affecting its H2A DUB activity. These cancer-derived mutations also revealed that auto-deubiquitination function of the enzyme is important for its proper nuclear localization. Thus, by separating the two activities of BAP1, we provide a biochemical paradigm for testing the involvement of other ubiquitin signaling cascades in regulating BAP1 function.

UBE2O acts as an atypical E2/E3 that ubiquitinates a subset of NLS-containing proteins

The evolution of protein conjugation pathways can be traced back to prokaryotic and archea cells. In eukaryotes, this system diversified resulting in establishment of the classical E1/E2/E3/substrate ubiquitin transfer cascade (Burroughs et al., 2012; Hochstrasser, 2009). UBE2O is highly conserved in plants and animals suggesting that it evolved from a common ancestor at least 1.6 billion years ago, when the prototypic animal and plant cell types were evolving (Meyerowitz, 2002). UBE2O seems to employ the properties of both E2 and E3 enzymes suggesting that it might recognize a limited number of substrates. In our study, we discovered that UBE2O specifically binds and ubiquitinates a subset of bipartite NLS that contain a VLI patch in their linker. Based on the consensus between two identified UBE2O substrates, i.e. BAP1 and UBE2O itself, we were able to predict the substrate specificity of the enzyme in turn allowing us to identify more putative UBE2O substrates including proteins involved in RNA processing, transcription, DNA replication, and chromatin remodelling. Thus, UBE2O might be involved in coordinating major signaling pathways in the cytoplasm, organelles, and nucleus that orchestrate cell function during proliferation and differentiation or in response to extracellular stimuli.

Although we were able to detect UBE2O expression in multiple cultured cell lines, its expression seems to be highly regulated. UBE2O levels were previously reported to increase during erythroid differentiation (Wefes et al., 1995). Chromatin of differentiating cells is subjected to multiple epigenetic and structural changes, requiring specific ubiquitin signaling pathways to promote the displacement of chromatin-associated regulators to activate or repress gene expression (Geng et al., 2012). Indeed, UBE2O promotes adipocyte differentiation and is also highly expressed in brain, heart, and skeletal muscle (Nagase et al., 2000; Yokota et al., 2001; Zhang et al., 2013a), all of which comprise post-mitotic cells that must finely coordinate gene expression programs to fulfill metabolically demanding requirements.

MATERIALS AND METHODS

Cell culture, transfections and western blot

Cells were cultured according to standard protocols. siRNA and plasmids were transfected using Lipofectamine or PEI. Total cell lysates were used for western blotting. Differentiation of 3T3L1 and additional details are provided in the supplemental text.

Imunoprecipitation of BAP1 and UBE2O

Cell lines stably expressing BAP1, ΔE631-A634, ΔK637-C638InsN, ΔCTD, ΔCC1 or UBE2O were generated following retroviral transduction and used for immunoprecipitation under native or denaturing conditions as indicated in the supplemental text.

Glycerol gradient fractionation

Molecular mass fractionation of nuclear extract was conduced using a 10-40 % glycerol gradient as indicated in the supplemental text.

***In vitro* interaction assays**

Recombinant GST-BAP1 fusion proteins were purified using glutathione agarose beads and incubated with His-UBE2O. The beads were extensively washed and bound proteins eluted in Laemmli buffer and subjected to western blotting. Additional details are described in the supplemental text.

***In vitro* and *in vivo* ubiquitination assay**

In vitro ubiquitination reactions were conducted using, human recombinant UBE1, BAP1 and UBE2O complexes or bacteria-purified enzymes. Additional details and Mass spectrometry analysis of ubiquitination sites was done as described in the supplemental text.

***In vitro* nucleosome deubiquitination assays**

Preparation of chromatin fractions from Flag-H2A transfected 293T cells and digestion with Micrococcal nuclease (MNase) were conducted with modification of the original protocol (Groisman et al., 2003). The procedure is described in the supplemental text.

Immunofluorescence

The procedure was carried out as previously described (Daou et al., 2011) with additional details provided in the supplemental text.

Protein sequence analysis, and structure modeling

Protein sequences were analyzed using Geneious 6.1.2 created by Biomatters, available from http://www.geneious.com. Other bioinformatics tools are described in the supplemental text.

ACKNOWLEDGMENTS. We thank Elliot Drobetsky, Eric Milot, Dindial Ramotar and Hugo Wurtele for the critical reading of the manuscript. We thank Diana Adjaoud for technical assistance. This work was supported by grants from the Canadian Institute of Health Research (CIHR) to EBA (MOP115132) and MT (MOP-93654). EBA is a scholar of the CIHR and Le Fonds de la Recherche en Santé du Québec. MT holds a Tier 1 Canada Research Chair in Intracellular Signaling. NM was supported by a PhD scholarship from the Fonds Québécois de la Recherche sur la Nature et les Technologies. The authors would like to dedicate this paper to the memory of Cecile M. Pickart for her original work that guided us to demonstrate that UBE2O is indeed an E2/E3 hybrid.

REFERENCES

Ahel, D., Horejsi, Z., Wiechens, N., Polo, S.E., Garcia-Wilson, E., Ahel, I., Flynn, H., Skehel, M., West, S.C., Jackson, S.P.*, et al.* (2009). Poly(ADP-ribose)-dependent regulation of DNA repair by the chromatin remodeling enzyme ALC1. Science *325*, 1240-1243.

Berleth, E.S., and Pickart, C.M. (1996). Mechanism of ubiquitin conjugating enzyme E2-230K: catalysis involving a thiol relay? Biochemistry *35*, 1664-1671.

Burgie, S.E., Bingman, C.A., Soni, A.B., and Phillips, G.N., Jr. (2011). Structural characterization of human Uch37. Proteins.

Burroughs, A.M., Iyer, L.M., and Aravind, L. (2012). The natural history of ubiquitin and ubiquitin-related domains. Frontiers in bioscience : a journal and virtual library *17*, 1433-1460.

Carbone, M., Yang, H., Pass, H.I., Krausz, T., Testa, J.R., and Gaudino, G. (2013). BAP1 and cancer. Nature reviews. Cancer *13*, 153-159.

Daou, S., Mashtalir, N., Hammond-Martel, I., Pak, H., Yu, H., Sui, G., Vogel, J.L., Kristie, T.M., and Affar el, B. (2011). Crosstalk between O-GlcNAcylation and proteolytic cleavage regulates the host cell factor-1 maturation pathway. Proceedings of the National Academy of Sciences of the United States of America *108*, 2747-2752.

Dey, A., Seshasayee, D., Noubade, R., French, D.M., Liu, J., Chaurushiya, M.S., Kirkpatrick, D.S., Pham, V.C., Lill, J.R., Bakalarski, C.E.*, et al.* (2012). Loss of the tumor suppressor BAP1 causes myeloid transformation. Science *337*, 1541-1546.

Geng, F., Wenzel, S., and Tansey, W.P. (2012). Ubiquitin and proteasomes in transcription. Annual review of biochemistry *81*, 177-201.

Groisman, R., Polanowska, J., Kuraoka, I., Sawada, J., Saijo, M., Drapkin, R., Kisselev, A.F., Tanaka, K., and Nakatani, Y. (2003). The ubiquitin ligase activity in the DDB2 and CSA complexes is differentially regulated by the COP9 signalosome in response to DNA damage. Cell *113*, 357-367.

Groulx, I., and Lee, S. (2002). Oxygen-dependent ubiquitination and degradation of hypoxia-inducible factor requires nuclear-cytoplasmic trafficking of the von Hippel-Lindau tumor suppressor protein. Molecular and cellular biology *22*, 5319-5336.

Hammond-Martel, I., Yu, H., and Affar el, B. (2012). Roles of ubiquitin signaling in transcription regulation. Cellular signalling *24*, 410-421.

Hao, Y.H., Doyle, J.M., Ramanathan, S., Gomez, T.S., Jia, D., Xu, M., Chen, Z.J., Billadeau, D.D., Rosen, M.K., and Potts, P.R. (2013). Regulation of WASH-Dependent Actin Polymerization and Protein Trafficking by Ubiquitination. Cell *152*, 1051-1064.

Harbour, J.W., Onken, M.D., Roberson, E.D., Duan, S., Cao, L., Worley, L.A., Council, M.L., Matatall, K.A., Helms, C., and Bowcock, A.M. (2010). Frequent mutation of BAP1 in metastasizing uveal melanomas. Science *330*, 1410-1413.

Hochstrasser, M. (2009). Origin and function of ubiquitin-like proteins. Nature *458*, 422-429.

Jackson, S.P., and Durocher, D. (2013). Regulation of DNA Damage Responses by Ubiquitin and SUMO. Molecular cell *49*, 795-807.

Jin, J., Cai, Y., Yao, T., Gottschalk, A.J., Florens, L., Swanson, S.K., Gutierrez, J.L., Coleman, M.K., Workman, J.L., Mushegian, A.*, et al.* (2005). A mammalian chromatin remodeling complex with similarities to the yeast INO80 complex. The Journal of biological chemistry *280*, 41207-41212.

Klemperer, N.S., Berleth, E.S., and Pickart, C.M. (1989). A novel, arsenite-sensitive E2 of the ubiquitin pathway: purification and properties. Biochemistry *28*, 6035-6041.

Lanzuolo, C., and Orlando, V. (2012). Memories from the polycomb group proteins. Annual review of genetics *46*, 561-589.

Lee, J.H., and Skalnik, D.G. (2005). CpG-binding protein (CXXC finger protein 1) is a component of the mammalian Set1 histone H3-Lys4 methyltransferase complex, the analogue of the yeast Set1/COMPASS complex. The Journal of biological chemistry *280*, 41725-41731.

Li, M., Brooks, C.L., Wu-Baer, F., Chen, D., Baer, R., and Gu, W. (2003). Mono- versus polyubiquitination: differential control of p53 fate by Mdm2. Science *302*, 1972-1975.

Machida, Y.J., Machida, Y., Vashisht, A.A., Wohlschlegel, J.A., and Dutta, A. (2009). The deubiquitinating enzyme BAP1 regulates cell growth via interaction with HCF-1. The Journal of biological chemistry *284*, 34179-34188.

Meray, R.K., and Lansbury, P.T., Jr. (2007). Reversible monoubiquitination regulates the Parkinson disease-associated ubiquitin hydrolase UCH-L1. The Journal of biological chemistry *282*, 10567-10575.

Meyerowitz, E.M. (2002). Plants compared to animals: the broadest comparative study of development. Science *295*, 1482-1485.

Misaghi, S., Ottosen, S., Izrael-Tomasevic, A., Arnott, D., Lamkanfi, M., Lee, J., Liu, J., O'Rourke, K., Dixit, V.M., and Wilson, A.C. (2009). Association of C-terminal ubiquitin hydrolase BRCA1-associated protein 1 with cell cycle regulator host cell factor 1. Molecular and cellular biology *29*, 2181-2192.

Nagase, T., Kikuno, R., Hattori, A., Kondo, Y., Okumura, K., and Ohara, O. (2000). Prediction of the coding sequences of unidentified human genes. XIX. The complete sequences of 100 new cDNA clones from brain which code for large proteins in vitro. DNA research : an international journal for rapid publication of reports on genes and genomes *7*, 347-355.

Nishitani, H., Lygerou, Z., Nishimoto, T., and Nurse, P. (2000). The Cdt1 protein is required to license DNA for replication in fission yeast. Nature *404*, 625-628.

Ruan, H.B., Han, X., Li, M.D., Singh, J.P., Qian, K., Azarhoush, S., Zhao, L., Bennett, A.M., Samuel, V.T., Wu, J.*, et al.* (2012). O-GlcNAc transferase/host cell factor C1 complex regulates gluconeogenesis by modulating PGC-1alpha stability. Cell metabolism *16*, 226-237.

Scheuermann, J.C., de Ayala Alonso, A.G., Oktaba, K., Ly-Hartig, N., McGinty, R.K., Fraterman, S., Wilm, M., Muir, T.W., and Muller, J. (2010). Histone H2A deubiquitinase activity of the Polycomb repressive complex PR-DUB. Nature *465*, 243-247.

Shabek, N., Herman-Bachinsky, Y., Buchsbaum, S., Lewinson, O., Haj-Yahya, M., Hejjaoui, M., Lashuel, H.A., Sommer, T., Brik, A., and Ciechanover, A. (2012). The size of the proteasomal substrate determines whether its degradation will be mediated by mono- or polyubiquitylation. Molecular cell *48*, 87-97.

Sowa, M.E., Bennett, E.J., Gygi, S.P., and Harper, J.W. (2009). Defining the human deubiquitinating enzyme interaction landscape. Cell *138*, 389-403.

van Wijk, S.J., and Timmers, H.T. (2010). The family of ubiquitin-conjugating enzymes (E2s): deciding between life and death of proteins. FASEB journal : official publication of the Federation of American Societies for Experimental Biology *24*, 981-993.

Vassilev, A., Yamauchi, J., Kotani, T., Prives, C., Avantaggiati, M.L., Qin, J., and Nakatani, Y. (1998). The 400 kDa subunit of the PCAF histone acetylase complex belongs to the ATM superfamily. Molecular cell *2*, 869-875.

Ventii, K.H., Devi, N.S., Friedrich, K.L., Chernova, T.A., Tighiouart, M., Van Meir, E.G., and Wilkinson, K.D. (2008). BRCA1-associated protein-1 is a tumor suppressor that requires deubiquitinating activity and nuclear localization. Cancer research *68*, 6953-6962.

Wefes, I., Mastrandrea, L.D., Haldeman, M., Koury, S.T., Tamburlin, J., Pickart, C.M., and Finley, D. (1995). Induction of ubiquitin-conjugating enzymes during terminal erythroid differentiation. Proceedings of the National Academy of Sciences of the United States of America *92*, 4982-4986.

Yokota, T., Nagai, H., Harada, H., Mine, N., Terada, Y., Fujiwara, H., Yabe, A., Miyazaki, K., and Emi, M. (2001). Identification, tissue expression, and chromosomal position of a novel gene encoding human ubiquitin-conjugating enzyme E2-230k. Gene *267*, 95-100.

Yu, H., Mashtalir, N., Daou, S., Hammond-Martel, I., Ross, J., Sui, G., Hart, G.W., Rauscher, F.J., 3rd, Drobetsky, E., Milot, E.*, et al.* (2010). The ubiquitin carboxyl hydrolase BAP1 forms a ternary complex with YY1 and HCF-1 and is a critical regulator of gene expression. Molecular and cellular biology *30*, 5071-5085.

Yu, H., Pak, H., Hammond-Martel, I., Ghram, M., Rodrigue, A., Daou, S., Barbour, H., Corbeil, L., Hebert, J., Drobetsky, E.*, et al.* (2014). Tumor suppressor and deubiquitinase BAP1 promotes DNA double-strand break repair. Proceedings of the National Academy of Sciences of the United States of America *111*, 285-290.

Zhang, X., Zhang, J., Bauer, A., Zhang, L., Selinger, D.W., Lu, C.X., and Ten Dijke, P. (2013a). Fine-tuning BMP7 signalling in adipogenesis by UBE2O/E2-230K-mediated monoubiquitination of SMAD6. The EMBO journal *32*, 996-1007.

Zhang, X., Zhang, J., Zhang, L., van Dam, H., and Ten Dijke, P. (2013b). UBE2O negatively regulates TRAF6-mediated NF-kappaB activation by inhibiting TRAF6 polyubiquitination. Cell research *23*, 366-377.

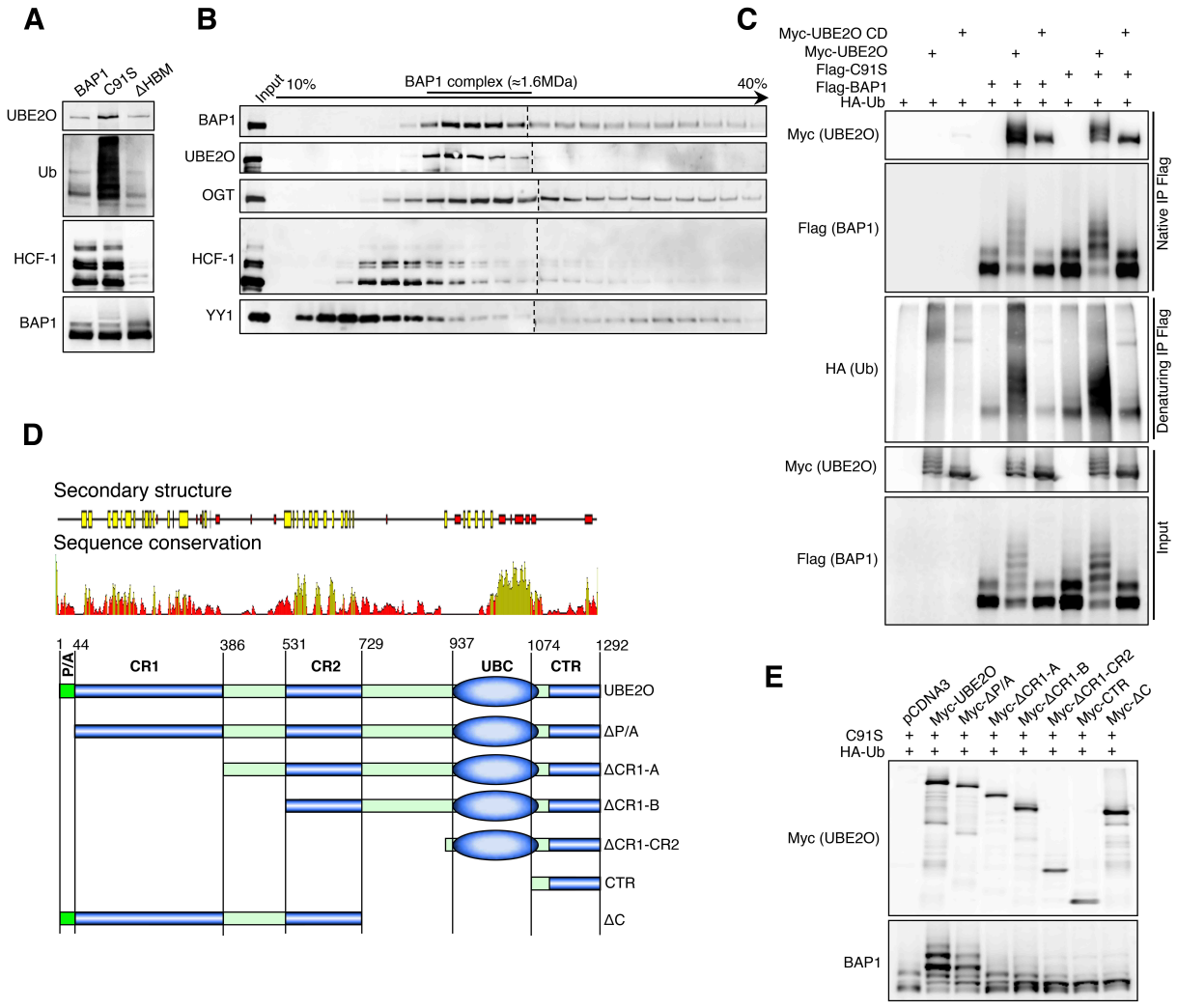

Figure 1. UBE2O interacts with and ubiquitinates BAP1 and this effect is actively counteracted by BAP1 auto-deubiquitination. (See also Figure S1).

A) Purified BAP1 complexes were used for western blot. **B)** HeLa nuclear extract was resolved by glycerol gradient, and used for western blot. **C)** 293T cells were co-transfected with 2 µg of HA-Ub, 2 µg of Myc-UBE2O (wild type or CD), and 1 µg of Flag-BAP1 (wild type or C91S) expression vectors, and cell extracts were used for immunoprecipitation. **D)** Top, schema representing the human UBE2O with secondary structure prediction (alpha helixes are in red and beta strands are in yellow). The main

predicted domains are indicated as CR1 (conserved region 1), CR2 (conserved region 2), UBC (ubiquitin conjugating) and CTR (C-terminal region). Bottom, schema representing UBE2O deletion mutants used for the ubiquitination assay. **E)** 293T cells were co-transfected with 2 μg of HA-Ub, 2 μg of Myc-UBE2O fragments, and 1 μg of C91S expression vectors, and cell extracts were used for western blot.

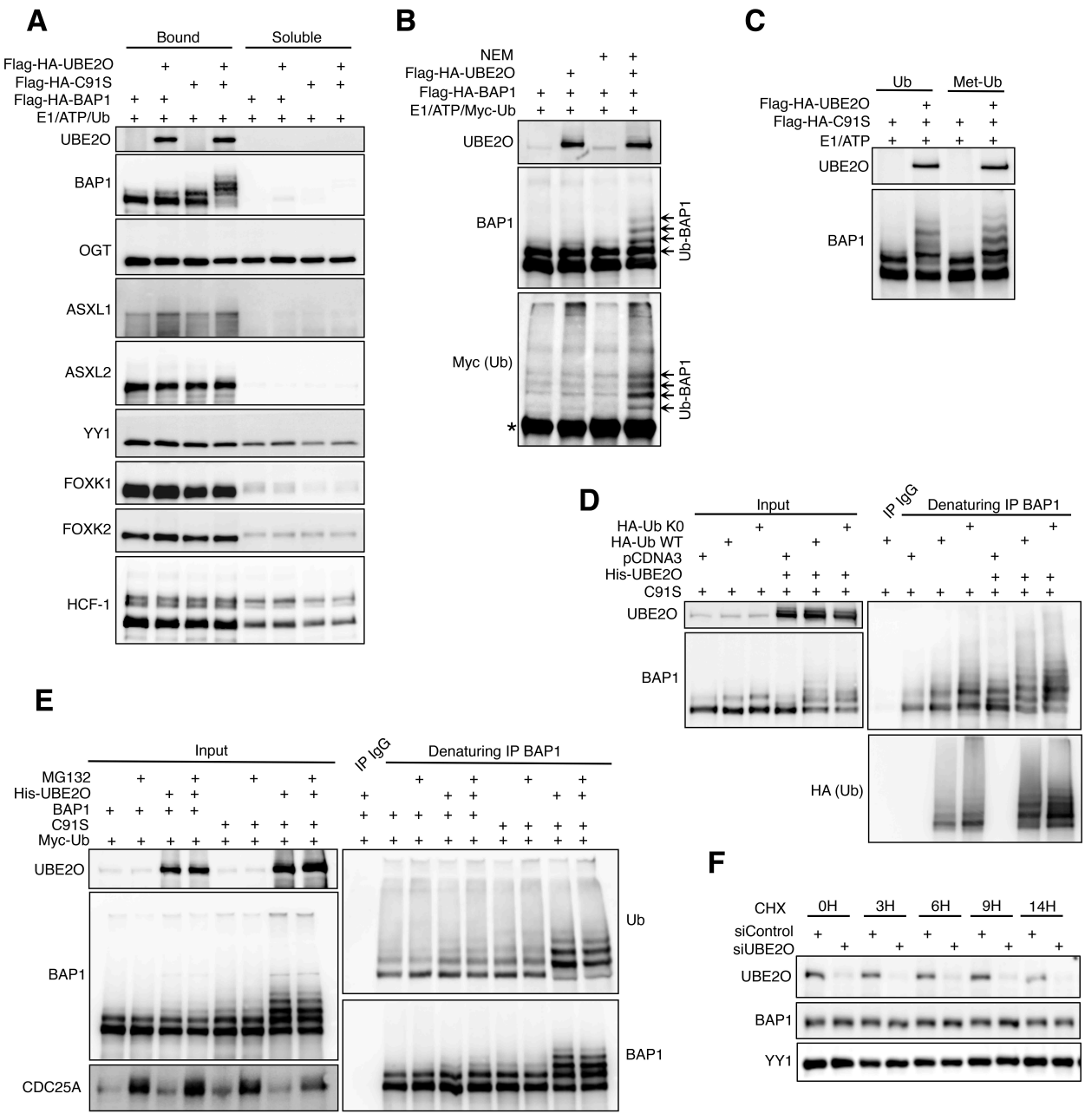

Figure 2. Characterization of UBE2O mediated ubiquitination of BAP1. (See also Figure S2).

A) *In vitro* ubiquitination reaction with beads-immobilized BAP1 or C91S complexes incubated with immunopurified UBE2O. Fractions were used for western blot detection of

components of the BAP1 complex. **B)** *In vitro* ubiquitination reaction using the BAP1 complex inhibited with NEM. **C)** The C91S complex was used for *in vitro* reaction with UBE2O and either unmodified or methylated ubiquitin. **D)** 293T cells were co-transfected with 2 μg of wild type ubiquitin or K0 mutant ubiquitin, 1 μg of BAP1 or C91S and 2 μg of empty vector or His-UBE2O expression vectors, and cell lysates were used for immunoprecipitation. **E)** 293T cells were co-transfected with 1 μg of HA-Ub, 2 μg of BAP1 or C91S and 1 μg of His-UBE2O expression vectors. Cells were treated with DMSO or 20 μM MG132 for 8 hours before immunoprecipitation. **F)** MCF7 cells were transfected with non-targeting or UBE2O siRNA for 96 hours, treated with 20 μg/ml of cycloheximide and analyzed by western blot. *indicates non-specific bands.

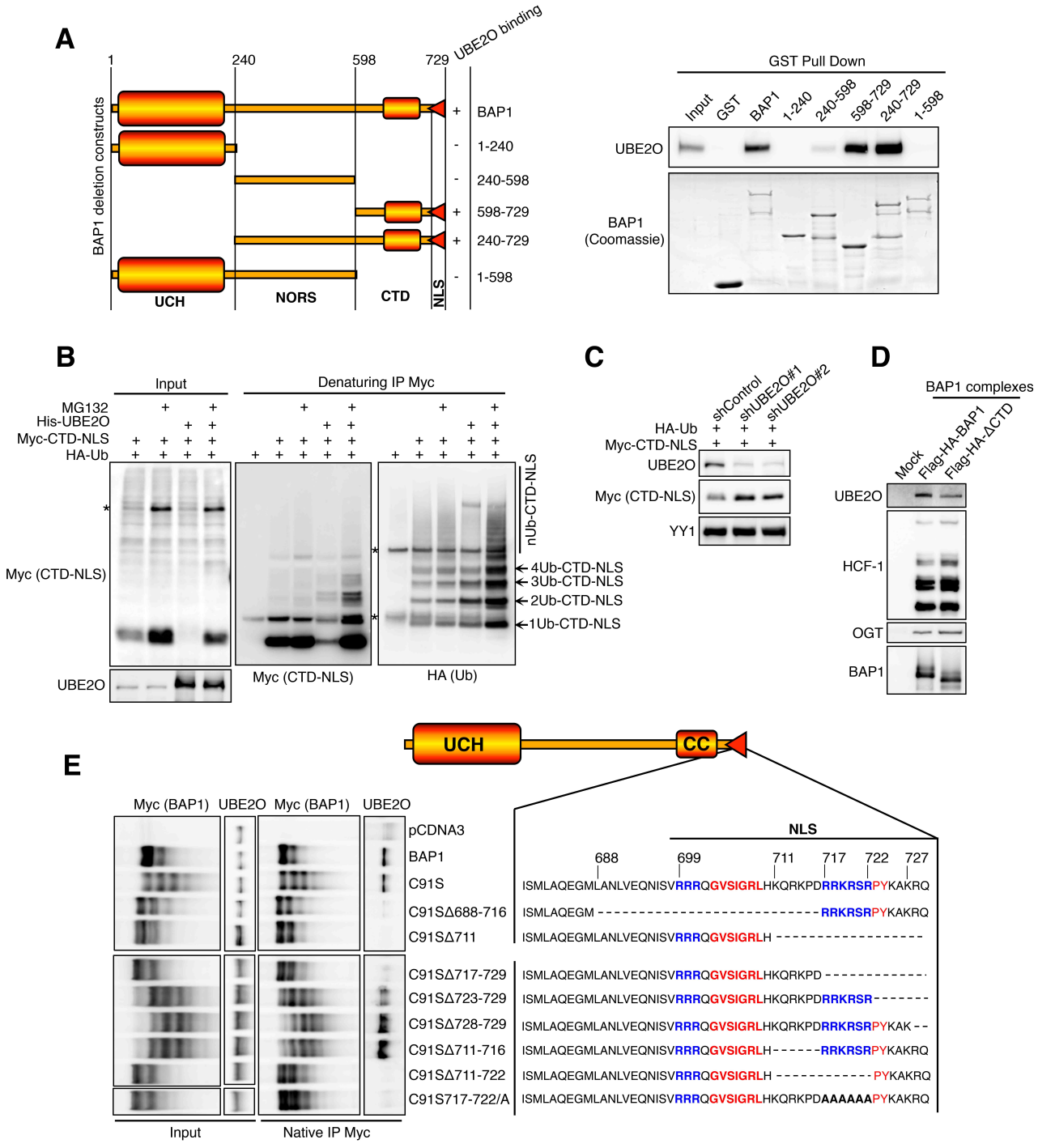

Figure 3. BAP1 NLS is required for its ubiquitination by UBE2O. (See also Figure S3). **A)** Schematic representation of GST-BAP1 fragments used for pull-down assay with His-UBE2O. **B)** 293T cells were co-transfected with 2 µg of HA-Ub, 2 µg of His-UBE2O, and

1 µg of Myc-CTD-NLS expression vectors, and cell extracts were used for immunoprecipitation. **C)** U2OS cells were co-transfected with 2 µg of shControl, shUBE2O#1 or shUBE2O#2 and 1 µg of HA-Ub and 0,5 µg of Myc-CTD-NLS expression vectors, and cell extracts were used for western blot. **D)** Purified complexes of BAP1 or BAP1 ΔCTD were used for western blot detection of components of BAP1 complex. **E)** 293T cells were co-transfected with 2 µg of HA-Ub, 2 µg of His-UBE2O, and 1 µg of Myc-BAP1 mutants expression vectors, and cell extracts were used for immunoprecipitation. * indicates non-specific bands.

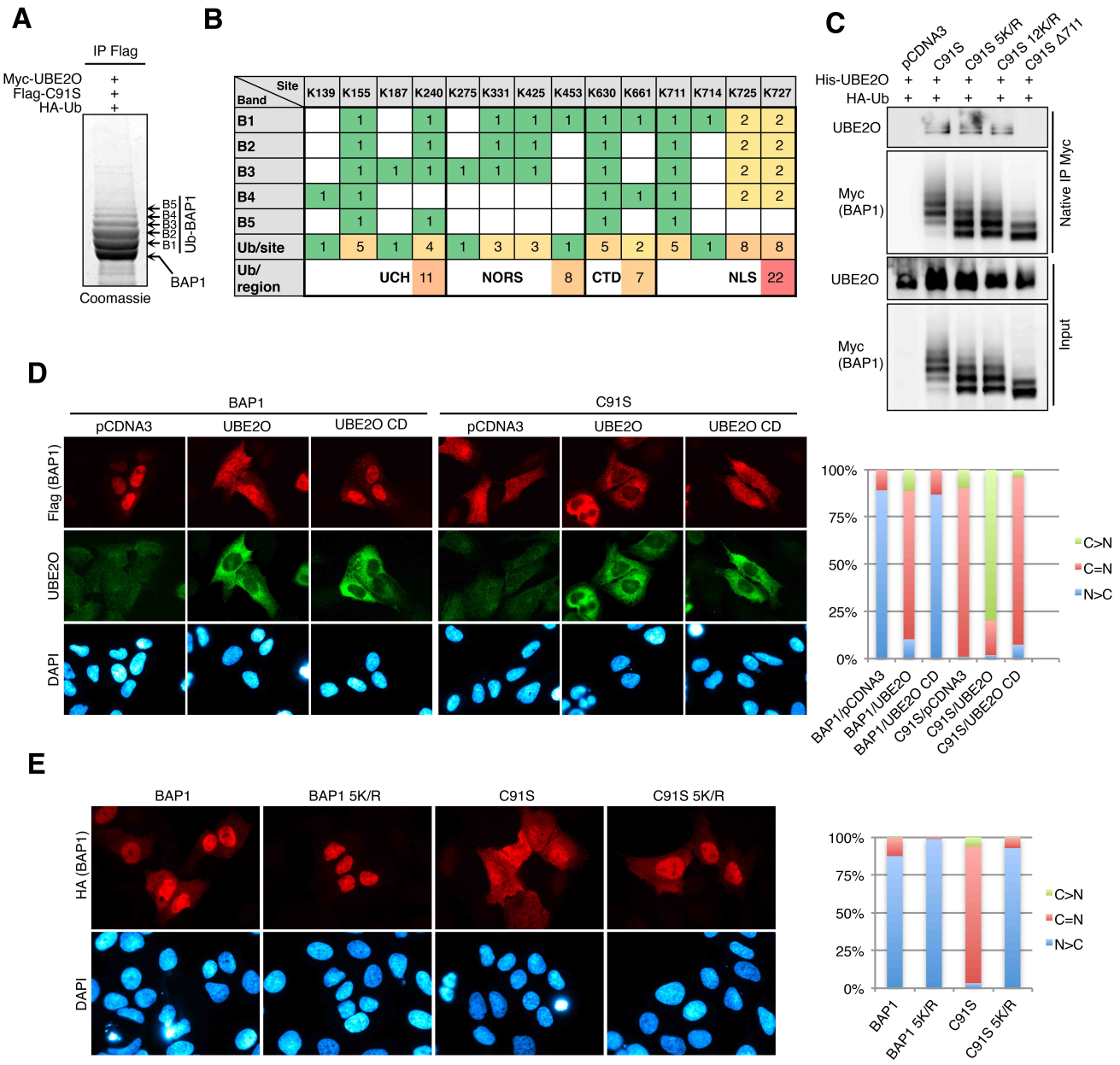

Figure 4. Ubiquitination of BAP1 NLS by UBE2O promotes its cytoplasmic sequestration. (See also Figure S4).

A) 293T cells were co-transfected with 2 µg of HA-Ub, 2 µg of Myc-UBE2O, and 1 µg of Flag-C91S, and cell extracts were used for Flag immunoprecipitation. The indicated bands were excised for MS analysis. **B)** Table of ubiquitination events detected by MS. **C)** Cells were co-transfected with 2 µg of HA-Ub, 2 µg of His-UBE2O, and 1 µg of Myc-tagged

BAP1 mutants expression vectors, and cell extracts were used for immunoprecipitation. **D)** U2OS cells were co-transfected with either 2 μg of empty vector, Myc-UBE2O or Myc-UBE2O CD and 3 μg of either Flag-HA-BAP1 or Flag-HA-C91S expression vectors and were used for immunofluorescence analysis. Representative cell counts for BAP1 subcellular localization are shown. C, cytoplasmic; N, Nuclear. **E)** U2OS cells were transfected with Flag-HA-BAP1 mutants expression vectors and used for immunofluorescence analysis as in panel D.

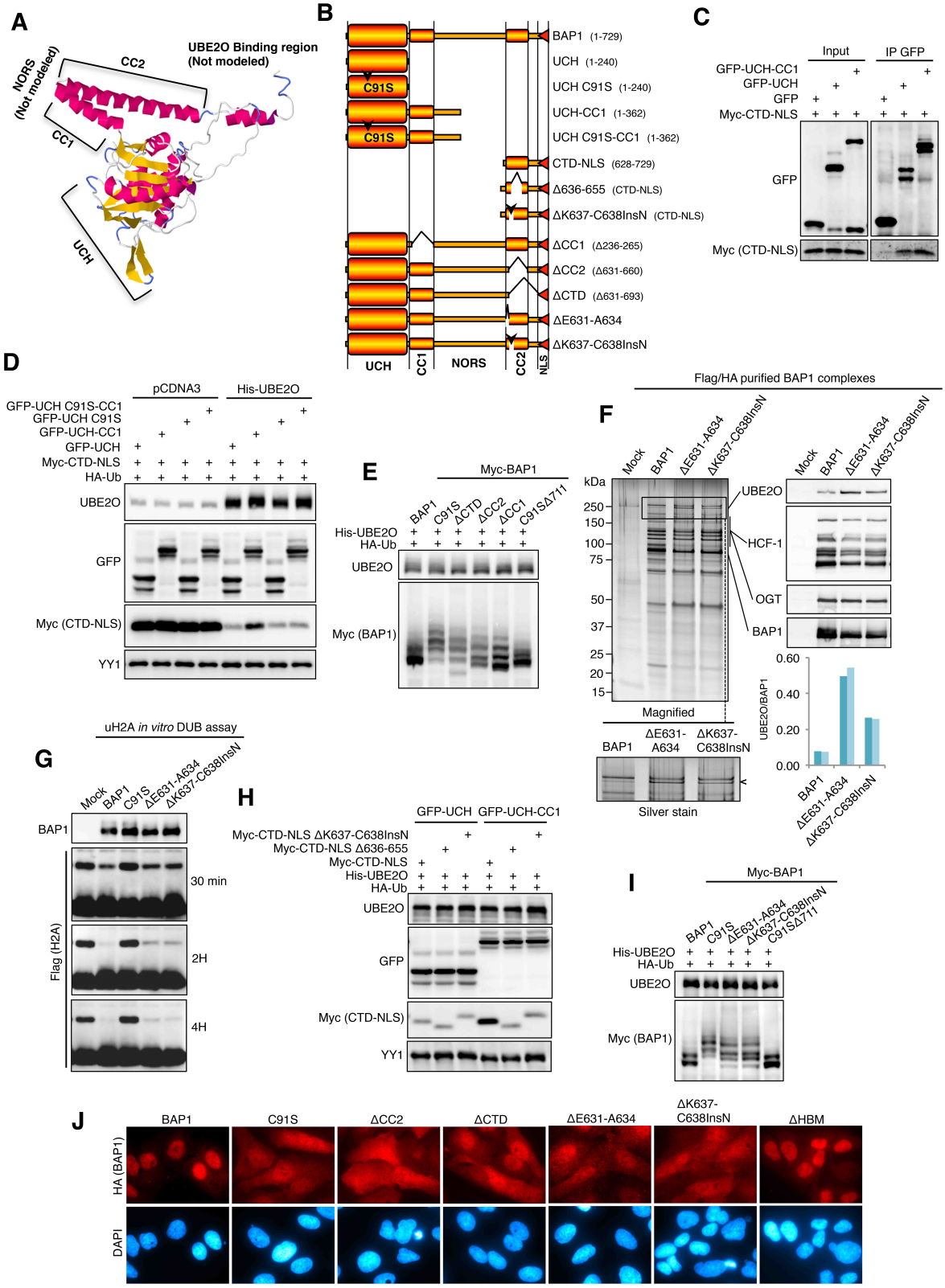
A
NORS (Not modeled)
CC2
UBE2O Binding region (Not modeled)
CC1
UCH
B
BAP1 (1-729)
UCH (1-240)
C91S
UCH C91S (1-240)
C91S
UCH-CC1 (1-362)
UCH C91S-CC1 (1-362)
CTD-NLS (628-729)
Δ636-655 (CTD-NLS)
ΔK637-C638InsN (CTD-NLS)
ΔCC1 (Δ236-265)
ΔCC2 (Δ631-660)
ΔCTD (Δ631-693)
ΔE631-A634
ΔK637-C638InsN
UCH
CC1
NORS
CC2
NLS
C
Input
IP GFP
GFP-UCH-CC1
GFP-UCH
GFP
Myc-CTD-NLS
GFP
Myc (CTD-NLS)
D
pCDNA3
His-UBE2O
GFP-UCH C91S-CC1
GFP-UCH C91S
GFP-UCH-CC1
GFP-UCH
Myc-CTD-NLS
HA-Ub
UBE2O
GFP
Myc (CTD-NLS)
YY1
E
Myc-BAP1
BAP1
C91S
ΔCTD
ΔCC2
ΔCC1
C91SΔ711
His-UBE2O
HA-Ub
UBE2O
Myc (BAP1)
F
Flag/HA purified BAP1 complexes
Mock
BAP1
ΔE631-A634
ΔK637-C638InsN
kDa
250
150
100
75
50
37
25
20
15
Magnified
BAP1
ΔE631-A634
ΔK637-C638InsN
Silver stain
UBE2O
HCF-1
OGT
BAP1
UBE2O/BAP1
0.60
0.40
0.20
0.00
G
uH2A in vitro DUB assay
Mock
BAP1
C91S
ΔE631-A634
ΔK637-C638InsN
BAP1
Flag (H2A)
30 min
2H
4H
H
GFP-UCH
GFP-UCH-CC1
Myc-CTD-NLS ΔK637-C638InsN
Myc-CTD-NLS Δ636-655
Myc-CTD-NLS
His-UBE2O
HA-Ub
UBE2O
GFP
Myc (CTD-NLS)
YY1
I
Myc-BAP1
BAP1
C91S
ΔE631-A634
ΔK637-C638InsN
C91SΔ711
His-UBE2O
HA-Ub
UBE2O
Myc (BAP1)
J
BAP1
C91S
ΔCC2
ΔCTD
ΔE631-A634
ΔK637-C638InsN
ΔHBM
HA (BAP1)
DAPI

Figure 5. BAP1 intramolecular interaction promotes auto-deubiquitination, a mechanism disrupted by cancer mutations. (See also Figure S5).

A) Predicted model of BAP1 UCH/CTD interface based on UCH37 crystal structure (PDB: 3IHR). Note that NLS and NORS are not present in UCH37, and thus not included in the model. **B)** Schematic representation of the mutants used for the complementation assay and the deletion mutants used in the context of full length BAP1. **C)** 293T cells were co-transfected with 2 μg of the indicated GFP fusion constructs and 2 μg of Myc-CTD-NLS expression vectors, and cell extracts were used for immunoprecipitation. **D)** 293T cells were co-transfected with 2 μg of HA-Ub and either 2 μg of empty vector or His-UBE2O, 1 μg of the indicated GFP fusion constructs and 1 μg of Myc-CTD-NLS expression vectors. **E)** 293T cells were co-transfected with 2 μg of HA-Ub, 2 μg of His-UBE2O, and 1 μg of Myc-BAP1 mutants expression vectors. **F**) Purified BAP1 complexes were analyzed by silver stain and western blotting. Densitometric ratios between UBE2O and BAP1 indicate its relative abundance in the complexes. The histogram shows two independent experiments. **G)** *In vitro* nucleosome deubiquitination reaction with purified BAP1 complexes. Samples were incubated at 37°C for the indicated times. **H)** 293T cells were co-transfected with 2 μg of HA-Ub, 2 μg of His-UBE2O expression vectors, 1 μg of indicated GFP fusion constructs and 1 μg of Myc-tagged constructs. **I)** 293T cells were co-transfected with 2 μg of HA-Ub, 2 μg of His-UBE2O, and 1 μg of Myc-tagged BAP1 mutants expression vectors. **J)** U2OS cell lines stably expressing Flag-HA-BAP1 and its mutant forms were used for immunofluorescence analysis.

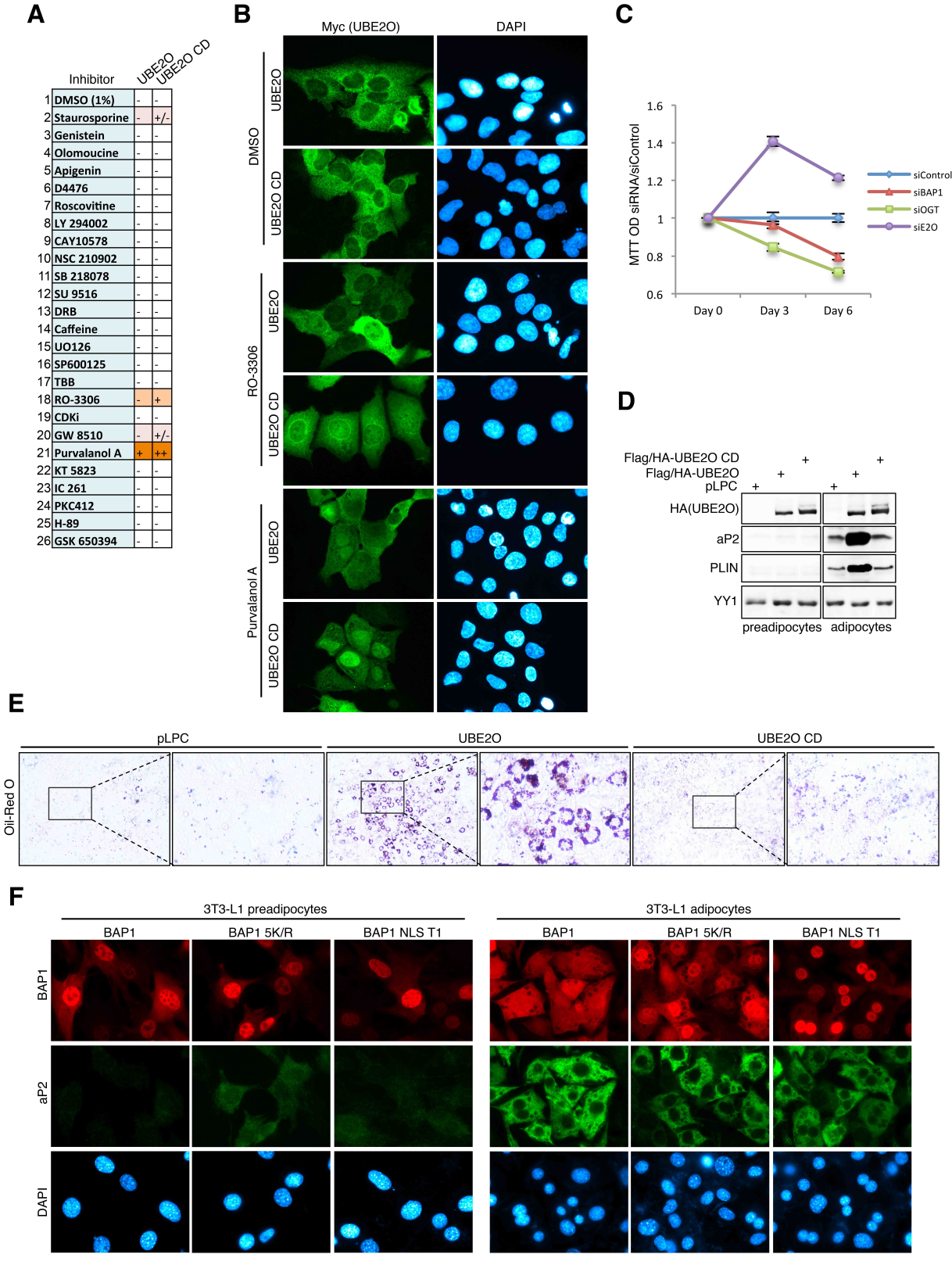
A
Inhibitor
UBE2O
UBE2O CD
1 DMSO (1%) - -
2 Staurosporine - +/-
3 Genistein - -
4 Olomoucine - -
5 Apigenin - -
6 D4476 - -
7 Roscovitine - -
8 LY 294002 - -
9 CAY10578 - -
10 NSC 210902 - -
11 SB 218078 - -
12 SU 9516 - -
13 DRB - -
14 Caffeine - -
15 UO126 - -
16 SP600125 - -
17 TBB - -
18 RO-3306 - +
19 CDKi - -
20 GW 8510 - +/-
21 Purvalanol A + ++
22 KT 5823 - -
23 IC 261 - -
24 PKC412 - -
25 H-89 - -
26 GSK 650394 - -
B
Myc (UBE2O)
DAPI
DMSO
RO-3306
Purvalanol A
UBE2O
UBE2O CD
C
MTT OD siRNA/siControl
1.6
1.4
1.2
1
0.8
0.6
Day 0
Day 3
Day 6
siControl
siBAP1
siOGT
siE2O
D
Flag/HA-UBE2O CD
Flag/HA-UBE2O
pLPC
HA(UBE2O)
aP2
PLIN
YY1
preadipocytes
adipocytes
E
pLPC
UBE2O
UBE2O CD
Oil-Red O
F
3T3-L1 preadipocytes
3T3-L1 adipocytes
BAP1
BAP1 5K/R
BAP1 NLS T1
aP2
DAPI

Figure 6. UBE2O shuttles between the nucleus and cytoplasm and promotes BAP1 cytoplasmic localization during adipocyte differentiation. (See also Figure S6).

A) Effect of kinase inhibition on nuclear localization of UBE2O. U2OS cells were transfected with 4 µg Myc-UBE2O or Myc-UBE2O CD expression vectors and then treated with a panel of kinase inhibitors for 24 hours prior harvesting for IF. + and - Indicate the relative intensity in the nuclear staining of UBE2O. **B)** Representative images of UBE2O localization in U2OS cells treated with CDK inhibitors. **C**) Effects of siRNA-depletion of UBE2O, BAP1 on cell proliferation, determined by MTT assay. siRNA for OGT is used as a control of decreased proliferation. Note that the values are relative to the non-target control siRNA for each time point. **D,E)** Effects of overexpression of UBE2O wild type or catalytic dead form on the differentiation of 3T3L1. Immunodetection of differentiation markers (E) and Oil-Red O staining (F). YY1 is used as a loading control. **F)** Localization of BAP1 and mutants during adipocyte differentiation. The BAP1 NLST1 corresponds to a mutant in which the NLS region of BAP1 which includes the UBE2O-binding motif is replaced with the T large antigen NLS. The BAP1 K/R mutant is mutated in the UBE2O-ubiquitination sites of the NLS.

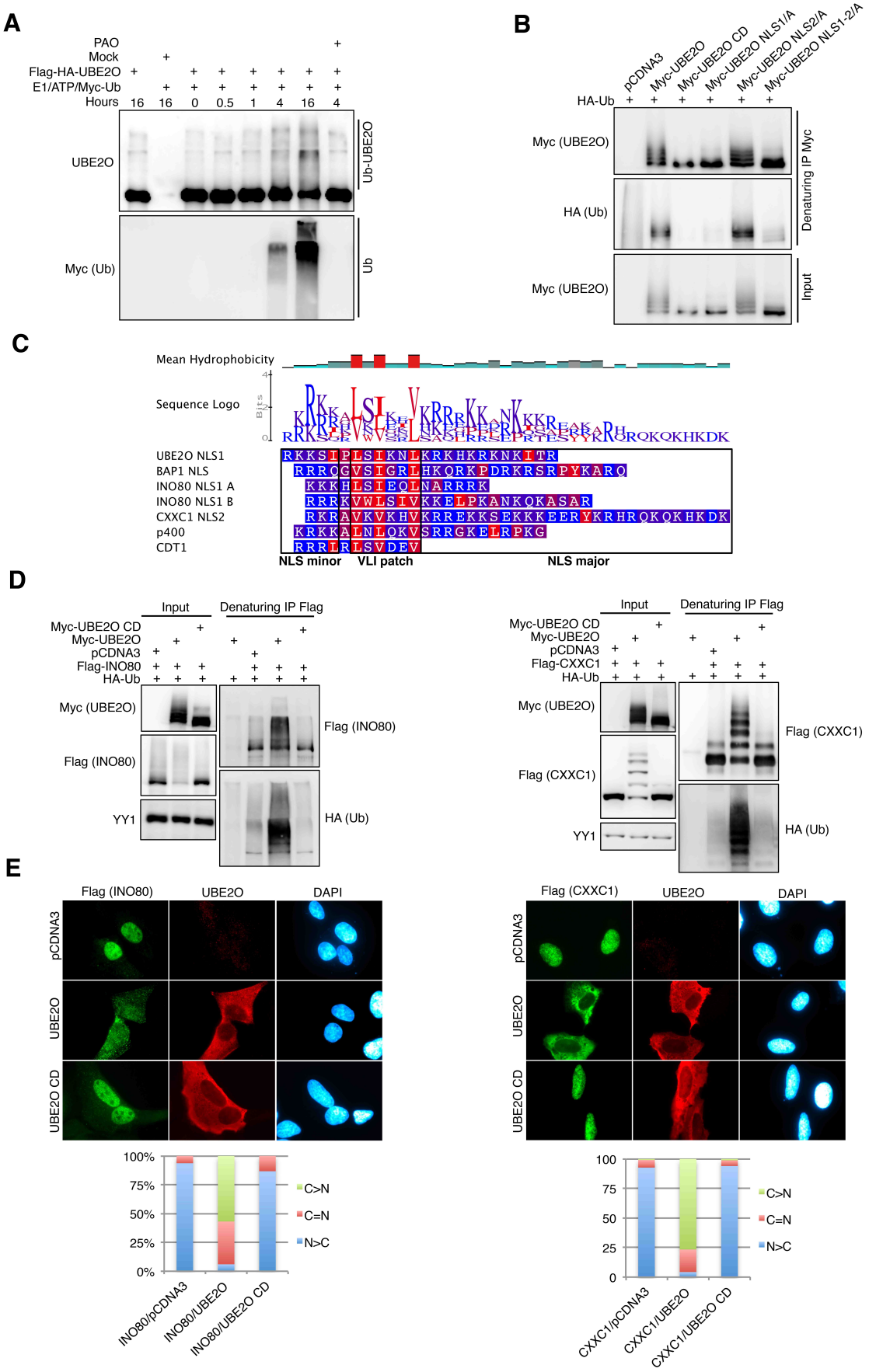
A
PAO
Mock
Flag-HA-UBE2O
E1/ATP/Myc-Ub
Hours
16 16 0 0.5 1 4 16 4
UBE2O
Ub-UBE2O
Myc (Ub)
Ub
B
pCDNA3
Myc-UBE2O
Myc-UBE2O CD
Myc-UBE2O NLS1/A
Myc-UBE2O NLS2/A
Myc-UBE2O NLS1-2/A
HA-Ub
Myc (UBE2O)
HA (Ub)
Myc (UBE2O)
Denaturing IP Myc
Input
C
Mean Hydrophobicity
Sequence Logo
Bits
UBE2O NLS1
BAP1 NLS
INO80 NLS1 A
INO80 NLS1 B
CXXC1 NLS2
p400
CDT1
NLS minor
VLI patch
NLS major
D
Input
Denaturing IP Flag
Myc-UBE2O CD
Myc-UBE2O
pCDNA3
Flag-INO80
HA-Ub
Myc (UBE2O)
Flag (INO80)
YY1
Flag (INO80)
HA (Ub)
Flag-CXXC1
Flag (CXXC1)
E
Flag (INO80)
UBE2O
DAPI
pCDNA3
UBE2O
UBE2O CD
100%
75%
50%
25%
0%
C>N
C=N
N>C
INO80/pCDNA3
INO80/UBE2O
INO80/UBE2O CD
Flag (CXXC1)
100
75
50
25
0
CXXC1/pCDNA3
CXXC1/UBE2O
CXXC1/UBE2O CD

Figure 7. UBE2O targets a subset of chromatin-associated proteins. (See also Figure S7). **A)** *In vitro* ubiquitination reaction with the purified UBE2O. Samples were incubated for the indicated times. **B)** 293T cells were co-transfected with 2 µg of HA-Ub and 2 µg of indicated Myc-UBE2O mutants, and cell extracts were used for immunoprecipitation. **C)** Sequence alignment between the UBE2O/BAP1 NLS and a subset of identified UBE2O substrates. Hydrophobic amino acids are in red and polar amino acids are in blue. A large N-terminal extension containing the NLS of CDT1 is not shown. **D)** 293T cells were co-transfected with 2 µg of HA-Ub and 1 µg of Flag-CXXC1 or 2 µg of Flag-INO80, and either 2 µg of empty vector, Myc-UBE2O or Myc-UBE2O CD expression vectors, and cell extracts were used for immunoprecipitation. **E)** U2OS cells were co-transfected with 0,5 µg of HA-Ub and either 1 µg of empty vector, Myc-UBE2O, Myc-UBE2O CD and 1 µg of either Flag-INO80 or Flag-CXXC1 expression vectors and used for immunofluorescence analysis. Representative cell counts are shown.

SUPPLEMENTAL INFORMATION INVENTORY

Figure S1. Related to Figure 1.

Contains the initial characterization of the UBE2O-independent BAP1 monoubiquitination, the comparison of UBE2O with other E2s, the *in vivo* ubiquitination controls for UBE2O specificity and UBE2O sequence conservation.

Figure S2. Related to Figure 2.

Contains schema of the protein purifications, the *in vitro* ubiquitination reactions and characterization of the effects of other E3 ligases on UBE2O-mediated ubiquitination of BAP1.

Figure S3. Related to Figure 3.

Contains the information about the degradation of CTD-NLS, the characterization of BAP1 NLS, the alanine mutagenesis screen in BAP1 NLS and the alignment of NLS regions of BAP1 orthologs.

Figure S4. Related to Figure 4.

Contains immunostaining of UBE2O overexpression and its effects on the localization of endogenous BAP1, YY1 and HCF-1.

Figure S5. Related to Figure 5.

Contains the characterization of UCH37 in respect to its auto-deubiquitination activity, the alignment of UCH37 and BAP1 C-terminal regions, crystal structure of UCH37, the characterization of the effect of the G13V mutation on BAP1 auto-deubiquitination activity and the establishment of the *in vitro* H2A DUB assay on nucleosomes.

Figure S6. Related to Figure 6.

Contains the mapping and characterization of UBE2O NLS regions, purification of UBE2O-associated proteins and schema of UBE2O and BAP1 post-translational modifications.

Figure S7. Related to Figure 7.

Contains the effects of the mutation in the VLI patch which disrupts UBE2O auto-catalytic activity, the effects of UBE2O on the degradation of p400 and CDT1 following expression of UBE2O, the characterization of the predicted UBE2O substrate ALC1 which tested negative for UBE2O-mediated ubiquitination and the list of the predicted UBE2O nuclear substrates based on the *[KR][KR][KR]-X(1,3)-[VLI]-X-[VLI]-X-X-[VLI]* consensus.

EXTENDED EXPERIMENTAL PROCEDURES

SUPPLEMENTAL REFERENCES

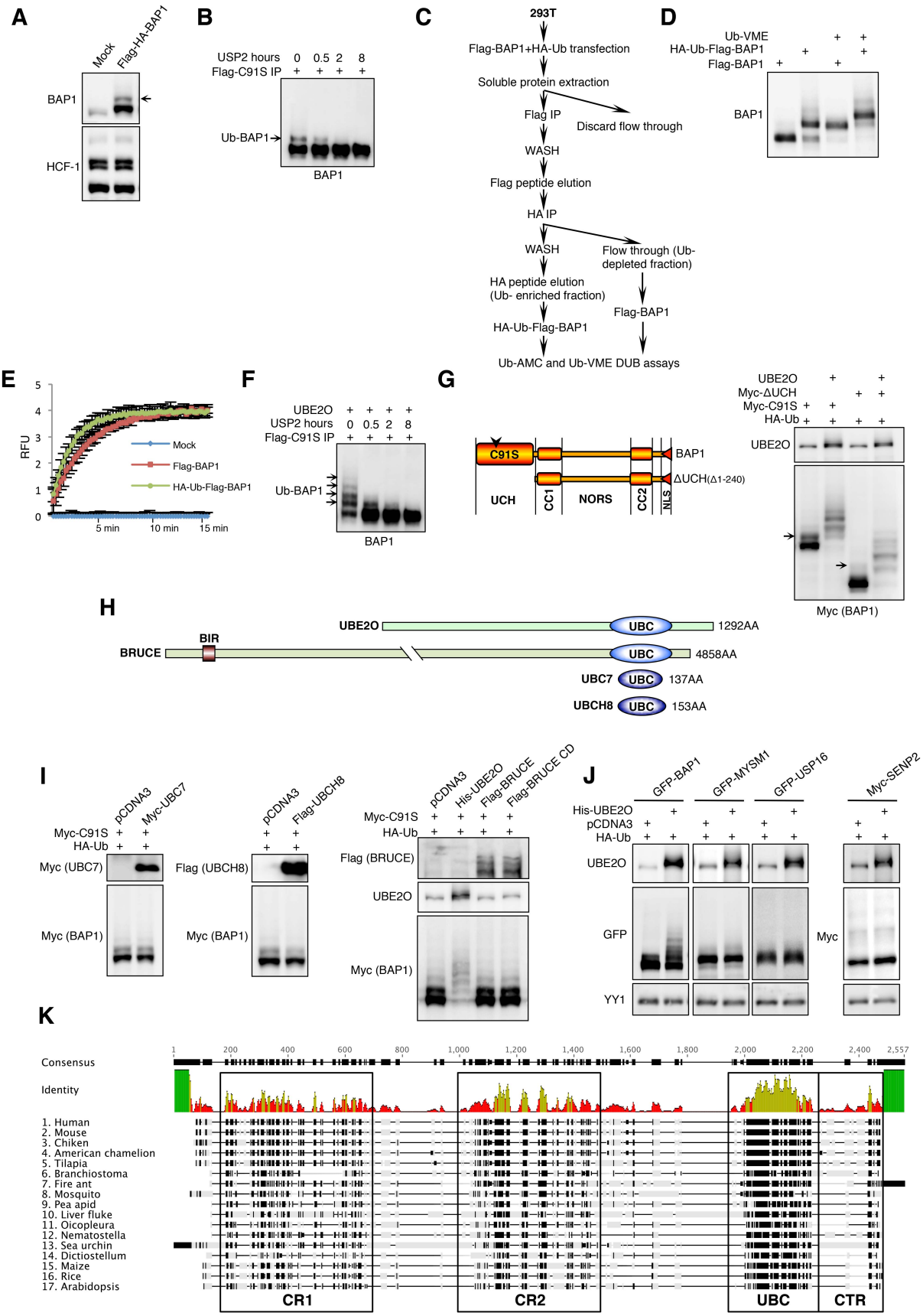
A
Mock
Flag-HA-BAP1
BAP1
HCF-1
B
USP2 hours 0 0.5 2 8
Flag-C91S IP + + + +
Ub-BAP1
BAP1
C
293T
Flag-BAP1+HA-Ub transfection
Soluble protein extraction
Flag IP
Discard flow through
WASH
Flag peptide elution
HA IP
WASH
Flow through (Ub-depleted fraction)
HA peptide elution (Ub- enriched fraction)
Flag-BAP1
HA-Ub-Flag-BAP1
Ub-AMC and Ub-VME DUB assays
D
Ub-VME + +
HA-Ub-Flag-BAP1 + +
Flag-BAP1 + +
BAP1
E
RFU
Mock
Flag-BAP1
HA-Ub-Flag-BAP1
5 min
10 min
15 min
F
UBE2O + + + +
USP2 hours 0 0.5 2 8
Flag-C91S IP + + + +
Ub-BAP1
BAP1
G
C91S
BAP1
ΔUCH(Δ1-240)
UCH
CC1
NORS
CC2
NLS
UBE2O + +
Myc-ΔUCH + +
Myc-C91S + +
HA-Ub + + + +
UBE2O
Myc (BAP1)
H
UBE2O
UBC
1292AA
BRUCE
BIR
UBC
4858AA
UBC7
UBC
137AA
UBCH8
UBC
153AA
I
pCDNA3
Myc-UBC7
Myc-C91S + +
HA-Ub + +
Myc (UBC7)
Myc (BAP1)
pCDNA3
Flag-UBCH8
+ +
Flag (UBCH8)
Myc (BAP1)
pCDNA3
His-UBE2O
Flag-BRUCE
Flag-BRUCE CD
Myc-C91S + + + +
HA-Ub + + + +
Flag (BRUCE)
UBE2O
Myc (BAP1)
J
GFP-BAP1
GFP-MYSM1
GFP-USP16
Myc-SENP2
His-UBE2O + +
pCDNA3 + + +
HA-Ub + + + + + +
UBE2O
GFP
Myc
YY1
K
Consensus
Identity
1. Human
2. Mouse
3. Chiken
4. American chamelion
5. Tilapia
6. Branchiostoma
7. Fire ant
8. Mosquito
9. Pea apid
10. Liver fluke
11. Oicopleura
12. Nematostella
13. Sea urchin
14. Dictiostellum
15. Maize
16. Rice
17. Arabidopsis
1 200 400 600 800 1,000 1,200 1,400 1,600 1,800 2,000 2,200 2,400 2,557
CR1
CR2
UBC
CTR

Figure S1 (Related to Figure 1).

Characterization of the UBE2O-independent mono-ubiquitination of BAP1.

A) Detection of the modified form of BAP1 in U2OS cells stably expressing Flag-HA-BAP1. U2OS cells were transduced with empty pOZ-N vector or pOZ-N-BAP1, selected with anti-IL2 receptor-coupled magnetic beads (4 rounds of selection), as previously described (Yu et al., 2010), and cell lysates were subjected to western blotting with the indicated antibodies. **B)** 293T cells were transfected with 3 μg of Flag-BAP1 C91S and harvested three days-post-transfection for immunoprecipitation. Anti-Flag column-purified C91S was incubated with 200 nM of recombinant USP2 catalytic domain and collected for western blotting at the indicated time points. Note the decrease of the constitutive ubiquitin modification. **C)** Schema of the double column purification strategy of ubiquitin-depleted and -enriched fractions of BAP1. **D)** Analysis of the anti-HA beads-bound and the flow through fractions revealed that the slower migrating band was enriched in the HA-bound fraction and depleted in the flow through fraction proving the monoubiquitination nature of the modification. Monoubiquitination of BAP1 does not influence its ability to incorporate the ubiquitin vinylmethylester (Ub-VME) suicide substrate. HA-Ub-Flag-BAP1 and unmodified Flag-BAP1 fractions where incubated with 1 μM of Ub-VME probe and analyzed by western blot as recently described (Yu et al., 2014). Note the similar efficiency of Ub-VME incorporation that corresponds to the slower migrating form of BAP1. **E)** Fluorometric analysis of the BAP1 activity towards the Ub-AMC DUB substrate. Adjusted amounts of the HA-Ub-Flag-BAP1 and unmodified Flag-BAP1 fractions where incubated with 100 nM of the Ub-AMC and fluorescence was analyzed in real time. Data are represented as mean +/- SD. Note that the modified form of BAP1 displays a similar DUB activity as the modified form towards this model substrate. **F)** The ubiquitinated forms of C91S can be efficiently deubiquitinated by USP2. The procedure was carried out essentially as in panel B except that UBE2O was included in the co-transfection. **G)** Similar UBE2O-mediated multi-mono-ubiquitination of BAP1 C91S or ΔUCH. 293T cells were co-transfected with 1 μg of Myc-C91S or Myc-BAP1 ΔUCH, 2 μg of HA-Ub and 2 μg of either empty vector or UBE2O. Three days later, cell lysates

were used for western blotting and probed with the indicated antibodies. Note the decrease of the constitutive BAP1 mono-ubiquitination upon the deletion of the UCH domain indicating that distinct activities modify BAP1.

Characterization of UBE2O specificity towards BAP1.

H) Comparison of several members of class I and IV ubiquitin carrier enzymes. **I)** To control for specificity, we evaluated other E2s (van Wijk and Timmers, 2010) including BRUCE, the closest evolutionary relative of UBE2O which was previously shown to act as an E2/E3 hybrid on other substrates (Bartke et al., 2004; Hao et al., 2004).

293T cells were co-transfected with 1 µg of Myc-C91S, 2 µg of HA-Ub and either 2 µg of empty vector, Myc-UBC7, Flag-UBCH8, 5 µg of Flag-BRUCE or 5 µg Flag-BRUCE CD (C4654S) expression vectors. Three days later, cell lysates were used for western blotting. **J)** We also tested two known H2A DUBs, i.e., USP16 and MYSM1 (Joo et al., 2007; Zhu et al., 2007), as well as the SUMO protease SENP2 (Kim et al., 2000). 293T cells were co-transfected with 2 µg of HA-Ub and either 2 µg of empty vector or 2 µg of His-UBE2O and either 1 µg of GFP-BAP1, GFP-MYSM1, GFP-USP16 or Myc-SENP2 expression vectors. Three days later, cell lysates were used for western blotting. **K)** Multiple sequence alignment of UBE2O orthologs, conserved regions are highlighted.

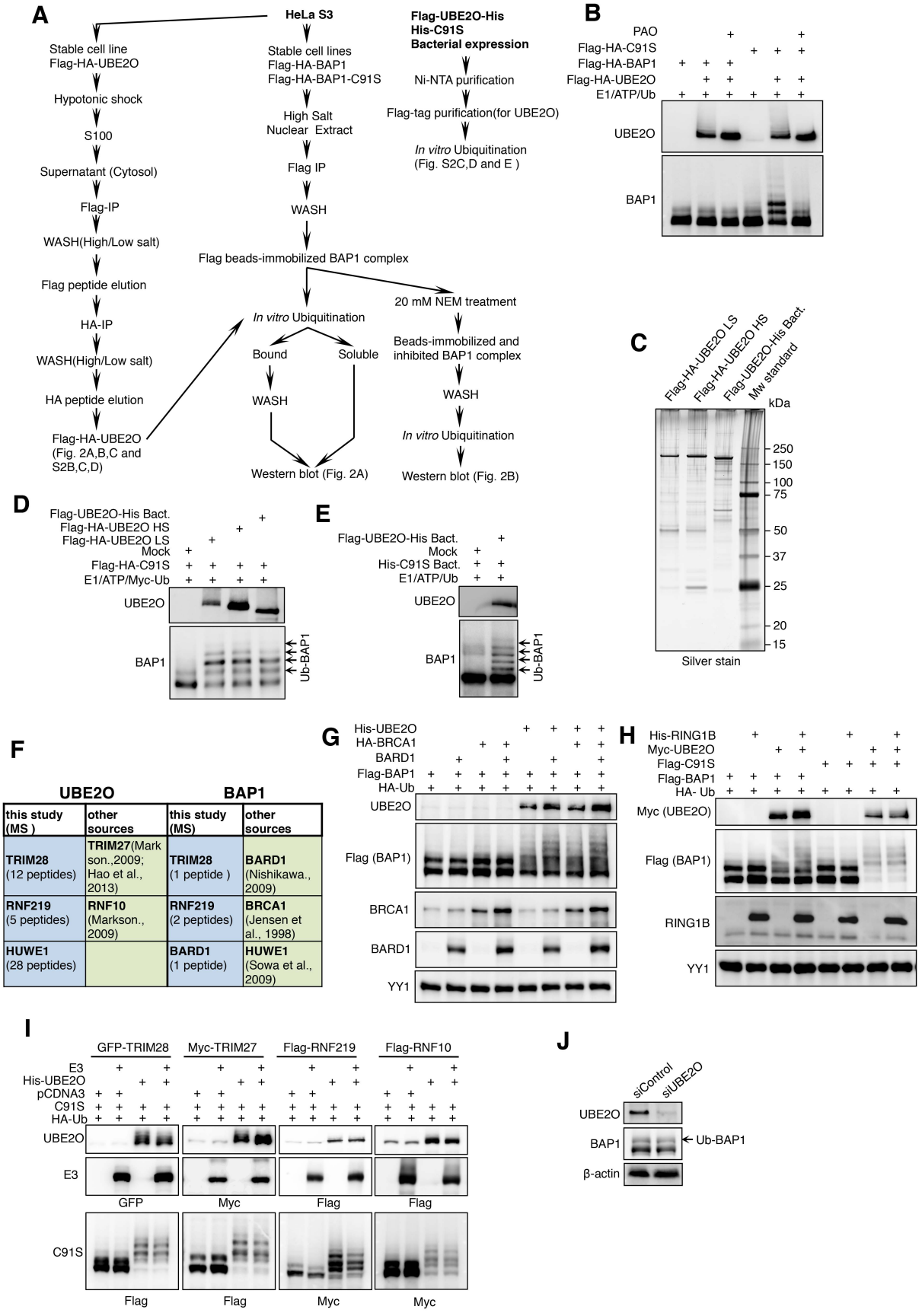
A
HeLa S3
Stable cell line
Flag-HA-UBE2O
Hypotonic shock
S100
Supernatant (Cytosol)
Flag-IP
WASH(High/Low salt)
Flag peptide elution
HA-IP
WASH(High/Low salt)
HA peptide elution
Flag-HA-UBE2O
(Fig. 2A,B,C and S2B,C,D)
Stable cell lines
Flag-HA-BAP1
Flag-HA-BAP1-C91S
High Salt
Nuclear Extract
Flag IP
WASH
Flag beads-immobilized BAP1 complex
In vitro Ubiquitination
Bound
Soluble
WASH
Western blot (Fig. 2A)
20 mM NEM treatment
Beads-immobilized and inhibited BAP1 complex
WASH
In vitro Ubiquitination
Western blot (Fig. 2B)
Flag-UBE2O-His
His-C91S
Bacterial expression
Ni-NTA purification
Flag-tag purification(for UBE2O)
In vitro Ubiquitination
(Fig. S2C,D and E)
B
PAO
Flag-HA-C91S
Flag-HA-BAP1
Flag-HA-UBE2O
E1/ATP/Ub
UBE2O
BAP1
C
Flag-HA-UBE2O LS
Flag-HA-UBE2O HS
Flag-UBE2O-His Bact.
Mw standard
kDa
250
150
100
75
50
37
25
20
15
Silver stain
D
Flag-UBE2O-His Bact.
Flag-HA-UBE2O HS
Flag-HA-UBE2O LS
Mock
Flag-HA-C91S
E1/ATP/Myc-Ub
UBE2O
BAP1
Ub-BAP1
E
Flag-UBE2O-His Bact.
Mock
His-C91S Bact.
E1/ATP/Ub
UBE2O
BAP1
Ub-BAP1
F
UBE2O
BAP1
this study (MS)
other sources
this study (MS)
other sources
TRIM28 (12 peptides)
TRIM27(Markson.,2009; Hao et al., 2013)
TRIM28 (1 peptide)
BARD1 (Nishikawa., 2009)
RNF219 (5 peptides)
RNF10 (Markson., 2009)
RNF219 (2 peptides)
BRCA1 (Jensen et al., 1998)
HUWE1 (28 peptides)
BARD1 (1 peptide)
HUWE1 (Sowa et al., 2009)
G
His-UBE2O
HA-BRCA1
BARD1
Flag-BAP1
HA-Ub
UBE2O
Flag (BAP1)
BRCA1
BARD1
YY1
H
His-RING1B
Myc-UBE2O
Flag-C91S
Flag-BAP1
HA- Ub
Myc (UBE2O)
Flag (BAP1)
RING1B
YY1
I
GFP-TRIM28
Myc-TRIM27
Flag-RNF219
Flag-RNF10
E3
His-UBE2O
pCDNA3
C91S
HA-Ub
UBE2O
E3
GFP
Myc
Flag
Flag
C91S
Flag
Flag
Myc
Myc
J
siControl
siUBE2O
UBE2O
BAP1
Ub-BAP1
β-actin

Figure S2 (Related to Figure 2).

Set up of the *in vitro* ubiquitination reaction.

A) Schema of protein purification and *in vitro* ubiquitination reactions for figure 2A, 2B, S2B, S2D and S2E. **B)** Purified BAP1 or C91S complexes were incubated with immunopurified UBE2O in an *in vitro* ubiquitination reaction. Samples were treated with 100 μM PAO as indicated. **C)** Mammalian Flag/HA or bacterial His/Flag purified UBE2O was loaded on a 4-12% gel and used for silver staining. **D)** Purified C91S complexes were incubated with UBE2O, purified from human cells or bacteria, in an *in vitro* ubiquitination reaction. Note that UBE2O maintains similar activity towards C91S independently of its origin and method of purification. HS and LS represent high salt and low salt washes, respectively. **E)** Ubiquitination with recombinant enzymes. His-C91S was purified from bacteria and used for *in vitro* reaction with bacteria purified Flag-UBE2O-His.

UBE2O- and BAP1-interacting ubiquitin ligases do not influence UBE2O ubiquitination activity towards BAP1.

F) Summary of potential UBE2O- and BAP1-interacting ubiquitin ligases. Our purification and mass spectrometry analysis of UBE2O- or BAP1-interacting proteins revealed additional substoichiometric E3 ligases that might participate in UBE2O-dependent or –independent ubiquitination of BAP1. Other E3 ligases previously reported as potential UBE2O- or BAP1-interacting enzymes are also included. **G)** 293T cells were transfected with 2 μg of HA-Ub, 1 μg of HA-BRCA1 and/or 0,5 μg of HA-BARD1, 1 μg of BAP1 and either 2 μg of empty vector or Myc-UBE2O expression vectors. Three days later, cell lysates were used for western blotting with the indicated antibodies. We note that BAP1 was described as a partner of the tumor suppressor and RING E3 ligase complex BRCA1/BARD1 that may perform ubiquitin chain elongation (Jensen et al., 1998; Wu-Baer et al., 2003). Nonetheless co-transfection with BRCA1/BARD1 did not significantly affect the pattern of BAP1 ubiquitination by UBE2O. **H)** Cells were transfected with 2 μg of HA-Ub, 1 μg of His-RING1B, 1 μg of BAP1 or C91S and either 2 μg of empty vector or Myc-UBE2O expression vectors. Three days later, cell lysates were used for western blotting with the indicated antibodies. BAP1 acts in concert with the RING1B E3 ligase to

regulate H2A ubiquitination (Carbone et al., 2013; Scheuermann et al., 2010). However, no direct ubiquitination of BAP1 or cooperation between RING1B and UBE2O were observed. **I)** Cells were transfected with 2 µg of HA-Ub, 0.5 µg of C91S, 2 µg of empty vector or His-UBE2O and 3 µg of GFP-TRIM28, Myc-TRIM27, Flag-RNF219 or Flag-RNF10 expression vectors. Three days later, cell lysates were used for western blotting with the indicated antibodies. Note the similar pattern of the C91S ubiquitination independently of the ubiquitin ligase co-expression. We were unable to express significant levels of HUWE1 (~500 kDa). Thus, we did not conclude about its potential effect alone or on UBE2O-mediated ubiquitination of BAP1. **J)** U2OS cell line stably expressing Flag-HA-BAP1 was transfected with control siRNA or siUBE2O. Three days later, cell lysates were used for western blotting with the indicated antibodies. Note that the knockdown of UBE2O has no effect on the constitutive monoubiquitination of BAP1 (described in Figure S1A-E, G).

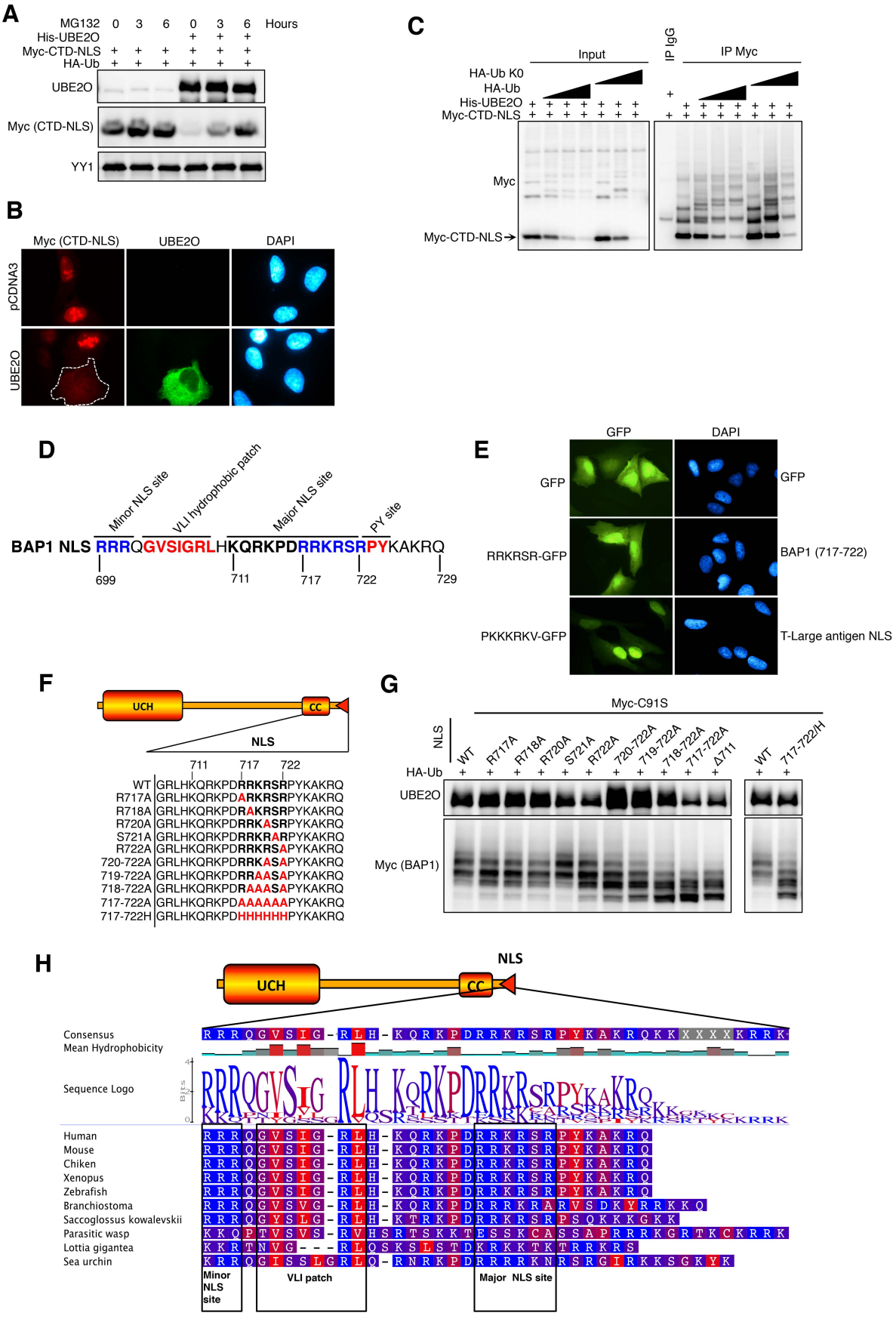
A
MG132 0 3 6 0 3 6 Hours
His-UBE2O + + +
Myc-CTD-NLS + + + + + +
HA-Ub + + + + + +
UBE2O
Myc (CTD-NLS)
YY1
B
Myc (CTD-NLS)
UBE2O
DAPI
pCDNA3
UBE2O
C
Input
IP IgG
IP Myc
HA-Ub K0
HA-Ub
His-UBE2O
Myc-CTD-NLS
Myc
Myc-CTD-NLS
D
Minor NLS site
VLI hydrophobic patch
Major NLS site
PY site
BAP1 NLS RRRQGVSIGRLHKQRKPDRRKRSRPYKAKRQ
699
711
717
722
729
E
GFP
DAPI
GFP
RRKRSR-GFP
PKKKRKV-GFP
GFP
BAP1 (717-722)
T-Large antigen NLS
F
UCH
CC
NLS
711 717 722
WT GRLHKQRKPDRRKRSRPYKAKRQ
R717A GRLHKQRKPDARKRSRPYKAKRQ
R718A GRLHKQRKPDRAKRSRPYKAKRQ
R720A GRLHKQRKPDRRKASRPYKAKRQ
S721A GRLHKQRKPDRRKRARPYKAKRQ
R722A GRLHKQRKPDRRKRSAPYKAKRQ
720-722A GRLHKQRKPDRRKASAPYKAKRQ
719-722A GRLHKQRKPDRRAASAPYKAKRQ
718-722A GRLHKQRKPDRAAASAPYKAKRQ
717-722A GRLHKQRKPDAAAAAPYKAKRQ
717-722H GRLHKQRKPDHHHHHPYKAKRQ
G
Myc-C91S
NLS
WT R717A R718A R720A S721A R722A 720-722A 719-722A 718-722A 717-722A Δ711 WT 717-722/H
HA-Ub
UBE2O
Myc (BAP1)
H
NLS
UCH
CC
Consensus
Mean Hydrophobicity
Sequence Logo
Bits
Human
Mouse
Chiken
Xenopus
Zebrafish
Branchiostoma
Saccoglossus kowalevskii
Parasitic wasp
Lottia gigantea
Sea urchin
Minor NLS site
VLI patch
Major NLS site

Figure S3 (Related to Figure 3).

UBE2O promotes degradation of BAP1 CTD-NLS.

A) 293T cells were co-transfected with 2 µg of HA-Ub, 2 µg of His-UBE2O, and 1 µg of Myc-CTD-NLS expression vectors. Three days later, cells were treated with 20 µM of MG132 for the indicated time points and harvested for western blotting. **B)** U2OS cells were co-transfected with 0,5 µg of HA-Ub, 1 µg of His-UBE2O and 1 µg of Myc-CTD-NLS expression vectors and plated on coverslips. Three days later, cells were fixed and used for immunofluorescence. **C)** 293T cells were co-transfected with increasing amounts of HA-Ub or HA-Ub K0 (0.5 µg, 1.5 µg or 4 µg), 2 µg of His-UBE2O, and 1 µg of Myc-CTD-NLS expression vectors. Three days later, cells extracts were analyzed by western blotting. Note that UBE2O promotes the Myc-CTD-NLS degradation in ubiquitin-dependent manner, and a similar degradation profile is obtained with either wild type or K0 ubiquitin mutant.

Characterization of the BAP1 NLS region.

D) Representation of the predicted BAP1 NLS. The basic regions are in blue and hydrophobic regions are in red. BAP1 possesses a complex NLS region that shares similarities with classical monopartite (Conti et al., 1998), bipartite (Robbins et al., 1991) and the atypical hydrophobic/basic PY NLS (Lee et al., 2006). **E)** U2OS cells were transfected with 0,5 µg of the indicated GFP fusion NLS. Three days later, cells were fixed and used for fluorescence microscope imaging. The region spanning a short stretch of basic amino acids RRKRSR (aa 717-722) is necessary for proper nuclear localization of BAP1 (Ventii et al., 2008). However, when fused to GFP, this motif was not sufficient to promote nuclear localization, i.e., additional sequences are required for NLS function. Therefore, we considered the entire aa 699-729 region as BAP1 NLS for further characterization.

Requirement of the major NLS site of BAP1 for UBE2O-mediated ubiquitination.

F) Schematic representation of the alanine screen mutants, mutations are indicated in red. **G)** 293T cells were co-transfected with 2 µg of HA-Ub, 2 µg of His-UBE2O, and 1 µg of Myc-C91S mutants expression vectors. Three days later, cell extracts were used for

western blotting and probed with the indicated antibodies. Single point mutations in the region did not cause significant reduction of C91S ubiquitination, but cumulative alanine mutations were able to gradually decrease the efficiency of ubiquitination. The substitution of RRKRSR to a similarly positively charged histidine stretch also strongly reduced the ubiquitination by UBE2O indicating that the arginine/lysine residues are critical

Sequence comparison of the NLS region from different BAP1 orthologs.

H) Multiple sequence alignment of the NLS regions of BAP1 from metazoan species using the Geneious tool, polar amino acids are in blue, hydrophobic amino acids are in red.

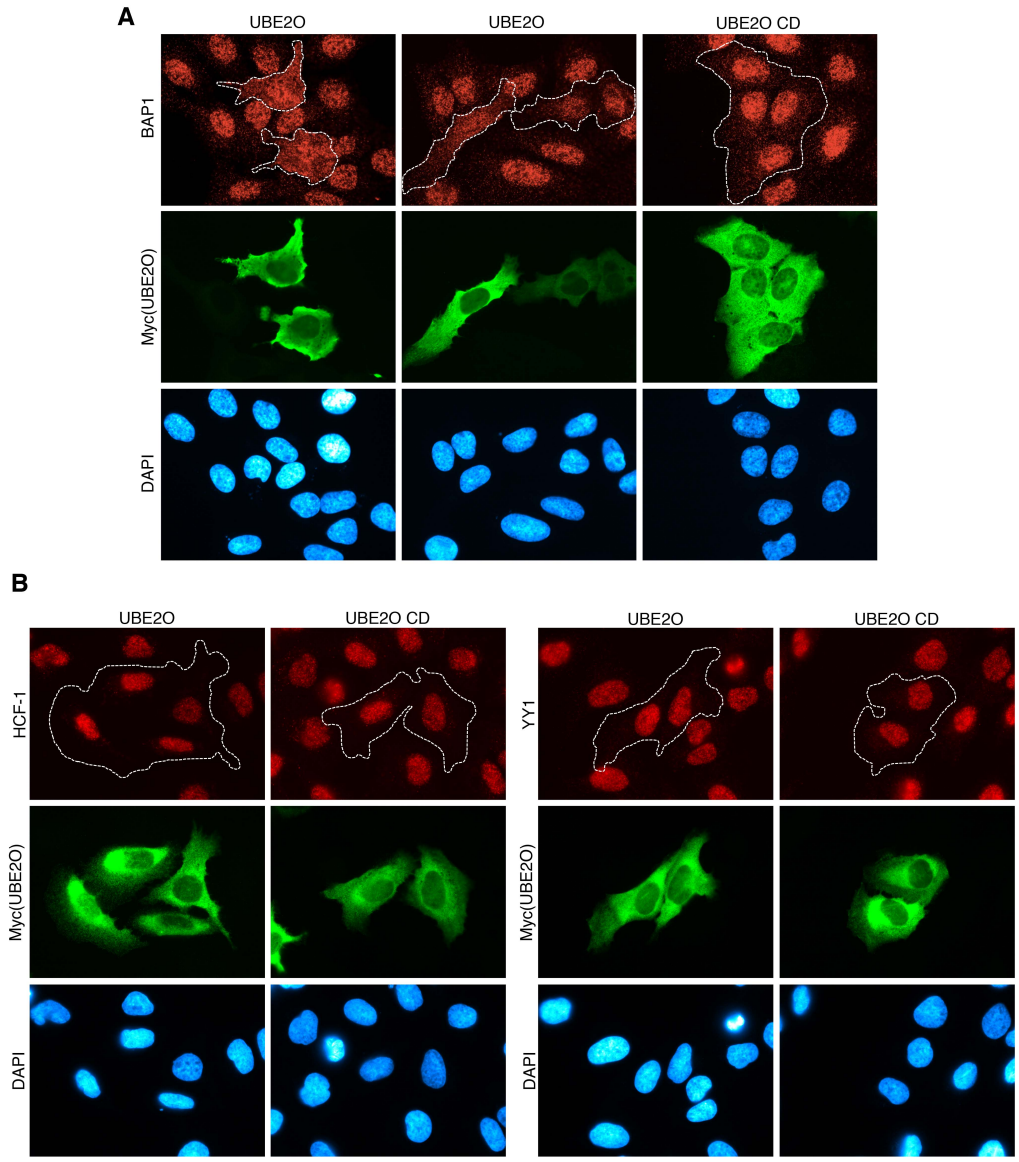

Figure S4 (Related to Figure 4).

Overexpression of UBE2O promotes cytoplasmic localization of endogenous BAP1. U2OS cells were transfected with 4 µg of the Myc-UBE2O or Myc-UBE2O CD. Three days later, cells were fixed and used for Immunofluorescence for BAP1 **(A)** or HCF-1 and YY1 **(B).** UBE2O promoted cytoplasmic localization of BAP1 but had no visible effect on YY1 and HCF-1.

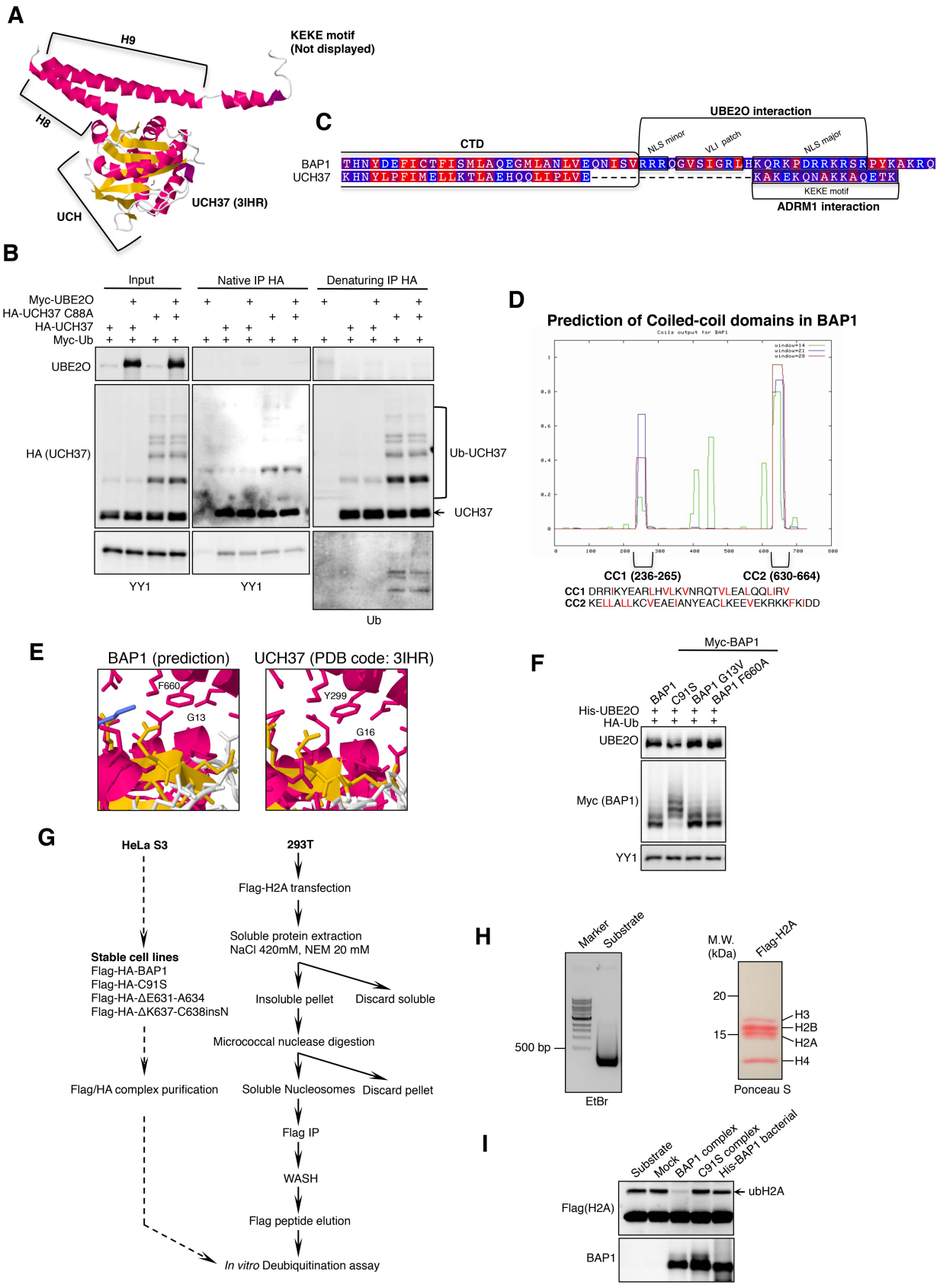
A
H9
H8
KEKE motif
(Not displayed)
UCH
UCH37 (3IHR)
C
UBE2O interaction
CTD
NLS minor
VLI patch
NLS major
BAP1
UCH37
KEKE motif
ADRM1 interaction
B
Input
Native IP HA
Denaturing IP HA
Myc-UBE2O
HA-UCH37 C88A
HA-UCH37
Myc-Ub
UBE2O
HA (UCH37)
Ub-UCH37
UCH37
YY1
YY1
Ub
D
Prediction of Coiled-coil domains in BAP1
CC1 (236-265)
CC2 (630-664)
CC1 DRRIKYEARLHVLKVNRQTVLEALQQLIRV
CC2 KELLALLKCVEAEIANYEACLKEEVEKRKKFKIDD
E
BAP1 (prediction)
UCH37 (PDB code: 3IHR)
F660
G13
Y299
G16
F
Myc-BAP1
BAP1
C91S
BAP1 G13V
BAP1 F660A
His-UBE2O
HA-Ub
UBE2O
Myc (BAP1)
YY1
G
HeLa S3
293T
Flag-H2A transfection
Soluble protein extraction
NaCl 420mM, NEM 20 mM
Stable cell lines
Flag-HA-BAP1
Flag-HA-C91S
Flag-HA-ΔE631-A634
Flag-HA-ΔK637-C638insN
Insoluble pellet
Discard soluble
Micrococcal nuclease digestion
Flag/HA complex purification
Soluble Nucleosomes
Discard pellet
Flag IP
WASH
Flag peptide elution
In vitro Deubiquitination assay
H
Marker
Substrate
500 bp
EtBr
M.W.
(kDa)
Flag-H2A
20
15
H3
H2B
H2A
H4
Ponceau S
I
Substrate
Mock
BAP1 complex
C91S complex
His-BAP1 bacterial
Flag(H2A)
ubH2A
BAP1

Figure S5 (Related to Figure 5).

BAP1 and UCH37 may employ a similar auto-deubiquitination mechanism.

A) Crystal structure of UCH37 (3IHR) (Burgie et al., 2011). **B)** UCH37 (UCHL5) is highly similar to BAP1 with respect to domain architecture (Sanchez-Pulido et al., 2012). Crystal structure of UCH37 suggests that an intramolecular interaction occurs between the UCH and the CTD. Therefore, we evaluated the possibility that UCH37 might also be regulated by UBE2O. 293T cells were co-transfected with 1 μg of Myc-Ub, 1 μg of HA-UCH37 wild type or HA-UCH37 C88A and either 2 μg of empty vector or Myc-UBE2O expression vectors. Three days later, cells lysates were used for IP with HA antibodies under native or denaturing conditions. Western blots were probed with the indicated antibodies. We detected ubiquitination of UCH37, which was more pronounced for its catalytic dead mutant (C88A), but this effect was independent of UBE2O. UCH37 also failed to interact with UBE2O in co-IP. Nonetheless, this result suggests that UCH37 may employ the same auto-deubiquitination mechanism as BAP1 to counteract the action of another, yet to be identified E3 ligase. Note that UCH37 co-immunoprecipitates endogenous YY1 providing an indication of IP validity (Yao et al., 2008). **C)** Alignment of human BAP1 and human UCH37 C-terminal regions, polar amino acids are in blue, hydrophobic amino acids are in red. Note the difference in the C-terminal region of both proteins, NLS in BAP1 and ADRM1-interacting region (KEKE) in UCH37 (Hamazaki et al., 2006; Yao et al., 2006). **D)** Prediction of coiled-coil domains in BAP1 using COILS program (Lupas et al., 1991). The amino acid sequences of CC1 and CC2 are presented. The hydrophobic amino acids are indicated in red.

G13V cancer mutant of BAP1 does not impair auto-deubiquitination of NLS.

We initially tested the G13V mutation recently described in renal carcinoma (Pena-Llopis et al., 2012). **E)** Prediction for the G13/F660 intra-molecular interaction (left) based on the crystal structure of UCH37 (3IHR)(right). **F)** 293T Cells were co-transfected with 2 μg of HA-Ub, 2 μg of His-UBE2O, and 1 μg of Myc-BAP1 expression vectors. Three days later, samples were used for western blotting and probed with the indicated antibodies. The G13

residue in UCH is predicted to interact with the F660 residue of the CC2; nonetheless G13V and F660A mutations did not have a noticeable effect on the auto-deubiquitination activity of BAP1.

Establishment of the *in vitro* nucleosome deubiquitination assay.

G) Schema representing the steps for the preparation of nucleosomes containing H2A mono-ubiquitinated on lysine 119 and the *in vitro* DUB assays. **H)** DNA from nucleosomal Flag elution was purified using phenol/chloroform separation and loaded on EtBr agarose gel (left). The Ponceau S staining of the nucleosomal Flag elution indicates the presence of all four histone types (right panel). **I)** *In vitro* nucleosome deubiquitination reaction with purified BAP1 complexes and bacteria purified BAP1. Samples were incubated at 37°C for 4 hours, reactions were stopped with 2X Laemmli buffer, and used for western blot with the indicated antibodies. Note that recombinant BAP1 (not assembled into its complex) does not deubiquitinate H2A .

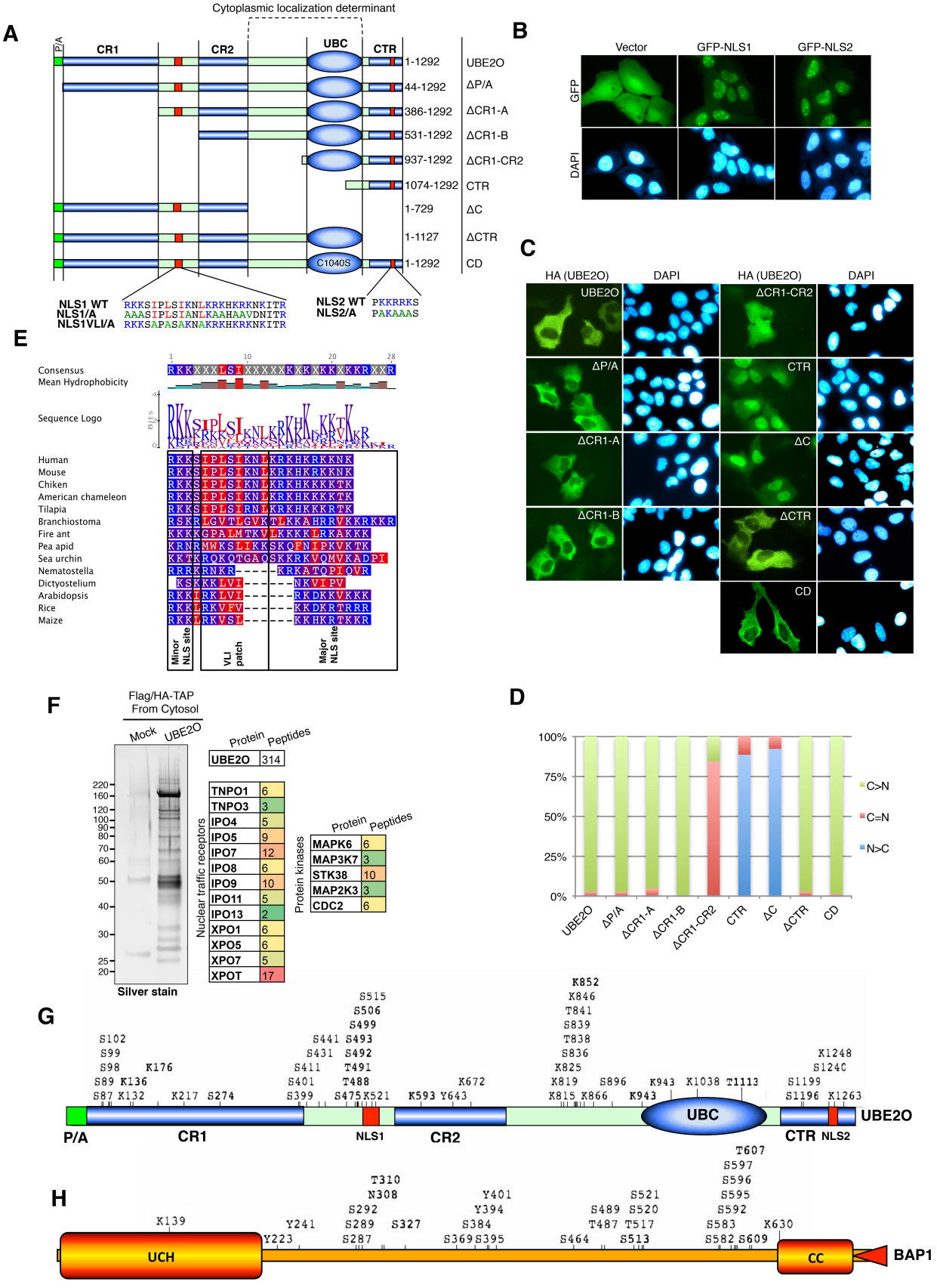
A
Cytoplasmic localization determinant
P/A
CR1
CR2
UBC
CTR
1-1292
UBE2O
44-1292
ΔP/A
386-1292
ΔCR1-A
531-1292
ΔCR1-B
937-1292
ΔCR1-CR2
1074-1292
CTR
1-729
ΔC
1-1127
ΔCTR
C1040S
1-1292
CD
NLS1 WT RKKSIPLSIKNLKRKHKRKNKITR
NLS1/A AAASIPLSIANLKAAHAAVDNITR
NLS1VLI/A RKKSAPASAKNAKRKHKRKNKITR
NLS2 WT PKKRRKS
NLS2/A PAKAAAS
B
Vector
GFP-NLS1
GFP-NLS2
GFP
DAPI
C
HA (UBE2O)
DAPI
UBE2O
ΔCR1-CR2
ΔP/A
CTR
ΔCR1-A
ΔC
ΔCR1-B
ΔCTR
CD
E
Consensus
Mean Hydrophobicity
Sequence Logo
Human
Mouse
Chiken
American chameleon
Tilapia
Branchiostoma
Fire ant
Pea apid
Sea urchin
Nematostella
Dictyostelium
Arabidopsis
Rice
Maize
Minor NLS site
VLI patch
Major NLS site
F
Flag/HA-TAP
From Cytosol
Mock
UBE2O
Silver stain
Protein
Peptides
UBE2O 314
Nuclear traffic receptors
TNPO1 6
TNPO3 3
IPO4 5
IPO5 9
IPO7 12
IPO8 6
IPO9 10
IPO11 5
IPO13 2
XPO1 6
XPO5 6
XPO7 5
XPOT 17
Protein kinases
MAPK6 6
MAP3K7 3
STK38 10
MAP2K3 3
CDC2 6
D
100%
75%
50%
25%
0%
C>N
C=N
N>C
UBE2O
ΔP/A
ΔCR1-A
ΔCR1-B
ΔCR1-CR2
CTR
ΔC
ΔCTR
CD
G
P/A
CR1
NLS1
CR2
UBC
CTR
NLS2
UBE2O
H
UCH
CC
BAP1

Figure S6 (Related to Figure 6).

Subcellular localization of UBE2O deletion mutants reveals nuclear and cytoplasmic targeting regions.

A) Schema of UBE2O mutants used to study its subcellular localization**. B)** U2OS cells were transfected with 1 µg of GFP fusion expression vectors of UBE2O NLS regions or empty vector and plated on coverslips. Two day later, cells were fixed and used for fluorescence microscopy analysis. **C)** U2OS cells were transfected with 3 µg of Flag-HA tagged expression vectors of UBE2O mutants and plated on coverslips. Two days later, cells were fixed and used for the immunofluorescence analysis with HA antibody. **D)** Representative cell counts for UBE2O subcellular localization are shown.

Multiple sequence alignment of NLS1 region from different UBE2O orthologs.

E) Multiple sequence alignment of NLS regions in UBE2O orthologs, polar amino acids are in blue, hydrophobic amino acids are in red.

F) Tandem affinity purification of UBE2O-associated proteins from HeLa cells followed by MS analysis. The regulators of nuclear traffic and protein kinases are presented

Post-translational modifications of UBE2O and BAP1.

G) Schema of known UBE2O phosphorylation and ubiquitination sites (modified from http://www.phosphosite.org/)

H) Schema of known BAP1 phosphorylation and ubiquitination sites (modified from http://www.phosphosite.org/)

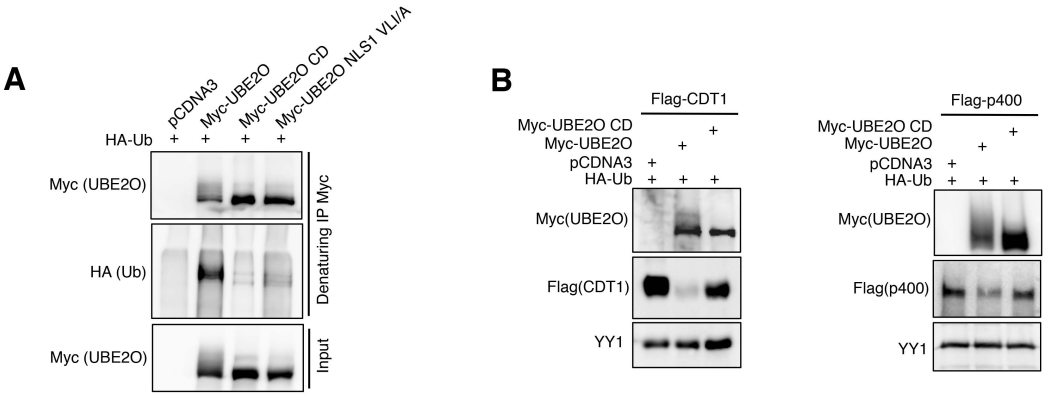

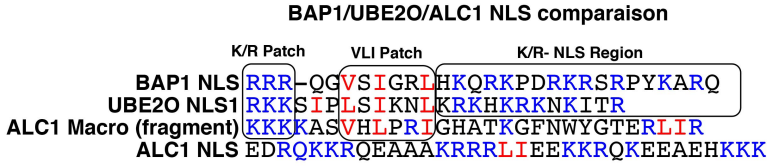

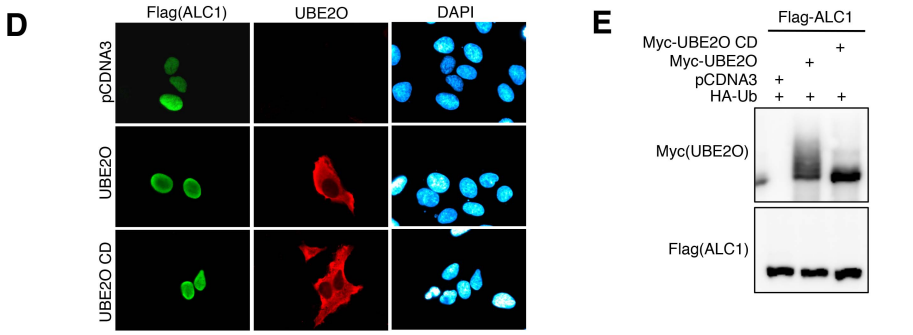

F

UniProt ID[a]	Name[b]	position[c]	Consensus sequence[d]	UBE2O substrate[e]
Q92560	**BAP1**	699-709	RRRqgVsIgrL	Yes
Q9C0C9	**UBE2O**	512-523	RKKsipLsIknL	Yes
Q9ULG1	**INO80**	264 - 273; 276 - 285	KKKh.LsIeqL; RRRk.VwLsiV	Yes
Q9H211	**CDT1**	67 - 77	RRRlrLsVdeV	Yes
Q9NS56	**TOPORS**	859 - 870	KRKtrsLsVeiV	unknown
Q9BRD0	**BUD13**	469 - 478	RKRn.LkLerL	unknown
Q5T5N4	**C6orf118**	172 - 182	RRReeLrLpdL	unknown
Q86WJ1	**ALC1**	833 - 843	KKKasVhLprI	NO
O43889	**CREB3**	192 - 202	RRKkkVyVggL	unknown
Q9P0U4	**CXXC1**	321 - 330	RKRa.VkVkhV	Yes
Q96L91	**EP400**	899 - 909	KRKkaLnLqkV	Yes
Q9NSI2	**FAM207A**	134 - 144	RRRatVvVgdL	unknown
O94915	**FRYL**	974 - 984	RRRdiLrVqlV	unknown
P5419	**HIRA**	628 - 638	KRKleLeVetV	unknown
Q32MZ4	**LRRF1**	578 - 588	KKKspVpVetL	unknown
O60942	**MCE1**	221 - 231	RRKerLkLgaI	unknown
O00566	**MPP10**	669 - 679	KKRqdIsVhkL	unknown
P35228	**NOS2**	509 - 518	KRRe.IpLkvL	unknown
Q86V59	**PNMAL1**	362 - 372	RKKkkVsLgpV	unknown
O60216	**RAD21**	319 - 329	KRKrkLiVdsV	unknown
P62979	**RS27A**	94 - 103	KRKk.VkLavL	unknown
P15822	**ZEP1**	1280 - 1289	KKKr.LrLaeI	unknown
Q9NQ69	**LHX9**	220 - 231	KRKspaLgVdiV	unknown
Q96NK8	**NEUROD6**	81 - 92	KKKttkLrLerV	unknown
Q96C28	**ZNF707**	166 - 177	RRKqraVeLsfI	unknown

Figure S7 (Related to Figure 7).

NLS1 hydrophobic VLI patch is required for auto-catalytic UBE2O targeting.

A) 293T cells were co-transfected with 2 µg of HA-Ub and 2 µg of indicated Myc-tagged UBE2O mutants, and cell extracts were used for immunoprecipitation.

UBE2O promotes degradation of p400 and CDT1.

B) 293T cells were co-transfected with 2 µg of HA-Ub and 2 µg of empty vector, Myc-UBE2O or Myc-UBE2O CD and either 1 µg of Flag-CDT1 or 5 µg Flag-p400 expression vectors. Three days later, samples were used for western blotting and probed with the indicated antibodies.

UBE2O does not ubiquitinate or promote localization change of ALC1, protein with unrelated NLS and the predicted consensus within Macro domain.

C) Sequence alignment between the UBE2O/BAP1 in comparison to ALC1 NLS. VLI patch is in red, and basic amino acids are in blue. Note that the K/R NLS region is absent downstream of the UBE2O consensus found in ALC1. The previously defined NLS sequence of ALC1 does not show similarities with the UBE2O consensus (Cheng et al., 2013). **D)** U2OS cells were co-transfected with 0,5 µg of HA-Ub and either 1 µg of empty vector, Myc-UBE2O or Myc-UBE2O CD and 1 µg of Flag-ALC1 expression vectors and plated on coverslips. Three days later, cells were fixed and used for immunofluorescence analysis with the indicated antibodies. **E)** 293T cells were co-transfected with 2 µg of HA-Ub and 2 µg of empty vector, Myc-UBE2O or Myc-UBE2O CD and 1µg of Flag-ALC1 expression vectors. Three days later, samples were used for western blotting and probed with the indicated antibodies.

Identification of potential UBE2O substrates

F) Prediction of UBE2O substrates based on BAP1/UBE2O NLS consensus

[a]UniProt accession number.

[b]protein name.

[c]protein positions of the *[KR][KR][KR]-X(1,3)-[VLI]-X-[VLI]-X-X-[VLI]* UBE2O binding consensus.

[d]consensus sequence (consensus-defined amino acids are capital).

[e]experimental evidence for the predicted UBE2O-mediated substrate ubiquitination (see Figures 7 and figure S7).

EXTENDED EXPERIMENTAL PROCEDURES

Plasmids and Antibodies

UBE2O and RING1B were cloned from HeLa total RNA by reverse transcription and inserted into pENTR D-Topo plasmid (Life Technologies). MYSM1 and USP16 were cloned from HeLa total RNA by reverse transcription and inserted into pEGFP-C1 plasmid. Human RNF10 and RNF219 were cloned from U2OS total RNA by reverse transcription and inserted into p3XFLAG-CMV™-7 expression vector (Sigma-Aldrich). UBE2O expression constructs were generated using LR clonase kit (Life Technologies) in pDEST-Myc, pDEST-His or retroviral pMSCV-Flag/HA-IRES-Puro (Sowa et al., 2009).

For bacterial expression, the UBE2O cDNA was cloned into pET-30a+ vector (Novagen), to generate N-terminal Flag- and the C- terminal His-tags for the double column purification.

The catalytically inactive UBE2O was generated by site-directed mutagenesis. Non-tagged pCDNA3-BAP1 and C91S were generated by subcloning the cDNA from pOZ-N BAP1 and pOZ-N C91S respectively. BAP1 cancer mutants ΔE631-A634, ΔK637-C638InsN, ΔCC2 and ΔCTD and UBE2O NLS mutants were generated using gene synthesis (BioBasic) and then subcloned into modified pENTR D-Topo plasmid.

BAP1 NLS mutants were generated by subcloning of annealed short adapters containing corresponding mutations in pENTR D-Topo BAP1 and/or C91S. NLS-GFP were generated by subcloning of annealed short adapters containing corresponding BAP1 or UBE2O NLS sequences in pOD35 plasmid provided by Dr. Paul Maddox (Institute for Research in Immunology and Cancer, Canada). All constructs were sequenced.

shRNAs for human UBE2O were from Sigma (#1 NM022066x814s1c1 and #2 NM022066x4103s1c1). The constructs used to produce recombinant full length GST-BAP1 and various deletion fragments, and BAP1 mutant deleted in the NHNY sequence

corresponding to the HCF-1 binding domain (ΔHBM) and BAP1 catalytic dead C91S were described (Yu et al., 2010).

Flag-INO80 expression vector was provided by Dr. Yang Shi (Harvard Medical School, USA) (Wu et al., 2007). Flag-p400 was provided by Dr. David M. Livingston (Harvard Medical School, USA) (Chan et al., 2005). Flag-CXXC1 expression vector was provided by Dr. David Skalnik (Indiana University-Purdue University Indianapolis, USA) (Tate et al., 2009). Flag-CDT1 expression vector was provided by Dr. Kevin Struhl (Harvard Medical School, USA) (Miotto and Struhl, 2011). Flag-ALC1 expression vector was provided by Dr. Simon Boulton (London Research Institute, UK) (Ahel et al., 2009). Flag-BRUCE and Flag-BRUCE CD expression vectors were from Dr. Stefan Jentsch (Max Planck Institute of Biochemistry, Germany) (Bartke et al., 2004). HA-UCH37 and HA-UCH37 C88A expression vectors were from Dr. Joan Conaway (Stowers Institute for Medical Research, USA) (Yao et al., 2008). Myc-UBC7 expression vector was provided by Dr. Allan M. Weissman (Center for Cancer Research National Cancer Institute, USA) (Tiwari and Weissman, 2001). Flag-UBCH8 expression vector was provided by Dr. Dong-Er Zhang (UC San Diego, USA) (Kim et al., 2004). GFP-TRIM28 expression vector was provided by Dr. Fanxiu Zhu (Florida State University USA) (Liang et al., 2011). Myc-TRIM27 expression vector was provided by Dr. Patrick R. Potts (UT Southwestern Dallas, USA) (Hao et al., 2013). HA-BRCA1 was generated by subcloning from the GFP-BRCA1 plasmid previously described (Hammond-Martel et al., 2010) into pCDNA3 plasmid. BARD1 expression vector was from Origene (SC119847). HA-wild type and K0 Ub expression vectors were from Dr. Ted Dawson (John Hopkins University, USA) (Lim et al., 2005).

The siRNA ON-TARGETplus® smart pool for human UBE2O and a non-target control were from Dharmacon (Thermo Scientific).

Rabbit polyclonal anti-UBE2O was from Novus Biologicals (NBP-03336). Mouse monoclonal anti-BAP1 (C4), rabbit polyclonal anti-BAP1 (H300), rabbit polyclonal anti-YY1 (H414), rabbit polyclonal anti-OGT (H300), mouse monoclonal anti-GFP (B2), rabbit polyclonal anti-GFP (FL), mouse monoclonal anti-RING1B (N-32), mouse monoclonal

anti-BRCA1 (D-9), mouse monoclonal anti-BARD1 (2059c4a), mouse monoclonal anti-CDC25A (F6), mouse monoclonal anti-Ubiquitin (P4D1) were from Santa Cruz. Rabbit polyclonal anti-HCF-1 (A301-400A) and rabbit polyclonal anti-ASXL2 (A302-037A) were from Bethyl Laboratories. Mouse monoclonal anti-Flag (M2) was from Sigma. Mouse monoclonal anti-Myc (9E10) and mouse monoclonal anti-HA (HA11) were from Covance. Rabbit polyclonal anti-HA (ab9110) was from Abcam. Rabbit monoclonal anti-Perilipin (PLIN) was from New England BioLabs (D1D8) XP®). Rabbit polyclonal anti-aP2 (FABP4) was from Cayman Chemicals. Mouse polyclonal anti-FOXK1 was provided by Dr. Xiao-Hua Li from Southwestern University of Texas. A rabbit polyclonal anti-FOXK2 was generated using a recombinant fragment of human FOXK2 by Pacific Immunology.

Chemicals and reagents

UBE1, USP2 CD, Ub-VME, Ub-AMC, recombinant Myc-Ub and Ub were from Boston Biochem. Cycloheximide (CHX), N-methylmaleimide (NEM), Phenylarsine oxide (PAO), MG132, Micrococcal nuclease (MNase) where from Sigma. Casein kinase II (CKII) inhibitor TBB (100 μM), Casein kinase I (CKI) inhibitor IC261 (10 μM), protein kinase G inhibitor KT5823 (10 μM), CDK1 inhibitor RO-3306 (10 μM) where purchased from Millipore. The CDK1, CDK2 and CDK5 inhibitor Roscovitine (10 μM), MEK1/2 inhibitor UO126 (20 μM) and the protein kinase A (PKA) inhibitor H-89 (20 μM) were purchased from Cell Signaling. The CDK2 inhibitor Purvalanol A (50 μM) was purchased from Abcam. Protein kinase C inhibitor PKC412 (20 μM) and STK inhibitor GSK 650394 (20 μM) were from Santa Cruz. The PI3-Kinase inhibitor caffeine (10 mM), CDK inhibitor CDKi (100 μM), CDK2 inhibitor GW8510 (20 μM) and JNK inhibitor SP600125 (30 μM) were from Sigma. SU 9516 (5 μM), Chk1 inhibitor SB 218078 (1 μM). Broad spectrum kinase inhibitor Staurosporine (100 nM), tyrosine kinase inhibitor Genistein (20 μM), CDK inhibitor Olomoucine (30 μM), CKII inhibitor Apigenin (20 μM), CKII and CDK inhibitor DRB (50 μM), PI3-Kinase inhibitor LY294002 (20 μM), CKII inhibitor NSC 210902 (15

μM), CKI inhibitor D 4476 (25 μM) and CKII inhibitor CAY10578 (15 μM) where from Cayman chemical.

Cell culture, transfections and western blot

HeLa S3 cervical cancer, MCF7 breast cancer, U2OS osteosarcoma, human embryonic kidney 293T, 293GPG virus-producing cells and 3T3-L1 mouse preadipocytes and human primary lung fibroblasts LF-1 were cultured in Dulbecco's modified Eagle's medium (DMEM) supplemented with 10% fetal bovine serum and penicillin/streptomycin.

siRNA and plasmid DNA were transfected in MCF7 and U2OS cells, respectively, using Lipofectamine 2000 (Life Technologies). HEK293T (293T) cells were transfected using PEI (Sigma).

Total cell lysates were prepared in buffer containing 25 mM Tris-HCl pH 7.5 and 1% SDS, samples were immediately boiled at 95°C for 10 min and sonicated to break down DNA. Samples were diluted using 2X or 4X Laemmli buffer (Laemmli, 1970). SDS-PAGE and western blotting were conducted according to standard procedures. Images were acquired using ImageQuant™ LAS 4000 biomolecular imager (GE Healthcare, USA). Densitometry quantification of western blot bands was performed using Gel-Pro Analyzer 3.1 (Media Cybernetics).

Stable cell lines

HeLa S3 cell lines stably expressing Flag-HA-BAP1, Flag-HA-C91S, Flag-HA-ΔE631-A634, Flag-HA-ΔK637-C638InsN, Flag-HA-ΔCTD, Flag-HA-ΔCC1 were

generated following retroviral transduction using pOZ-N-based retroviral constructs and selected using anti-IL2 magnetic beads (Life Technologies) as previously described (Yu et al., 2010).

U2OS cell lines stably expressing Flag-HA-BAP1, Flag-HA-C91S, Flag-HA-ΔE631-A634, Flag-HA-ΔK637-C638InsN, Flag-HA-ΔCTD, Flag-HA-ΔCC1 were generated following retroviral transduction of pMSCV-Flag/HA-IRES-Puro based constructs and selected with 3 μg/ml of puromycin.

3T3-L1 cell lines stably expressing Flag-HA-BAP1, Flag-HA-BAP1 5 K/R, Flag-HA-BAP1 NLS T1, Flag-HA-UBE2O and Flag-HA-UBE2O CD were generated following retroviral transduction of pMSCV-Flag/HA-IRES-Puro based constructs and selected with 3 μg/ml of puromycin.

Stable HeLa S3 Flag-HA-UBE2O cell line was generated following retroviral transduction of pMSCV-Flag/HA UBE2O-IRES-Puro and selected with 2 μg/ml of puromycin.

Purification of BAP1 complexes and UBE2O-interacting proteins

HeLa S3 (~12 X 10^9) cells stably expressing Flag-HA-BAP1, Flag-HA-C91S, Flag-HA-ΔE631-A634, Flag-HA-ΔK637-C638InsN, Flag-HA-ΔCTD and Flag-HA-UBE2O were grown in spinner flasks. The cytosolic fraction was used for the purification of UBE2O with Flag and HA immunoaffinity columns essentially as previously described (Groisman et al., 2003) the Flag and HA columns were washed with either low salt buffer containing 100 mM KCl (Flag-HA-UBE2O LS) or 300 mM NaCl (Flag-HA-UBE2O HS) (Figure S2A, C, D)). The BAP1 protein complexes were purified from total soluble protein extracts in EBcom (50 mM Tris-HCl pH 7.5, 150 mM NaCl, 0,5% NP-40, 50 mM NaF, 10 mM β-glycerophosphat, 1 mM Na_3VO_4 1 mM DTT, 1 mM EDTA, 1 mM PMSF and protease inhibitors cocktail (Sigma)). The extracts were clarified by centrifugation at 30,000g for 1 hour, with subsequent filtration of supernatants through a 0,45 μm pore

filter. The extracts were incubated with the anti-Flag M2 resin overnight and extensively washed with EBcom. The resin was eluted three times with EBcom containing 200 ng/ml of Flag peptide. The eluted fractions were incubated with anti-HA resin overnight, and the procedure was repeated as for the previous column. The HA eluted fractions were used for silver stain, western blot and in vitro DUB assay. Mass spectrometric identification of UBE2O-interacting proteins was done at the Taplin Mass Spectrometry facility (Harvard, USA). Identification of additional BAP1-interacting proteins was done at the Proteomics Platform of the Quebec Genomics Center (CHUQ, Laval University, Canada).

Immunoprecipitation

Cells were lysed in buffer EB150 (50 mM Tris-HCl pH 7.5, 150 mM NaCl, 1% NP-40, 10 mM β-mercaptoethanol, 1 mM PMSF and protease inhibitors cocktail (Sigma)) and the lysates were clarified by centrifugation at 21,000 g for 30 min. The supernatants were incubated with indicated antibodies for 3 hours and then protein-G beads were added and incubated for an additional hour. The samples were extensively washed with EB150 and re-suspended in 2X Laemmli buffer. For an IP under denaturing conditions, the cells were harvested as described for western blot, and diluted in EB300 (50 mM Tris-HCl pH 7.5, 300 mM NaCl, 1% NP-40, 10 mM β-mercaptoethanol). The lysates were incubated overnight with antibody and protein-G beads. The beads were washed several times with EB300 and resuspended in 2X Laemmli buffer.

Mass spectrometric identification of ubiquitination sites

293T (~1 X 10^9) cells were transfected with HA-Ub, Flag-C91S, and His-UBE2O expression vectors. 96 hours later, the cells were lysed in EB300 containing 20 mM NEM and protease inhibitor cocktail. The extracts were clarified by centrifugation at 30,000g for

1 hour. The extracts were incubated with the anti-Flag M2 resin overnight and extensively washed with EB300. The resin was eluted three times with EB300 containing 200 ng/ml of Flag peptide. The eluted fractions were combined and concentrated using TCA (trichloroacetic acid) precipitation and loaded on the NuPAGE® Bis-Tris Precast Gel (Life Technologies). The gel was stained with Coomassie G-250 and the modified C91S bands were excised and sent for MS analysis at Taplin Mass Spectrometry facility (Harvard, USA).

Glycerol gradient

Molecular mass fractionation of nuclear extract was conduced using a 10-40 % glycerol gradient prepared in 20 mM Tris-HCl, pH 7.9; 100 mM KCl; 5 mM $MgCl_2$; 1 mM PMSF; 0.1% NP40 and 10 mM β-mercaptoethanol. The samples were centrifuged for 12 hours at 50,000 RPM (SW55Ti rotor, Beckman,) at 4 ºC. Individual fractions were then collected from top to bottom and analyzed by western blotting. The BAP1 complex is estimated to have a molecular mass of 1.6 MDa.

***In vitro* interaction assays**

Recombinant GST-BAP1 fusion proteins were purified from bacteria using glutathione agarose beads (Sigma) and 2 to 3 µg of bound proteins were incubated with His-UBE2O for 6 to 8 hours at 4 ºC in pull down buffer (50 mM Tris-HCl, pH 7.5; 50 mM NaCl; 0.02% Tween 20; 1 mM PMSF and 500 µM dithiothreitol). The beads were extensively washed with the same buffer, and bound proteins eluted in 2X Laemmli buffer and subjected to western blotting.

In vitro ubiquitination assay

Ubiquitination reactions were conducted in a total volume of 30 µl containing 25 mM Tris-HCl pH 7.5, 10 mM $MgCl_2$, 5 mM ATP, 50 ng/µl Ub, 250 ng of human recombinant UBE1 and 1 mM β-mercaptoethanol. Purified Flag-HA-BAP1, Flag-HA-C91S, His-C91S (bacterial recombinant), Flag-UBE2O-His (bacterial recombinant) and Flag-HA-UBE2O were added as indicated.

Reaction on the beads-immobilized complexes was performed when indicated. Briefly, the anti-Flag M2 beads were incubated with high salt nuclear extracts from HeLa S3 Flag-HA-BAP1 or Flag-HA-C91S for 5 hour and washed 8 times with buffer containing 20 mM Tris-HCl pH 7.5, 100 mM KCl, 1 mM $MgCl_2$, 5 mM EDTA, 0.1% Triton X-100 and 1 mM PMSF. The last wash was performed using buffer containing 25 mM Tris-HCl pH 7.5 and 10 mM $MgCl_2$. The beads-bound complexes (25 µl) were used for the reaction essentially in the same conditions as for the reaction in solution. Reactions were incubated at 37ºC with constant shaking overnight. Met-Ub was previously described (Kirisako et al., 2006)

Purification of the nucleosomes and *In vitro* nucleosome DUB assay

Preparation of chromatin fractions and digestion with Micrococcal nuclease (MNase Sigma) were conducted as previously described (Groisman et al., 2003), with some modifications. The 293T cellular pellet was resuspended in EB420 (50 mM Tris-HCl pH 7.5, 420 mM NaCl, 1% NP-40, 10 mM β-mercaptoethanol, 20 mM NEM and protease inhibitor cocktail). The soluble fraction was discarded and the pellet was extensively washed with MNase buffer (20 mM Tris-HCl pH 7.5, 100 mM KCl, 2 mM $MgCl_2$, 1 mM $CaCl_2$, 0.3 M sucrose, 0.1% NP-40, and protease inhibitor cocktail). Following MNase treatment (3 U/ml for 10 min at room temperature), the reaction was quenched with 5 mM of EGTA and 5 mM of EDTA. The samples were then centrifuged at 20,000g for 10

minutes at 4°C to obtain the soluble chromatin fraction. The extract was incubated with anti-Flag M2 resin overnight and washed with EB300 buffer. The beads then were eluted with EB300 containing 200 ng/ml of Flag peptide.

The eluted soluble chromatin fraction was incubated with the indicated Flag/HA purified BAP1 complexes and used for western blotting.

Immunofluorescence

The procedure was carried over essentially as previously described (Daou et al., 2011). Briefly cells were fixed in 3% PFA-PBS and permeabilized using PBS 0.1% NP-40. Anti-mouse Alexa Fluor® 594 and Anti-mouse Alexa Fluor® 488 (Life Technologies) were used as secondary antibodies. Nuclei were stained with 4',6-diamidino-2-phenylindole (DAPI).

Images were acquired using Zeiss. Z2 microscope and Plan Apochrmat 40X/0.95 Korr, Plan Apochrmat 63X/1.4 Oil DIC and Plan Apochrmat 100X/1.4 Oil DIC objectives and AxioCam MRm camera. Images were processed using WCIF-ImageJ program (NIH).

Adipogenic differentiation of 3T3-L1 preadipocytes.

3T3-L1 cell lines stably expressing BAP1 or UBE2O were plated at the same density, upon reaching of confluency the growth media was changed to induction media containing 10% fetal bovine serum, penicillin/streptomycin, 1 μM dexamethasone, 1 μg/ml insulin and 500 μM IBMX (Sigma). Two days post-induction, the media was changed to maintenance media containing 10 % fetal bovine serum, penicillin/streptomycin, 1 μg/ml

insulin. The cells were fixed with PFA or harvested for western blotting two to three days post-induction. Lipid droplet content was evaluated using Oil-Red O lipid stain (Sigma).

Protein sequence analysis, and structure modeling

Protein sequences were analyzed and aligned using Geneious 6.1.2 created by Biomatters, available from http://www.geneious.com. NLS consensus were analyzed using ProSite (Sigrist et al., 2013) and NLStradamus (Nguyen Ba et al., 2009). Coiled-coil regions were predicted using COILS (Lupas et al., 1991). BAP1 3D structure modeling was performed using SWISS-MODEL (Arnold et al., 2006) and crystal structure of UCH37 (Burgie et al., 2011) (PDB code: 3IHR).

Supplemental References

Ahel, D., Horejsi, Z., Wiechens, N., Polo, S.E., Garcia-Wilson, E., Ahel, I., Flynn, H., Skehel, M., West, S.C., Jackson, S.P., *et al.* (2009). Poly(ADP-ribose)-dependent regulation of DNA repair by the chromatin remodeling enzyme ALC1. Science *325*, 1240-1243.

Arnold, K., Bordoli, L., Kopp, J., and Schwede, T. (2006). The SWISS-MODEL workspace: a web-based environment for protein structure homology modelling. Bioinformatics *22*, 195-201.

Bartke, T., Pohl, C., Pyrowolakis, G., and Jentsch, S. (2004). Dual role of BRUCE as an antiapoptotic IAP and a chimeric E2/E3 ubiquitin ligase. Molecular cell *14*, 801-811.

Burgie, S.E., Bingman, C.A., Soni, A.B., and Phillips, G.N., Jr. (2011). Structural characterization of human Uch37. Proteins.

Carbone, M., Yang, H., Pass, H.I., Krausz, T., Testa, J.R., and Gaudino, G. (2013). BAP1 and cancer. Nature reviews. Cancer *13*, 153-159.

Chan, H.M., Narita, M., Lowe, S.W., and Livingston, D.M. (2005). The p400 E1A-associated protein is a novel component of the p53 --> p21 senescence pathway. Genes & development *19*, 196-201.

Cheng, W., Su, Y., and Xu, F. (2013). CHD1L: a novel oncogene. Molecular cancer *12*, 170.

Conti, E., Uy, M., Leighton, L., Blobel, G., and Kuriyan, J. (1998). Crystallographic analysis of the recognition of a nuclear localization signal by the nuclear import factor karyopherin alpha. Cell *94*, 193-204.

Daou, S., Mashtalir, N., Hammond-Martel, I., Pak, H., Yu, H., Sui, G., Vogel, J.L., Kristie, T.M., and Affar el, B. (2011). Crosstalk between O-GlcNAcylation and proteolytic cleavage regulates the host cell factor-1 maturation pathway. Proceedings of the National Academy of Sciences of the United States of America *108*, 2747-2752.

Groisman, R., Polanowska, J., Kuraoka, I., Sawada, J., Saijo, M., Drapkin, R., Kisselev, A.F., Tanaka, K., and Nakatani, Y. (2003). The ubiquitin ligase activity in the DDB2 and CSA complexes is differentially regulated by the COP9 signalosome in response to DNA damage. Cell *113*, 357-367.

Hamazaki, J., Iemura, S., Natsume, T., Yashiroda, H., Tanaka, K., and Murata, S. (2006). A novel proteasome interacting protein recruits the deubiquitinating enzyme UCH37 to 26S proteasomes. The EMBO journal *25*, 4524-4536.

Hammond-Martel, I., Pak, H., Yu, H., Rouget, R., Horwitz, A.A., Parvin, J.D., Drobetsky, E.A., and Affar el, B. (2010). PI 3 kinase related kinases-independent proteolysis of BRCA1 regulates Rad51 recruitment during genotoxic stress in human cells. PloS one *5*, e14027.

Hao, Y., Sekine, K., Kawabata, A., Nakamura, H., Ishioka, T., Ohata, H., Katayama, R., Hashimoto, C., Zhang, X., Noda, T.*, et al.* (2004). Apollon ubiquitinates SMAC and caspase-9, and has an essential cytoprotection function. Nature cell biology *6*, 849-860.

Hao, Y.H., Doyle, J.M., Ramanathan, S., Gomez, T.S., Jia, D., Xu, M., Chen, Z.J., Billadeau, D.D., Rosen, M.K., and Potts, P.R. (2013). Regulation of WASH-Dependent Actin Polymerization and Protein Trafficking by Ubiquitination. Cell *152*, 1051-1064.

Jensen, D.E., Proctor, M., Marquis, S.T., Gardner, H.P., Ha, S.I., Chodosh, L.A., Ishov, A.M., Tommerup, N., Vissing, H., Sekido, Y.*, et al.* (1998). BAP1: a novel ubiquitin hydrolase which binds to the BRCA1 RING finger and enhances BRCA1-mediated cell growth suppression. Oncogene *16*, 1097-1112.

Joo, H.Y., Zhai, L., Yang, C., Nie, S., Erdjument-Bromage, H., Tempst, P., Chang, C., and Wang, H. (2007). Regulation of cell cycle progression and gene expression by H2A deubiquitination. Nature *449*, 1068-1072.

Kim, K.I., Baek, S.H., Jeon, Y.J., Nishimori, S., Suzuki, T., Uchida, S., Shimbara, N., Saitoh, H., Tanaka, K., and Chung, C.H. (2000). A new SUMO-1-specific protease, SUSP1, that is highly expressed in reproductive organs. The Journal of biological chemistry *275*, 14102-14106.

Kim, K.I., Giannakopoulos, N.V., Virgin, H.W., and Zhang, D.E. (2004). Interferon-inducible ubiquitin E2, Ubc8, is a conjugating enzyme for protein ISGylation. Molecular and cellular biology *24*, 9592-9600.

Kirisako, T., Kamei, K., Murata, S., Kato, M., Fukumoto, H., Kanie, M., Sano, S., Tokunaga, F., Tanaka, K., and Iwai, K. (2006). A ubiquitin ligase complex assembles linear polyubiquitin chains. The EMBO journal *25*, 4877-4887.

Laemmli, U.K. (1970). Cleavage of structural proteins during the assembly of the head of bacteriophage T4. Nature *227*, 680-685.

Lee, B.J., Cansizoglu, A.E., Suel, K.E., Louis, T.H., Zhang, Z., and Chook, Y.M. (2006). Rules for nuclear localization sequence recognition by karyopherin beta 2. Cell *126*, 543-558.

Liang, Q., Deng, H., Li, X., Wu, X., Tang, Q., Chang, T.H., Peng, H., Rauscher, F.J., 3rd, Ozato, K., and Zhu, F. (2011). Tripartite motif-containing protein 28 is a small ubiquitin-related modifier E3 ligase and negative regulator of IFN regulatory factor 7. Journal of immunology *187*, 4754-4763.

Lim, K.L., Chew, K.C., Tan, J.M., Wang, C., Chung, K.K., Zhang, Y., Tanaka, Y., Smith, W., Engelender, S., Ross, C.A.*, et al.* (2005). Parkin mediates nonclassical, proteasomal-independent ubiquitination of synphilin-1: implications for Lewy body formation. The Journal of neuroscience : the official journal of the Society for Neuroscience *25*, 2002-2009.

Lupas, A., Van Dyke, M., and Stock, J. (1991). Predicting coiled coils from protein sequences. Science *252*, 1162-1164.

Miotto, B., and Struhl, K. (2011). JNK1 phosphorylation of Cdt1 inhibits recruitment of HBO1 histone acetylase and blocks replication licensing in response to stress. Molecular cell *44*, 62-71.

Nguyen Ba, A.N., Pogoutse, A., Provart, N., and Moses, A.M. (2009). NLStradamus: a simple Hidden Markov Model for nuclear localization signal prediction. BMC bioinformatics *10*, 202.

Pena-Llopis, S., Vega-Rubin-de-Celis, S., Liao, A., Leng, N., Pavia-Jimenez, A., Wang, S., Yamasaki, T., Zhrebker, L., Sivanand, S., Spence, P.*, et al.* (2012). BAP1 loss defines a new class of renal cell carcinoma. Nature genetics *44*, 751-759.

Robbins, J., Dilworth, S.M., Laskey, R.A., and Dingwall, C. (1991). Two interdependent basic domains in nucleoplasmin nuclear targeting sequence: identification of a class of bipartite nuclear targeting sequence. Cell *64*, 615-623.

Sanchez-Pulido, L., Kong, L., and Ponting, C.P. (2012). A common ancestry for BAP1 and Uch37 regulators. Bioinformatics *28*, 1953-1956.

Scheuermann, J.C., de Ayala Alonso, A.G., Oktaba, K., Ly-Hartig, N., McGinty, R.K., Fraterman, S., Wilm, M., Muir, T.W., and Muller, J. (2010). Histone H2A deubiquitinase activity of the Polycomb repressive complex PR-DUB. Nature *465*, 243-247.

Sigrist, C.J., de Castro, E., Cerutti, L., Cuche, B.A., Hulo, N., Bridge, A., Bougueleret, L., and Xenarios, I. (2013). New and continuing developments at PROSITE. Nucleic acids research *41*, D344-347.

Sowa, M.E., Bennett, E.J., Gygi, S.P., and Harper, J.W. (2009). Defining the human deubiquitinating enzyme interaction landscape. Cell *138*, 389-403.

Tate, C.M., Lee, J.H., and Skalnik, D.G. (2009). CXXC finger protein 1 contains redundant functional domains that support embryonic stem cell cytosine methylation, histone methylation, and differentiation. Molecular and cellular biology *29*, 3817-3831.

Tiwari, S., and Weissman, A.M. (2001). Endoplasmic reticulum (ER)-associated degradation of T cell receptor subunits. Involvement of ER-associated ubiquitin-conjugating enzymes (E2s). The Journal of biological chemistry *276*, 16193-16200.

van Wijk, S.J., and Timmers, H.T. (2010). The family of ubiquitin-conjugating enzymes (E2s): deciding between life and death of proteins. FASEB journal : official publication of the Federation of American Societies for Experimental Biology *24*, 981-993.

Ventii, K.H., Devi, N.S., Friedrich, K.L., Chernova, T.A., Tighiouart, M., Van Meir, E.G., and Wilkinson, K.D. (2008). BRCA1-associated protein-1 is a tumor suppressor that requires deubiquitinating activity and nuclear localization. Cancer research *68*, 6953-6962.

Wu, S., Shi, Y., Mulligan, P., Gay, F., Landry, J., Liu, H., Lu, J., Qi, H.H., Wang, W., Nickoloff, J.A., *et al.* (2007). A YY1-INO80 complex regulates genomic stability through homologous recombination-based repair. Nature structural & molecular biology *14*, 1165-1172.

Wu-Baer, F., Lagrazon, K., Yuan, W., and Baer, R. (2003). The BRCA1/BARD1 heterodimer assembles polyubiquitin chains through an unconventional linkage involving lysine residue K6 of ubiquitin. The Journal of biological chemistry *278*, 34743-34746.

Yao, T., Song, L., Jin, J., Cai, Y., Takahashi, H., Swanson, S.K., Washburn, M.P., Florens, L., Conaway, R.C., Cohen, R.E., *et al.* (2008). Distinct modes of regulation of the Uch37 deubiquitinating enzyme in the proteasome and in the Ino80 chromatin-remodeling complex. Molecular cell *31*, 909-917.

Yao, T., Song, L., Xu, W., DeMartino, G.N., Florens, L., Swanson, S.K., Washburn, M.P., Conaway, R.C., Conaway, J.W., and Cohen, R.E. (2006). Proteasome recruitment and activation of the Uch37 deubiquitinating enzyme by Adrm1. Nature cell biology *8*, 994-1002.

Yu, H., Mashtalir, N., Daou, S., Hammond-Martel, I., Ross, J., Sui, G., Hart, G.W., Rauscher, F.J., 3rd, Drobetsky, E., Milot, E., *et al.* (2010). The ubiquitin carboxyl hydrolase BAP1 forms a ternary complex with YY1 and HCF-1 and is a critical regulator of gene expression. Molecular and cellular biology *30*, 5071-5085.

Yu, H., Pak, H., Hammond-Martel, I., Ghram, M., Rodrigue, A., Daou, S., Barbour, H., Corbeil, L., Hebert, J., Drobetsky, E., *et al.* (2014). Tumor suppressor and deubiquitinase BAP1 promotes DNA double-strand break repair. Proceedings of the National Academy of Sciences of the United States of America *111*, 285-290.

Zhu, P., Zhou, W., Wang, J., Puc, J., Ohgi, K.A., Erdjument-Bromage, H., Tempst, P., Glass, C.K., and Rosenfeld, M.G. (2007). A histone H2A deubiquitinase complex coordinating histone acetylation and H1 dissociation in transcriptional regulation. Molecular cell *27*, 609-621.

Discussion

Regulation of the OGT/HCF-1 complex by O-GlcNAcylation and limited proteolysis.

Although the OGT/HCF-1 are found in several chromatin regulatory complexes, our initial interest in these factors was driven by their presence as components of the BAP1 complex. OGT/HCF-1 appears to be important for the functions of the BAP1 complex in chromatin function, tumor suppression as well as maintenance of the metabolic balance (Pena-Llopis et al., 2012; Ruan et al., 2012). Therefore the information about their cross-regulation is crucial to our understanding of the function and significance of the OGT/HCF-1/BAP1 complex. We initially contributed to the understanding of how OGT/HCF-1 regulate each other through a complex crosstalk (Daou et al., 2011).

Regulation of OGT protein levels by HCF-1

We found that OGT and HCF-1 constitute a tight complex, and that their normal function is dependent on each other. We found that almost half of the cellular pool of OGT is complexed with HCF-1 (Daou et al., 2011). We showed that about half of OGT protein interacts within HCF-1 in the nucleus. Indeed, depletion of HCF-1 by shRNA-mediated knockdown decreased the total levels of OGT by around 50%. Notably, immunofluorescence microscopy confirmed that the levels of nuclear OGT were affected the most following depletion of HCF-1. This observation strongly suggests that the function of OGT as an epigenetic regulator is coordinated by HCF-1.

Co-stabilization of the subunits of the same complex by each other is shared among multiple transcription regulators; including, for instance, the previously discussed BAP1/ASXL1/2 complex (Daou et al., submitted) (Scheuermann et al., 2010) and SUZ12/EZH2 components of the PRC2 complex (Cao and Zhang, 2004).

The mechanism by which HCF-1 stabilizes OGT remains unknown. Since HCF-1 is a highly abundant transcriptional regulator and often implicated in transcription activation, it may regulate the expression level of OGT. However, the knockdown of HCF-1 did not affect the mRNA levels of OGT and moreover HCF-1 seems to be poorly enriched at the OGT promoter. These results indicate that transcription of the OGT gene is not regulated by HCF-1. Furthermore, overexpression of HCF-1 stabilized endogenous OGT. These data indicate that OGT is stabilized by HCF-1 via direct physical interaction.

Several mechanisms might explain the role of HCF-1 in stabilizing OGT. The first possibility is that the interaction of HCF-1 with OGT competes with the recruitment of ubiquitin E3 ligase or its adapter protein. Indeed we were able to detect the ubiquitination of OGT, represented by several monoubiquitination bands as well as polyubiquitin chain conjugates (see the results section). However, cycloheximide chase experiments did not reveal a drastic change in OGT protein levels, which can be explained by the long half-life of the protein.

Another possibility, which was not addressed in our study, is that the depletion of

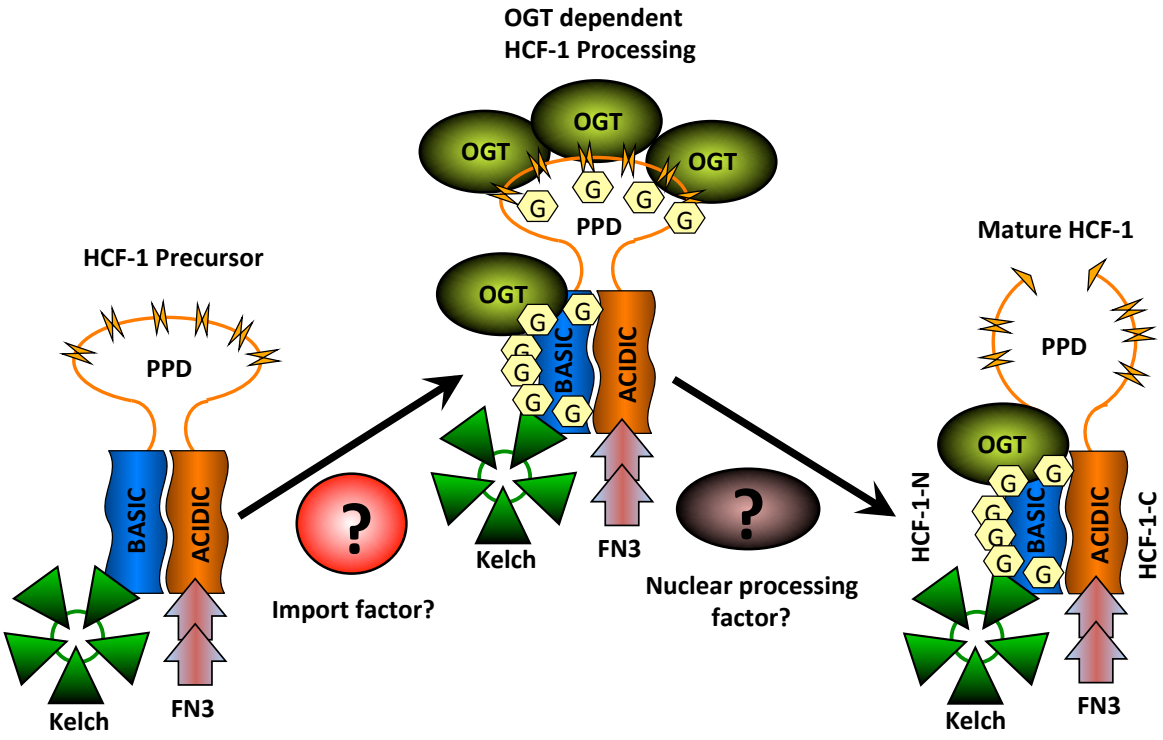

Figure 6. Regulation of HCF-1 proteolytic processing by OGT (Daou et al., 2011)

HCF-1 exposes the aggregation/misfolding prone surfaces of the OGT, which might result in the loss of its native structure or/and solubility inducing OGT aggregation. We were unable to detect visible OGT inclusions in the HCF-1 depleted cells, although the intracellular chaperone/heat shock and aggregate degrading systems may clear out damaged and misfolded OGT by recruiting the ubiquitin ligase CHIP (McDonough and Patterson, 2003). The other possibility is that the cellular autophagy machinery might degrade the misfolded OGT. In this case the ubiquitinated aggregates would recruit several well described ubiquitination/autophagy mediators such as the ubiquitin receptor p62 and the AAA+ type ATPase/unfoldase p97/VCP. At the later steps of this process the ubiquitin/substrate aggregates would be recruited to the autophagosome and degraded (Meyer et al., 2012). The latter process may have far reaching implications for energy balance sensing and metabolic regulation as OGT has been implicated as an intracellular energy sensor. Perturbation of the intracellular energy level could promote the micro- and macro-autophagy pathways with the subsequent decrease of OGT levels, thus reducing O-GlcNAcylation of transcription regulators and signaling proteins and promoting adequate cellular response.

OGT is required for HCF-1 proteolytic processing.

Previous studies identified OGT as a component of the HCF-1 complex (Wysocka et al., 2003). These studies used the N-terminal region of the HCF-1 as a bait for affinity capture studies and were able to recover a significant amount of OGT. We found that HCF-1 possesses at least two major OGT interaction regions. One of these, as previously described, is localized to N-terminal basic region of HCF-1. We further mapped the region to the short fragment of the basic region (termed OBM). Notably, although this region was able to bind OGT, its deletion had no impact on the level of OGT in the context of the full length HCF-1. This can be explained by the identification of the second site for OGT

binding in the HCF-1 central region termed PPD. The affinity of OGT to this domain seems to be at least 10 fold higher when compared to the OBM region in the N-terminus. We showed that the PPD region was required to stabilize OGT, which in turn promoted the proteolytic processing of the HCF-1 at the PPD. Although the OGT itself does not possess any known protease domain its catalytic activity and O-GlcNAcylation are required for the proteolytic cleavage of HCF-1.

Limited proteolysis is usually performed by endoproteases, although attempts to purify the HCF-1 specific protease activity failed to reveal the occurrence of such an enzyme. This can be explained by the requirement of O-GlcNAcylation for this process, which involves several factors including the UDP-GlcNAc, OGT itself and the protease. A study by W. Herr group proposed that OGT itself possesses the proteolytic activity towards the PPD (Capotosti et al., 2011; Lazarus et al., 2013). Indeed some evidence suggests that this mechanism may indeed be executed by OGT. The bacteria-purified OGT was able to promote, to some extent, the processing of the bacteria-purified PPD. However, this does not exclude the possible contamination of the purified reagents by a bacterial protease, which might promote, to some extent, the proteolysis of O-GlcNAcylated PPD. In support of the direct role of OGT in mediating proteolysis, Walker and Herr groups recently published a study of the crystal structure of the OGT catalytic domain and the PPD and proposed a biochemical mechanism for the reaction (Lazarus et al., 2013).

It is worth mentioning that previous studies on the bacteria-expressed HCF-1 showed that it might possess an intrinsic proteolytic activity (Vogel and Kristie, 2000a; Wilson et al., 1995). The bacterially expressed HCF-1 PPD was able to be auto-processed without the involvement of OGT (Vogel and Kristie, 2000a; Wilson et al., 1995). In these assays, the use of a series of conventional protease inhibitors resulted in an unusual inhibitor sensitivity profile with most of the compounds having weak or no effect on the PPD processing, with the exception of the AEBSF serine protease inhibitor that completely blocked the processing. This result suggests that PPD might possess protease activity, which can be enhanced by O-GlcNAcylation, although the contribution of bacteria proteases cannot be firmly excluded. Nonetheless, the O-GlcNAcylation of the PPD by the

OGT might promote conformational changes within the proteolytic repeat that would facilitate the autocatalytic processing.

Interestingly, we noticed that the PPD domain itself cannot be efficiently processed when co-expressed with OGT even though the PPD had a strong stabilizing effect on OGT and was able to promote the sequestration of OGT to the cytoplasm, indicating stable interaction (Daou et al., 2011). In contrast, a dramatic enhancement of the proteolytic process was achieved when the PPD was forced to enter the nucleus, by fusing it with the strong NLS sequence of the SV40 T-large antigen. This result indicates that the nuclear import and/or nuclear localization of both components were required for the PPD processing. Therefore, an additional nuclear factor or possibly a protease might be required for the process, and that OGT is required but not sufficient to promote the efficient proteolytic processing of HCF-1 *in vivo*. Unfortunately so far we do not have any information on the missing proteolytic processing factor. The studies of the PPD-associated proteome may shed light on the intriguing mechanism of HCF-1 maturation.

Another important question is the significance of HCF-1 cleavage. The limited proteolysis in the cell usually occurs for a number of reasons. The regulatory proteolysis of proteins promotes their activation, or inactivation. A number of proteins are kept inactive until specific signals induce their cleavage. The limited proteolysis in the Notch signaling pathway promotes the cleavage of the Notch receptor cytoplasmic NICD tail (Notch intracellular domain) upon ligand-mediated receptor activation. The NICD acts as a signal mediator, that is transported to the nucleus and promotes the assembly of the transcription regulatory complex to promote gene expression (Guruharsha et al., 2012). Several proteases are proteolytically processed from their inactive proenzymes (zymogens). This mechanism prevents their uncontrolled catalytic activity towards the cellular proteins. The activation of caspases upon the induction of apoptosis results in their autocatalytic processing that promotes their dimerisation and activation (Raina et al., 2005; Renatus et al., 2001). On the other hand the caspase mediated proteolysis of the substrates often remove their regulatory regions/domains and result in their inactivation or constitutive activation (Affar et al., 2001).

The proteolytic processing of HCF-1 is required for the proper execution of the cell cycle. Previous studies indicated that the N-terminal region is sufficient to promote the G1/S transition, while the C terminal domain is necessary for normal cytokinesis (Julien and Herr, 2003, 2004). HCF-1 mutant with a deletion of the PPD failed to rescue the cytokinesis defects induced by RNAi-mediated depletion of HCF-1, suggesting that proteolytic processing is necessary to activate the C-terminal region (Julien and Herr, 2003). It remains unknown, why the N- and C-terminal parts of HCF-1 have to be separated and further structural studies are needed to address these questions. A recent study solved the structure of the HCF-1 SAS (Self association sequence) domain along with the C-terminal FN3 (Fibronectin type domain 3) domains (Park et al., 2012; Wilson et al., 2000). The SAS is a part of the FN3-1 of the C-terminus. It is thus possible that the unprocessed HCF-1 is unable to properly assemble the SAS/FN3-1 structure, and that the PPD processing ensures this association. On the other hand the HCF-1 C-terminus was sufficient to rescue the mitotic aberration phenotype caused by HCF-1 depletion, suggesting that the SAS/FN3-1 is not required. Therefore the inhibitory function might be contained within the N-terminus and this inhibitory effect is abrogated upon HCF-1 maturation.

Future work regarding HCF-1/OGT complex

The study of the HCF-1/OGT complex has far reaching implications for the basic understanding of chromatin function and transcription regulation in physiological as well as human pathological processes such as metabolic, neurological and neoplastic disorders.

The HCF-1/OGT complex may serve as a link between the energy balance, epigenetic modifications and cell cycle regulation. The HCF-1 is one of the most heavily O-GlcNAcylated proteins in the nucleus, containing at least 20-40 O-GlcNAcylation sites. We showed the O-GlcNAcylation of the PPD resulted in its cleavage. But most of the O-GlcNAcylation occurs in the HCF-1 N-terminal basic region. The function of these modifications remains unclear, as mutation of the multiple O-GlcNAcylation sites in the N-

terminal basic region did not affect HCF-1 maturation. Nonetheless, the basic region acts as an interaction platform for multiple HCF-1 partners (i.e. SIN3A, OGT, GABP, Miz-1 also see the introduction section), and it is possible that the O-GlcNAcylation of this region might enhance or disrupt the binding of these co-factors. The O-GlcNAcylation might also play the role as competitive post-translational modification towards phosphorylation of serine and threonine. Indeed, numerous proteomic studies revealed that HCF-1 is also extensively phosphorylated, often on overlapping sites with O-GlcNAcylation in the N-terminal basic region (Huttlin et al., 2010; Myers et al., 2013; Olsen et al., 2010).

Since O-GlcNAcylation is highly dependent on the availability of energy, one can speculate that changes in the energy balance would have proportional effects on the O-GlcNAcylation of HCF-1 basic region. A gradual modification of the HCF-1 N-terminus may act as a rheostat that converts the energy status input information into gene expression/epigenetic output. The participation of HCF-1/OGT in the multiple chromatin modifying complexes (BAP1 complex, TET 2/3 complexes, MLL and BAP1 complexes, CLOCK/BMAL1 complex (Cai et al., 2010; Chen et al., 2013; Deplus et al., 2013; Ito et al., 2014; Li et al., 2013; Yu et al., 2010) would link the energy balance sensing to gene expression regulation during ES cell maintenance and differentiation cell cycle progression, DNA demethylation, tumor suppression and the circadian rhythm regulation.

The metabolic alterations during cellular transformation are recognized as one of the major hallmarks of cancer (Hanahan and Weinberg, 2011). Indeed, convoluted and often counterintuitive reorganization of the cell metabolism is required for tumorigenesis in multiple types of cancer. Tumor cells switch their metabolic pathways to promote the generation of metabolites/catabolites that ensure the survival and proliferation of cancer cells. OGT expression and protein O-GlcNAcylation profile are disrupted in multiple types of cancers such as pancreatic, breast and prostate cancer (Caldwell et al., 2010; Huang et al., 2013). Indeed, abnormally high levels of O-GlcNAcylation were implicated in the cancer cell proliferation, tumor angiogenesis and metastasis as well as maintenance of constant pro-inflammatory signaling. (Hart et al., 2011; Ma and Vosseller, 2013; Wang et al., 2012). The suggested role of the OGT in the PI3K signaling also predicts its possible

role in receptor tyrosine kinases (RTK) signaling, one of the most prominent oncogenic pathways. OGT functions as a negative regulator of Akt signaling at the level of insulin receptor activation, and also acts as an insulin desensitizer. It would be interesting to determine if OGT also acts as an agonist/antagonist of the well-established oncogenic RTKs pathways, i.e., EGFR, HER, Met and VEGFR, although the function of the OGT in these pathways may be independent of HCF-1. The immediate effects of the receptor protein signaling on the chromatin landscape are much less studied, and the HCF-1/OGT complex might provide the link between the RTK signaling and chromatin modifications.

The OGT/HCF-1 is associated with multiple tumor suppressors such as BAP1 and TET 2/3 and proto-oncogenes such as MLL1 and MLL5. Mutations of the OGT and HCF-1 have been detected in human malignancies, but their role in tumor development is unknown. The importance of the OGT/HCF-1 complex for cell cycle progression suggests that any loss of function mutations would not be beneficial for the cancer cell, therefore the gain of function mutation would be more likely to play a role in this process. Further studies are needed to understand the role of such mutations in cancer development. The study of the role of the HCF-1/OGT in the oncogenic process may shed light on the mechanisms of tumor suppression/oncogenesis and provide a platform for the development of targeted anticancer therapeutic strategies.

Regulation of the tumor suppressor BAP1 by the atypical ubiquitin ligase UBE2O

The last decade of research in the field of DUBs uncovered numerous functions for this family of enzymes. DUBs were shown to play important roles in almost every aspect of ubiquitin signaling, from ubiquitin processing, to protein degradation and ubiquitin recycling. Despite all the progress in the field, the mechanisms of DUB regulation remain much less understood.

The recent rise of interest in BAP1 resulted from the discovery of its role as a tumor

suppressor in a plethora of human malignancies. Although the exact mechanism of BAP1 action still remains elusive, it is clear that it is involved in transcription regulation and DSB repair through its DUB activity towards the histone repressive mark, the ubiquitinated H2A (K119) (Scheuermann et al., 2010; Yu et al., 2010; Yu et al., 2014). The multiple BAP1 partners (LSD2, HAT1, OGT) may act in the concert with its core subunit (BAP1) and promote coordinated demethylation, acetylation and O-GlcNAcylation in order to ensure specific chromatin associated events (Carbone et al., 2013; Fang et al., 2010; Hart et al., 2011; Parthun, 2007).

Our work describes a novel regulatory circuit between the DUB BAP1 and the unusual ubiquitin-conjugating enzyme UBE2O. We found that UBE2O dynamically and reversibly ubiquitinates BAP1 on its NLS. Notably, this process promotes the sequestration of BAP1 to the cytoplasm. The BAP1 auto-deubiquitination mechanism counteracts the action of UBE2O and ensures its proper localization. We found that the auto-deubiquitination ability of BAP1 is targeted by mutations in the CTD region that disable this activity and promote its cytoplasmic localization. Together our data indicate that ubiquitination/deubiquitination play a dynamic role of in the regulation of BAP1 function.

In addition to histone H2A and itself, BAP1 also appears to act on other substrates. This includes the abundant BAP1 partners HCF-1 and OGT (Dey et al., 2012; Machida et al., 2009; Misaghi et al., 2009). The two independent studies showed that the HCF-1 is deubiquitinated by BAP1, although the sites and even the regions of the protein were different. The first study showed that BAP1 deubiquitinates HCF-1 on their interaction interface that contained the ubiquitination sites within the HCF-1 Kelch domain (Misaghi et al., 2009). The parallel study showed that the HCF-1 is deubiquitinated by BAP1 on its ubiquitination sites localized within the C-terminal region (Machida et al., 2009). In both studies BAP1 had a marginal effect on HCF-1 stability suggesting possible regulatory role for HCF-1 ubiquitination, rather than its degradation. Two independent studies also revealed that BAP1 deubiquitinate and stabilize OGT (Dey et al., 2012). Notably the study by Dixit group found that the conditional knockout of BAP1 displayed dramatic drop in OGT as well as HCF-1 protein levels, supporting the idea of BAP1 as a DUB for OGT and

HCF-1 that may regulate their stability.

UBE2O as an atypical ubiquitin E2/E3 hybrid

The fact that UBE2O can act as an ubiquitin ligase was already suggested by earlier studies (Berleth and Pickart, 1996; Klemperer et al., 1989; Zhang et al., 2013a). The Class IV ubiquitin carriers emerged as E3 independent enzymes (Bartke et al., 2004; Berleth and Pickart, 1996). The very limited number of enzymes of this group (only three in human genome) suggests a unique mechanism of ubiquitin transfer. From the chemical point of view, the ubiquitination reaction does not require any other enzymes apart an E1, which activate the ubiquitin by forming the thioester ubiquitin adduct. The subsequent reactions of the ubiquitin transfer funnel the ubiquitin cascade to specific subsets of substrates and specify the particular type of ubiquitin chain. The fact that UBE2O directly engages and ubiquitinates the NLS of BAP1 is unusual but quite plausible from the biochemical point of view. The mechanism of this atypical UBE2O mediated E2/E3 ubiquitination reaction is unknown. The sensitivity of the enzyme to PAO indicates an internal ubiquitin thioester relay mechanism (Berleth and Pickart, 1996).

UBE2O can be viewed as a hypothetical fusion between the E2 carrier enzyme and the HECT domain ubiquitin ligase. According to this model, upon the E2-Ub thioester formation, the ubiquitin is being further transferred to the catalytic cysteine of the HECT domain and then to the target lysine of the substrate. UBE2O shares no similarity with any HECT domain ligase, but it may employ a similar strategy for the ubiquitination of substrates. Moreover, UBE2O sequence analysis revealed at least three putative protein domains (including the UBC), reinforcing the possibility that these regions may act similarly to the lobes of the HECT domain in complex with the E2. According to the crystal structure of the HECT/E2 complex (i.e. E6AP/UbcH7 (Huang et al., 1999)), the N-lobe of the HECT domain acts as a bridge between the UBC catalytic domain (UbcH7) and the C-

catalytic lobe of the ligase. The C-lobe and UBC oppose each other through a relatively large gap of around 40 Å. The charged UBC stimulates conformational changes that allow the closure of the gap and transfer of the ubiquitin to the C-lobe catalytic cysteine, and than to the substrate.

If we extrapolate this data, the CR1 domain of UBE2O would act as a HECT C-lobe, the CR2 domain of UBE2O as the N-lobe and the UBC domain of t UBE2O would correspond to the HECT recruited E2 (UbcH7). According to our data the CR1 region is absolutely required for substrate ubiquitination, which, to some extend, support this model.

The sensitivity of UBE2O to the PAO suggests the existence of at least two catalytically active cysteine sites. In an effort do decipher the mechanism of UBE2O mediated catalysis we analyzed the conservation of the UBE2O sequence across its orthologs in metazoans and plants. As expected, the catalytic cysteine of the enzyme (C1040 in humans) is the most conserved residue across the UBE2O orthologs. The analysis of the other 23 cysteine residues of human UBE2O did not reveal a consistent pattern of conservation that ranged from nonconserved (for example found only in mammals) to more conserved (found in most metazoans). The C230, which resides within the CR1 domain and is conserved across metazoans (apart the *Drosophila*) and plant species, was selected for mutagenesis. Unfortunately the C230S mutation did not affect the catalytic activity of UBE2O (Nazar Mashtalir and El Bachir Affar unpublished data). This result can be explained by the possible redundancy of the cysteine residues within a specific domain of UBE2O that may promote further ubiquitin transfer. Otherwise the C230S may simply not be the required site for ubiquitin transfer and other less conserved cysteine residues may play a role. A more systematic mutagenesis approach would provide insights into the mechanism of UBE2O-mediated ubiquitin transfer.

The mechanism of substrate binding by UBE2O is unknown. Our attempts to identify the substrate-binding domain failed to pinpoint the exact UBE2O region, meaning that substrate binding might involve the combination of multiple domains (Nazar Mashtalir and El Bachir Affar unpublished data).

On the other hand the other member of the class IV ubiquitin conjugating enzymes

BRUCE (BIRC6) also ubiquitinates a subset of substrates in an E3-independent manner (Bartke et al., 2004; Hao et al., 2004). UBE2O and BRUCE share similarities only in their UBC domain. BRUCE and UBE2O are likely to use their non-catalytic protein sequences to engage the substrate and promote ubiquitination by UBC. Indeed, the crystal structure of the UBC domain of BRUCE revealed the classical core fold with the addition of a subset of atypical structures with unknown functions (PDB code 3CEG). The typical ubiquitin charged E2 cannot easily transfer the ubiquitin moiety to the target lysine. The ligation reaction requires the recruitment of the E3 enzyme, for example the RING domain ligase, which stimulates the conformational shift within the Ub-UBC to promote ubiquitin discharge. The structures found in BRUCE (and in UBE2O by similarity) can be involved in the E3-independent ubiquitin discharge upon substrate binding. According to this model, the UBC of and the rest of the domains might be involved in substrate binding and proper orientation towards the catalytic site.

Auto-deubiquitination as an anti-E3 self defense mechanism

The principle of autocatalytic regulation is widely spread among the enzymes, i.e. kinases, ubiquitin ligases and proteases (Bakkenist and Kastan, 2003; Chen et al., 2002; Chen and Hochstrasser, 1996; Raina et al., 2005). This ability of autocatalysis usually results in the positive regulation of the enzyme by either exposing the catalytic site, removal of the negative regulatory sequence or the stimulation of protein/protein interaction. The auto-deubiquitination activity of DUBs stands aside of other autocatalytic reactions since it is being imposed by E3 ligases. The DUBs are often regarded as antagonists of E3 ligases since they reverse the substrate ubiquitination. The notion that the ligases also can directly and negatively regulate DUBs is much less studied, with only few papers published.

One of the studies on another UCH family DUB member UCH-L1 described its

potential regulatory mechanism by ubiquitination/autodeubiquitination (Meray and Lansbury, 2007). The UCH-L1 is a DUB highly expressed in the neural tissues (up to 10% of all the protein biomass in the brain) and is used as one of these tissues histological markers. The exact function of the enzyme is not well understood; nonetheless some studies showed that it might be implicated in the development of Parkinson disease (Lowe et al., 1990).

UCH-L1 is monoubiquitinated and displays an autodeubiquitination activity. Indeed, the catalytic dead mutant of UCH-L1 (C90S) had more pronounced ubiquitin signal than the wild type protein. The ubiquitination sites of the UCH-L1 are scattered through all the lysine residues of the enzyme including the N-terminus, but are frequently located in the vicinity of the catalytic site (Meray and Lansbury, 2007). The exact function of UCH-L1 deubiquitination remains unclear, but the monoubiquitinated UCH-L1 displayed lower ubiquitin binding affinity, indicating that ubiquitination of UCH-L1 may regulate its catalytic activity or/and substrate binding.

Since UCH-L1 consists of just one single UCH catalytic domain, the auto-deubiquitination mechanism is probably different from the one we described for UBE2O/BAP1, which involves intramolecular binding followed by autodeubiquitination of the NLS. Nonetheless, we found some ubiquitination sites in the UCH domain of BAP1 indicating possible additional mechanism similar to UCH-L1 (see the results section).

The other DUBs that display the auto-deubiquitinase activity are the muscle specific DUB USP25m (Denuc et al., 2009) and the histone H2A DUB MYSM1 (Nazar Mashtalir and El Bachir Affar unpublished data). The exact function of this E3 counteractions are unknown and may act as a protective mechanism against degradation or might act as enzymatic activity regulatory mechanisms.

In our study, we found that the BAP1 and its close relative UCH37 display the auto-deubiquitination activity. We found that the atypical class IV E2 UBE2O acts as an ubiquitin E3 ligase for the BAP1 NLS region. Notably, UBE2O was highly specific to BAP1, and displayed no activity towards UCH37, which is ubiquitinated by other unknown ubiquitin E3 ligase.

BAP1 auto-deubiquitination mechanism and its disruption in cancer

UCH37 and BAP1 share common ancestry and are highly similar in their N- and C-terminal regions (Figure 4). The UCH37 crystal structure revealed that the CTD domain is engaged in an intramolecular interaction between the UCH domain and the H8/H9 helices in its C-terminus. This coiled-coil fold positions the C-terminal region of UCH37 in proximity of the UCH domain of the protein. The very last 30 aa (ADRM1 interaction region or the KEKE motif) of the protein are not defined by the crystal structure as a result of the unstructured nature of the region (Burgie et al., 2011; Yao et al., 2008; Yao et al., 2006). Nonetheless, it is highly likely that the intramolecular interaction might facilitate the targeting of the KEKE motif on UCH37. The experimental evidence of the ubiquitination of the C88A UCH37 catalytic dead mutant also supports this notion (se the result section).

The main structural differences between BAP1 and UCH37 proteins are represented by the presence of the NLS region at the C-terminus of BAP1, as well as the acquisition of the large (400 aa) NORS region between the CC1 (corresponds to H8 in UCH37) and the CC2 (corresponds to H9 in UCH37). Despite such a drastic protein sequence acquisitions, the intramolecular interaction between the CC1 and the CC2 regions remained conserved (see result section).

The importance of the BAP1 auto-deubiquitination mechanism is further confirmed by the identification of cancer mutations in the CC2 that abrogate this ability of BAP1. Mutations of BAP1 target the catalytic domain, the HBM and the NLS regions. In addition, our studies revealed that additional cancer-associated mutations that promote the loss of ASXL1/2 inducing a loss of DUB activity toward H2A or induce a disruption of autocatalytic activity (Salima Daou, et al., submitted).

The mechanism of the BAP1 and UBE2O nuclear import and export

We described the effect of UBE2O-mediated ubiquitination of BAP1, which promoted the accumulation of this DUB in the cytoplasm. Although the mechanism of this process remains to be defined, several molecular signaling scenarios may take place.

The simple explanation of the BAP1 cytoplasmic retention by UBE2O may be the result of the interference with the NLS binding by the nuclear import machinery imposed by the ubiquitin moiety. The structural studies of the NLS recognition indicate that the NLS sequence has to remain accessible to the HEAT repeats of karyopherins, moreover the charges of lysine and arginine residues is crucial for the interaction (Conti et al., 1998; Lee et al., 2006). Therefore, the bulky nature of ubiquitin may physically interfere with the proper binding with karyopherin. This effect may be further increased by targeting multiple lysine residues of the NLS (we found at lest 4 sites in BAP1 NLS region). This mechanism predicts that BAP1 would be engaged by UBE2O in the cytoplasm and would remain retained in this compartment unable to be imported into the nucleus. The mono-ubiquitinated BAP1 might be subsequently targeted by the ubiquitin chain extending E3 ligases and degraded in a proteasome-dependent manner.

The other possibility would require the UBE2O import into the nucleus and subsequent BAP1 ubiquitination. Being predominantly cytoplasmic, the UBE2O possesses two functional NLS regions. The reason for such unexpected localization remains unclear, though it is possible that UBE2O in its inactive form remains in a “locked” conformation with masked NLS region. On the other hand, the MS analysis of the TAP purified UBE2O interacting proteins revealed numerous components on the protein import and export machinery, such as several types of the NLS receptors and nuclear import factors (i.e. TNPO1, IPO7, IPO9) as well as the components of nuclear protein and RNA export factors (i.e. XPOT, XPO1 (CRM1), XPO7, XPO5) (se the results section). This data suggest that a dynamic equilibrium may exist between the export and import of UBE2O, with export mechanism being more efficient than import, resulting in the cytoplasmic localization of the protein. The MS analysis also identified a subset of protein kinases that may be

involved in the regulation of UBE2O. One might predict that phosphorylation/dephosphorylation would stimulate the shift of the equilibrium towards the import of UBE2O. This would provide UBE2O access to BAP1 and other substrates inducing their subsequent nuclear export.

In an effort to identify the condition we performed a focused screen that included several kinase/phosphatase inhibitors and stress inducers. The subset of CDK inhibitors (Purvalanol A and RO3306) promoted the nuclear localization of UBE2O in catalytic activity-dependent manner, with the catalytic dead mutant being more responsive to the treatment. This result indicates that the nucleocytoplasmic transport of UBE2O is regulated at multiple levels involving protein kinases and ubiquitin conjugation mechanisms. The involvement of ubiquitination in regulating UBE2O localization is further supported by the observation of autocatalytic activity towards its own NLS (NLS1). The ubiquitination targeting of NLS1 is predicted to inactivate it and promote UBE2O export or block its import. Therefore, the higher sensitivity of UBE2O CD towards CDK inhibitors may occur as a result of combination of both factors. Taken together this data indicate the multilayer regulatory mechanism behind the UBE2O activity and nucleocytoplasmic transport.

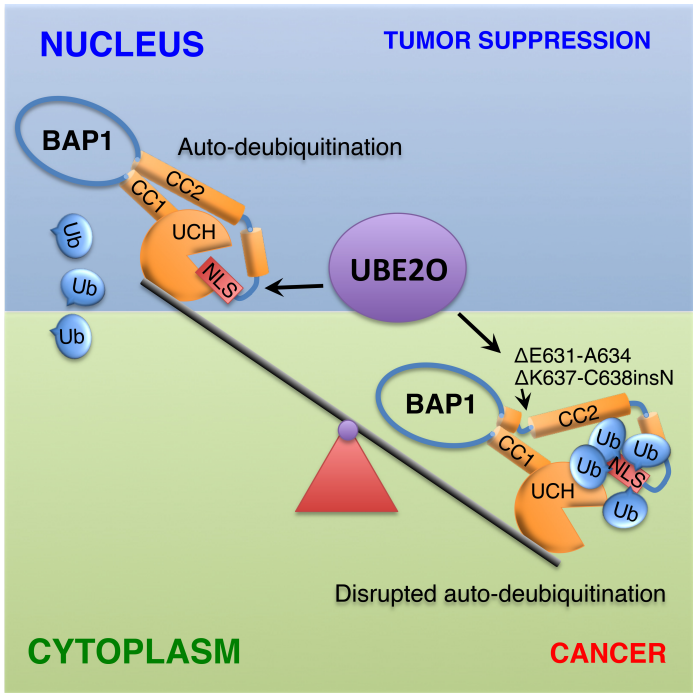

Figure 7. Regulation of BAP1 nucleocytoplasmic transport by UBE2O

We identified the region of UBE2O responsible for the dominant cytoplasmic localization of this enzyme. This region included the UBC domain along with the upstream region of 300 amino acid residues.

The classical CRM1 inhibitor Leptomycin-B, which promotes the accumulation of dynamically exported proteins in the nucleus, had no effect on the subcellular localization of UBE2O. The sequence analysis of UBE2O for the CRM1 mediated protein export signal (nuclear export signal NES) identified two degenerate LXXLXL motifs that proved to be non-functional (as GFP fusions) (la Cour et al., 2004). This explains the insensitivity of UBE2O localization to CRM1 inhibition confirming that CRM1 is not directly involved in the cytoplasmic retention of UBE2O (Nazar Mashtalir and El Bachir Affar unpublished data)

The UBC catalytic activity and Ub charging were shown to be required for proper nuclear import of one of the class III E2 enzymes UbcM2. UbcM2 was able to interact with importin-11 only when charged with ubiquitin. Therefore, the catalytic dead mutant of the UbcM2 was retained in the cytoplasm (Plafker et al., 2004). In respect to the UBE2O, the charging does not seem to be involved in the import process, since the UBE2O WT as well as CD were both predominantly cytoplasmic. Nevertheless, the auto-ubiquitination of the UBE2O NLS1 seems to play an important role in its cytoplasmic retention (see the result section).

There are two main possibilities that describe the mechanism of action of cytoplasmic retention region. First, the region may represent, or incorporate the atypical export sequence, that promotes UBE2O nuclear export in concert with exportin factors. Second, the region might mask the NLS motif via intramolecular or intermolecular interactions. To date our results suggest that the main pool of UBE2O under normal growth conditions remains mostly cytoplasmic, with the possibility of a small fraction being imported to the nucleus with very short residence time as a result of its efficient export

mechanism. Otherwise, an unidentified signal might promote the unmasking of the NLS sequence, with its subsequent nuclear import, and quick export back to the cytoplasm.

There is no information about the fate of BAP1 in the cytoplasm. The most likely scenario is that it is being targeted by ubiquitin chain extending E3 ligase with its subsequent proteasomal degradation. Such a mechanism was described for several transcription factors such as HIF-1a and p53 as well as ubiquitin ligase factor DCN1 (Boyd et al., 2000; Groulx and Lee, 2002; Li et al., 2003; Wu et al., 2011). The plausible explanation of the mechanism would predict the nuclear ubiquitin receptor recognizes the monoubiquitinated NLS and promotes its export to the cytoplasm.

The alignment of BAP1 and UBE2O NLS regions allowed us to identify the UBE2O recognition consensus that led to the identification of multiple UBE2O substrates, notably three of them INO80, p400 and CDT1 where degraded in UBE2O co-expression experiments. No monoubiquitinated products where detected for either of proteins suggesting that the polyubiquitinated protein products where rapidly degraded possibly as a result of ubiquitin chain extension by another E3. Therefore the fate of the UBE2O ubiquitinated protein probably depends on additional factors and specific signaling pathways.

Under normal conditions, BAP1 is highly stable and there is no evidence for its regulation by ubiquitin mediated degradation. Since BAP1 is involved in the regulation of normal cell proliferation and differentiation, we decided to test whether UBE2O may play a role in its regulation during cell cycle exit. Indeed, UBE2O was shown to be involved in the regulation of cell differentiation, and down regulation of this enzyme in primary cells promoted their increased proliferation. In contrast BAP1 knockdown induced a delay in cell cycle progression. This prompted us to study the role of UBE2O and BAP1 during cell cycle exit (see the result section).

Indeed, we observed the increased cytoplasmic localization of BAP1 during terminal cell cycle exit in differentiating 3T3-L1 preadipocytes, and this effect was dependent on the ubiquitination of BAP1 NLS. Moreover, the overexpression of UBE2O but not its CD form promoted 3T3-L1 differentiation. Taken together, these results suggest

that UBE2O may play a major role in the regulation of cell cycle and cell differentiation. UBE2O was indeed shown to be upregulated in several models of cellular differentiation including neuronal, erythroid and muscle (Berleth and Pickart, 1996; Yokota et al., 2001). The data from *Arabidopsis thaliana* have shown that UBE2O ortholog *UBP23* was promptly and highly upregulated during the induction of abscisic acid and ethylene signaling, major plant signaling pathways of abscission, senescence and fruit ripening (De Paepe et al., 2004; Hoth et al., 2002), Taken together this data defines a conserved role of UBE2O in the regulation of cell proliferation and differentiation.

References:

Abdel-Rahman, M.H., Pilarski, R., Cebulla, C.M., Massengill, J.B., Christopher, B.N., Boru, G., Hovland, P., and Davidorf, F.H. (2011). Germline BAP1 mutation predisposes to uveal melanoma, lung adenocarcinoma, meningioma, and other cancers. Journal of medical genetics *48*, 856-859.

Abdel-Wahab, O., and Dey, A. (2013). The ASXL-BAP1 axis: new factors in myelopoiesis, cancer and epigenetics. Leukemia *27*, 10-15.

Adams, M.D., Celniker, S.E., Holt, R.A., Evans, C.A., Gocayne, J.D., Amanatides, P.G., Scherer, S.E., Li, P.W., Hoskins, R.A., Galle, R.F.*, et al.* (2000). The genome sequence of Drosophila melanogaster. Science *287*, 2185-2195.

Affar, E.B., Germain, M., Winstall, E., Vodenicharov, M., Shah, R.G., Salvesen, G.S., and Poirier, G.G. (2001). Caspase-3-mediated processing of poly(ADP-ribose) glycohydrolase during apoptosis. The Journal of biological chemistry *276*, 2935-2942.

Ahel, D., Horejsi, Z., Wiechens, N., Polo, S.E., Garcia-Wilson, E., Ahel, I., Flynn, H., Skehel, M., West, S.C., Jackson, S.P.*, et al.* (2009). Poly(ADP-ribose)-dependent regulation of DNA repair by the chromatin remodeling enzyme ALC1. Science *325*, 1240-1243.

Ajuh, P., Chusainow, J., Ryder, U., and Lamond, A.I. (2002). A novel function for human factor C1 (HCF-1), a host protein required for herpes simplex virus infection, in pre-mRNA splicing. The EMBO journal *21*, 6590-6602.

Ajuh, P.M., Browne, G.J., Hawkes, N.A., Cohen, P.T., Roberts, S.G., and Lamond, A.I. (2000). Association of a protein phosphatase 1 activity with the human factor C1 (HCF) complex. Nucleic acids research *28*, 678-686.

Akimoto, Y., Kreppel, L.K., Hirano, H., and Hart, G.W. (2000). Increased O-GlcNAc transferase in pancreas of rats with streptozotocin-induced diabetes. Diabetologia *43*, 1239-1247.

Amerik, A., Swaminathan, S., Krantz, B.A., Wilkinson, K.D., and Hochstrasser, M. (1997). In vivo disassembly of free polyubiquitin chains by yeast Ubp14 modulates rates of protein degradation by the proteasome. The EMBO journal *16*, 4826-4838.

Avery, O.T., Macleod, C.M., and McCarty, M. (1944). STUDIES ON THE CHEMICAL NATURE OF THE SUBSTANCE INDUCING TRANSFORMATION OF PNEUMOCOCCAL TYPES : INDUCTION OF TRANSFORMATION BY A DESOXYRIBONUCLEIC ACID FRACTION ISOLATED FROM PNEUMOCOCCUS TYPE III. The Journal of experimental medicine *79*, 137-158.

Avramova, Z.V. (2002). Heterochromatin in animals and plants. Similarities and differences. Plant physiology *129*, 40-49.

Bakkenist, C.J., and Kastan, M.B. (2003). DNA damage activates ATM through intermolecular autophosphorylation and dimer dissociation. Nature *421*, 499-506.

Bartke, T., Pohl, C., Pyrowolakis, G., and Jentsch, S. (2004). Dual role of BRUCE as an antiapoptotic IAP and a chimeric E2/E3 ubiquitin ligase. Molecular cell *14*, 801-811.

Bekes, M., Okamoto, K., Crist, S.B., Jones, M.J., Chapman, J.R., Brasher, B.B., Melandri, F.D., Ueberheide, B.M., Denchi, E.L., and Huang, T.T. (2013). DUB-resistant ubiquitin to survey ubiquitination switches in mammalian cells. Cell reports *5*, 826-838.

Bentley, M.L., Corn, J.E., Dong, K.C., Phung, Q., Cheung, T.K., and Cochran, A.G. (2011). Recognition of UbcH5c and the nucleosome by the Bmi1/Ring1b ubiquitin ligase complex. The EMBO journal *30*, 3285-3297.

Berleth, E.S., and Pickart, C.M. (1996). Mechanism of ubiquitin conjugating enzyme E2-230K: catalysis involving a thiol relay? Biochemistry *35*, 1664-1671.

Bernstein, B.E., Humphrey, E.L., Erlich, R.L., Schneider, R., Bouman, P., Liu, J.S., Kouzarides, T., and Schreiber, S.L. (2002). Methylation of histone H3 Lys 4 in coding regions of active genes. Proceedings of the National Academy of Sciences of the United States of America *99*, 8695-8700.

Blattler, S.M., Cunningham, J.T., Verdeguer, F., Chim, H., Haas, W., Liu, H., Romanino, K., Ruegg, M.A., Gygi, S.P., Shi, Y.*, et al.* (2012). Yin Yang 1 deficiency in skeletal muscle protects against rapamycin-induced diabetic-like symptoms through activation of insulin/IGF signaling. Cell metabolism *15*, 505-517.

Bott, M., Brevet, M., Taylor, B.S., Shimizu, S., Ito, T., Wang, L., Creaney, J., Lake, R.A., Zakowski, M.F., Reva, B.*, et al.* (2011). The nuclear deubiquitinase BAP1 is commonly inactivated by somatic mutations and 3p21.1 losses in malignant pleural mesothelioma. Nature genetics *43*, 668-672.

Boya, P., Reggiori, F., and Codogno, P. (2013). Emerging regulation and functions of autophagy. Nature cell biology *15*, 713-720.

Boyd, S.D., Tsai, K.Y., and Jacks, T. (2000). An intact HDM2 RING-finger domain is required for nuclear exclusion of p53. Nature cell biology *2*, 563-568.

Boyer, L.A., Plath, K., Zeitlinger, J., Brambrink, T., Medeiros, L.A., Lee, T.I., Levine, S.S., Wernig, M., Tajonar, A., Ray, M.K.*, et al.* (2006). Polycomb complexes repress developmental regulators in murine embryonic stem cells. Nature *441*, 349-353.

Bradbury, E.M. (1992). Reversible histone modifications and the chromosome cell cycle. BioEssays : news and reviews in molecular, cellular and developmental biology *14*, 9-16.

Branco, M.R., Ficz, G., and Reik, W. (2012). Uncovering the role of 5-hydroxymethylcytosine in the epigenome. Nature reviews. Genetics *13*, 7-13.

Breen, T.R., and Harte, P.J. (1991). Molecular characterization of the trithorax gene, a positive regulator of homeotic gene expression in Drosophila. Mechanisms of development *35*, 113-127.

Bridges, C.B. (1921). Current Maps of the Location of the Mutant Genes of Drosophila Melanogaster. Proceedings of the National Academy of Sciences of the United States of America *7*, 127-132.

Burgie, S.E., Bingman, C.A., Soni, A.B., and Phillips, G.N., Jr. (2011). Structural characterization of human Uch37. Proteins.

Cai, Y., Jin, J., Swanson, S.K., Cole, M.D., Choi, S.H., Florens, L., Washburn, M.P., Conaway, J.W., and Conaway, R.C. (2010). Subunit composition and substrate specificity of a MOF-containing histone acetyltransferase distinct from the male-specific lethal (MSL) complex. The Journal of biological chemistry *285*, 4268-4272.

Caldwell, S.A., Jackson, S.R., Shahriari, K.S., Lynch, T.P., Sethi, G., Walker, S., Vosseller, K., and Reginato, M.J. (2010). Nutrient sensor O-GlcNAc transferase regulates breast cancer tumorigenesis through targeting of the oncogenic transcription factor FoxM1. Oncogene *29*, 2831-2842.

Campos, E.I., and Reinberg, D. (2009). Histones: annotating chromatin. Annual review of genetics *43*, 559-599.

Cao, Q., Wang, X., Zhao, M., Yang, R., Malik, R., Qiao, Y., Poliakov, A., Yocum, A.K., Li, Y., Chen, W.*, et al.* (2014). The central role of EED in the orchestration of polycomb group complexes. Nature communications *5*, 3127.

Cao, R., Wang, L., Wang, H., Xia, L., Erdjument-Bromage, H., Tempst, P., Jones, R.S., and Zhang, Y. (2002). Role of histone H3 lysine 27 methylation in Polycomb-group silencing. Science *298*, 1039-1043.

Cao, R., and Zhang, Y. (2004). SUZ12 is required for both the histone methyltransferase activity and the silencing function of the EED-EZH2 complex. Molecular cell *15*, 57-67.

Capotosti, F., Guernier, S., Lammers, F., Waridel, P., Cai, Y., Jin, J., Conaway, J.W., Conaway, R.C., and Herr, W. (2011). O-GlcNAc transferase catalyzes site-specific proteolysis of HCF-1. Cell *144*, 376-388.

Capotosti, F., Hsieh, J.J., and Herr, W. (2007). Species selectivity of mixed-lineage leukemia/trithorax and HCF proteolytic maturation pathways. Molecular and cellular biology *27*, 7063-7072.

Carbone, M., Ferris, L.K., Baumann, F., Napolitano, A., Lum, C.A., Flores, E.G., Gaudino, G., Powers, A., Bryant-Greenwood, P., Krausz, T.*, et al.* (2012). BAP1 cancer syndrome: malignant mesothelioma, uveal and cutaneous melanoma, and MBAITs. Journal of translational medicine *10*, 179.

Carbone, M., Yang, H., Pass, H.I., Krausz, T., Testa, J.R., and Gaudino, G. (2013). BAP1 and cancer. Nature reviews. Cancer *13*, 153-159.

Cardoso, W.V. (1995). Transcription factors and pattern formation in the developing lung. The American journal of physiology *269*, L429-442.

Caretti, G., Di Padova, M., Micales, B., Lyons, G.E., and Sartorelli, V. (2004). The Polycomb Ezh2 methyltransferase regulates muscle gene expression and skeletal muscle differentiation. Genes & development *18*, 2627-2638.

Carroll, S.B. (1995). Homeotic genes and the evolution of arthropods and chordates. Nature *376*, 479-485.

Caterino, T.L., and Hayes, J.J. (2011). Structure of the H1 C-terminal domain and function in chromatin condensation. Biochemistry and cell biology = Biochimie et biologie cellulaire *89*, 35-44.

Chamberlain, S.J., Yee, D., and Magnuson, T. (2008). Polycomb repressive complex 2 is dispensable for maintenance of embryonic stem cell pluripotency. Stem cells *26*, 1496-1505.

Chan, H.M., Narita, M., Lowe, S.W., and Livingston, D.M. (2005). The p400 E1A-associated protein is a novel component of the p53 --> p21 senescence pathway. Genes & development *19*, 196-201.

Chen, A., Kleiman, F.E., Manley, J.L., Ouchi, T., and Pan, Z.Q. (2002). Autoubiquitination of the BRCA1*BARD1 RING ubiquitin ligase. The Journal of biological chemistry *277*, 22085-22092.

Chen, L., Cai, Y., Jin, J., Florens, L., Swanson, S.K., Washburn, M.P., Conaway, J.W., and Conaway, R.C. (2011). Subunit organization of the human INO80 chromatin remodeling complex: an evolutionarily conserved core complex catalyzes ATP-dependent nucleosome remodeling. The Journal of biological chemistry *286*, 11283-11289.

Chen, P., and Hochstrasser, M. (1996). Autocatalytic subunit processing couples active site formation in the 20S proteasome to completion of assembly. Cell *86*, 961-972.

Chen, Q., Chen, Y., Bian, C., Fujiki, R., and Yu, X. (2013). TET2 promotes histone O-GlcNAcylation during gene transcription. Nature *493*, 561-564.

Chi, P., Allis, C.D., and Wang, G.G. (2010). Covalent histone modifications--miswritten, misinterpreted and mis-erased in human cancers. Nature reviews. Cancer *10*, 457-469.

Chou, D.M., Adamson, B., Dephoure, N.E., Tan, X., Nottke, A.C., Hurov, K.E., Gygi, S.P., Colaiacovo, M.P., and Elledge, S.J. (2010). A chromatin localization screen reveals poly (ADP ribose)-regulated recruitment of the repressive polycomb and NuRD complexes to sites of DNA damage. Proceedings of the National Academy of Sciences of the United States of America *107*, 18475-18480.

Clarke, A.J., Hurtado-Guerrero, R., Pathak, S., Schuttelkopf, A.W., Borodkin, V., Shepherd, S.M., Ibrahim, A.F., and van Aalten, D.M. (2008). Structural insights into mechanism and specificity of O-GlcNAc transferase. The EMBO journal *27*, 2780-2788.

Comtesse, N., Maldener, E., and Meese, E. (2001). Identification of a nuclear variant of MGEA5, a cytoplasmic hyaluronidase and a beta-N-acetylglucosaminidase. Biochemical and biophysical research communications *283*, 634-640.

Conti, E., Uy, M., Leighton, L., Blobel, G., and Kuriyan, J. (1998). Crystallographic analysis of the recognition of a nuclear localization signal by the nuclear import factor karyopherin alpha. Cell *94*, 193-204.

Cooper, E.M., Cutcliffe, C., Kristiansen, T.Z., Pandey, A., Pickart, C.M., and Cohen, R.E. (2009). K63-specific deubiquitination by two JAMM/MPN+ complexes: BRISC-associated Brcc36 and proteasomal Poh1. The EMBO journal *28*, 621-631.

Daou, S., Mashtalir, N., Hammond-Martel, I., Pak, H., Yu, H., Sui, G., Vogel, J.L., Kristie, T.M., and Affar el, B. (2011). Crosstalk between O-GlcNAcylation and proteolytic

cleavage regulates the host cell factor-1 maturation pathway. Proceedings of the National Academy of Sciences of the United States of America *108*, 2747-2752.

de Napoles, M., Mermoud, J.E., Wakao, R., Tang, Y.A., Endoh, M., Appanah, R., Nesterova, T.B., Silva, J., Otte, A.P., Vidal, M.*, et al.* (2004). Polycomb group proteins Ring1A/B link ubiquitylation of histone H2A to heritable gene silencing and X inactivation. Developmental cell *7*, 663-676.

De Paepe, A., Vuylsteke, M., Van Hummelen, P., Zabeau, M., and Van Der Straeten, D. (2004). Transcriptional profiling by cDNA-AFLP and microarray analysis reveals novel insights into the early response to ethylene in Arabidopsis. The Plant journal : for cell and molecular biology *39*, 537-559.

Dejardin, J., Rappailles, A., Cuvier, O., Grimaud, C., Decoville, M., Locker, D., and Cavalli, G. (2005). Recruitment of Drosophila Polycomb group proteins to chromatin by DSP1. Nature *434*, 533-538.

Dejosez, M., Levine, S.S., Frampton, G.M., Whyte, W.A., Stratton, S.A., Barton, M.C., Gunaratne, P.H., Young, R.A., and Zwaka, T.P. (2010). Ronin/Hcf-1 binds to a hyperconserved enhancer element and regulates genes involved in the growth of embryonic stem cells. Genes & development *24*, 1479-1484.

Dekker, J., Rippe, K., Dekker, M., and Kleckner, N. (2002). Capturing chromosome conformation. Science *295*, 1306-1311.

Denuc, A., Bosch-Comas, A., Gonzalez-Duarte, R., and Marfany, G. (2009). The UBA-UIM domains of the USP25 regulate the enzyme ubiquitination state and modulate substrate recognition. PloS one *4*, e5571.

Deplus, R., Delatte, B., Schwinn, M.K., Defrance, M., Mendez, J., Murphy, N., Dawson, M.A., Volkmar, M., Putmans, P., Calonne, E.*, et al.* (2013). TET2 and TET3 regulate

GlcNAcylation and H3K4 methylation through OGT and SET1/COMPASS. The EMBO journal *32*, 645-655.

Deshaies, R.J., and Joazeiro, C.A. (2009). RING domain E3 ubiquitin ligases. Annual review of biochemistry *78*, 399-434.

Dey, A., Seshasayee, D., Noubade, R., French, D.M., Liu, J., Chaurushiya, M.S., Kirkpatrick, D.S., Pham, V.C., Lill, J.R., Bakalarski, C.E*., et al.* (2012). Loss of the tumor suppressor BAP1 causes myeloid transformation. Science *337*, 1541-1546.

Dias, W.B., and Hart, G.W. (2007). O-GlcNAc modification in diabetes and Alzheimer's disease. Molecular bioSystems *3*, 766-772.

Dikic, I., Wakatsuki, S., and Walters, K.J. (2009). Ubiquitin-binding domains - from structures to functions. Nature reviews. Molecular cell biology *10*, 659-671.

Dillon, S.C., and Dorman, C.J. (2010). Bacterial nucleoid-associated proteins, nucleoid structure and gene expression. Nature reviews. Microbiology *8*, 185-195.

Dolle, P., Izpisua-Belmonte, J.C., Brown, J., Tickle, C., and Duboule, D. (1993). Hox genes and the morphogenesis of the vertebrate limb. Progress in clinical and biological research *383A*, 11-20.

Dorigo, B., Schalch, T., Kulangara, A., Duda, S., Schroeder, R.R., and Richmond, T.J. (2004). Nucleosome arrays reveal the two-start organization of the chromatin fiber. Science *306*, 1571-1573.

Dostie, J., Richmond, T.A., Arnaout, R.A., Selzer, R.R., Lee, W.L., Honan, T.A., Rubio, E.D., Krumm, A., Lamb, J., Nusbaum, C*., et al.* (2006). Chromosome Conformation Capture Carbon Copy (5C): a massively parallel solution for mapping interactions between genomic elements. Genome research *16*, 1299-1309.

Eissenberg, J.C., and Shilatifard, A. (2010). Histone H3 lysine 4 (H3K4) methylation in development and differentiation. Developmental biology *339*, 240-249.

Endoh, M., Endo, T.A., Endoh, T., Isono, K., Sharif, J., Ohara, O., Toyoda, T., Ito, T., Eskeland, R., Bickmore, W.A.*, et al.* (2012). Histone H2A mono-ubiquitination is a crucial step to mediate PRC1-dependent repression of developmental genes to maintain ES cell identity. PLoS genetics *8*, e1002774.

Eskeland, R., Leeb, M., Grimes, G.R., Kress, C., Boyle, S., Sproul, D., Gilbert, N., Fan, Y., Skoultchi, A.I., Wutz, A.*, et al.* (2010). Ring1B compacts chromatin structure and represses gene expression independent of histone ubiquitination. Molecular cell *38*, 452-464.

Fang, J., Chen, T., Chadwick, B., Li, E., and Zhang, Y. (2004). Ring1b-mediated H2A ubiquitination associates with inactive X chromosomes and is involved in initiation of X inactivation. The Journal of biological chemistry *279*, 52812-52815.

Fang, R., Barbera, A.J., Xu, Y., Rutenberg, M., Leonor, T., Bi, Q., Lan, F., Mei, P., Yuan, G.C., Lian, C.*, et al.* (2010). Human LSD2/KDM1b/AOF1 regulates gene transcription by modulating intragenic H3K4me2 methylation. Molecular cell *39*, 222-233.

Filion, G.J., van Bemmel, J.G., Braunschweig, U., Talhout, W., Kind, J., Ward, L.D., Brugman, W., de Castro, I.J., Kerkhoven, R.M., Bussemaker, H.J.*, et al.* (2010). Systematic protein location mapping reveals five principal chromatin types in Drosophila cells. Cell *143*, 212-224.

Finley, D. (2009). Recognition and processing of ubiquitin-protein conjugates by the proteasome. Annual review of biochemistry *78*, 477-513.

Flemming, W. (1882). Zellsubstanz, Kern und Zelltheilung (Leipzig: Vogel).

Francis, N.J., Follmer, N.E., Simon, M.D., Aghia, G., and Butler, J.D. (2009). Polycomb proteins remain bound to chromatin and DNA during DNA replication in vitro. Cell *137*, 110-122.

Freiman, R.N., and Herr, W. (1997). Viral mimicry: common mode of association with HCF by VP16 and the cellular protein LZIP. Genes & development *11*, 3122-3127.

Fujiki, R., Chikanishi, T., Hashiba, W., Ito, H., Takada, I., Roeder, R.G., Kitagawa, H., and Kato, S. (2009). GlcNAcylation of a histone methyltransferase in retinoic-acid-induced granulopoiesis. Nature *459*, 455-459.

Fujiki, R., Hashiba, W., Sekine, H., Yokoyama, A., Chikanishi, T., Ito, S., Imai, Y., Kim, J., He, H.H., Igarashi, K.*, et al.* (2011). GlcNAcylation of histone H2B facilitates its monoubiquitination. Nature *480*, 557-560.

Fussner, E., Ching, R.W., and Bazett-Jones, D.P. (2011). Living without 30nm chromatin fibers. Trends in biochemical sciences *36*, 1-6.

Gambetta, M.C., Oktaba, K., and Muller, J. (2009). Essential role of the glycosyltransferase sxc/Ogt in polycomb repression. Science *325*, 93-96.

Gaspar-Maia, A., Alajem, A., Meshorer, E., and Ramalho-Santos, M. (2011). Open chromatin in pluripotency and reprogramming. Nature reviews. Molecular cell biology *12*, 36-47.

Gearhart, M.D., Corcoran, C.M., Wamstad, J.A., and Bardwell, V.J. (2006). Polycomb group and SCF ubiquitin ligases are found in a novel BCOR complex that is recruited to BCL6 targets. Molecular and cellular biology *26*, 6880-6889.

Geng, F., Wenzel, S., and Tansey, W.P. (2012). Ubiquitin and proteasomes in transcription. Annual review of biochemistry *81*, 177-201.

Gieni, R.S., Ismail, I.H., Campbell, S., and Hendzel, M.J. (2011). Polycomb group proteins in the DNA damage response: a link between radiation resistance and "stemness". Cell cycle *10*, 883-894.

Goff, S.A., Ricke, D., Lan, T.H., Presting, G., Wang, R., Dunn, M., Glazebrook, J., Sessions, A., Oeller, P., Varma, H.*, et al.* (2002). A draft sequence of the rice genome (Oryza sativa L. ssp. japonica). Science *296*, 92-100.

Goll, M.G., and Bestor, T.H. (2005). Eukaryotic cytosine methyltransferases. Annual review of biochemistry *74*, 481-514.

Gornik, S.G., Ford, K.L., Mulhern, T.D., Bacic, A., McFadden, G.I., and Waller, R.F. (2012). Loss of nucleosomal DNA condensation coincides with appearance of a novel nuclear protein in dinoflagellates. Current biology : CB *22*, 2303-2312.

Grau, D.J., Chapman, B.A., Garlick, J.D., Borowsky, M., Francis, N.J., and Kingston, R.E. (2011). Compaction of chromatin by diverse Polycomb group proteins requires localized regions of high charge. Genes & development *25*, 2210-2221.

Griffith, F. (1928). The Significance of Pneumococcal Types. The Journal of hygiene *27*, 113-159.

Groulx, I., and Lee, S. (2002). Oxygen-dependent ubiquitination and degradation of hypoxia-inducible factor requires nuclear-cytoplasmic trafficking of the von Hippel-Lindau tumor suppressor protein. Molecular and cellular biology *22*, 5319-5336.

Gupta, R.A., Shah, N., Wang, K.C., Kim, J., Horlings, H.M., Wong, D.J., Tsai, M.C., Hung, T., Argani, P., Rinn, J.L.*, et al.* (2010). Long non-coding RNA HOTAIR reprograms chromatin state to promote cancer metastasis. Nature *464*, 1071-1076.

Guruharsha, K.G., Kankel, M.W., and Artavanis-Tsakonas, S. (2012). The Notch signalling system: recent insights into the complexity of a conserved pathway. Nature reviews. Genetics *13*, 654-666.

Haldeman, M.T., Finley, D., and Pickart, C.M. (1995). Dynamics of ubiquitin conjugation during erythroid differentiation in vitro. The Journal of biological chemistry *270*, 9507-9516.

Hallson, G., Hollebakken, R.E., Li, T., Syrzycka, M., Kim, I., Cotsworth, S., Fitzpatrick, K.A., Sinclair, D.A., and Honda, B.M. (2012). dSet1 is the main H3K4 di- and tri-methyltransferase throughout Drosophila development. Genetics *190*, 91-100.

Hammond-Martel, I., Yu, H., and Affar el, B. (2012). Roles of ubiquitin signaling in transcription regulation. Cellular signalling *24*, 410-421.

Hanahan, D., and Weinberg, R.A. (2011). Hallmarks of cancer: the next generation. Cell *144*, 646-674.

Hanna, J., Meides, A., Zhang, D.P., and Finley, D. (2007). A ubiquitin stress response induces altered proteasome composition. Cell *129*, 747-759.

Hansen, K.H., Bracken, A.P., Pasini, D., Dietrich, N., Gehani, S.S., Monrad, A., Rappsilber, J., Lerdrup, M., and Helin, K. (2008). A model for transmission of the H3K27me3 epigenetic mark. Nature cell biology *10*, 1291-1300.

Hao, Y., Sekine, K., Kawabata, A., Nakamura, H., Ishioka, T., Ohata, H., Katayama, R., Hashimoto, C., Zhang, X., Noda, T.*, et al.* (2004). Apollon ubiquitinates SMAC and caspase-9, and has an essential cytoprotection function. Nature cell biology *6*, 849-860.

Hao, Y.H., Doyle, J.M., Ramanathan, S., Gomez, T.S., Jia, D., Xu, M., Chen, Z.J., Billadeau, D.D., Rosen, M.K., and Potts, P.R. (2013). Regulation of WASH-Dependent Actin Polymerization and Protein Trafficking by Ubiquitination. Cell *152*, 1051-1064.

Harbour, J.W., Onken, M.D., Roberson, E.D., Duan, S., Cao, L., Worley, L.A., Council, M.L., Matatall, K.A., Helms, C., and Bowcock, A.M. (2010). Frequent mutation of BAP1 in metastasizing uveal melanomas. Science *330*, 1410-1413.

Hart, G.W., Housley, M.P., and Slawson, C. (2007). Cycling of O-linked beta-N-acetylglucosamine on nucleocytoplasmic proteins. Nature *446*, 1017-1022.

Hart, G.W., Slawson, C., Ramirez-Correa, G., and Lagerlof, O. (2011). Cross talk between O-GlcNAcylation and phosphorylation: roles in signaling, transcription, and chronic disease. Annual review of biochemistry *80*, 825-858.

He, A., Shen, X., Ma, Q., Cao, J., von Gise, A., Zhou, P., Wang, G., Marquez, V.E., Orkin, S.H., and Pu, W.T. (2012). PRC2 directly methylates GATA4 and represses its transcriptional activity. Genes & development *26*, 37-42.

Herr, W. (1998). The herpes simplex virus VP16-induced complex: mechanisms of combinatorial transcriptional regulation. Cold Spring Harbor symposia on quantitative biology *63*, 599-607.

Ho, L., and Crabtree, G.R. (2010). Chromatin remodelling during development. Nature *463*, 474-484.

Hoth, S., Morgante, M., Sanchez, J.P., Hanafey, M.K., Tingey, S.V., and Chua, N.H. (2002). Genome-wide gene expression profiling in Arabidopsis thaliana reveals new targets of abscisic acid and largely impaired gene regulation in the abi1-1 mutant. Journal of cell science *115*, 4891-4900.

Hu, M., Li, P., Song, L., Jeffrey, P.D., Chenova, T.A., Wilkinson, K.D., Cohen, R.E., and Shi, Y. (2005). Structure and mechanisms of the proteasome-associated deubiquitinating enzyme USP14. The EMBO journal *24*, 3747-3756.

Huang, L., Kinnucan, E., Wang, G., Beaudenon, S., Howley, P.M., Huibregtse, J.M., and Pavletich, N.P. (1999). Structure of an E6AP-UbcH7 complex: insights into ubiquitination by the E2-E3 enzyme cascade. Science *286*, 1321-1326.

Huang, T.T., Nijman, S.M., Mirchandani, K.D., Galardy, P.J., Cohn, M.A., Haas, W., Gygi, S.P., Ploegh, H.L., Bernards, R., and D'Andrea, A.D. (2006). Regulation of monoubiquitinated PCNA by DUB autocleavage. Nature cell biology *8*, 339-347.

Huang, X., Pan, Q., Sun, D., Chen, W., Shen, A., Huang, M., Ding, J., and Geng, M. (2013). O-GlcNAcylation of Cofilin Promotes Breast Cancer Cell Invasion. The Journal of biological chemistry *288*, 36418-36425.

Huttlin, E.L., Jedrychowski, M.P., Elias, J.E., Goswami, T., Rad, R., Beausoleil, S.A., Villen, J., Haas, W., Sowa, M.E., and Gygi, S.P. (2010). A tissue-specific atlas of mouse protein phosphorylation and expression. Cell *143*, 1174-1189.

Ingham, P.W. (1985). A clonal analysis of the requirement for the trithorax gene in the diversification of segments in Drosophila. Journal of embryology and experimental morphology *89*, 349-365.

Ismail, I.H., Andrin, C., McDonald, D., and Hendzel, M.J. (2010). BMI1-mediated histone ubiquitylation promotes DNA double-strand break repair. The Journal of cell biology *191*, 45-60.

Ito, R., Katsura, S., Shimada, H., Tsuchiya, H., Hada, M., Okumura, T., Sugawara, A., and Yokoyama, A. (2014). TET3-OGT interaction increases the stability and the presence of OGT in chromatin. Genes to cells : devoted to molecular & cellular mechanisms *19*, 52-65.

Iyer, S.P., and Hart, G.W. (2003). Roles of the tetratricopeptide repeat domain in O-GlcNAc transferase targeting and protein substrate specificity. The Journal of biological chemistry *278*, 24608-24616.

Jacob, F., and Monod, J. (1961). Genetic regulatory mechanisms in the synthesis of proteins. Journal of molecular biology *3*, 318-356.

James, T.W., Frias-Staheli, N., Bacik, J.P., Levingston Macleod, J.M., Khajehpour, M., Garcia-Sastre, A., and Mark, B.L. (2011). Structural basis for the removal of ubiquitin and interferon-stimulated gene 15 by a viral ovarian tumor domain-containing protease. Proceedings of the National Academy of Sciences of the United States of America *108*, 2222-2227.

Je, E.M., Lee, S.H., and Yoo, N.J. (2012). Somatic mutation of a tumor suppressor gene BAP1 is rare in breast, prostate, gastric and colorectal cancers. APMIS : acta pathologica, microbiologica, et immunologica Scandinavica *120*, 855-856.

Jensen, D.E., Proctor, M., Marquis, S.T., Gardner, H.P., Ha, S.I., Chodosh, L.A., Ishov, A.M., Tommerup, N., Vissing, H., Sekido, Y.*, et al.* (1998). BAP1: a novel ubiquitin hydrolase which binds to the BRCA1 RING finger and enhances BRCA1-mediated cell growth suppression. Oncogene *16*, 1097-1112.

Ji, L., Minna, J.D., and Roth, J.A. (2005). 3p21.3 tumor suppressor cluster: prospects for translational applications. Future oncology *1*, 79-92.

Jin, J., Li, X., Gygi, S.P., and Harper, J.W. (2007). Dual E1 activation systems for ubiquitin differentially regulate E2 enzyme charging. Nature *447*, 1135-1138.

Johnston, S.C., Riddle, S.M., Cohen, R.E., and Hill, C.P. (1999). Structural basis for the specificity of ubiquitin C-terminal hydrolases. The EMBO journal *18*, 3877-3887.

Joo, H.Y., Zhai, L., Yang, C., Nie, S., Erdjument-Bromage, H., Tempst, P., Chang, C., and Wang, H. (2007). Regulation of cell cycle progression and gene expression by H2A deubiquitination. Nature *449*, 1068-1072.

Juan, A.H., Kumar, R.M., Marx, J.G., Young, R.A., and Sartorelli, V. (2009). Mir-214-dependent regulation of the polycomb protein Ezh2 in skeletal muscle and embryonic stem cells. Molecular cell *36*, 61-74.

Julien, E., and Herr, W. (2003). Proteolytic processing is necessary to separate and ensure proper cell growth and cytokinesis functions of HCF-1. The EMBO journal *22*, 2360-2369.

Julien, E., and Herr, W. (2004). A switch in mitotic histone H4 lysine 20 methylation status is linked to M phase defects upon loss of HCF-1. Molecular cell *14*, 713-725.

Kaneko, S., Li, G., Son, J., Xu, C.F., Margueron, R., Neubert, T.A., and Reinberg, D. (2010). Phosphorylation of the PRC2 component Ezh2 is cell cycle-regulated and up-regulates its binding to ncRNA. Genes & development *24*, 2615-2620.

Kennison, J.A. (1995). The Polycomb and trithorax group proteins of Drosophila: trans-regulators of homeotic gene function. Annual review of genetics *29*, 289-303.

Kerscher, O., Felberbaum, R., and Hochstrasser, M. (2006). Modification of proteins by ubiquitin and ubiquitin-like proteins. Annual review of cell and developmental biology *22*, 159-180.

Khorasanizadeh, S. (2004). The nucleosome: from genomic organization to genomic regulation. Cell *116*, 259-272.

Kimura, Y., and Tanaka, K. (2010). Regulatory mechanisms involved in the control of ubiquitin homeostasis. Journal of biochemistry *147*, 793-798.

Klemperer, N.S., Berleth, E.S., and Pickart, C.M. (1989). A novel, arsenite-sensitive E2 of the ubiquitin pathway: purification and properties. Biochemistry *28*, 6035-6041.

Klose, R.J., and Zhang, Y. (2007). Regulation of histone methylation by demethylimination and demethylation. Nature reviews. Molecular cell biology *8*, 307-318.

Klymenko, T., Papp, B., Fischle, W., Kocher, T., Schelder, M., Fritsch, C., Wild, B., Wilm, M., and Muller, J. (2006). A Polycomb group protein complex with sequence-specific DNA-binding and selective methyl-lysine-binding activities. Genes & development *20*, 1110-1122.

Kohli, R.M., and Zhang, Y. (2013). TET enzymes, TDG and the dynamics of DNA demethylation. Nature *502*, 472-479.

Kolas, N.K., Chapman, J.R., Nakada, S., Ylanko, J., Chahwan, R., Sweeney, F.D., Panier, S., Mendez, M., Wildenhain, J., Thomson, T.M.*, et al.* (2007). Orchestration of the DNA-damage response by the RNF8 ubiquitin ligase. Science *318*, 1637-1640.

Komander, D., Clague, M.J., and Urbe, S. (2009). Breaking the chains: structure and function of the deubiquitinases. Nature reviews. Molecular cell biology *10*, 550-563.

Kornberg, R.D. (1974). Chromatin structure: a repeating unit of histones and DNA. Science *184*, 868-871.

Koshland, D.E., Jr. (2002). Special essay. The seven pillars of life. Science *295*, 2215-2216.

Koundrioukoff, S., Polo, S., and Almouzni, G. (2004). Interplay between chromatin and cell cycle checkpoints in the context of ATR/ATM-dependent checkpoints. DNA repair *3*, 969-978.

Krebs, A.R., Karmodiya, K., Lindahl-Allen, M., Struhl, K., and Tora, L. (2011). SAGA and ATAC histone acetyl transferase complexes regulate distinct sets of genes and ATAC defines a class of p300-independent enhancers. Molecular cell *44*, 410-423.

Krogan, N.J., Dover, J., Khorrami, S., Greenblatt, J.F., Schneider, J., Johnston, M., and Shilatifard, A. (2002). COMPASS, a histone H3 (Lysine 4) methyltransferase required for telomeric silencing of gene expression. The Journal of biological chemistry *277*, 10753-10755.

Kruithof, M., Chien, F.T., Routh, A., Logie, C., Rhodes, D., and van Noort, J. (2009). Single-molecule force spectroscopy reveals a highly compliant helical folding for the 30-nm chromatin fiber. Nature structural & molecular biology *16*, 534-540.

Kulathu, Y., and Komander, D. (2012). Atypical ubiquitylation - the unexplored world of polyubiquitin beyond Lys48 and Lys63 linkages. Nature reviews. Molecular cell biology *13*, 508-523.

Kuzmichev, A., Nishioka, K., Erdjument-Bromage, H., Tempst, P., and Reinberg, D. (2002). Histone methyltransferase activity associated with a human multiprotein complex containing the Enhancer of Zeste protein. Genes & development *16*, 2893-2905.

la Cour, T., Kiemer, L., Molgaard, A., Gupta, R., Skriver, K., and Brunak, S. (2004). Analysis and prediction of leucine-rich nuclear export signals. Protein engineering, design & selection : PEDS *17*, 527-536.

Lagarou, A., Mohd-Sarip, A., Moshkin, Y.M., Chalkley, G.E., Bezstarosti, K., Demmers, J.A., and Verrijzer, C.P. (2008). dKDM2 couples histone H2A ubiquitylation to histone H3 demethylation during Polycomb group silencing. Genes & development *22*, 2799-2810.

Lairson, L.L., Henrissat, B., Davies, G.J., and Withers, S.G. (2008). Glycosyltransferases: structures, functions, and mechanisms. Annual review of biochemistry *77*, 521-555.

Landeira, D., Sauer, S., Poot, R., Dvorkina, M., Mazzarella, L., Jorgensen, H.F., Pereira, C.F., Leleu, M., Piccolo, F.M., Spivakov, M*., et al.* (2010). Jarid2 is a PRC2 component in embryonic stem cells required for multi-lineage differentiation and recruitment of PRC1 and RNA Polymerase II to developmental regulators. Nature cell biology *12*, 618-624.

Lanzuolo, C., and Orlando, V. (2012). Memories from the polycomb group proteins. Annual review of genetics *46*, 561-589.

Lazarus, M.B., Jiang, J., Kapuria, V., Bhuiyan, T., Janetzko, J., Zandberg, W.F., Vocadlo, D.J., Herr, W., and Walker, S. (2013). HCF-1 is cleaved in the active site of O-GlcNAc transferase. Science *342*, 1235-1239.

Lee, B.J., Cansizoglu, A.E., Suel, K.E., Louis, T.H., Zhang, Z., and Chook, Y.M. (2006). Rules for nuclear localization sequence recognition by karyopherin beta 2. Cell *126*, 543-558.

Lee, I., and Schindelin, H. (2008). Structural insights into E1-catalyzed ubiquitin activation and transfer to conjugating enzymes. Cell *134*, 268-278.

Lee, M.G., Villa, R., Trojer, P., Norman, J., Yan, K.P., Reinberg, D., Di Croce, L., and Shiekhattar, R. (2007). Demethylation of H3K27 regulates polycomb recruitment and H2A ubiquitination. Science *318*, 447-450.

Lelli, K.M., Slattery, M., and Mann, R.S. (2012). Disentangling the many layers of eukaryotic transcriptional regulation. Annual review of genetics *46*, 43-68.

Leonard, N., Chaggar, R., Jones, C., Takahashi, M., Nikitopoulou, A., and Lakhani, S.R. (2001). Loss of heterozygosity at cylindromatosis gene locus, CYLD, in sporadic skin adnexal tumours. Journal of clinical pathology *54*, 689-692.

Levine, S.S., Weiss, A., Erdjument-Bromage, H., Shao, Z., Tempst, P., and Kingston, R.E. (2002). The core of the polycomb repressive complex is compositionally and functionally conserved in flies and humans. Molecular and cellular biology *22*, 6070-6078.

Lewis, E.B. (1978). A gene complex controlling segmentation in Drosophila. Nature *276*, 565-570.

Li, M., Brooks, C.L., Wu-Baer, F., Chen, D., Baer, R., and Gu, W. (2003). Mono- versus polyubiquitination: differential control of p53 fate by Mdm2. Science *302*, 1972-1975.

Li, M.D., Ruan, H.B., Hughes, M.E., Lee, J.S., Singh, J.P., Jones, S.P., Nitabach, M.N., and Yang, X. (2013). O-GlcNAc signaling entrains the circadian clock by inhibiting BMAL1/CLOCK ubiquitination. Cell metabolism *17*, 303-310.

Li, X., Wang, S., Li, Y., Deng, C., Steiner, L.A., Xiao, H., Wu, C., Bungert, J., Gallagher, P.G., Felsenfeld, G.*, et al.* (2011). Chromatin boundaries require functional collaboration between the hSET1 and NURF complexes. Blood *118*, 1386-1394.

Liang, Y., Vogel, J.L., Narayanan, A., Peng, H., and Kristie, T.M. (2009). Inhibition of the histone demethylase LSD1 blocks alpha-herpesvirus lytic replication and reactivation from latency. Nature medicine *15*, 1312-1317.

Lieberman-Aiden, E., van Berkum, N.L., Williams, L., Imakaev, M., Ragoczy, T., Telling, A., Amit, I., Lajoie, B.R., Sabo, P.J., Dorschner, M.O.*, et al.* (2009). Comprehensive mapping of long-range interactions reveals folding principles of the human genome. Science *326*, 289-293.

Liu, C., van Dyk, D., Xu, P., Choe, V., Pan, H., Peng, J., Andrews, B., and Rao, H. (2010). Ubiquitin chain elongation enzyme Ufd2 regulates a subset of Doa10 substrates. The Journal of biological chemistry *285*, 10265-10272.

Liu, Y., Hengartner, M.O., and Herr, W. (1999). Selected elements of herpes simplex virus accessory factor HCF are highly conserved in Caenorhabditis elegans. Molecular and cellular biology *19*, 909-915.

Lowe, J., McDermott, H., Landon, M., Mayer, R.J., and Wilkinson, K.D. (1990). Ubiquitin carboxyl-terminal hydrolase (PGP 9.5) is selectively present in ubiquitinated inclusion bodies characteristic of human neurodegenerative diseases. The Journal of pathology *161*, 153-160.

Luger, K., Dechassa, M.L., and Tremethick, D.J. (2012). New insights into nucleosome and chromatin structure: an ordered state or a disordered affair? Nature reviews. Molecular cell biology *13*, 436-447.

Luger, K., and Hansen, J.C. (2005). Nucleosome and chromatin fiber dynamics. Current opinion in structural biology *15*, 188-196.

Luger, K., Mader, A.W., Richmond, R.K., Sargent, D.F., and Richmond, T.J. (1997). Crystal structure of the nucleosome core particle at 2.8 A resolution. Nature *389*, 251-260.

Lynch, V.J., and Wagner, G.P. (2009). Multiple chromosomal rearrangements structured the ancestral vertebrate Hox-bearing protochromosomes. PLoS genetics *5*, e1000349.

Ma, Z., and Vosseller, K. (2013). O-GlcNAc in cancer biology. Amino acids *45*, 719-733.

Machida, Y.J., Machida, Y., Vashisht, A.A., Wohlschlegel, J.A., and Dutta, A. (2009). The deubiquitinating enzyme BAP1 regulates cell growth via interaction with HCF-1. The Journal of biological chemistry *284*, 34179-34188.

Mahajan, S.S., and Wilson, A.C. (2000). Mutations in host cell factor 1 separate its role in cell proliferation from recruitment of VP16 and LZIP. Molecular and cellular biology *20*, 919-928.

Mailand, N., Bekker-Jensen, S., Faustrup, H., Melander, F., Bartek, J., Lukas, C., and Lukas, J. (2007). RNF8 ubiquitylates histones at DNA double-strand breaks and promotes assembly of repair proteins. Cell *131*, 887-900.

Mak, W., Baxter, J., Silva, J., Newall, A.E., Otte, A.P., and Brockdorff, N. (2002). Mitotically stable association of polycomb group proteins eed and enx1 with the inactive x chromosome in trophoblast stem cells. Current biology : CB *12*, 1016-1020.

Margueron, R., Justin, N., Ohno, K., Sharpe, M.L., Son, J., Drury, W.J., 3rd, Voigt, P., Martin, S.R., Taylor, W.R., De Marco, V*., et al.* (2009). Role of the polycomb protein EED in the propagation of repressive histone marks. Nature *461*, 762-767.

Margueron, R., Li, G., Sarma, K., Blais, A., Zavadil, J., Woodcock, C.L., Dynlacht, B.D., and Reinberg, D. (2008). Ezh1 and Ezh2 maintain repressive chromatin through different mechanisms. Molecular cell *32*, 503-518.

Margueron, R., and Reinberg, D. (2011). The Polycomb complex PRC2 and its mark in life. Nature *469*, 343-349.

Marshall, S., Bacote, V., and Traxinger, R.R. (1991). Discovery of a metabolic pathway mediating glucose-induced desensitization of the glucose transport system. Role of hexosamine biosynthesis in the induction of insulin resistance. The Journal of biological chemistry *266*, 4706-4712.

Martinez-Fleites, C., Macauley, M.S., He, Y., Shen, D.L., Vocadlo, D.J., and Davies, G.J. (2008). Structure of an O-GlcNAc transferase homolog provides insight into intracellular glycosylation. Nature structural & molecular biology *15*, 764-765.

Mashtalir, N., Daou, S., Barbour, H., Sen, N.N., Gagnon, J., Hammond-Martel, I., Dar, H.H., Therrien, M., and Affar, E.B. (2014). Autodeubiquitination Protects the Tumor

Suppressor BAP1 from Cytoplasmic Sequestration Mediated by the Atypical Ubiquitin Ligase UBE2O. Molecular cell.

Mattiroli, F., Vissers, J.H., van Dijk, W.J., Ikpa, P., Citterio, E., Vermeulen, W., Marteijn, J.A., and Sixma, T.K. (2012). RNF168 ubiquitinates K13-15 on H2A/H2AX to drive DNA damage signaling. Cell *150*, 1182-1195.

Mazars, R., Gonzalez-de-Peredo, A., Cayrol, C., Lavigne, A.C., Vogel, J.L., Ortega, N., Lacroix, C., Gautier, V., Huet, G., Ray, A.*, et al.* (2010). The THAP-zinc finger protein THAP1 associates with coactivator HCF-1 and O-GlcNAc transferase: a link between DYT6 and DYT3 dystonias. The Journal of biological chemistry *285*, 13364-13371.

McDonough, H., and Patterson, C. (2003). CHIP: a link between the chaperone and proteasome systems. Cell stress & chaperones *8*, 303-308.

McGinnis, W., Garber, R.L., Wirz, J., Kuroiwa, A., and Gehring, W.J. (1984a). A homologous protein-coding sequence in Drosophila homeotic genes and its conservation in other metazoans. Cell *37*, 403-408.

McGinnis, W., Levine, M.S., Hafen, E., Kuroiwa, A., and Gehring, W.J. (1984b). A conserved DNA sequence in homoeotic genes of the Drosophila Antennapedia and bithorax complexes. Nature *308*, 428-433.

Meray, R.K., and Lansbury, P.T., Jr. (2007). Reversible monoubiquitination regulates the Parkinson disease-associated ubiquitin hydrolase UCH-L1. The Journal of biological chemistry *282*, 10567-10575.

Mevissen, T.E., Hospenthal, M.K., Geurink, P.P., Elliott, P.R., Akutsu, M., Arnaudo, N., Ekkebus, R., Kulathu, Y., Wauer, T., El Oualid, F.*, et al.* (2013). OTU deubiquitinases reveal mechanisms of linkage specificity and enable ubiquitin chain restriction analysis. Cell *154*, 169-184.

Meyer, H., Bug, M., and Bremer, S. (2012). Emerging functions of the VCP/p97 AAA-ATPase in the ubiquitin system. Nature cell biology *14*, 117-123.

Misaghi, S., Ottosen, S., Izrael-Tomasevic, A., Arnott, D., Lamkanfi, M., Lee, J., Liu, J., O'Rourke, K., Dixit, V.M., and Wilson, A.C. (2009). Association of C-terminal ubiquitin hydrolase BRCA1-associated protein 1 with cell cycle regulator host cell factor 1. Molecular and cellular biology *29*, 2181-2192.

Mohan, M., Lin, C., Guest, E., and Shilatifard, A. (2010). Licensed to elongate: a molecular mechanism for MLL-based leukaemogenesis. Nature reviews. Cancer *10*, 721-728.

Morizane, Y., Honda, R., Fukami, K., and Yasuda, H. (2005). X-linked inhibitor of apoptosis functions as ubiquitin ligase toward mature caspase-9 and cytosolic Smac/DIABLO. Journal of biochemistry *137*, 125-132.

Morrison, A.J., and Shen, X. (2009). Chromatin remodelling beyond transcription: the INO80 and SWR1 complexes. Nature reviews. Molecular cell biology *10*, 373-384.

Mousavi, K., Zare, H., Wang, A.H., and Sartorelli, V. (2012). Polycomb protein Ezh1 promotes RNA polymerase II elongation. Molecular cell *45*, 255-262.

Mueller, R.D., Yasuda, H., Hatch, C.L., Bonner, W.M., and Bradbury, E.M. (1985). Identification of ubiquitinated histones 2A and 2B in Physarum polycephalum. Disappearance of these proteins at metaphase and reappearance at anaphase. The Journal of biological chemistry *260*, 5147-5153.

Muller, J., and Kassis, J.A. (2006). Polycomb response elements and targeting of Polycomb group proteins in Drosophila. Current opinion in genetics & development *16*, 476-484.

Myers, S.A., Daou, S., Affar el, B., and Burlingame, A. (2013). Electron transfer dissociation (ETD): the mass spectrometric breakthrough essential for O-GlcNAc protein

site assignments-a study of the O-GlcNAcylated protein host cell factor C1. Proteomics *13*, 982-991.

Nagase, T., Kikuno, R., Hattori, A., Kondo, Y., Okumura, K., and Ohara, O. (2000). Prediction of the coding sequences of unidentified human genes. XIX. The complete sequences of 100 new cDNA clones from brain which code for large proteins in vitro. DNA research : an international journal for rapid publication of reports on genes and genomes *7*, 347-355.

Nakagawa, T., Kajitani, T., Togo, S., Masuko, N., Ohdan, H., Hishikawa, Y., Koji, T., Matsuyama, T., Ikura, T., Muramatsu, M.*, et al.* (2008). Deubiquitylation of histone H2A activates transcriptional initiation via trans-histone cross-talk with H3K4 di- and trimethylation. Genes & development *22*, 37-49.

Nakayama, K.I., and Nakayama, K. (2006). Ubiquitin ligases: cell-cycle control and cancer. Nature reviews. Cancer *6*, 369-381.

Narlikar, G.J., Sundaramoorthy, R., and Owen-Hughes, T. (2013). Mechanisms and functions of ATP-dependent chromatin-remodeling enzymes. Cell *154*, 490-503.

Nekrasov, M., Klymenko, T., Fraterman, S., Papp, B., Oktaba, K., Kocher, T., Cohen, A., Stunnenberg, H.G., Wilm, M., and Muller, J. (2007). Pcl-PRC2 is needed to generate high levels of H3-K27 trimethylation at Polycomb target genes. The EMBO journal *26*, 4078-4088.

Ng, H.H., Robert, F., Young, R.A., and Struhl, K. (2003). Targeted recruitment of Set1 histone methylase by elongating Pol II provides a localized mark and memory of recent transcriptional activity. Molecular cell *11*, 709-719.

Nishikawa, H., Wu, W., Koike, A., Kojima, R., Gomi, H., Fukuda, M., and Ohta, T. (2009). BRCA1-associated protein 1 interferes with BRCA1/BARD1 RING heterodimer activity. Cancer research *69*, 111-119.

Nishino, Y., Eltsov, M., Joti, Y., Ito, K., Takata, H., Takahashi, Y., Hihara, S., Frangakis, A.S., Imamoto, N., Ishikawa, T.*, et al.* (2012). Human mitotic chromosomes consist predominantly of irregularly folded nucleosome fibres without a 30-nm chromatin structure. The EMBO journal *31*, 1644-1653.

Noordermeer, D., Leleu, M., Splinter, E., Rougemont, J., De Laat, W., and Duboule, D. (2011). The dynamic architecture of Hox gene clusters. Science *334*, 222-225.

Oberdoerffer, P., and Sinclair, D.A. (2007). The role of nuclear architecture in genomic instability and ageing. Nature reviews. Molecular cell biology *8*, 692-702.

Ogawa, H., Ishiguro, K., Gaubatz, S., Livingston, D.M., and Nakatani, Y. (2002). A complex with chromatin modifiers that occupies E2F- and Myc-responsive genes in G0 cells. Science *296*, 1132-1136.

Ohta, T., Sato, K., and Wu, W. (2011). The BRCA1 ubiquitin ligase and homologous recombination repair. FEBS letters *585*, 2836-2844.

Olins, A.L., and Olins, D.E. (1974). Spheroid chromatin units (v bodies). Science *183*, 330-332.

Olins, D.E., and Olins, A.L. (2003). Chromatin history: our view from the bridge. Nature reviews. Molecular cell biology *4*, 809-814.

Olsen, J.V., Vermeulen, M., Santamaria, A., Kumar, C., Miller, M.L., Jensen, L.J., Gnad, F., Cox, J., Jensen, T.S., Nigg, E.A.*, et al.* (2010). Quantitative phosphoproteomics reveals widespread full phosphorylation site occupancy during mitosis. Science signaling *3*, ra3.

Oudet, P., Gross-Bellard, M., and Chambon, P. (1975). Electron microscopic and biochemical evidence that chromatin structure is a repeating unit. Cell *4*, 281-300.

Park, J., Lammers, F., Herr, W., and Song, J.J. (2012). HCF-1 self-association via an interdigitated Fn3 structure facilitates transcriptional regulatory complex formation. Proceedings of the National Academy of Sciences of the United States of America *109*, 17430-17435.

Parker, J.L., and Ulrich, H.D. (2009). Mechanistic analysis of PCNA poly-ubiquitylation by the ubiquitin protein ligases Rad18 and Rad5. The EMBO journal *28*, 3657-3666.

Parthun, M.R. (2007). Hat1: the emerging cellular roles of a type B histone acetyltransferase. Oncogene *26*, 5319-5328.

Pasini, D., Cloos, P.A., Walfridsson, J., Olsson, L., Bukowski, J.P., Johansen, J.V., Bak, M., Tommerup, N., Rappsilber, J., and Helin, K. (2010). JARID2 regulates binding of the Polycomb repressive complex 2 to target genes in ES cells. Nature *464*, 306-310.

Patel, D.J., and Wang, Z. (2013). Readout of epigenetic modifications. Annual review of biochemistry *82*, 81-118.

Pearson, J.C., Lemons, D., and McGinnis, W. (2005). Modulating Hox gene functions during animal body patterning. Nature reviews. Genetics *6*, 893-904.

Pena-Llopis, S., Vega-Rubin-de-Celis, S., Liao, A., Leng, N., Pavia-Jimenez, A., Wang, S., Yamasaki, T., Zhrebker, L., Sivanand, S., Spence, P.*, et al.* (2012). BAP1 loss defines a new class of renal cell carcinoma. Nature genetics *44*, 751-759.

Pendleton, J.W., Nagai, B.K., Murtha, M.T., and Ruddle, F.H. (1993). Expansion of the Hox gene family and the evolution of chordates. Proceedings of the National Academy of Sciences of the United States of America *90*, 6300-6304.

Peng, H., Nogueira, M.L., Vogel, J.L., and Kristie, T.M. (2010). Transcriptional coactivator HCF-1 couples the histone chaperone Asf1b to HSV-1 DNA replication components. Proceedings of the National Academy of Sciences of the United States of America *107*, 2461-2466.

Perez-Cabrera, A., Kofman-Alfaro, S., and Zenteno, J.C. (2002). Mutational analysis of HOXD13 and HOXA13 genes in the triphalangeal thumb-brachyectrodactyly syndrome. Journal of orthopaedic research : official publication of the Orthopaedic Research Society *20*, 899-901.

Pickart, C.M. (2004). Back to the future with ubiquitin. Cell *116*, 181-190.

Piluso, D., Bilan, P., and Capone, J.P. (2002). Host cell factor-1 interacts with and antagonizes transactivation by the cell cycle regulatory factor Miz-1. The Journal of biological chemistry *277*, 46799-46808.

Plafker, S.M., Plafker, K.S., Weissman, A.M., and Macara, I.G. (2004). Ubiquitin charging of human class III ubiquitin-conjugating enzymes triggers their nuclear import. The Journal of cell biology *167*, 649-659.

Pohl, C., and Jentsch, S. (2008). Final stages of cytokinesis and midbody ring formation are controlled by BRUCE. Cell *132*, 832-845.

Pontarotti, P. (2009). Evolutionary biology : concept, modeling, and application (Dordrecht Netherlands ; London ; New York: Springer).

Postow, L., Hardy, C.D., Arsuaga, J., and Cozzarelli, N.R. (2004). Topological domain structure of the Escherichia coli chromosome. Genes & development *18*, 1766-1779.

Qin, S., and Parthun, M.R. (2002). Histone H3 and the histone acetyltransferase Hat1p contribute to DNA double-strand break repair. Molecular and cellular biology *22*, 8353-8365.

Raina, D., Pandey, P., Ahmad, R., Bharti, A., Ren, J., Kharbanda, S., Weichselbaum, R., and Kufe, D. (2005). c-Abl tyrosine kinase regulates caspase-9 autocleavage in the apoptotic response to DNA damage. The Journal of biological chemistry *280*, 11147-11151.

Ravid, T., and Hochstrasser, M. (2008). Diversity of degradation signals in the ubiquitin-proteasome system. Nature reviews. Molecular cell biology *9*, 679-690.

Ren, B., Robert, F., Wyrick, J.J., Aparicio, O., Jennings, E.G., Simon, I., Zeitlinger, J., Schreiber, J., Hannett, N., Kanin, E.*, et al.* (2000). Genome-wide location and function of DNA binding proteins. Science *290*, 2306-2309.

Renatus, M., Stennicke, H.R., Scott, F.L., Liddington, R.C., and Salvesen, G.S. (2001). Dimer formation drives the activation of the cell death protease caspase 9. Proceedings of the National Academy of Sciences of the United States of America *98*, 14250-14255.

Reyes-Turcu, F.E., Horton, J.R., Mullally, J.E., Heroux, A., Cheng, X., and Wilkinson, K.D. (2006). The ubiquitin binding domain ZnF UBP recognizes the C-terminal diglycine motif of unanchored ubiquitin. Cell *124*, 1197-1208.

Rinn, J.L., Kertesz, M., Wang, J.K., Squazzo, S.L., Xu, X., Brugmann, S.A., Goodnough, L.H., Helms, J.A., Farnham, P.J., Segal, E.*, et al.* (2007). Functional demarcation of active and silent chromatin domains in human HOX loci by noncoding RNAs. Cell *129*, 1311-1323.

Rotin, D., and Kumar, S. (2009). Physiological functions of the HECT family of ubiquitin ligases. Nature reviews. Molecular cell biology *10*, 398-409.

Ruan, H.B., Han, X., Li, M.D., Singh, J.P., Qian, K., Azarhoush, S., Zhao, L., Bennett, A.M., Samuel, V.T., Wu, J.*, et al.* (2012). O-GlcNAc transferase/host cell factor C1 complex regulates gluconeogenesis by modulating PGC-1alpha stability. Cell metabolism *16*, 226-237.

Ruthenburg, A.J., Li, H., Patel, D.J., and Allis, C.D. (2007). Multivalent engagement of chromatin modifications by linked binding modules. Nature reviews. Molecular cell biology *8*, 983-994.

Sakabe, K., Wang, Z., and Hart, G.W. (2010). Beta-N-acetylglucosamine (O-GlcNAc) is part of the histone code. Proceedings of the National Academy of Sciences of the United States of America *107*, 19915-19920.

Sakaidani, Y., Nomura, T., Matsuura, A., Ito, M., Suzuki, E., Murakami, K., Nadano, D., Matsuda, T., Furukawa, K., and Okajima, T. (2011). O-linked-N-acetylglucosamine on extracellular protein domains mediates epithelial cell-matrix interactions. Nature communications *2*, 583.

Sato, Y., Yoshikawa, A., Yamagata, A., Mimura, H., Yamashita, M., Ookata, K., Nureki, O., Iwai, K., Komada, M., and Fukai, S. (2008). Structural basis for specific cleavage of Lys 63-linked polyubiquitin chains. Nature *455*, 358-362.

Scarr, R.B., and Sharp, P.A. (2002). PDCD2 is a negative regulator of HCF-1 (C1). Oncogene *21*, 5245-5254.

Schalch, T., Duda, S., Sargent, D.F., and Richmond, T.J. (2005). X-ray structure of a tetranucleosome and its implications for the chromatin fibre. Nature *436*, 138-141.

Scheuermann, J.C., de Ayala Alonso, A.G., Oktaba, K., Ly-Hartig, N., McGinty, R.K., Fraterman, S., Wilm, M., Muir, T.W., and Muller, J. (2010). Histone H2A deubiquitinase activity of the Polycomb repressive complex PR-DUB. Nature *465*, 243-247.

Schoeftner, S., Sengupta, A.K., Kubicek, S., Mechtler, K., Spahn, L., Koseki, H., Jenuwein, T., and Wutz, A. (2006). Recruitment of PRC1 function at the initiation of X inactivation independent of PRC2 and silencing. The EMBO journal *25*, 3110-3122.

Schuettengruber, B., Chourrout, D., Vervoort, M., Leblanc, B., and Cavalli, G. (2007). Genome regulation by polycomb and trithorax proteins. Cell *128*, 735-745.

Schummer, M., Scheurlen, I., Schaller, C., and Galliot, B. (1992). HOM/HOX homeobox genes are present in hydra (Chlorohydra viridissima) and are differentially expressed during regeneration. The EMBO journal *11*, 1815-1823.

Scott, M.P., and Weiner, A.J. (1984). Structural relationships among genes that control development: sequence homology between the Antennapedia, Ultrabithorax, and fushi tarazu loci of Drosophila. Proceedings of the National Academy of Sciences of the United States of America *81*, 4115-4119.

Scott, M.P., Weiner, A.J., Hazelrigg, T.I., Polisky, B.A., Pirrotta, V., Scalenghe, F., and Kaufman, T.C. (1983). The molecular organization of the Antennapedia locus of Drosophila. Cell *35*, 763-776.

Sealfon, S.C., and Chu, T.T. (2011). RNA and DNA microarrays. Methods in molecular biology *671*, 3-34.

Sedkov, Y., Cho, E., Petruk, S., Cherbas, L., Smith, S.T., Jones, R.S., Cherbas, P., Canaani, E., Jaynes, J.B., and Mazo, A. (2003). Methylation at lysine 4 of histone H3 in ecdysone-dependent development of Drosophila. Nature *426*, 78-83.

Senior, M.B., Olins, A.L., and Olins, D.E. (1975). Chromatin fragments resembling v bodies. Science *187*, 173-175.

Shah, N., and Sukumar, S. (2010). The Hox genes and their roles in oncogenesis. Nature reviews. Cancer *10*, 361-371.

Shahbazian, M.D., and Grunstein, M. (2007). Functions of site-specific histone acetylation and deacetylation. Annual review of biochemistry *76*, 75-100.

Shen, X., Kim, W., Fujiwara, Y., Simon, M.D., Liu, Y., Mysliwiec, M.R., Yuan, G.C., Lee, Y., and Orkin, S.H. (2009). Jumonji modulates polycomb activity and self-renewal versus differentiation of stem cells. Cell *139*, 1303-1314.

Shen, X., Liu, Y., Hsu, Y.J., Fujiwara, Y., Kim, J., Mao, X., Yuan, G.C., and Orkin, S.H. (2008). EZH1 mediates methylation on histone H3 lysine 27 and complements EZH2 in maintaining stem cell identity and executing pluripotency. Molecular cell *32*, 491-502.

Shenk, M.A., Bode, H.R., and Steele, R.E. (1993). Expression of Cnox-2, a HOM/HOX homeobox gene in hydra, is correlated with axial pattern formation. Development *117*, 657-667.

Shi, Y., Lee, J.S., and Galvin, K.M. (1997). Everything you have ever wanted to know about Yin Yang 1. Biochimica et biophysica acta *1332*, F49-66.

Shilatifard, A. (2006). Chromatin modifications by methylation and ubiquitination: implications in the regulation of gene expression. Annual review of biochemistry *75*, 243-269.

Shilatifard, A. (2008). Molecular implementation and physiological roles for histone H3 lysine 4 (H3K4) methylation. Current opinion in cell biology *20*, 341-348.

Silva, J., Mak, W., Zvetkova, I., Appanah, R., Nesterova, T.B., Webster, Z., Peters, A.H., Jenuwein, T., Otte, A.P., and Brockdorff, N. (2003). Establishment of histone h3

methylation on the inactive X chromosome requires transient recruitment of Eed-Enx1 polycomb group complexes. Developmental cell *4*, 481-495.

Sinclair, D.A., Syrzycka, M., Macauley, M.S., Rastgardani, T., Komljenovic, I., Vocadlo, D.J., Brock, H.W., and Honda, B.M. (2009). Drosophila O-GlcNAc transferase (OGT) is encoded by the Polycomb group (PcG) gene, super sex combs (sxc). Proceedings of the National Academy of Sciences of the United States of America *106*, 13427-13432.

Sing, A., Pannell, D., Karaiskakis, A., Sturgeon, K., Djabali, M., Ellis, J., Lipshitz, H.D., and Cordes, S.P. (2009). A vertebrate Polycomb response element governs segmentation of the posterior hindbrain. Cell *138*, 885-897.

Smith, E.R., Cayrou, C., Huang, R., Lane, W.S., Cote, J., and Lucchesi, J.C. (2005). A human protein complex homologous to the Drosophila MSL complex is responsible for the majority of histone H4 acetylation at lysine 16. Molecular and cellular biology *25*, 9175-9188.

Sowa, M.E., Bennett, E.J., Gygi, S.P., and Harper, J.W. (2009). Defining the human deubiquitinating enzyme interaction landscape. Cell *138*, 389-403.

Spedale, G., Timmers, H.T., and Pijnappel, W.W. (2012). ATAC-king the complexity of SAGA during evolution. Genes & development *26*, 527-541.

Stewart, G.S., Panier, S., Townsend, K., Al-Hakim, A.K., Kolas, N.K., Miller, E.S., Nakada, S., Ylanko, J., Olivarius, S., Mendez, M.*, et al.* (2009). The RIDDLE syndrome protein mediates a ubiquitin-dependent signaling cascade at sites of DNA damage. Cell *136*, 420-434.

Stock, J.K., Giadrossi, S., Casanova, M., Brookes, E., Vidal, M., Koseki, H., Brockdorff, N., Fisher, A.G., and Pombo, A. (2007). Ring1-mediated ubiquitination of H2A restrains

poised RNA polymerase II at bivalent genes in mouse ES cells. Nature cell biology *9*, 1428-1435.

Stojic, L., Jasencakova, Z., Prezioso, C., Stutzer, A., Bodega, B., Pasini, D., Klingberg, R., Mozzetta, C., Margueron, R., Puri, P.L.*, et al.* (2011). Chromatin regulated interchange between polycomb repressive complex 2 (PRC2)-Ezh2 and PRC2-Ezh1 complexes controls myogenin activation in skeletal muscle cells. Epigenetics & chromatin *4*, 16.

Strahl, B.D., and Allis, C.D. (2000). The language of covalent histone modifications. Nature *403*, 41-45.

Tan, M., Luo, H., Lee, S., Jin, F., Yang, J.S., Montellier, E., Buchou, T., Cheng, Z., Rousseaux, S., Rajagopal, N.*, et al.* (2011). Identification of 67 histone marks and histone lysine crotonylation as a new type of histone modification. Cell *146*, 1016-1028.

Tavares, L., Dimitrova, E., Oxley, D., Webster, J., Poot, R., Demmers, J., Bezstarosti, K., Taylor, S., Ura, H., Koide, H.*, et al.* (2012). RYBP-PRC1 complexes mediate H2A ubiquitylation at polycomb target sites independently of PRC2 and H3K27me3. Cell *148*, 664-678.

Testa, J.R., Cheung, M., Pei, J., Below, J.E., Tan, Y., Sementino, E., Cox, N.J., Dogan, A.U., Pass, H.I., Trusa, S.*, et al.* (2011). Germline BAP1 mutations predispose to malignant mesothelioma. Nature genetics *43*, 1022-1025.

Tomko, R.J., Jr., and Hochstrasser, M. (2013). Molecular architecture and assembly of the eukaryotic proteasome. Annual review of biochemistry *82*, 415-445.

Tong, Z.T., Cai, M.Y., Wang, X.G., Kong, L.L., Mai, S.J., Liu, Y.H., Zhang, H.B., Liao, Y.J., Zheng, F., Zhu, W.*, et al.* (2012). EZH2 supports nasopharyngeal carcinoma cell aggressiveness by forming a co-repressor complex with HDAC1/HDAC2 and Snail to inhibit E-cadherin. Oncogene *31*, 583-594.

Trojer, P., Cao, A.R., Gao, Z., Li, Y., Zhang, J., Xu, X., Li, G., Losson, R., Erdjument-Bromage, H., Tempst, P.*, et al.* (2011). L3MBTL2 protein acts in concert with PcG protein-mediated monoubiquitination of H2A to establish a repressive chromatin structure. Molecular cell *42*, 438-450.

Tsou, W.L., Burr, A.A., Ouyang, M., Blount, J.R., Scaglione, K.M., and Todi, S.V. (2013). Ubiquitination regulates the neuroprotective function of the deubiquitinase ataxin-3 in vivo. The Journal of biological chemistry *288*, 34460-34469.

Tuskan, G.A., Difazio, S., Jansson, S., Bohlmann, J., Grigoriev, I., Hellsten, U., Putnam, N., Ralph, S., Rombauts, S., Salamov, A.*, et al.* (2006). The genome of black cottonwood, Populus trichocarpa (Torr. & Gray). Science *313*, 1596-1604.

Tyagi, S., Chabes, A.L., Wysocka, J., and Herr, W. (2007). E2F activation of S phase promoters via association with HCF-1 and the MLL family of histone H3K4 methyltransferases. Molecular cell *27*, 107-119.

van der Veen, A.G., and Ploegh, H.L. (2012). Ubiquitin-like proteins. Annual review of biochemistry *81*, 323-357.

van Wijk, S.J., and Timmers, H.T. (2010). The family of ubiquitin-conjugating enzymes (E2s): deciding between life and death of proteins. FASEB journal : official publication of the Federation of American Societies for Experimental Biology *24*, 981-993.

Varshavsky, A. (2006). The early history of the ubiquitin field. Protein science : a publication of the Protein Society *15*, 647-654.

Venter, J.C., Adams, M.D., Myers, E.W., Li, P.W., Mural, R.J., Sutton, G.G., Smith, H.O., Yandell, M., Evans, C.A., Holt, R.A.*, et al.* (2001). The sequence of the human genome. Science *291*, 1304-1351.

Ventii, K.H., Devi, N.S., Friedrich, K.L., Chernova, T.A., Tighiouart, M., Van Meir, E.G., and Wilkinson, K.D. (2008). BRCA1-associated protein-1 is a tumor suppressor that requires deubiquitinating activity and nuclear localization. Cancer research *68*, 6953-6962.

Vercauteren, K., Gleyzer, N., and Scarpulla, R.C. (2008). PGC-1-related coactivator complexes with HCF-1 and NRF-2beta in mediating NRF-2(GABP)-dependent respiratory gene expression. The Journal of biological chemistry *283*, 12102-12111.

Vogel, J.L., and Kristie, T.M. (2000a). Autocatalytic proteolysis of the transcription factor-coactivator C1 (HCF): a potential role for proteolytic regulation of coactivator function. Proceedings of the National Academy of Sciences of the United States of America *97*, 9425-9430.

Vogel, J.L., and Kristie, T.M. (2000b). The novel coactivator C1 (HCF) coordinates multiprotein enhancer formation and mediates transcription activation by GABP. The EMBO journal *19*, 683-690.

Vogel, J.L., and Kristie, T.M. (2006). Site-specific proteolysis of the transcriptional coactivator HCF-1 can regulate its interaction with protein cofactors. Proceedings of the National Academy of Sciences of the United States of America *103*, 6817-6822.

Wadt, K., Choi, J., Chung, J.Y., Kiilgaard, J., Heegaard, S., Drzewiecki, K.T., Trent, J.M., Hewitt, S.M., Hayward, N.K., Gerdes, A.M.*, et al.* (2012). A cryptic BAP1 splice mutation in a family with uveal and cutaneous melanoma, and paraganglioma. Pigment cell & melanoma research *25*, 815-818.

Wang, H., Wang, L., Erdjument-Bromage, H., Vidal, M., Tempst, P., Jones, R.S., and Zhang, Y. (2004). Role of histone H2A ubiquitination in Polycomb silencing. Nature *431*, 873-878.

Wang, S., Huang, X., Sun, D., Xin, X., Pan, Q., Peng, S., Liang, Z., Luo, C., Yang, Y., Jiang, H.*, et al.* (2012). Extensive crosstalk between O-GlcNAcylation and phosphorylation regulates Akt signaling. PloS one *7*, e37427.

Wang, Z., Udeshi, N.D., Slawson, C., Compton, P.D., Sakabe, K., Cheung, W.D., Shabanowitz, J., Hunt, D.F., and Hart, G.W. (2010). Extensive crosstalk between O-GlcNAcylation and phosphorylation regulates cytokinesis. Science signaling *3*, ra2.

Watson, J.D., and Crick, F.H. (1953). Molecular structure of nucleic acids; a structure for deoxyribose nucleic acid. Nature *171*, 737-738.

Wefes, I., Mastrandrea, L.D., Haldeman, M., Koury, S.T., Tamburlin, J., Pickart, C.M., and Finley, D. (1995). Induction of ubiquitin-conjugating enzymes during terminal erythroid differentiation. Proceedings of the National Academy of Sciences of the United States of America *92*, 4982-4986.

Weiler, K.S., and Wakimoto, B.T. (1995). Heterochromatin and gene expression in Drosophila. Annual review of genetics *29*, 577-605.

Wellik, D.M. (2009). Hox genes and vertebrate axial pattern. Current topics in developmental biology *88*, 257-278.

Wells, J. (2011). The myth of junk DNA, 1st edn (Seattle, WA: Discovery Institute Press).

Wells, L., Vosseller, K., and Hart, G.W. (2001). Glycosylation of nucleocytoplasmic proteins: signal transduction and O-GlcNAc. Science *291*, 2376-2378.

Wertz, I.E., O'Rourke, K.M., Zhou, H., Eby, M., Aravind, L., Seshagiri, S., Wu, P., Wiesmann, C., Baker, R., Boone, D.L.*, et al.* (2004). De-ubiquitination and ubiquitin ligase domains of A20 downregulate NF-kappaB signalling. Nature *430*, 694-699.

Wiesner, T., Murali, R., Fried, I., Cerroni, L., Busam, K., Kutzner, H., and Bastian, B.C. (2012). A distinct subset of atypical Spitz tumors is characterized by BRAF mutation and loss of BAP1 expression. The American journal of surgical pathology *36*, 818-830.

Wiesner, T., Obenauf, A.C., Murali, R., Fried, I., Griewank, K.G., Ulz, P., Windpassinger, C., Wackernagel, W., Loy, S., Wolf, I.*, et al.* (2011). Germline mutations in BAP1 predispose to melanocytic tumors. Nature genetics *43*, 1018-1021.

Wilkinson, F., Pratt, H., and Atchison, M.L. (2010). PcG recruitment by the YY1 REPO domain can be mediated by Yaf2. Journal of cellular biochemistry *109*, 478-486.

Wilkinson, K.D. (2005). The discovery of ubiquitin-dependent proteolysis. Proceedings of the National Academy of Sciences of the United States of America *102*, 15280-15282.

Williams, S.A., Maecker, H.L., French, D.M., Liu, J., Gregg, A., Silverstein, L.B., Cao, T.C., Carano, R.A., and Dixit, V.M. (2011). USP1 deubiquitinates ID proteins to preserve a mesenchymal stem cell program in osteosarcoma. Cell *146*, 918-930.

Wilson, A.C., Boutros, M., Johnson, K.M., and Herr, W. (2000). HCF-1 amino- and carboxy-terminal subunit association through two separate sets of interaction modules: involvement of fibronectin type 3 repeats. Molecular and cellular biology *20*, 6721-6730.

Wilson, A.C., LaMarco, K., Peterson, M.G., and Herr, W. (1993). The VP16 accessory protein HCF is a family of polypeptides processed from a large precursor protein. Cell *74*, 115-125.

Wilson, A.C., Peterson, M.G., and Herr, W. (1995). The HCF repeat is an unusual proteolytic cleavage signal. Genes & development *9*, 2445-2458.

Wong, J.T., New, D.C., Wong, J.C., and Hung, V.K. (2003). Histone-like proteins of the dinoflagellate Crypthecodinium cohnii have homologies to bacterial DNA-binding proteins. Eukaryotic cell *2*, 646-650.

Woo, C.J., Kharchenko, P.V., Daheron, L., Park, P.J., and Kingston, R.E. (2010). A region of the human HOXD cluster that confers polycomb-group responsiveness. Cell *140*, 99-110.

Wu, K., Kovacev, J., and Pan, Z.Q. (2010). Priming and extending: a UbcH5/Cdc34 E2 handoff mechanism for polyubiquitination on a SCF substrate. Molecular cell *37*, 784-796.

Wu, K., Yan, H., Fang, L., Wang, X., Pfleger, C., Jiang, X., Huang, L., and Pan, Z.Q. (2011). Mono-ubiquitination drives nuclear export of the human DCN1-like protein hDCNL1. The Journal of biological chemistry *286*, 34060-34070.

Wu, S., Shi, Y., Mulligan, P., Gay, F., Landry, J., Liu, H., Lu, J., Qi, H.H., Wang, W., Nickoloff, J.A.*, et al.* (2007). A YY1-INO80 complex regulates genomic stability through homologous recombination-based repair. Nature structural & molecular biology *14*, 1165-1172.

Wu, X., Johansen, J.V., and Helin, K. (2013). Fbxl10/Kdm2b recruits polycomb repressive complex 1 to CpG islands and regulates H2A ubiquitylation. Molecular cell *49*, 1134-1146.

Wysocka, J., and Herr, W. (2003). The herpes simplex virus VP16-induced complex: the makings of a regulatory switch. Trends in biochemical sciences *28*, 294-304.

Wysocka, J., Myers, M.P., Laherty, C.D., Eisenman, R.N., and Herr, W. (2003). Human Sin3 deacetylase and trithorax-related Set1/Ash2 histone H3-K4 methyltransferase are tethered together selectively by the cell-proliferation factor HCF-1. Genes & development *17*, 896-911.

Xi, H., Yu, Y., Fu, Y., Foley, J., Halees, A., and Weng, Z. (2007). Analysis of overrepresented motifs in human core promoters reveals dual regulatory roles of YY1. Genome research *17*, 798-806.

Xu, K., Wu, Z.J., Groner, A.C., He, H.H., Cai, C., Lis, R.T., Wu, X., Stack, E.C., Loda, M., Liu, T.*, et al.* (2012). EZH2 oncogenic activity in castration-resistant prostate cancer cells is Polycomb-independent. Science *338*, 1465-1469.

Yang, X., Ongusaha, P.P., Miles, P.D., Havstad, J.C., Zhang, F., So, W.V., Kudlow, J.E., Michell, R.H., Olefsky, J.M., Field, S.J.*, et al.* (2008). Phosphoinositide signalling links O-GlcNAc transferase to insulin resistance. Nature *451*, 964-969.

Yang, X., Zhang, F., and Kudlow, J.E. (2002). Recruitment of O-GlcNAc transferase to promoters by corepressor mSin3A: coupling protein O-GlcNAcylation to transcriptional repression. Cell *110*, 69-80.

Yao, T., Song, L., Jin, J., Cai, Y., Takahashi, H., Swanson, S.K., Washburn, M.P., Florens, L., Conaway, R.C., Cohen, R.E.*, et al.* (2008). Distinct modes of regulation of the Uch37 deubiquitinating enzyme in the proteasome and in the Ino80 chromatin-remodeling complex. Molecular cell *31*, 909-917.

Yao, T., Song, L., Xu, W., DeMartino, G.N., Florens, L., Swanson, S.K., Washburn, M.P., Conaway, R.C., Conaway, J.W., and Cohen, R.E. (2006). Proteasome recruitment and activation of the Uch37 deubiquitinating enzyme by Adrm1. Nature cell biology *8*, 994-1002.

Ye, Y., Akutsu, M., Reyes-Turcu, F., Enchev, R.I., Wilkinson, K.D., and Komander, D. (2011). Polyubiquitin binding and cross-reactivity in the USP domain deubiquitinase USP21. EMBO reports *12*, 350-357.

Yokota, T., Nagai, H., Harada, H., Mine, N., Terada, Y., Fujiwara, H., Yabe, A., Miyazaki, K., and Emi, M. (2001). Identification, tissue expression, and chromosomal position of a novel gene encoding human ubiquitin-conjugating enzyme E2-230k. Gene *267*, 95-100.

Yokoyama, A., Wang, Z., Wysocka, J., Sanyal, M., Aufiero, D.J., Kitabayashi, I., Herr, W., and Cleary, M.L. (2004). Leukemia proto-oncoprotein MLL forms a SET1-like histone methyltransferase complex with menin to regulate Hox gene expression. Molecular and cellular biology *24*, 5639-5649.

Yoshikawa, Y., Sato, A., Tsujimura, T., Emi, M., Morinaga, T., Fukuoka, K., Yamada, S., Murakami, A., Kondo, N., Matsumoto, S.*, et al.* (2012). Frequent inactivation of the BAP1 gene in epithelioid-type malignant mesothelioma. Cancer science *103*, 868-874.

Yu, H., Mashtalir, N., Daou, S., Hammond-Martel, I., Ross, J., Sui, G., Hart, G.W., Rauscher, F.J., 3rd, Drobetsky, E., Milot, E.*, et al.* (2010). The ubiquitin carboxyl hydrolase BAP1 forms a ternary complex with YY1 and HCF-1 and is a critical regulator of gene expression. Molecular and cellular biology *30*, 5071-5085.

Yu, H., Pak, H., Hammond-Martel, I., Ghram, M., Rodrigue, A., Daou, S., Barbour, H., Corbeil, L., Hebert, J., Drobetsky, E.*, et al.* (2014). Tumor suppressor and deubiquitinase BAP1 promotes DNA double-strand break repair. Proceedings of the National Academy of Sciences of the United States of America *111*, 285-290.

Yu, Y., Teng, Y., Liu, H., Reed, S.H., and Waters, R. (2005). UV irradiation stimulates histone acetylation and chromatin remodeling at a repressed yeast locus. Proceedings of the National Academy of Sciences of the United States of America *102*, 8650-8655.

Zacharias, E. (1894). Über Beziehungen des Zellenwachstum zur Beschaffenheit des Zellkerns, [Sonderdr.] edn.

Zhang, E.E., Liu, A.C., Hirota, T., Miraglia, L.J., Welch, G., Pongsawakul, P.Y., Liu, X., Atwood, A., Huss, J.W., 3rd, Janes, J.*, et al.* (2009). A genome-wide RNAi screen for modifiers of the circadian clock in human cells. Cell *139*, 199-210.

Zhang, X., Zhang, J., Bauer, A., Zhang, L., Selinger, D.W., Lu, C.X., and Ten Dijke, P. (2013a). Fine-tuning BMP7 signalling in adipogenesis by UBE2O/E2-230K-mediated monoubiquitination of SMAD6. The EMBO journal *32*, 996-1007.

Zhang, X., Zhang, J., Zhang, L., van Dam, H., and Ten Dijke, P. (2013b). UBE2O negatively regulates TRAF6-mediated NF-kappaB activation by inhibiting TRAF6 polyubiquitination. Cell research *23*, 366-377.

Zhao, C., Collins, M.N., Hsiang, T.Y., and Krug, R.M. (2013). Interferon-induced ISG15 pathway: an ongoing virus-host battle. Trends in microbiology *21*, 181-186.

Zhao, G.Y., Sonoda, E., Barber, L.J., Oka, H., Murakawa, Y., Yamada, K., Ikura, T., Wang, X., Kobayashi, M., Yamamoto, K.*, et al.* (2007). A critical role for the ubiquitin-conjugating enzyme Ubc13 in initiating homologous recombination. Molecular cell *25*, 663-675.

Zhao, Z., Tavoosidana, G., Sjolinder, M., Gondor, A., Mariano, P., Wang, S., Kanduri, C., Lezcano, M., Sandhu, K.S., Singh, U.*, et al.* (2006). Circular chromosome conformation capture (4C) uncovers extensive networks of epigenetically regulated intra- and interchromosomal interactions. Nature genetics *38*, 1341-1347.